

**Role of glutathione S-transferases and the
mercapturic acid pathway in the biotransformation
potential of two zebrafish (*Danio rerio*) test systems:
early life stages and PAC2 cells**

Présentée le 6 août 2020

à la Faculté de l'environnement naturel, architectural et construit
Laboratoire de toxicologie de l'environnement
Programme doctoral en génie civil et environnement

pour l'obtention du grade de Docteur ès Sciences

par

Alena TIERBACH

Acceptée sur proposition du jury

Prof. U. von Gunten, président du jury
Prof. K. Schirmer, Dr M. J.-F. Suter, directeurs de thèse
Prof. S. Sturla, rapporteuse
Prof. P. Picotti, rapporteuse
Prof. S. Gerber, rapporteuse

Abstract

Zebrafish (*Danio rerio*) early life stages provide an important model for chemical risk assessment due to their genetic similarity to humans and the availability of well-established high-throughput techniques. Cells isolated from zebrafish conserve all these advantages and can, in addition, be multiplied in the laboratory to an unlimited extent. However, the biotransformation capacities of both systems have not been fully characterized. One biotransformation pathway, which is of utmost importance for the clearance of electrophilic compounds and phase I biotransformation products, is the mercapturic acid pathway. Its first step is the conjugation of the electrophile with glutathione, catalyzed by glutathione S-transferases (GSTs). The glutathione conjugates are usually further biotransformed within the mercapturic acid pathway by sequential removal of the glutamyl- and glycyl-moieties and an acetylation step followed by elimination of the mercapturate. Considering the significance of this biotransformation route for the outcome of toxicological investigations, this thesis aims to close some major knowledge gaps regarding the protein expression of GSTs and the functionality of the mercapturic acid pathway in two test systems, zebrafish early life stages and the embryo-derived cell line PAC2.

To investigate the repertoire of cytosolic GSTs and their expression dynamics, a targeted proteomics method using electrospray ionization (ESI) was developed. Zebrafish embryos showed a basal expression of GST isoenzymes belonging to the classes alpha, mu, pi and rho as early as 4 hours post fertilization, indicating maternal transfer. After hatching, all cytosolic GST classes could be detected in the free-swimming larvae. The embryo-derived cell line PAC2 also expressed all cytosolic GST classes, except class alpha. Motivated by the abundant expression of GSTs in the zebrafish models, focus was set on the potential of GSTs to biotransform a model substrate (1-chloro-2,4-dinitrobenzene, CDNB) and to initiate its further biotransformation within the mercapturic acid pathway. Since CDNB has no acid/base properties, an atmospheric pressure chemical ionization (APCI) method based on electron capture was developed for CDNB analysis at and below the nontoxic concentrations. For the determination of CDNB biotransformation products of the mercapturic acid pathway, an ESI method was developed. In both test systems, the expression of cytosolic GSTs was not affected by non-toxic concentrations of the model substrate CDNB. Furthermore, both test systems disclosed a fully functional mercapturic acid pathway with the first (glutathione conjugate) and last (mercapturate) biotransformation product being produced and excreted in zebrafish early life stages and PAC2 cells.

To conclude, this thesis reveals the expression of a large GST repertoire and a functional mercapturic acid pathway in zebrafish early life stages and PAC2 cells. The presence of this important chemical activation/deactivation and clearance route supports the application of these test systems as alternative models in toxicology and chemical hazard assessment.

Keywords

Glutathione S-transferases, targeted proteomics, mercapturic acid pathway, biotransformation, CDNB, electron capture APCI, zebrafish, PAC2, alternatives to animal testing

Zusammenfassung

Die frühen Lebensstadien des Zebrafischblings (*Danio rerio*) sind aufgrund ihrer genetischen Ähnlichkeit mit Menschen und der Verfügbarkeit automatisierter Hochdurchsatzverfahren ein wichtiges Modell für die Risikobewertung von Chemikalien. Aus dem Zebrafischbling isolierte Zellen bewahren all diese Vorteile und können darüber hinaus im Labor unbegrenzt vermehrt werden. Die Biotransformationskapazitäten beider Systeme sind jedoch noch nicht vollständig charakterisiert. Die Bildung von Mercaptursäure-Derivaten ist ein wichtiger Biotransformationsprozess, der für die Entgiftung von elektrophilen Verbindungen und Phase-I-Biotransformationsprodukten von größter Bedeutung ist. Die zentrale Rolle bei diesem Vorgang spielen Glutathion S-Transferasen (GST), welche das Glutathion mit verschiedenen elektrophilen Verbindungen konjugieren. Nach der Konjugation wird der Glycyl- und Glutamylrest des Glutathions abgespalten und die Substanz wird nach einer Konjugation mit Acetyl-CoA als Mercaptursäure-Derivat ausgeschieden. Angesichts der Bedeutung dieses Prozesses für toxikologische Studien, befasst sich die vorliegende Arbeit mit Wissenslücken in Bezug auf die Proteinexpression von GST und der Bildung von Mercaptursäure-Derivaten in zwei Testsystemen, Frühstadien des Zebrafischblings und in der vom Embryo abgeleiteten Zelllinie PAC2.

Um das Repertoire der zytosolischen GSTs und ihre Expressionsdynamik zu untersuchen, wurde eine Targeted-Proteomics-Methode mit Elektrospray-Ionisierung (ESI) entwickelt. Embryonen des Zebrafischblings zeigten bereits 4 Stunden nach der Befruchtung eine basale Expression von GST-Isoenzymen der Klassen alpha, mu, pi und rho, was auf einen maternalen Transfer hindeutet. Nach dem Schlüpfen konnten in den freischwimmenden Larven alle zytosolischen GST-Klassen nachgewiesen werden. Die von Embryonen abgeleitete PAC2 Zelllinie exprimierte ebenfalls alle zytosolischen GST-Klassen, mit Ausnahme der Klasse alpha. Motiviert durch die Expression von GSTs in beiden Zebrafischmodellen, wurde der Schwerpunkt auf das GST Potenzial, das Modells substrat (1-Chlor-2,4-dinitrobenzol, CDNB) mit Glutathion zu konjugieren und somit die Bildung von Mercaptursäure-Derivaten zu initiieren, gelegt. Da CDNB keine Säure / Base-Eigenschaften aufweist, wurde für die CDNB-Analyse ein Verfahren zur chemischen Ionisierung bei Atmosphärendruck (APCI) entwickelt, welches die Bestimmung von CDNB unter nichttoxischen Konzentrationen erlaubt. Für die Analyse von CDNB-Biotransformationsprodukten wurde eine ESI-Methode entwickelt. In beiden Testsystemen wurde die Expression von zytosolischen GSTs durch nichttoxische Konzentrationen des Modells substrats CDNB nicht beeinflusst. Weiterhin beinhalteten beide Testsysteme einen voll funktionsfähigen Biotransformationsprozess zur Bildung von Mercaptursäure-Derivaten. Wir konnten beobachten, dass das erste (Glutathionkonjugat) und

das letzte (Mercaptursäure-Derivat) Biotransformationsprodukt in frühen Lebensstadien des Zebrafisches und in PAC2-Zellen gebildet und ausgeschieden wurden.

Zusammenfassend lässt sich sagen, dass die Ergebnisse der vorliegenden Arbeit, insbesondere die grosse Bandbreite der exprimierten GSTs und die Funktionalität der Bildung von Mercaptursäure-Derivaten, die Anwendung dieser Testsysteme als alternative Modelle in der Toxikologie und Risikobewertung unterstützen.

Schlüsselwörter

Glutathion S-Transferasen, Targeted Proteomics, Mercaptursäure-Derivate, Biotransformation, CDNB, Elektroneneinfang APCI, Zebrafisch, PAC2, Alternativen zu Tierversuchen

Table of contents

Abstract.....	i
Zusammenfassung	iii
Chapter 1 Introduction.....	1
1.1 Zebrafish is an immensely versatile model.....	2
1.1.1 Zebrafish early life stages facilitate the development of high-throughput approaches	3
1.1.2 Zebrafish cell lines have the potential to substitute <i>in vivo</i> tests in selected research areas	4
1.2 Knowledge gaps regarding the biotransformation potential of different test systems exist	5
1.2.1 Biotransformation is a complex interplay of enzyme-catalyzed reactions	7
1.2.2 Glutathione S-transferases play a crucial role in detoxification of reactive electrophiles.....	8
1.2.3 Protein expression data provide a sound picture of a model's biotransformation enzyme repertoire	10
1.2.4 Glutathione conjugates are further biotransformed within the mercapturic acid pathway.....	10
1.2.5 Analysis of biotransformation products provides a complete picture of a pathway's functionality	13
1.3 Research objectives.....	14
1.3.1 Scope of Chapter 2: Glutathione S-transferase protein expression in different life stages of zebrafish (<i>Danio rerio</i>).....	14
1.3.2 Scope of Chapter 3: LC-APCI(-)-MS determination of 1-chloro-2,4-dinitrobenzene, a model substrate for glutathione S-transferases	15
1.3.3 Scope of Chapter 4: Biotransformation capacity of zebrafish (<i>Danio rerio</i>) early life stages: Functionality of the mercapturic acid pathway.....	16
1.3.4 Scope of Chapter 5: Expression of cytosolic glutathione S-transferases and performance of the mercapturic acid pathway in the zebrafish embryo cell line, PAC2	17
Chapter 2 Glutathione S-transferase protein expression in different life stages of zebrafish (<i>Danio rerio</i>).....	19
2.1 Abstract.....	20
2.2 Introduction	21
2.3 Materials and methods.....	23
2.3.1 Zebrafish maintenance and sampling	23
2.3.2 Protein extraction and preparation of tryptic digests	25
2.3.3 Selection of peptides and MRM method development	25
2.3.4 LC and MS settings.....	27
2.3.5 Data analysis.....	27
2.3.6 Supplementary information Chapter 2.....	28
2.4 Results	29
2.4.1 GST classes and isoenzymes show distinct expression patterns throughout zebrafish development	29
2.4.2 GST classes and isoenzymes show distinct expression patterns in organs of adult zebrafish	32
2.5 Discussion.....	34
2.5.1 GST expression in early life stages of zebrafish reflects important developmental events	34
2.5.2 GST expression in adult organs is organ-specific and variable among individuals	36
2.5.3 GSTs expressed in zebrafish show similarities to humans	37

Chapter 3	LC-APCI(-)-MS determination of 1-chloro-2,4-dinitrobenzene, a model substrate for glutathione S-transferases	39
3.1	Abstract	40
3.2	Introduction	41
3.3	Materials and methods	42
3.3.1	Chemicals and reagents	42
3.3.2	Mass spectrometry	42
3.3.3	Chromatography	43
3.3.4	Verification of exposure levels in CDNB toxicity studies	43
3.3.5	Data processing and evaluation	44
3.3.6	Supplementary information Chapter 3	44
3.4	Results and discussion	45
3.4.1	CDNB undergoes dissociative and non-dissociative EC in APCI(-)	45
3.4.2	Dissociative EC in APCI(-) allows to measure CDNB load in common toxicity studies	47
3.5	Conclusion	49
Chapter 4	Biotransformation capacity of zebrafish (<i>Danio rerio</i>) early life stages: Functionality of the mercapturic acid pathway	50
4.1	Abstract	51
4.2	Introduction	52
4.3	Materials and methods	55
4.3.1	Chemicals and reagents	55
4.3.2	Zebrafish maintenance and breeding	55
4.3.3	CDNB toxicity study	55
4.3.4	CDNB exposure experiments for biotransformation analysis	56
4.3.5	Metabolite depuration analysis	57
4.3.6	Preparation of standards for method development and normalization	57
4.3.7	Extraction of CDNB metabolites from tissue	58
4.3.8	LC-HRMS analysis of CDNB metabolites	59
4.3.9	Protein expression analysis	59
4.3.10	Data evaluation	60
4.3.11	Supplementary information Chapter 4	61
4.4	Results	62
4.4.1	LC-MS can be used to analyze CDNB biotransformation products	62
4.4.2	CDNB induces toxicity in zebrafish early life stages at concentrations higher than 25 ng/ml	62
4.4.3	Metabolites of the mercapturic acid pathway are formed upon exposure to the non-toxic concentration of CDNB	64
4.4.4	Zebrafish embryo and larvae excrete mercapturic acid metabolites	64
4.4.5	Exposure to the non-toxic concentration of CDNB does not affect GST protein expression	66
4.5	Discussion	66
4.5.1	Mercapturic acid pathway is functional in zebrafish early life stages	66
4.6	Exposure to the NtC of a model electrophile does not affect GST protein expression	69

4.6.1	Functionality of mercapturic acid pathway has consequences for the manifestation of toxicity	69
Chapter 5	Expression of cytosolic glutathione S-transferases and performance of the mercapturic acid pathway in the zebrafish embryo cell line, PAC2	71
5.1	Abstract	72
5.2	Introduction	73
5.3	Materials and methods	75
5.3.1	Chemicals and reagents	75
5.3.2	Routine PAC2 cell culture	75
5.3.3	CDNB toxicity study	76
5.3.4	Exposure experiments for the analysis of CDBN biotransformation and GST expression	77
5.3.5	Analysis of CDBN biotransformation products in PAC2 cells and exposure medium	78
5.3.6	Protein expression analysis	78
5.3.7	Data evaluation	79
5.3.8	Supplementary information Chapter 5	79
5.4	Results	80
5.4.1	Determination of EC ₅₀ and non-toxic CDBN concentrations	80
5.4.2	Kinetics of CDBN in the culture system	81
5.4.3	Identification of biotransformation products of the mercapturic acid pathway	83
5.4.4	Analysis of GST protein expression upon exposure to CDBN	83
5.5	Discussion	85
5.5.1	CDBN concentrations in cell-free and cell-containing systems show different kinetics	85
5.5.2	CDBN acute toxicity in PAC2 cells is similar to acute toxicity in other aquatic organisms	85
5.5.3	All but one cytosolic GST class is detectable in the PAC2 cell line	86
5.5.4	Cytosolic GST protein expression is not affected by low concentrations of a model substrate	87
5.5.5	Mercapturic acid pathway is functional in PAC2 cells	87
Chapter 6	Conclusion and outlook	89
6.1	Future directions in the study of glutathione S-transferases	91
6.2	Further analysis of the mercapturic acid pathway and its branches	92
6.3	Innovations in cell culture technologies to mimic certain <i>in vivo</i> conditions	93
6.4	Concluding statement	94
Bibliography		95
Glossary		105
Supplementary information Chapter 2		107
Supplementary information Chapter 3		132
Supplementary information Chapter 4		134
Generation of DNP-C through gas-phase reactions in the ESI source		142
Supplementary information Chapter 5		155
Generation of DNP-CG through gas-phase reactions in the ESI source		162
Acknowledgements		175
Curriculum Vitae – Alena Tierbach		177

List of figures

Chapter 1

Figure 1: Different organism levels used in research with zebrafish combined with the graphical representation of processes involved in phase I and phase II biotransformation	6
Figure 2: The catalytic conjugation reaction performed by glutathione S-transferases	9
Figure 3: The mercapturic acid pathway	12
Figure 4: The targeted proteomic technique used in Chapter 2	15
Figure 5: The procedure used in Chapter 3.....	16
Figure 6: The procedure used in Chapter 4.....	17
Figure 7: The procedure used in Chapter 5.....	18

Chapter 2

Figure 8: The experimental workflow and schematic representation of the MRM technique.....	24
Figure 9: Schematic amino acid sequence alignment of GST classes.....	26
Figure 10: GST expression patterns observed during zebrafish early development	30
Figure 11: GST expression in zebrafish embryos and larvae.....	31
Figure 12: GST expression in different organs of adult female and male zebrafish	33

Chapter 3

Figure 13: Structural formula of 1-chloro-2,4-dinitrobenzene and proposed chemical formula of ions produced with APCI(-)-MS electron capture.....	46
Figure 14: Mass spectra of ions produced with APCI(-)-MS electron capture	48

Chapter 4

Figure 15: The biotransformation of 1-chloro-2,4-dinitrobenzene through the mercapturic acid pathway	54
Figure 16: Precursor ions of 2,4-dinitrophenyl-S-glutathione and 2,4-dinitrophenyl N-acetylcysteine in combination with the proposed structures of the fragment ions produced by higher energy collisional dissociation.	60
Figure 17: Formation and depuration of biotransformation products during zebrafish exposure to the non-toxic concentration of 1-chloro-2,4-dinitrobenzene and during a subsequent depuration period.....	63
Figure 18: Expression of cytosolic GSTs in zebrafish early life stages exposed to the non-toxic concentration of 1-chloro-2,4-dinitrobenzene	65

Chapter 5

Figure 19: The biotransformation of 1-chloro-2,4-dinitrobenzene through the mercapturic acid pathway in cell lines.....	74
Figure 20: Measured 1-chloro-2,4-dinitrobenzene medium concentrations in cell-free and cell-containing systems.....	81
Figure 21: Biotransformation products present in PAC2 cell lines and medium upon cell exposure to the non-toxic concentration of 1-chloro-2,4-dinitrobenzene	82
Figure 22: Expression of cytosolic GSTs in the PAC2 cell line exposed to the non-toxic concentration of 1-chloro-2,4-dinitrobenzene	84

Chapter 6

Figure 23: Schematic representation of the mercapturic acid pathway..	90
---	----

List of supplementary figures

Supplementary information Chapter 3

SI Figure 1: Calibration series over the concentration range of 0 to 2 µg/ml in reconstituted water and L15 medium with 5% FBS.....	133
---	-----

Supplementary information Chapter 4

SI Figure 2: Experimental workflow Chapter 4	134
SI Figure 3: Recovery of 2,4-dinitrophenyl-S-glutathione.....	135
SI Figure 4: Dose-response curve for lethal effects of 1-chloro-2,4-dinitrobenzene.....	135
SI Figure 5: Dose-response curve for sublethal effects of 1-chloro-2,4-dinitrobenzene	136
SI Figure 6: Chromatogram and mass spectra of 2,4-dinitrophenyl-S-glutathione.....	140
SI Figure 7: Chromatogram and mass spectra of 2,4-dinitrophenyl N-acetylcysteine	141

Supplementary information Chapter 5

SI Figure 8: Dose-response curves representing cell viability.....	156
SI Figure 9: Chromatogram in full scan mode and mass spectra of 2,4-dinitrotoluene-S-glutathione .	157
SI Figure 10: Chromatogram in full scan mode and mass spectra of 2,4-dinitrophenyl-S-glutathione, 2,4-dinitrophenyl cysteinylglycine and 2,4-dinitrophenyl N-acetylcysteine.....	158
SI Figure 11: Reconstructed ion chromatogram of the m/z=474.09 precursor ion and MS2 accurate mass spectra of the monoisotopic fragment ions.....	160
SI Figure 12: Expression of cytosolic GSTs within PAC2 cells.....	161
SI Figure 13: Kinetic model of 1-chloro-2,4-dinitrobenzene concentration in T75 cell culture flasks .	162

List of supplemental tables

Supplementary information Chapter 2

SI Table 1: Summary of the GST family classes, nomenclature of the isoforms and gene and protein reference sequences obtained from NCBI Reference Sequence Database.....	107
SI Table 2: Summary of synthetic peptides that have been purchased from JPT, Innovative Peptide Solutions, Germany.....	107
SI Table 3: Summary of proteotypic peptides and shared peptides, detected in zebrafish embryos and in organs of adult zebrafish.....	110
SI Table 4: CLUSTAL O (1.2.4) multiple sequence alignments of isoenzymes belonging to the same class.....	111
SI Table 5: Peak area of proteotypic peptides and shared peptides detected in zebrafish embryo	114
SI Table 6: Peak area of proteotypic peptides and shared peptides detected in organs of adult zebrafish	119
SI Table 7: Indexed retention time values for the respective peptides	130

Supplementary information Chapter 3

SI Table 8: Measured and predicted mass-to-charge ratio, the intensities and the relative intensities of isotopes.....	132
SI Table 9: Nominal and measured concentrations of 1-chloro-2,4-dinitrobenzene used for toxicity studies in reconstituted water and L15 medium with 5% FBS.....	133

Supplementary information Chapter 4

SI Table 10: Physico-chemical calculations and predictions for 2,4-dinitrotoluene-S-glutathione, 2,4-dinitrophenyl-S-glutathione, 2,4-dinitrophenyl cysteinylglycine, 2,4-dinitrophenyl cysteine, 2,4-dinitrophenyl N-acetylcysteine.....	137
SI Table 11: Difference between the measured and predicted masses of the precursor ion 2,4-dinitrophenyl-S-glutathione in full scan and of the fragment ions	140
SI Table 12: Difference between the measured and predicted masses of the precursor ion 2,4-dinitrophenyl N-acetylcysteine in full scan and of the fragment ions.	141
SI Table 13: Analysis of biotransformation products in 1-chloro-2,4-dinitrobenzene exposure experiments	143
SI Table 14: Analysis of biotransformation products in 1-chloro-2,4-dinitrobenzene depuration experiments.....	147
SI Table 15: Cytosolic GST expression in zebrafish embryos and larvae exposed to 1-chloro-2,4-dinitrobenzene non toxic concentration.	150

Supplementary information Chapter 5

<i>SI Table 16: Nominal and measured 1-chloro-2,4-dinitrobenzene concentrations in the medium at the beginning of each toxicity study</i>	<i>155</i>
<i>SI Table 17: Measured 1-chloro-2,4-dinitrobenzene concentrations at the beginning and at the end of the experiment in addition to the geometric mean.....</i>	<i>155</i>
<i>SI Table 18: Mean of EC₅₀ and NtC values measured with the three fluorescent dyes.....</i>	<i>155</i>
<i>SI Table 19: Difference between the measured and predicted isotopes of the protonated molecular ions of 2,4-dinitrotoluene-S-glutathione, 2,4-dinitrophenyl-S-glutathione, 2,4-dinitrophenyl cysteinglycine and 2,4-dinitrophenyl N-acetylcysteine in full scan.....</i>	<i>159</i>
<i>SI Table 20: Analysis of biotransformation products in PAC2 cells during 1-chloro-2,4-dinitrobenzene exposure experiments.....</i>	<i>163</i>
<i>SI Table 21: Analysis of biotransformation products in medium during 1-chloro-2,4-dinitrobenzene exposure experiments.....</i>	<i>166</i>
<i>SI Table 22: Cytosolic GST expression in PAC2 cells exposed to 1-chloro-2,4-dinitrobenzene non-toxic concentration.....</i>	<i>170</i>
<i>SI Table 23: Analysis of 1-chloro-2,4-dinitrobenzene in medium during the exposure experiments. ..</i>	<i>173</i>

Chapter 1 Introduction

In Switzerland and many European countries, the regulatory framework dealing with animal experimentation consists of a combination of deontological and consequentialist elements; describing some absolute limits (deontological) and case by case weighing of benefits and costs of an experiment (consequentialist). By following the consequentialist approach, animal experiments can be justified only if the aggregation of benefits (i.e. gain in knowledge, medical advancement, environmental protection) outweighs the cumulative harms imposed on an animal (i.e. pain, impairment of mobility, impairment of growth). For the benefit of ethical balancing and to improve animal welfare, scientific and legislative developments in Switzerland and the European Union have promoted a gradual implementation of the 3R principles (Russell and Burch, 1959). This implies that animal experiments should, whenever possible, be replaced with non-animal test systems (Replace), the number of animals used in experiments should be limited to the essential number (Reduce) and the harm imposed on an animal should be minimized (Refine). To fulfill these principles and to reduce the use of vertebrate animal models, the scientific community has developed different approaches, including *in vitro* systems, non-invasive diagnostic techniques and the use of less sentient life stages.

One popular vertebrate animal model, which is frequently used in life sciences and ecotoxicology alike, is the zebrafish (*Danio rerio*). Although many scientific studies still require adult animals, test systems have been developed with the aim to refine and replace studies with adult fish. A possible refinement of toxicity tests with adult animals is the use of non-feeding development stages. The non-feeding embryo and larvae are considered as the least sentient life stages in fish development because they do not yet show signs of pain experience, long-term memory, complex learning and behavioral versatility (Authority 2005). Based on this reasoning, live stages incapable of independent feeding do not require permission by authorities (European Commission 2010). Additionally, the use of cell cultures has great potential to replace animal experimentations in selected fields. The importance of cell cultures for modern science has recently been acknowledged with the 3R Swiss Competence Centre (3RCC) award, honoring the establishment of the ISO guideline for the assessment of acute fish toxicity using a fish gill cell line (ISO 21115:2019).

However, it would be irrational to claim that early life stages or cell lines completely represent the complex adult organism. One important aspect that needs to be kept in mind is biotransformation, a process by which

a xenobiotic is biochemically modified within an organism. A chemical, for instance, can have contrasting effects on different life stages (e.g. non-feeding larvae *versus* adult fish) which differ in their biotransformation capacity. Furthermore, some chemicals are biotransformed within interorgan pathways. A cell culture derived from only one organ or early life stage may therefore lack the enzymes responsible for a compound's activation or detoxification. It is therefore necessary to assess the repertoire of biotransformation enzymes and define metabolic limitations of alternatives, such as zebrafish early life stages and cell cultures.

With the aim to broaden the application field of zebrafish early life stages and an embryonic zebrafish cell line (PAC2), this thesis focuses on the expression of biotransformation enzymes involved in the phase II biotransformation (glutathione S-transferases) and the functionality of the mercapturic acid pathway within these test systems. The introduction aims to provide a profound background on the chosen model systems, the enzymes involved in biotransformation with the focus on glutathione S-transferases (GSTs), and the mercapturic acid pathway.

1.1 Zebrafish is an immensely versatile model

The small tropical fish – zebrafish (*Danio rerio*) – has evolved into a powerful model organism for research on vertebrate development, physiology, genetics and drug metabolism (Graham and Cheng 2009; Langheinrich 2003; Rennekamp and Peterson 2015). Due to its small size (3 to 4 cm) and schooling behavior, a large number of animals can be maintained in a small space. The short generation time of 3 to 4 months allows a fast breeding of zebrafish lines for specific research questions. Female zebrafish spawn all-season every 2 to 3 days, producing hundreds of eggs, which develop *ex utero*. They can easily be collected with spawning trays and genetically manipulated at any life stage. In addition, the embryo and its chorion are translucent, which allows the observation of the organ development with optical microscopy (Dahm and Geisler 2006). This facilitated the establishment of large mutant libraries for the detailed understanding of vertebrate development and pathogenesis. Zebrafish show significant homology with human physiology and genetics (Goldsmith and Jobin 2012; Howe et al. 2014). The whole-genome sequencing initiative performed by the Sanger Institute showed that 69% of zebrafish genes have at least one human orthologue. When looking into human disease-related genes, the similarity between zebrafish and humans becomes even more pronounced. 82% of known human disease-related genes can be associated with at least one zebrafish orthologue (Howe et al. 2013).

In combination with the zebrafish genome project, a substantial body of information collected in developmental biology and molecular genetics, contributed to the popularity of the zebrafish model. It has evolved into one of the most important vertebrates for human disease research and has proven its high potential as a representative system for human pharmacology and toxicology (Bailey et al. 2013; Dooley and Zon 2000; Rennekamp and Peterson 2015). The release of pharmaceuticals, pesticides, industrial chemicals, and the degradation products of these into the environment also increased the need for ecotoxicological studies with the focus on chemical fate and effects in fish, again with zebrafish being one of the most important toxicological vertebrate models (Bambino and Chu 2017).

1.1.1 Zebrafish early life stages facilitate the development of high-throughput approaches

Especially the embryonic life stages contributed to the popularity of zebrafish as a model organism (Di Paolo et al. 2015; Hill et al. 2005; Scholz et al. 2008). They are easy to maintain, less space-consuming than adult fish, require low volumes of test substance, and they develop fast, which favors the development of large-scale, high-throughput screening systems for chemicals and therapeutic drugs (Scholz et al. 2008). Furthermore, the lack of pigmentation at early stages (McGrath and Li 2008) offers the opportunity to monitor effects of chemicals throughout the development and to include non-lethal endpoints such as malformation of organs. As the early larvae does not start feeding before 120 hours post fertilization (hpf) (Kimmel et al. 1995; Strahle et al. 2012), it is considered an extension of the embryonic development phase (eleutheroembryo) and hence is not protected by the legislation on animal welfare (Strahle et al. 2012). Within the first 120 hpf, zebrafish represent a unique organism that allows the analysis of cells within a multiorgan structure by maintaining all advantages of an *in vitro* system (Kimmel et al. 1995; Veldman and Lin 2008).

Chemical screens with zebrafish led to the establishment of new targets and new uses for existing bioactive compounds and accelerated the discovery of novel compound classes (Rennekamp and Peterson 2015). Zebrafish early life stages are also a suitable model for the study and development of Adverse Outcome Pathways (AOP). AOP-oriented studies can be applied to identify useful screening and prioritization strategies for chemicals and to collect data for the establishment and training of predictive models for toxicity. Such an approach is not only favorable for economic reasons but is also a strategy to reduce the number of animals required for toxicity testing (Villeneuve et al. 2014; Volz et al. 2011). Consequently, zebrafish embryos are a

widely used model system in pharmacology, toxicology and for monitoring of environmental contaminants (Busquet et al. 2014; Dooley and Zon 2000; FederalLawGazette 2005; Knobel et al. 2012; Rennekamp and Peterson 2015). The advantages of the embryo model have for instance been exploited in environmental risk assessment to refine the 96 hours acute fish toxicity test (AFT) with adult fish. Since the implementation of REACH, every chemical, which is produced or imported in volumes \geq one tonne per year, needs to be registered by the manufacturer or importer through the provision of a registration dossier to the European Chemicals Agency (ECHA). For the registration of chemicals with a tonnage \geq 10 tons per year, the provision of data from the AFT remains an important requirement (European Commission 2006). The AFT is, however, not only time and resource consuming, but also expected to increase the number of fish used in animal testing (Breithaupt 2006; Embry et al. 2010; Rovida and Hartung 2009). As a refinement to the AFT, toxicity studies with zebrafish early life stages are therefore an attractive possibility. In Germany, zebrafish embryos have already replaced adult fish testing for the determination of wastewater effluent toxicity since January 2005 (Federal Law Gazette 2005) and thus contribute to the substitution of conventional animal tests. Due to the fact that the REACH policy promotes the submission of data from alternative test systems, much effort has been put into the standardization and validation of the zebrafish embryo acute toxicity (zFET) test, to strengthen its application as a refinement system for AFT (Belanger et al. 2013; Busquet et al. 2014; Knobel et al. 2012).

1.1.2 Zebrafish cell lines have the potential to substitute *in vivo* tests in selected research areas

Research with immortal cell lines has revolutionized modern approaches to study gene functions, uncover molecular mechanisms and test drug efficacy and safety. Permanent cell cultures offer several advantages as compared to primary cells and *in vivo* experiments. They are cost effective, provide an unlimited supply of homogenous samples and are not subject to the same ethical concerns as *in vivo* animal experimentation. Currently, the global biological materials resource and standards organization (American Type Culture Collection, ATCC) offers an inventory of animal cell lines from over 150 species, including zebrafish. Although not included in the inventory, the embryonic zebrafish cell line PAC2 is occasionally used as an *in vitro* alternative to zebrafish embryos. The PAC2 cell line is a fibroblast line, generated from 24 hpf old embryos (Lin et al. 1994). It can be cultivated at approximately 28 °C in a conventional Leibovitz medium without CO₂ enriched

atmosphere (Senghaas and Koster 2009), which is cost-efficient and has a lower risk of contamination compared to mammalian lines. PAC2 cells are a promising model for toxicological studies as they have previously been successfully used in studies focusing on antibiotics, flame-retardants and model genotoxins (Klobucar et al. 2013; Srut et al. 2015; van Boxtel et al. 2008; van Boxtel et al. 2010).

1.2 Knowledge gaps regarding the biotransformation potential of different test systems exist

In order to replace animal testing, especially in chemical risk assessment, the refinement or alternative tests should be available as a standardized method that has successfully completed a comprehensive validation process. For this, it is required that the test is highly reproducible and shows a robust relationship with the test system it aims to replace. Hence, comprehensive validation studies have been performed with the aim to determine the intra- and interlaboratory reproducibility of toxicity test results with zebrafish embryos (Busquet et al. 2014; Knobel et al. 2012). Additionally, a rainbow trout (*Oncorhynchus mykiss*) gill cell line (RTgill-W1) was tested for the potential to provide reproducible and representative toxicity data for the whole organism (Fischer et al. 2019; Tanneberger et al. 2013). For the validation, zebrafish embryos and RTgill-WT cells were exposed to organic chemicals with multiple modes of action and physicochemical properties. The chemical concentrations causing a reduction of embryo survival (median lethal concentration, LC_{50}) or of cell viability (median effect concentration, EC_{50}) by 50% were measured and compared to the adult fish LC_{50} data from literature and databases.

Overall, a good repeatability and reproducibility (intra- and interlaboratory variability) of the two test systems was reported and both showed a strong correlation with the toxicity data collected with juvenile or adult fish (Fischer et al. 2019; Knobel et al. 2012; Tanneberger et al. 2013). However, despite the strong correlation, a few chemicals emerged as outliers. These included two neurotoxins (permethrin and lindane) and one compound (allyl alcohol) that undergoes enzymatic activation to its toxic biotransformation product (acrolein) only if the respective enzyme (alcohol dehydrogenase) is sufficiently expressed within the test system (Kluver et al. 2014; Knobel et al. 2012). In zebrafish embryos, the expression of alcohol dehydrogenase (*adh8a*) can be observed for the first time at 120 hpf. Before that, enzymatic oxidation of allyl alcohol to acrolein is not detectable, resulting in a lower toxicity (Kluver et al. 2014). This example underlines the importance of enzymatic

biotransformation processes, which strongly influence a compound's toxicity. Gene expression can also significantly differ. He et al. (2006) demonstrated that different zebrafish cell lines, zebrafish embryos and adult fish could be distinguished in their transcriptome profile.

A different repertoire or/and differing expression levels of biotransformation enzymes can result in under- or overestimation of a compound's efficacy and safety. Yet, comprehensive studies dealing with the developmental expression of xenobiotic-metabolizing enzymes in zebrafish embryos and cell lines are scarce.

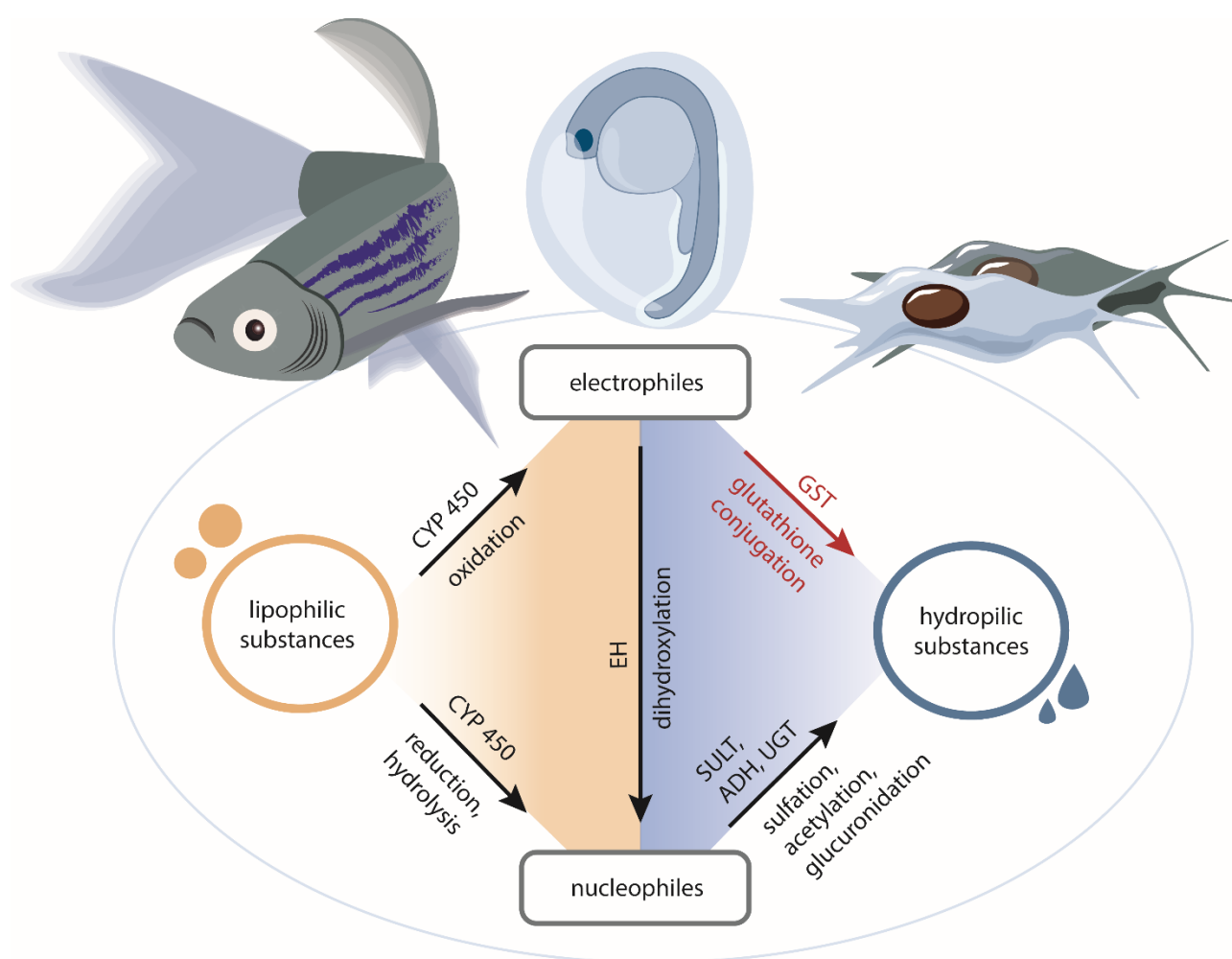


Figure 1: Schematic representation of different organism levels used in research with zebrafish - from left to right: male/female adult zebrafish, zebrafish early developmental stages and zebrafish cell cultures, combined with the graphical representation of processes involved in phase I (yellow) and phase II (blue) biotransformation performed by the enzyme families cytochrome P450s (CYP450), epoxide hydrolases (EH), glutathione S-transferases (GST), sulfotransferases (SULT), alcohol dehydrogenases (ADH) and uridine 5'-diphosphoglucuronosyltransferases (UGT).

1.2.1 Biotransformation is a complex interplay of enzyme-catalyzed reactions

Biotransformation is a process catalyzed by enzymes and their cofactors, capable of modifying the chemical structure of the parent compound through different reactions, such as oxidation, reduction, hydrolysis and conjugation with endogenous molecules (Figure 1). It can be regarded as a two-phase process, which generally alters the chemistry of lipophilic, non-polar compounds to more hydrophilic, polar ones. Predominantly, the resulting products are easier to excrete, less reactive and thus less toxic. It is, however, possible that the introduction of chemical groups that increase the polarity of the substance results in highly reactive metabolites with higher hazardous potential than their parent compound (Testa 2009; Testa et al. 2012). The first phase (phase I) reaction either exposes or adds a polar group to the substance. This group can be used in a conjugation reaction – in the second phase (phase II) – to link the substance to an endogenous compound with high hydrophilicity. However, these processes do not necessarily occur one after another. It is rather a complex network of reactions where some pathways are more or less favored depending on the chemical structure of the substance (Testa 2009; Testa et al. 2012). Differences in the expression of enzymes involved in phase I and phase II biotransformation can lead to changes in concentrations of the parent compound as well as the resulting biotransformation products.

Phase I reactions are mainly performed by cytochrome P450 (CYP450) oxidoreductases. They play a major role in the biotransformation of xenobiotic compounds through oxidative processes (Figure 1). Phase I reactions often lead to the production of highly reactive intermediates that need to be inactivated through phase II conjugation reactions. Reduced metabolic capacity of phase II enzymes can lead to an accumulation of reactive intermediates and to adverse effects within the organism. Quantitatively, enzymatic glutathione (GSH) conjugation is the second most important process in phase II biotransformation in humans, exceeded only by glucuronidation (Testa et al. 2012). For the detoxification of electrophiles however, GSH conjugation is the most important process. Key enzymes that catalyze the conjugation of electrophilic compounds with GSH are glutathione S-transferases (GSTs) (Glisic et al. 2015; Testa et al. 2012). Nonetheless, the repertoire and expression levels of GSTs in organisms used for chemical risk assessment is largely unexplored.

1.2.2 Glutathione S-transferases play a crucial role in detoxification of reactive electrophiles

Glutathione S-transferases (GSTs) are a family of enzymes capable of catalyzing different types of reactions, which enables GSTs to serve as peroxidases, isomerases or chaperones (Hayes and Pulford 1995). The enzyme family name is derived from the ability of GSTs to catalyze nucleophilic addition (Michael addition) of reduced glutathione (γ -L-glutamyl-L-cysteinylglycine, GSH, intracellular concentration of 0.1-10 mM (Ruzza and Calderan 2013)) onto electrophilic compounds, resulting in the formation of glutathione conjugates (Figure 2) (Hayes et al. 2005). Although GSH conjugation reactions can also occur non-catalytically, the Michael addition rate is considerably enhanced in the presence of GSTs (Higgins and Hayes 2011; Stoelting and Tjeerdema 2000). Under physiological conditions (pH \sim 7.4), GSH exists in its relatively unreactive form. Binding of GSH to the GST catalytic center greatly increases its reactivity towards electrophiles through a decrease of its apparent pK_a from approximately 9 to 6.5. In addition, the binding to GSTs brings GSH into proximity with the hydrophobic electrophile, which is bound to the substrate-binding site. This then accelerates the formation of the GSH conjugate (Hayes and Pulford 1995; Kumagai and Abiko 2017). GSH conjugation is involved in the protection of the cell from a variety of harmful compounds, including products of oxidative stress (such as 4-hydroxynon-2-enal and organic hydroperoxides), reactive phase I biotransformation products (such as benzo[a]pyrene-7,8-diol-9,10-epoxide and aflatoxin-8,9-epoxide), pesticides (such as alachlor, atrazine) and drugs (such as diuretic ethacrynic acid and chlorambucil) (Hayes and Pulford 1995; Ruzza and Calderan 2013). Relatedly, multiple studies suggest that the repertoire of GST isoenzymes and their expression level influences the organisms' sensitivity to a wide range of xenobiotic compounds, the susceptibility to certain cancer types (such as bladder and colon) and the development of drug resistance (Hayes and Pulford 1995; Townsend and Tew 2003). Furthermore, regulation of GSTs can indicate an adaptive response caused by chemical stress (Knight et al. 2008; Mitchell et al. 1997). Thus, insights into the GST expression and regulation within model organisms are essential for understanding toxicological outcomes and for extrapolation of the toxicity data from cells to organisms and from one organism to another.

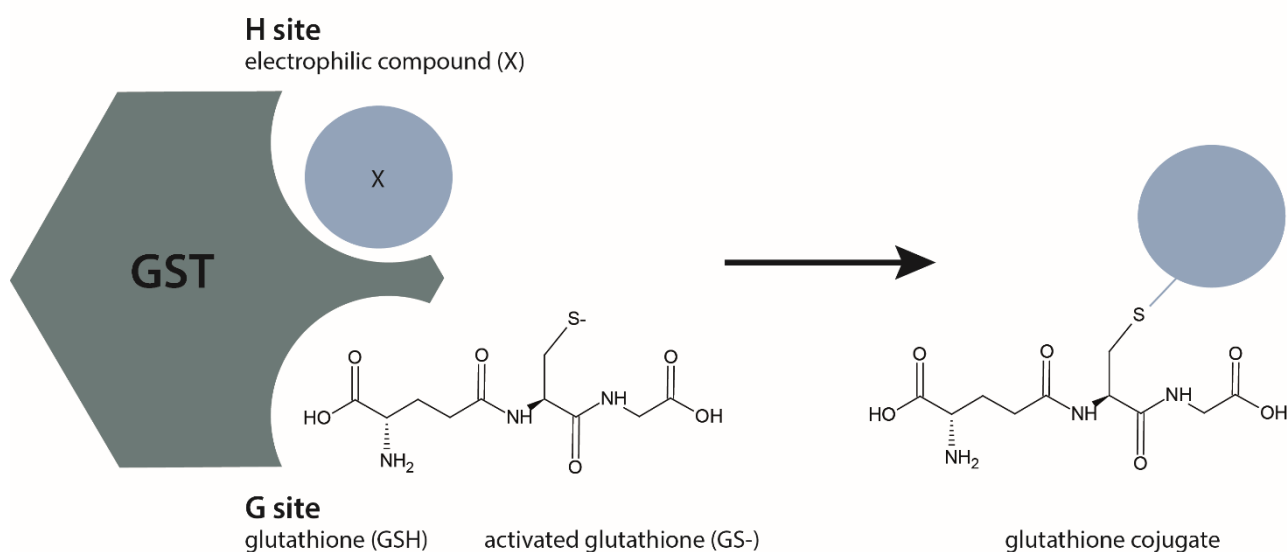


Figure 2: Schematic representation of the catalytic conjugation reaction performed by glutathione S-transferases (GSTs).

Enzymes belonging to the GST family are subdivided into three groups: membrane associated, mitochondrial, and cytosolic (Glisic et al. 2015; Hayes et al. 2005). These groups are further subdivided into classes based on sequence similarities (Glisic et al. 2015; Hayes et al. 2005; Sheehan et al. 2001). Membrane-associated GSTs form the MGST or MAPEG class (Membrane-Associated Proteins in Eicosanoid and Glutathione metabolism). Those membrane-associated enzymes are involved in the biosynthesis of leukotrienes and prostanooids (Glisic et al. 2015; Jakobsson et al. 1999). Mitochondrial GSTs belong to the kappa class. The cytosolic GSTs have been classified as alpha, zeta, theta, mu, pi, rho, and omega, with members of the rho class only being found in cephalo-chordates and teleosts (Glisic et al. 2015). Cytosolic GSTs are dimeric enzymes consisting of either two identical (homodimers) or closely related (heterodimers) subunits. The diversification of cytosolic GSTs into multiple classes and the potential to form heterodimers provides a broad substrate specificity and underlines their involvement not only in endogenous processes but also in the inactivation of potentially harmful endogenous and xenobiotic compounds (Glisic et al. 2015).

1.2.3 Protein expression data provide a sound picture of a model's biotransformation enzyme repertoire

Despite the versatile application of zebrafish in research, current understanding of the protein expression of GSTs is limited. Instead, relative mRNA expression is often used to investigate the expression pattern of GST classes within different life stages of zebrafish (Glisic et al. 2015; Glisic et al. 2016; Timme-Laragy et al. 2013). The correlation between the protein and mRNA expression level is, however, poor (Abreu et al. 2009; Vogel and Marcotte 2012). Yet, it is possible to analyze proteins within complex biological samples *via* mass spectrometry-based targeted proteomics (Picotti and Aebersold 2012). This technique uses multiple reaction monitoring (MRM), which allows sensitive and precise measurement of *a priori*-selected proteins (Bereman et al. 2012; Lange et al. 2008; Picotti and Aebersold 2012; Surinova et al. 2013).

Glutathione S-transferases have a size of approximately 25 kDa (200 to 230 residues in length). However, the amino acid sequence identity of enzymes belonging to the same class is relatively high, which limits the spectrum of suitable proteotypic peptides (peptides that have a sequence, which is unique to one isoenzyme). On the other hand, there are also peptide sequences shared between isoenzymes, but unique to one class. These can be used to quantify the sum of all isoenzymes of one specific enzyme class.

1.2.4 Glutathione conjugates are further biotransformed within the mercapturic acid pathway

The formation of glutathione conjugates is only the first step in the detoxification of electrophiles. Since the building blocks of glutathione are very valuable to the organism, they are sequentially clipped off and recycled after the first inactivation of the potentially toxic molecule. The formation of the glutathione conjugates and the subsequent series of biotransformation reactions along the mercapturic acid pathway are shown in Figure 3 (Armstrong et al. 2018; Cooper and Hanigan 2018).

After the initial conjugation of the electrophilic compounds with the sulfhydryl group of GSH by GSTs, the conjugate is actively transported to the cell surface by members of the ATP-binding cassette/multidrug resistance-associated protein transporter family (ABCC/MRP) (Ballatori et al. 2009; Ursic et al. 2009). In close proximity to the cell surface, integral membrane enzymes, specifically γ -glutamyl transferases and peptidases, remove the γ -glutamyl and glycyl group one by one from the glutathione moiety (Cooper and Hanigan 2018;

Pompella et al. 2006). This results in the formation of intermediate biotransformation products of the mercapturic acid pathway, i.e. the cysteinylglycine S-conjugate and cysteine S-conjugate. The latter re-enters the cell *via* transporters and is biotransformed by *N*-acetyl transferases to the mercapturic acid form of the chemical, the *N*-acetyl-L-cysteine S-conjugate (Cooper and Hanigan 2018; Dilda et al. 2008; Garnier et al. 2014; Hinchman et al. 1998). The *N*-acetyl-L-cysteine S-conjugate is generally non-reactive and highly hydrophilic. In this form, the conjugated chemical is excreted by the cells and eliminated from the body through the kidneys (Cooper and Hanigan 2018; Monks et al. 1990).

Although the mercapturic acid pathway is generally considered a detoxification route, it can facilitate the distribution of a xenobiotic within the body, if the conjugation reaction is reversible such as in case of isothiocyanates, isocyanates and α,β -unsaturated ketones (Monks et al. 1990; Vamvakas and Anders 1991). A deviation from the mercapturic acid pathway may also lead to the production of reactive transformation products. For instance, instead of being acetylated to the mercapturate, the cysteine S-conjugates of e.g. haloalkenes can be biotransformed through β -elimination to form reactive thiols by the enzyme β -lyase (Armstrong et al. 2018; Bakke and Gustafsson 1984; Monks et al. 1990; Vamvakas and Anders 1991). However, despite being harmful in general, those activation reactions can be exploited in cancer therapy to treat tumors with GST overexpression (Ramsay and Dilda 2014; Ruzza and Calderan 2013). Various candidate anticancer prodrugs have been designed which act as cytotoxic agents only after being biotransformed by GSTs or other enzymes of the mercapturic acid pathway (Ramsay and Dilda 2014; Ruzza and Calderan 2013).

To facilitate the selection of an appropriate model organism for toxicity studies and risk assessment, it is important to have knowledge about the functionality of the mercapturic acid pathway within the test system. A smooth biotransformation of an electrophile to the mercapturate strongly affects the compounds intracellular concentration and body clearance. Disruptions of the pathway, however, can increase the chance that branching pathways, such as the transformation of the cysteine conjugate by the enzyme β -lyase, metabolically activate intermediate biotransformation products, thus increasing their toxic potential.

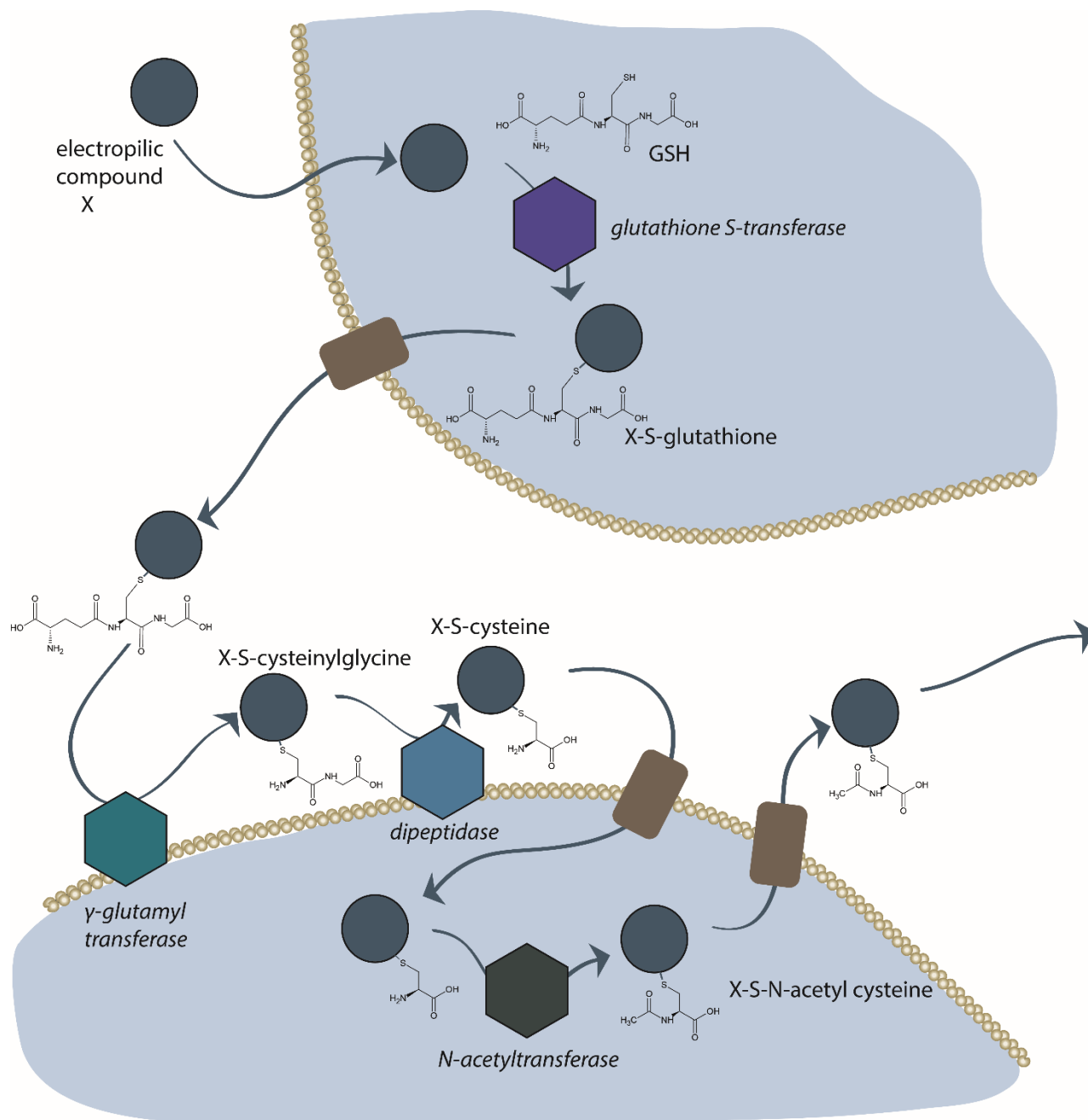


Figure 3: Schematic representation of the mercapturic acid pathway. After entering the cell, the electrophilic compound (X) is enzymatically conjugated to the glutathione conjugate (X-S-glutathione). After being transported to the cell surface, the conjugate is further biotransformed to the cysteinylglycine (X-S-cysteinylglycine) and cysteine (X-S-cysteine) conjugate, taken up by the cell, acetylated and finally excreted as mercapturic acid (X-S-N-acetyl cysteine). The electrophile is represented as a circle while the enzymes are shown as hexagons. Rounded rectangles represent different types of transporters. Intracellular space is depicted in grey while the intercellular space is shown in white.

1.2.5 Analysis of biotransformation products provides a complete picture of a pathway's functionality

For the study of the mercapturic acid pathway within a model system, mRNA and protein expression analyses of the enzymes involved can be useful, but do not necessarily reveal its functionality. To investigate if a model system is capable to convert the glutathione conjugate to the mercapturate and subsequently excrete the biotransformed substance, a targeted measurement of the biotransformation products of the mercapturic acid pathway is needed.

A known model substrate for GSTs is 1-chloro-2,4-dinitrobenzene (CDNB), which is often used to measure the activity of glutathione S-transferases. It has become a popular model substrate due to the fact that the parent compound as well as its biotransformation products can be distinguished spectrophotometrically. High-performance liquid chromatography (HPLC) coupled with ultraviolet (UV) detection is traditionally used for simultaneous CDNB and CDNB-metabolite analysis in various biological matrices (Hinchman et al. 1991; Simmons et al. 1991; Stoelting and Tjeerdema 2000; Trevisan et al. 2016; Vaidya and Gerk 2007). By using this method, the mercapturic acid pathway has been analyzed in different biological systems, such as rodents and mollusks (Hinchman et al. 1991; Simmons et al. 1991; Trevisan et al. 2016). However, HPLC-UV only allows the analysis of CDNB at relatively high concentrations (limit of quantification > 0.2 μ M for CDNB (Vaidya and Gerk 2007), which are already in the toxic range for most aquatic organisms. At toxic concentrations, however, enzymes might be adversely affected. Thus, it is important to use non-toxic concentrations to precisely analyze the metabolic capacity of organisms.

A very powerful technique for the analysis of biotransformation products in biological samples is high-resolution mass spectrometry (HRMS). It allows the measurement of a molecule's exact mass and with that, its differentiation from other biotransformation products and endogenous substances. HRMS can be exploited to analyze the biotransformation products of the mercapturic acid pathway upon exposure to non-toxic concentration of a xenobiotic compound.

1.3 Research objectives

Facing the persisting knowledge gaps regarding the biotransformation capacity of alternative approaches to conventional animal tests, I took an initiative towards characterizing one of the major biotransformation pathways, the mercapturic acid pathway, in zebrafish early life stages and the zebrafish embryo-derived PAC2 cell line.

The following chapters report on the succession of studies that contributed key pieces to the pathway characterization: starting from studying the expression of the pathway-initiating enzyme family, the GSTs, to the establishment of techniques for the detection of a model substrate and its biotransformation products, to the clarification of similarities and differences between zebrafish early life stages and PAC2 cells.

1.3.1 Scope of Chapter 2: Glutathione S-transferase protein expression in different life stages of zebrafish (*Danio rerio*)

The expression level and type of GSTs present in a model organism can define its sensitivity towards potentially toxic electrophilic compounds. Focusing on cytosolic glutathione S-transferases (GSTs), I established a targeted proteomic technique that enables the analysis of the complete repertoire of cytosolic GST classes present in zebrafish. This technique was used in Chapter 2 to perform the first proteomics study focused on biotransformation enzymes in zebrafish. Here, I show that GST family members are expressed during early zebrafish development and in organs of adult zebrafish, indicating that GSH conjugation is a functional detoxification pathway (Figure 4).

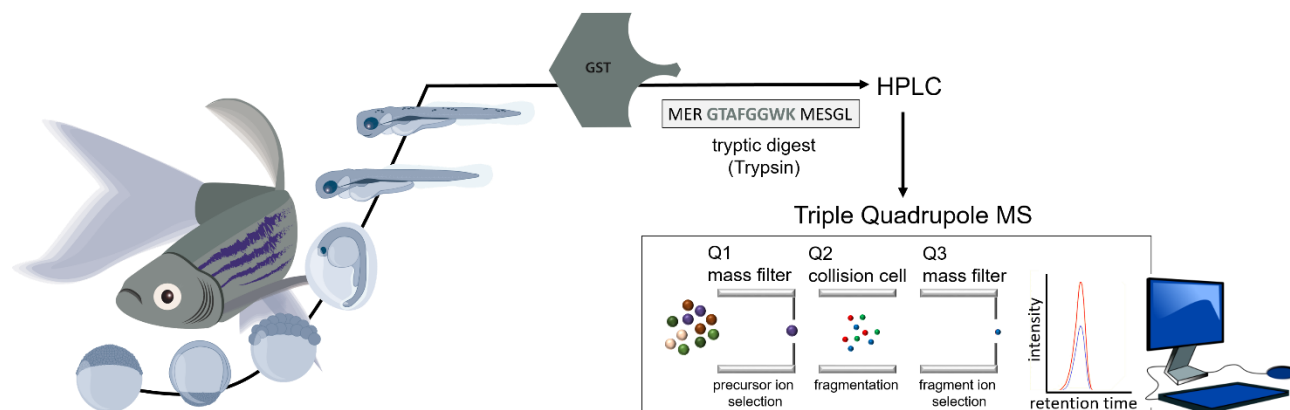


Figure 4: Schematic representation of the targeted proteomic technique used in Chapter 2 to analyze cytosolic glutathione S-transferase expression in the developing embryo and in different organs of adult zebrafish. HPLC - high-performance liquid chromatography, MS - mass spectrometry.

1.3.2 Scope of Chapter 3: LC-APCI(-)-MS determination of 1-chloro-2,4-dinitrobenzene, a model substrate for glutathione S-transferases

A sensitive technique for substrate quantification is of importance for enzyme activity assays because it allows a high degree of flexibility in experimental design. Facing the limitation of spectrophotometric techniques traditionally used for the analysis of CDNB, I exploited the possibilities of atmospheric pressure chemical ionization (APCI) and developed a sensitive liquid chromatography-mass spectrometry (LC-MS) technique. This technique is based on dissociative and non-dissociative electron capture ionization, using APCI in negative ion mode. It allows the analysis of CDNB down to 17 ng/ml, without the need of enrichment, which is an order of magnitude more sensitive than the traditional spectrophotometry. Using early life stages of the model organism zebrafish (*Danio rerio*) and the zebrafish cell line, PAC2, I showed that electron capture APCI(-) can be used to measure the whole concentration range applied in typical toxicity assays, including non-toxic concentrations (Figure 5).

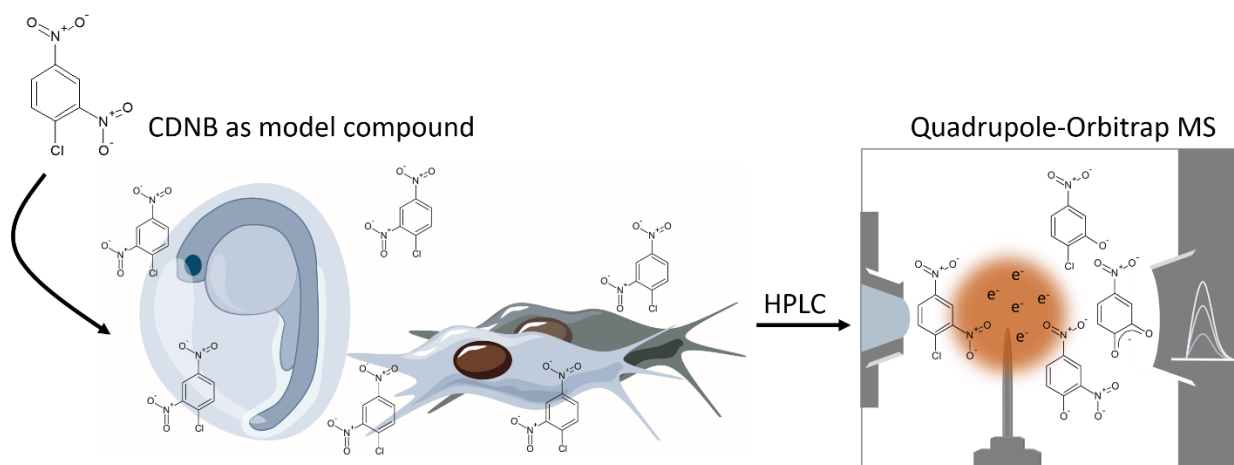


Figure 5: Schematic representation of the procedure used in Chapter 3 to analyze the model substrate 1-chloro-2,4-dinitrobenzene (CDNB) in exposure media via atmospheric pressure chemical ionization. HPLC - high-performance liquid chromatography, MS - mass spectrometry.

1.3.3 Scope of Chapter 4: Biotransformation capacity of zebrafish (*Danio rerio*) early life stages: Functionality of the mercapturic acid pathway

The mercapturic acid pathway is a key biotransformation pathway, which protects the organism from harmful electrophilic compounds. To be fully functional, the pathway requires a succession of enzymatic reactions performed by different enzyme families. Focusing on *in vivo* biotransformation of the model compound 1-chloro-2,4-dinitrobenzene (CDNB), I developed an LC-MS method to simultaneously analyze the biotransformation products of the mercapturic acid pathway. In Chapter 4, I present the first study demonstrating the completeness and functionality of the mercapturic acid pathway in zebrafish early life stages. Additionally, I show that non-toxic concentrations of CDNB do not affect the expression of GSTs, analyzed by using the targeted proteomics method described in Chapter 2 (Figure 6).

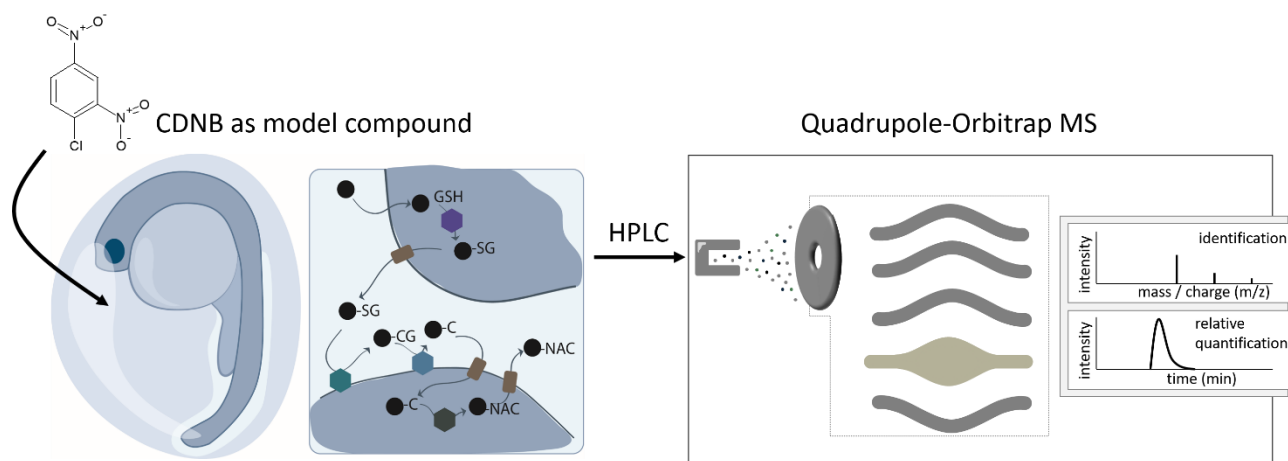


Figure 6: Schematic representation of the procedure used in Chapter 4 to analyze biotransformation products of the model substrate 1-chloro-2,4-dinitrobenzene (CDNB) via high-resolution mass spectrometry during zebrafish early life stage development. GSH - glutathione, ●-SG - glutathione conjugate, ●-CG - cysteinylglycine conjugate, ●-C - cysteine conjugate and ●-NAC - mercapturic acid. HPLC - high-performance liquid chromatography, MS - mass spectrometry.

1.3.4 Scope of the Chapter 5: Expression of cytosolic glutathione S-transferases and performance of the mercapturic acid pathway in the zebrafish embryo cell line, PAC2

In complex organisms, the mercapturic acid pathway is considered a multiorgan-process that requires an efficient transfer of the biotransformation products from one enzyme to another. In Chapter 5, I show for the first time that the fibroblast cell line, PAC2, isolated from zebrafish embryos (age 24 hpf), has the potential to perform biotransformation of electrophilic substances within the mercapturic acid pathway. However, although all important players of the pathway are present in the cell line, the transfer of the biotransformation products from one enzyme to another appears less efficient than in zebrafish early life stages. This difference is likely to be caused by the cell culture setup and the dilution of the intermediate biotransformation products in the culture medium. Additionally, I showed that within PAC2 cells, similar to zebrafish embryos, non-toxic concentrations of CDNB do not affect the expression of GSTs. To investigate the biotransformation potential of the PAC2 cell line, I successfully applied the three techniques developed in previous chapters (Figure 7).

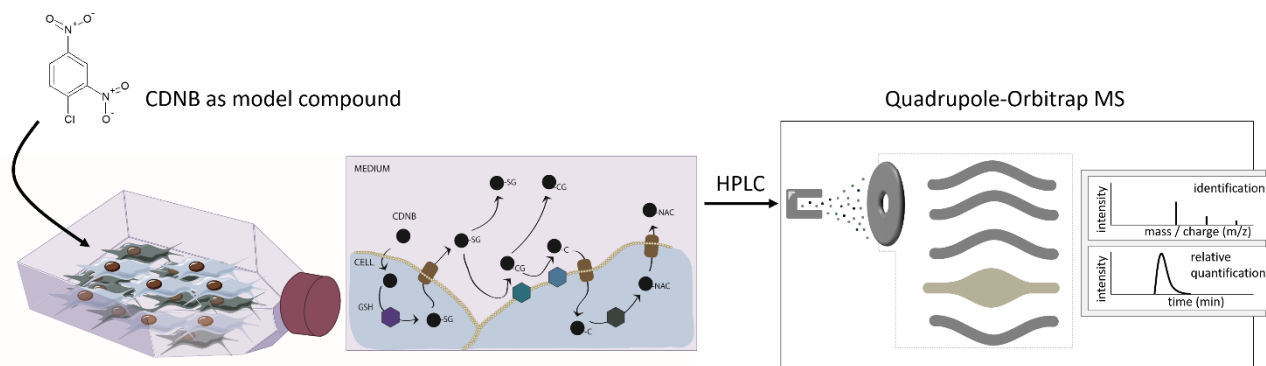


Figure 7: Schematic representation of the procedure used in Chapter 5 to analyze biotransformation products of the model substrate 1-chloro-2,4-dinitrobenzene (CDNB) via high-resolution mass spectrometry in the PAC2 cell line. GSH - glutathione, ●-SG - glutathione conjugate, ●-CG - cysteinylglycine conjugate, ●-C - cysteine conjugate and ●-NAC - mercapturic acid. HPLC - high-performance liquid chromatography, MS - mass spectrometry.

Chapter 2 Glutathione S-transferase protein expression in different life stages of zebrafish (*Danio rerio*)

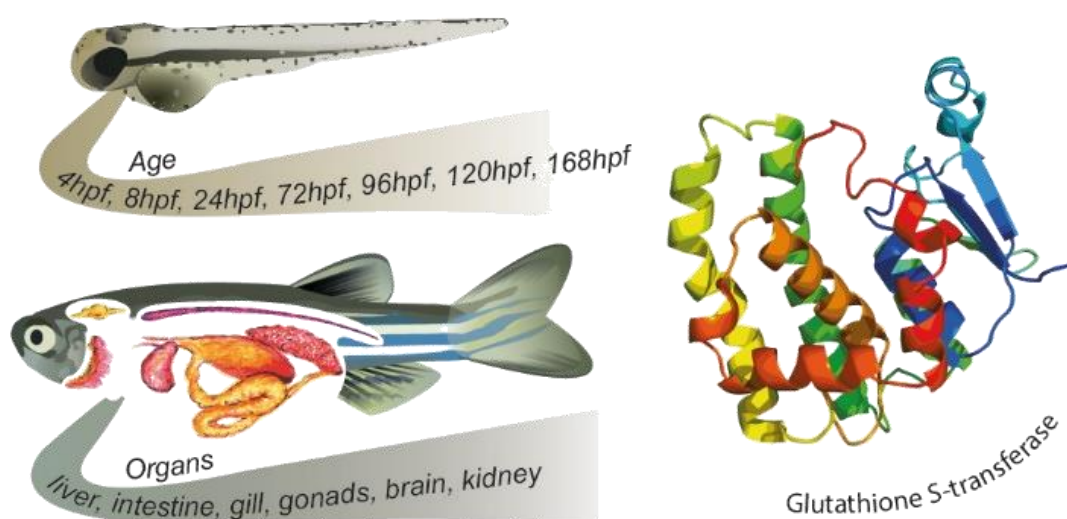
Alena Tierbach, Ksenia J Groh, René Schönenberger, Kristin Schirmer, Marc J-F Suter

Published in *Toxicological Sciences*

<https://doi.org/10.1093/toxsci/kfx293>

Publishing date: 19 January 2018

Note: Editors' Choice



Contributions

I was supported within this project in the following ways:

- Technical assistance in mass spectrometric analysis: René Schönenberger
- Experimental design and discussions: Ksenia J Groh, Kristin Schirmer, Marc J-F Suter
- Reviewing & editing: Ksenia J Groh, Kristin Schirmer, Marc J-F Suter

2.1 Abstract

Zebrafish is a widely used animal model in biomedical sciences and toxicology. Although evidence for the presence of phase I and phase II xenobiotic defense mechanisms in zebrafish exists on the transcriptional and enzyme activity level, little is known about the protein expression of xenobiotic metabolizing enzymes. Given the important role of glutathione S-transferases (GSTs) in phase II biotransformation, we analyzed cytosolic GST proteins in zebrafish early life stages and different organs of adult male and female fish, using a targeted proteomics approach. The established multiple reaction monitoring-based assays enable the measurement of the relative abundance of specific GST isoenzymes and GST classes in zebrafish through a combination of proteotypic peptides and peptides shared within the same class.

GSTs of the classes alpha, mu, pi and rho are expressed in zebrafish embryo as early as 4 hours post fertilization (hpf). The majority of GST enzymes are present at 72 hpf followed by a continuous increase in expression thereafter. In adult zebrafish, GST expression is organ-dependent, with most of the GST classes showing the highest expression in the liver. The expression of a wide range of cytosolic GST isoenzymes and classes in zebrafish early life stages and adulthood supports the use of zebrafish as a model organism in chemical-related investigations.

2.2 Introduction

Assessing the risk posed by chemicals to human and environmental health requires appropriate models to investigate the chemicals' biological activity and toxicity. Especially vertebrate models, which are suitable for mechanistic investigations and medium- to high-throughput approaches, are needed in order to comply with the requirements imposed by 21st century toxicology (Krewski et al. 2010). Zebrafish (*Danio rerio*) is such a model. It shares a high degree of homology with other vertebrates, including humans, and zebrafish early life stages attract attention owing to their small size and transparency (Dahm and Geisler 2006). Yet, despite its popularity and increasing use in biomedical research as well as human and environmental toxicology, knowledge gaps still exist concerning the capacity of zebrafish to biotransform and detoxify chemicals, particularly at early life stages.

The biotransformation potential of zebrafish has been the focus of previous studies, which provided transcriptional evidence for enzymes involved in phase I and phase II metabolism, including cytochrome P450 (Cyp450), uridine 5'-diphospho-glucuronosyltransferase (UGT) and glutathione S-transferases (GSTs), already in early stages of the development (Christen and Fent 2014; Glisic et al. 2016; Goldstone et al. 2010; Timme-Laragy et al. 2013). Additionally, Otte et al. (2017) mapped intrinsic activities of representative enzymes involved in xenobiotic metabolism. The study demonstrated that selected phase I and phase II enzymes, such as Cyp450 and GSTs, are already active in early developmental stages.

GSTs are an enzyme family that plays a major role in phase II biotransformation processes by catalyzing the conjugation reaction of the tripeptide glutathione (GSH) with electrophilic substrates (Sheehan et al. 2001). This reaction typically results in the formation of more hydrophilic and readily excretable products. Accordingly, GST activity is considered a critical contributor to detoxification and clearance of various intracellular metabolites, but also natural toxins and xenobiotic compounds, including drugs, and their reactive intermediates (Hayes et al. 2005; Sau et al. 2010).

The GST family consists of three major groups: membrane-associated, mitochondrial and cytosolic proteins (Glisic et al. 2015; Hayes et al. 2005). Membrane-associated GSTs belong to the microsomal GST (MGST) or Membrane-Associated Proteins in Eicosanoid and Glutathione metabolism class (MAPEG), and are involved in the biosynthesis of leukotrienes and prostanoids (Glisic et al. 2015; Jakobsson et al. 1999). Mitochondrial GSTs form the kappa-class (Thomson et al. 2004). Cytosolic GSTs are subdivided into several classes based

on enzyme sequence similarities (Glisic et al. 2015; Hayes et al. 2005; Sheehan et al. 2001). These classes are alpha, zeta, theta, mu, pi and omega. In mammalian species, a further cytosolic class, sigma, is present, whereas the cytosolic class rho is specific to teleosts and cephalo-chordates (Glisic et al. 2015). The diversification of cytosolic GSTs into multiple classes provides a broad substrate specificity for the inactivation of potentially harmful endogenous and exogenous compounds, including xenobiotics (Glisic et al. 2015). Increasing our knowledge about cytosolic GSTs therefore will help to better understand the xenobiotic defense mechanisms and their contribution to sensitivity differences among species or life stages.

To date, zebrafish GST studies have focused on two levels: GST enzymatic activity (Best et al. 2002; Notch et al. 2011; Otte et al. 2017; Pavagadhi et al. 2012; Wiegand et al. 2000) and mRNA expression (Abunnaja et al. 2017; Glisic et al. 2015; Glisic et al. 2016; Timme-Laragy et al. 2013). GST enzymatic activity was detected within the first four hours of zebrafish development (Notch et al. 2011; Otte et al. 2017; Wiegand et al. 2000) as well as in all examined organs of adult zebrafish (Pavagadhi et al. 2012). Members of all cytosolic GST classes were detectable on the mRNA level during zebrafish development (Glisic et al. 2016; Timme-Laragy et al. 2013). In adult zebrafish, GST mRNA expression levels were found to be tissue- and sex-dependent (Glisic et al. 2015).

Although enzyme activity and mRNA abundance studies give a valuable overview of the GST family in zebrafish, they have certain limits. Non-specific substrates used for activity measurements, such as 1-chloro-2,4-dinitrobenzene (CDNB), do not allow to differentiate between GST isoenzymes (Glisic et al. 2015; Habig et al. 1974). While the detection of selected isoenzymes is possible via mRNA analysis, the correlation with the protein data is usually poor (Li et al. 2014; Schwanhaussner et al. 2011). Proteins are the biomolecules carrying out biotransformation reactions, yet studies mapping GST expression on the protein level are missing in zebrafish. It is, however, possible to analyze enzymes on the protein level within complex biological samples using mass spectrometry-based targeted proteomics (Picotti and Aebersold 2012). With the multiple reaction monitoring (MRM) technique (Figure 8), multiple pairs of peptide precursor and fragment ions can be monitored over a chromatographic run, allowing the analysis of several proteins within one measurement (Bereman et al. 2012; Lange et al. 2008; Picotti and Aebersold 2012; Surinova et al. 2013).

We performed MRM-based targeted analyses to investigate how cytosolic GST proteins evolve in zebrafish during early life stages and how they are expressed in organs of adult male and female fish. This involved the

development of MRM assays for a panel of proteotypic peptides and peptides shared within the same class, enabling the analysis of the relative abundance of specific GST isoenzymes and GST classes in zebrafish.

2.3 Materials and methods

2.3.1 Zebrafish maintenance and sampling

Wild-type zebrafish with mixed genetic background from WiK (Max Planck Institute for Developmental Biology, Tübingen, Germany), OBI (Helmholtz Centre for Environmental Research established from OBI Baumarkt, Leipzig, Germany) and Qualipet (pet shop, Switzerland) strains were maintained and bred in our facility according to recommended procedures (Nüsslein-Volhard 2002). Fish were reared in a flow-through system filled with a 1:2 mixture of reconstituted water (294.0 mg/l $\text{CaCl}_2 \cdot 2\text{H}_2\text{O}$, 123.2 mg/l $\text{MgSO}_4 \cdot 7\text{H}_2\text{O}$, 64.7 mg/l NaHCO_3 and 5.7 mg/l KCl; ISO 15088:2007(E); 2007) and tap water. Water temperature ranged from 26 to 28 °C; light/dark cycle was 14/10 h. Zebrafish were fed with live food (*Artemia nauplia*) and dry vitamin flakes (TetraMin, USA) twice daily. Zebrafish eggs were obtained from group crosses. Eggs were collected 1 h after the light in the facility was switched on, washed with reconstituted water and raised in Petri dishes in an incubator at 28 °C, 14/10 h light/dark cycle. Zebrafish samples were collected at 4, 8, 24, 48, 72, 96, 120 and 168 hours post fertilization (hpf) in order to cover a range of life stages, starting from early embryo and continuing until the end of the transition phase from non-feeding to larvae capable of independent feeding. Zebrafish embryos and larvae were washed in ice-cold phosphate-buffered saline and snap frozen in liquid nitrogen (60 embryos/sample) in Eppendorf LoBind microcentrifuge tubes (Sigma-Aldrich, United States). The embryos collected at 24 and 48 hpf were dechorionated with forceps prior to sampling, in order to remove chorion proteins. The organs (liver, intestine, gills, brain, gonads and kidney) were obtained from adult animals aged ~1.5 years. For organ collection, adult fish were euthanized with tricaine methanesulfonate (MS222) and dissected. Organs from four fish of the same sex were pooled for one replicate. The organs were snap frozen in liquid nitrogen in Eppendorf LoBind microcentrifuge tubes (Sigma-Aldrich, United States). Samples were stored at -80 °C until further processing. All procedures were in accordance with the animal protection guidelines and approved by the Cantonal Veterinary Office Zurich, Switzerland.

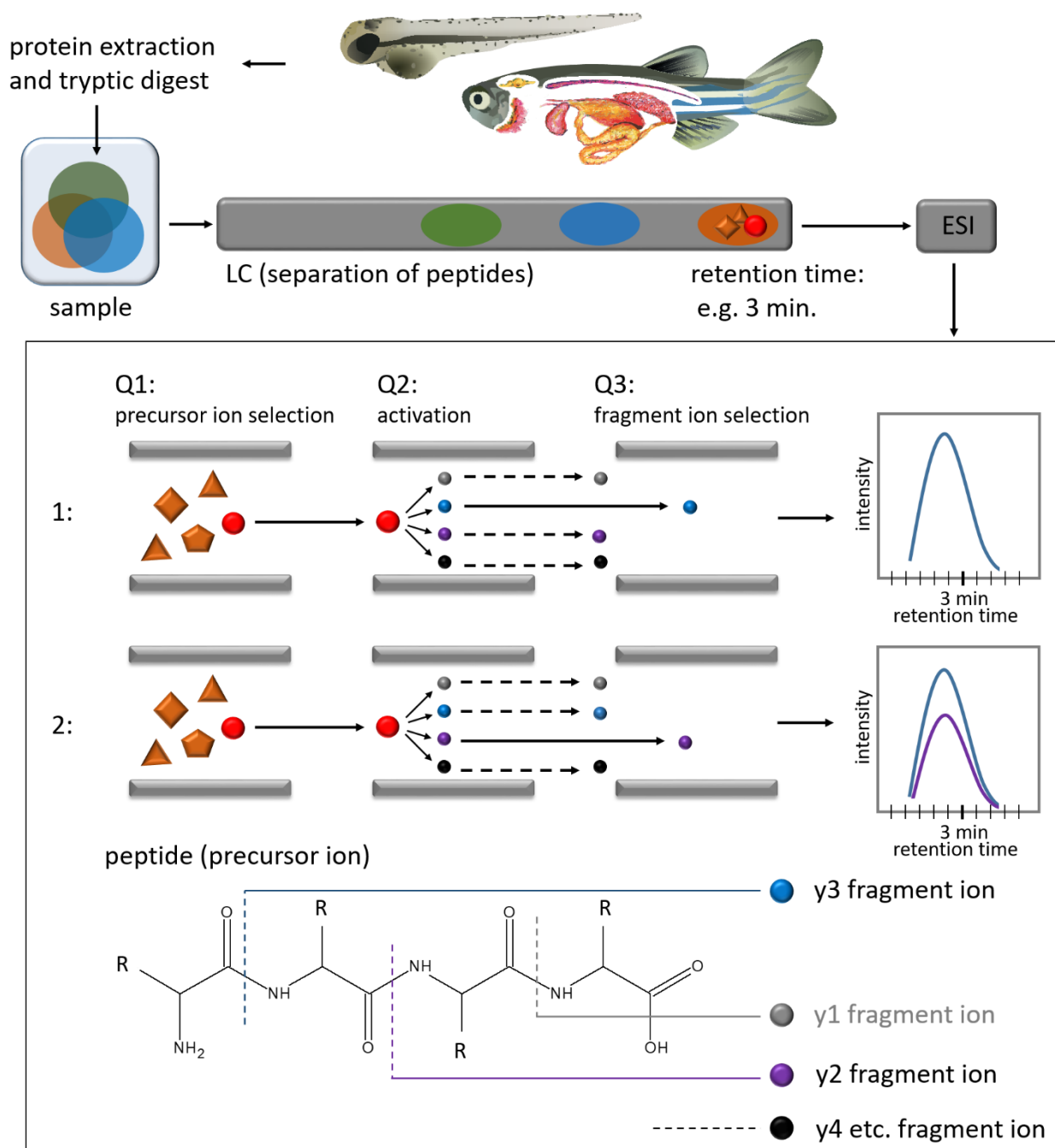


Figure 8: Overview of the experimental workflow and schematic representation of the MRM technique. The proteins are extracted from tissue, tryptically digested into peptides, separated with liquid chromatography (LC), ionized via electrospray ionization (ESI) and transferred into the triple-quadrupole mass spectrometer (Q1–Q3). In Q1—the precursor ion (peptide) is selected, in Q2 the peptide is fragmented into fragment ions (y1, y2, y3, etc.), in Q3 the selection of the fragment ion takes place. Subsequently, the intensity of the fragment ion is measured over time. Within one measurement, several transitions (peptide and fragment ion) can be monitored.

2.3.2 Protein extraction and preparation of tryptic digests

Protein extraction and trypsin digestion were performed as reported previously (Groh et al. 2013) with some modifications. Briefly, samples were taken up in 600 µl ice-cold lysis buffer immediately upon thawing (9 M urea, 2 M thiourea, 0.1 M Tris-HCl, 4% CHAPS, 100 mM DTT, 1× Protease Inhibitor Cocktail, pH 8.5) and homogenized with the soft tissue homogenizing kit (Bertin Instruments, France) using a FastPrep-24 Homogenizer (MP Biomedicals, United States). The sample lysate was centrifuged at 14'000×g for 15 min at 4 °C and the supernatant was aliquoted in 150 µl amounts into fresh Eppendorf LoBind microcentrifuge tubes (Sigma-Aldrich, United States). Proteins were precipitated from the supernatant using the methanol/chloroform method. The protein pellet was isolated, air-dried for 4 min, wetted with 5 µl NaOH (0.2 M) and re-dissolved in 25 µl re-solubilization buffer (9 M urea, 2 M thiourea, 50 mM Tris HCl, pH 8). Aliquots of the same sample were re-combined and protein concentration determined by the Bradford method. Subsequently, proteins within each sample were diluted with re-solubilization buffer to a final protein concentration of 2.5 µg/µl. Samples were reduced with tris(2-carboxyethyl)phosphine (5 mM final concentration) for 30 min in the dark at room temperature, alkylated (carbamidomethylated) with iodacetamide (25 mM final concentration) for 30 min in the dark at room temperature and digested with trypsin (trypsin:protein ratio of 1:100, trypsin sequencing grade, Roche, Switzerland) at 37 °C for 16 h. Prior to the trypsin digestion, adult organ samples were spiked with the standards apomyoglobin from equine skeletal muscle and the MS Qual/Quant QC Mix (Sigma-Aldrich, United States). The digestion was terminated through addition of formic acid (1% final concentration). The samples were desalted using reversed-phase cartridges (Sep-Pak Vac tC18, Waters, United States), eluted in 800 µl 80% acetonitrile solution with 0.1% (v/v) formic acid, evaporated using a vacuum centrifuge at 30 °C, re-dissolved in 100 µl nanopure water with 0.1% formic acid and filtered through Amicon Ultrafree centrifugal filters, 0.45 µm cut-off (Millipore, United States). The samples were then stored at 4 °C or immediately measured on the TSQ Vantage (Thermo Scientific, United States).

2.3.3 Selection of peptides and MRM method development

Protein reference sequences for the cytosolic GSTs were retrieved from NCBI (SI Table 1), imported into Skyline (MacLean et al. 2010) as FASTA files and *in silico* digested with trypsin. Only fully tryptic peptides in a range of 6-21 amino acids were selected for further processing. Proteotypic peptides (peptides that uniquely identify the protein of interest) and peptides that cover conserved domains (characteristic for two or more isoenzymes of the same class, see Figure 9) were selected by running a protein-protein BLAST search against

the non-redundant protein sequences from *Danio rerio* (taxid:7955). As suggested previously (Lange et al. 2008), peptides containing the RP/KP motive, two neighboring amino acids (K and/or R) at either cleavage site, and amino acids that are prone to chemical modifications (e.g. alkylation, deamination and oxidation) were avoided whenever possible. In total, 86 peptides representing isoenzymes of the cytosolic GSTs were chosen and commercially synthesized as small scale, unpurified peptides with carbamidomethyl-modified cysteine and C-terminal lysine or arginine (SpikeTides, JPT Innovative Peptide Technologies, Germany, see SI Table 2). Their sequence and position within the protein are shown in SI Table 3 and 4 and the chromatograms can be downloaded from the Dryad Digital Repository. The synthetic peptides (~ 54 nmol) were re-suspended in 150 µl aqueous solution containing 20% acetonitrile and 1% formic acid under gentle agitation (30 min, room temperature), aliquoted in volumes of 35 µl and kept at -80 °C for long term storage. For measurements, a pool of all synthetic peptides was generated (10 µl each), evaporated under vacuum at 30 °C, re-dissolved in nanopure water with 0.1% formic acid and stored at 4 °C until use.

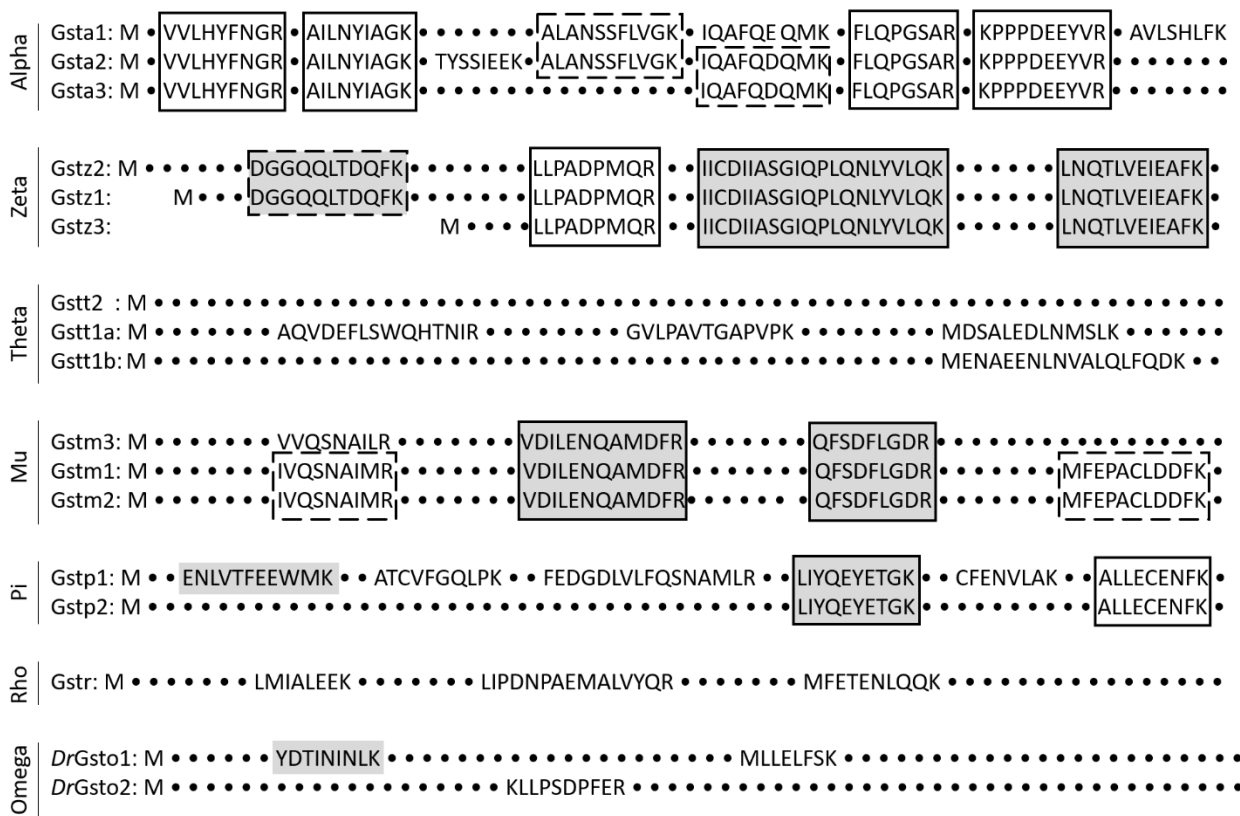


Figure 9: Schematic amino acid sequence alignment of GST classes for the visualization of proteotypic peptides (no frame), shared peptides that cover a sequence present in some isoenzymes (dashed frame) and shared peptides that cover a sequence present in all isoenzymes of the respective enzyme class (solid frame). Peptides which were detected only in organs of adult zebrafish are shown with a gray background. All others were also found at certain stages of zebrafish early development.

The MRM methods were developed with Skyline. The charge state of the precursor ions was set to +2 for peptides < 15 amino acids and +2 and +3 for peptides > 15 amino acids. Only singly charged fragment ions with $m/z > \text{precursor}$ were considered. The collision energy for each peptide was calculated for the Thermo TSQ Vantage using Skyline. Cysteine was set to be carbamidomethyl-modified and peptides containing methionine were synthesized and monitored in the oxidized and reduced form.

The synthetic standard mixture in nanopure water with 0.1% formic acid was run on a TSQ Vantage to validate the MRM methods and to obtain peptide retention time (RT) information. The data was processed using Skyline. The two to three strongest MRM transitions of detected synthetic peptides were then selected for the analysis of the endogenous peptides.

2.3.4 LC and MS settings

Samples were injected onto a Poroshell 120 EC - C18 (2.7 μm particle size, 2.1x100 mm column - Agilent) and separated at a flow rate of 150 $\mu\text{l}/\text{min}$ using a 38 min linear gradient from 100% solvent A (1% methanol in water, 0.2% formic acid) to 100% solvent B (98.8% methanol, 0.2% formic acid), followed by a washing step (4 min with 100% solvent B) and a re-equilibration step (8 min with 100% solvent A). The measurements were performed on a TSQ Vantage operating in MRM mode with a scan width of 0.3 m/z and a dwell time of 30 ms. In order to measure all desired transitions with an optimal cycle time, the number of peptides monitored simultaneously was limited to a maximum of 60 per segment. With this, the resulting cycle time was < 1.7 s in all segments. The de-clustering potential was set to zero, the collision cell entrance and exit potential to 10 and 12, respectively. Figure 8 shows the overview of experimental workflow and schematic representation of the MRM technique.

2.3.5 Data analysis

The profiles from endogenous peptides were digitally transformed (Savitzky-Golay smoothing) and evaluated based on the following criteria: retention time deviation from the synthetic standard should be ≤ 1 min, overlapping peak profiles of the transitions, intensity ratio of the monitored transitions and the peak shape comparable to the corresponding synthetic standard, signal intensity > 1000 arbitrary units (au) and the signal-to-noise ratio (S/N) > 10. The most sensitive criteria were the overlapping peak profiles and corresponding intensity ratio. All peptides passing these criteria were selected for further analysis. Their sequence and location

within the protein sequence is provided in SI Table 3 and 4, respectively. The chromatograms can be downloaded from the Dryad Digital Repository.

To account for variations in the efficiency of sample digestion and peptide recovery after desalting, as well as for variations between injections, the signal intensities of the target peptides were normalized. For the samples from early life stages (embryos and larvae), an intense and stably expressed housekeeping protein, glyceraldehyde 3-phosphate dehydrogenase (GAPDH), was used for normalization. However, within the organs of adult male and female fish, the expression levels of all tested housekeeping proteins (GAPDH, beta-actin and 40S ribosomal protein S18) were organ dependent and therefore could not be used for normalization across different tissues. For this reason, the signal intensities of the target peptides within the adult organs were normalized to a standard protein, apomyoglobin from equine skeletal muscle (Sigma-Aldrich, United States), spiked before digestion. Normalized peak areas of peptides detected in zebrafish embryo and organs of adult zebrafish are summarized in SI Table 5 and SI Table 6, respectively.

2.3.6 Supplementary information Chapter 2

Protein reference sequences of the cytosolic GSTs (SI Table 1), summary of synthetic peptides (SI Table 2) and peptides detected in zebrafish early life stages and organs of adult fish (SI Table 3) are provided in the Supplemental Information (Chapter 2). In addition, Supplemental Information provides multiple sequence alignments of GST isoenzymes belonging to the same class (SI Table 4), normalized peak areas for the peptides detected during zebrafish development (SI Table 5) and in organs of adult fish (SI Table 6). To facilitate the usage of the targeted proteomics technique for GST analysis in different laboratories, indexed retention time (iRT) values for all the all used peptides are provided in SI Table 7.

2.4 Results

We established methods for a set of peptides in order to analyze GST classes and GST isoenzymes in zebrafish. Out of 86 peptides preselected according to the criteria described in “Materials and methods”, 34 peptides could be detected in zebrafish samples, covering all classes of cytosolic GSTs. Eight of those peptides were detected only in tissues of adult zebrafish and with low intensity (SI Table 2). The observed peptides were of two types: proteotypic and shared peptides. Proteotypic peptides cover non-conserved protein regions and allow the differentiation of isoenzymes with high sequence homology. In this way, we were able to unequivocally identify GST isoenzymes belonging to the GST classes alpha (Gsta1, Gsta2), theta (Gstt1a, Gstt1b), mu (Gstm3), pi (Gstp1), rho (Gstr), and omega (Gsto1 and Gsto2) (Figure 9, SI Table 2). The shared peptides cover conserved sequences of two or three isoenzymes and enable the monitoring of GST class-specific protein expression. We were able to detect shared peptides for the GST classes alpha, zeta, mu and pi (Figure 9, SI Table 2). GST isoenzymes that share the peptide sequence are indicated through the isoenzyme number separated by comma (e.g. peptide shared between isoenzymes Gsta1 and Gsta2 would be indicated as Gsta1,2).

2.4.1 GST classes and isoenzymes show distinct expression patterns throughout zebrafish development

By comparing the time-resolved abundance of cytosolic GSTs, we identified three distinct expression patterns: (i) early detection followed by continuous increase throughout the development (Figure 10, A), (ii) first occurrence after 72 hpf, followed by a continuous increase (Figure 10, B) and (iii) variable trend with no consistent change (Figure 10, C). The expression pattern of shared peptides generally was similar to the expression of one dominating isoenzyme. For instance, the expression patterns of the shared peptides Gsta1,2,3 and Gsta1,2 were similar to those exhibited by Gsta1 whereas Gsta2,3 showed a pattern comparable to Gsta2 (Figure 10).

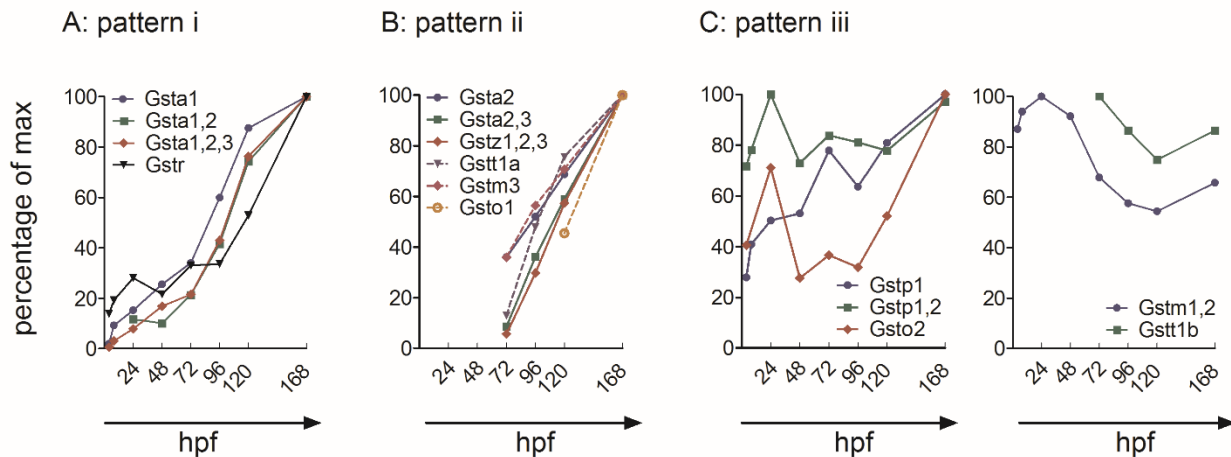


Figure 10: GST expression patterns observed during zebrafish early development. A, Early detection followed by continuous increase throughout the development (pattern i). B, First occurrence after 72 hpf, followed by an increase (pattern ii), and (C), variable trend with no consistent change (pattern iii). Median of the normalized peak area is shown as percentage of the maximal value.

Members of the class alpha and Gstr followed the expression pattern (i) (Figure 11A). Gsta1, Gsta1,2,3 and Gstr were detected as early as 4 hpf and their expression level increased throughout the development. In case of Gsta1, Gsta1,2 and Gsta1,2,3 we observed a strong increase in the expression already after 24 hpf, whereas the difference between 120 and 168 hpf was less distinct. For Gstr, the expression increased slowly but continuously until 96 hpf, and only after 96 hpf a sharp increase in the expression level was observed. The majority of GSTs (Gsta2, Gsta2,3, Gsta1,2,3, Gsta1a, Gstm3 and Gsto1) could be assigned to the expression pattern (ii) (Figure 11B). Those enzymes were first detected after hatching (72 hpf) and their expression subsequently increased. In some cases, the GST expression showed no consistent or strong change with age (Figure 11C). Gstp1 and Gstp1,2 were detected already at 4 hpf in all replicates. Whereas Gstp1 expression increased slightly over time, Gstp1,2 showed a steady expression throughout the development. Gsto2 was detected at 4, 24 and 48 hpf in one replicate each; at 72 and 96 hpf the expression level stayed constant and increased only after 120 hpf.

The expression level of Gstm1,2 appeared to be highly dynamic. It was detected at 4 hpf, decreased at 72 hpf and stayed at a constant level thereafter. However, this dynamic trend could only be observed for one peptide that covered a conserved sequence of Gstm1 and 2. The second shared peptide was observed only after hatching (72 hpf) and expression continuously increased until 168 hpf (Figure 11C, SI Table 5). Gstm1b was first observed after hatching and was expressed at a constant level until 168 hpf.

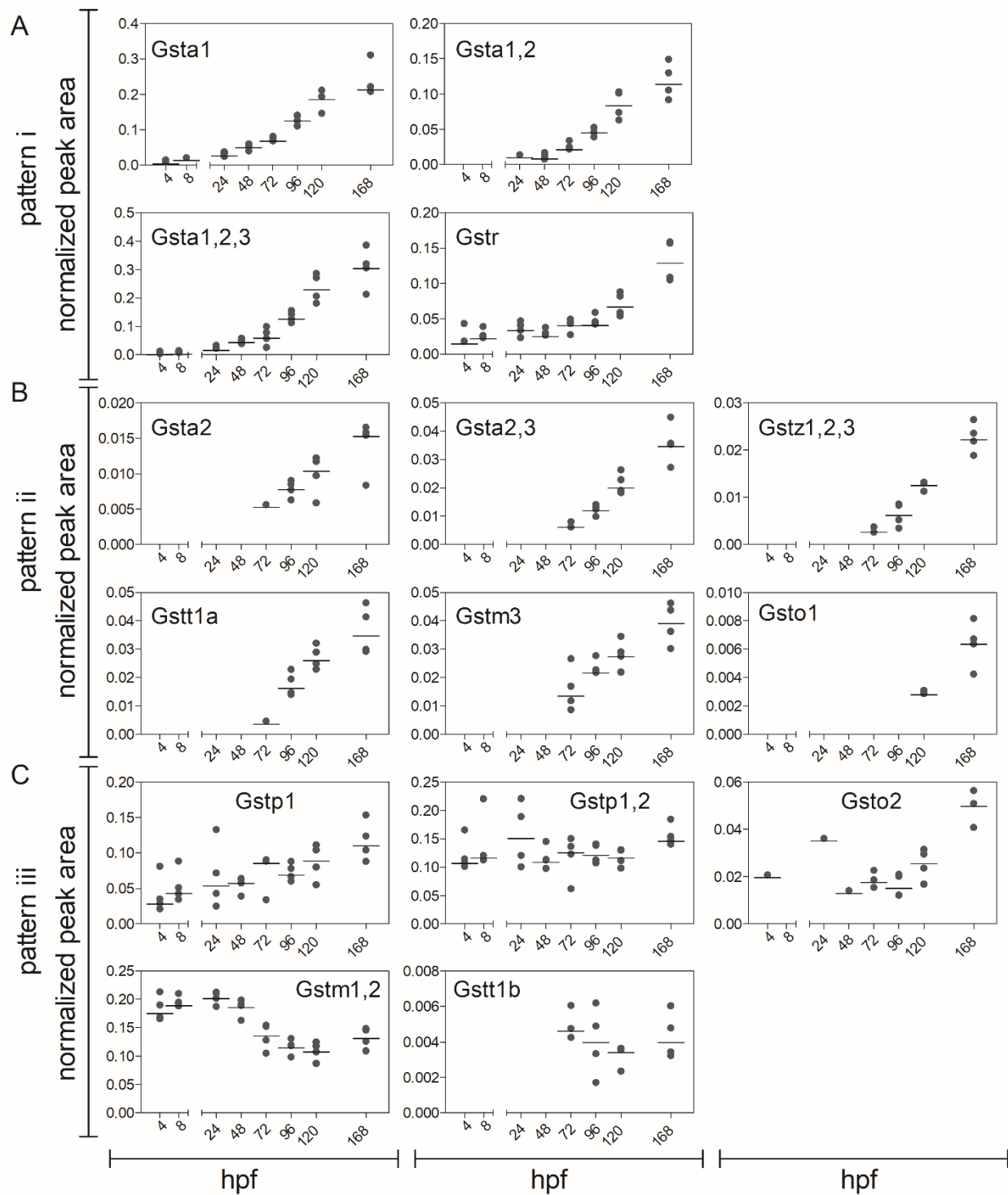


Figure 11: GST expression in zebrafish embryos and larvae. The graphs are sorted in accordance to the expression patterns described in Figure 10. Data are shown as peak area normalized to the housekeeping protein GAPDH at 4, 8, 24, 48, 72, 96, 120, and 168 hpf. Each replicate (a sample of 60 pooled embryos) is shown in addition to the median (black line). For visualization, the normalized peak area of peptides belonging to the same enzyme (in case of proteotypic peptides) or several isoenzymes from the same class (in case of shared peptides) were cumulated. The number and characteristics of the cumulated peptides are summarized in SI Table 2 and 5.

Altogether, representatives of four classes (alpha, mu, pi and rho) could be detected as early as 4 hpf in more than one replicate. Representatives of the remaining classes (zeta, theta and omega) were expressed after hatching (72 hpf). In general, the expression level of most GST classes increased throughout the zebrafish development.

2.4.2 GST classes and isoenzymes show distinct expression patterns in organs of adult zebrafish

The majority of cytosolic GSTs were expressed in all examined organs of both male and female adult zebrafish (liver, intestine, gill, gonads, brain and kidney). However, Gstm1a was not observed in the brain, and Gstm1,2 was not detected in the intestine (Figure 12). Differences in the class- and isoenzyme-specific expression level among organs of adult zebrafish were distinguishable despite the partly high variability of GST expression in replicates. All representatives of the alpha-class (except Gsta2), as well as Gstm1a, Gstm1,2, Gstm1,2,3 and Gstm1, were predominantly expressed in the liver. The members of the pi-class showed a higher expression in liver and gill compared to other organs. The highest expression of Gstm3, Gstm1,2,3 and Gstm2 was observed in the gills, whereby the expression of Gstm2 was also elevated in the intestine. Gstm1 was predominantly expressed in the intestine. In contrast, the expression of Gstm1,2 in the intestine was below the median of other organs (Figure 12). The signal intensity of Gsta2 and Gstm1b (SI Table 6) was low, and in some organs the proteins could be observed in only one replicate. Therefore, it was not possible to estimate the organ specific expression of these enzymes. We did not observe strong sex-dependent differences in the GST expression within most organs. Only female gonads showed a generally low expression of all measured GSTs, with the exception of Gstm1,2. The isoenzyme Gstm1 and the shared peptide Gstm1,2 were even below the limit of detection in female gonads.

Data available from the Dryad Digital Repository: <https://doi.org/10.5061/dryad.5s32v>

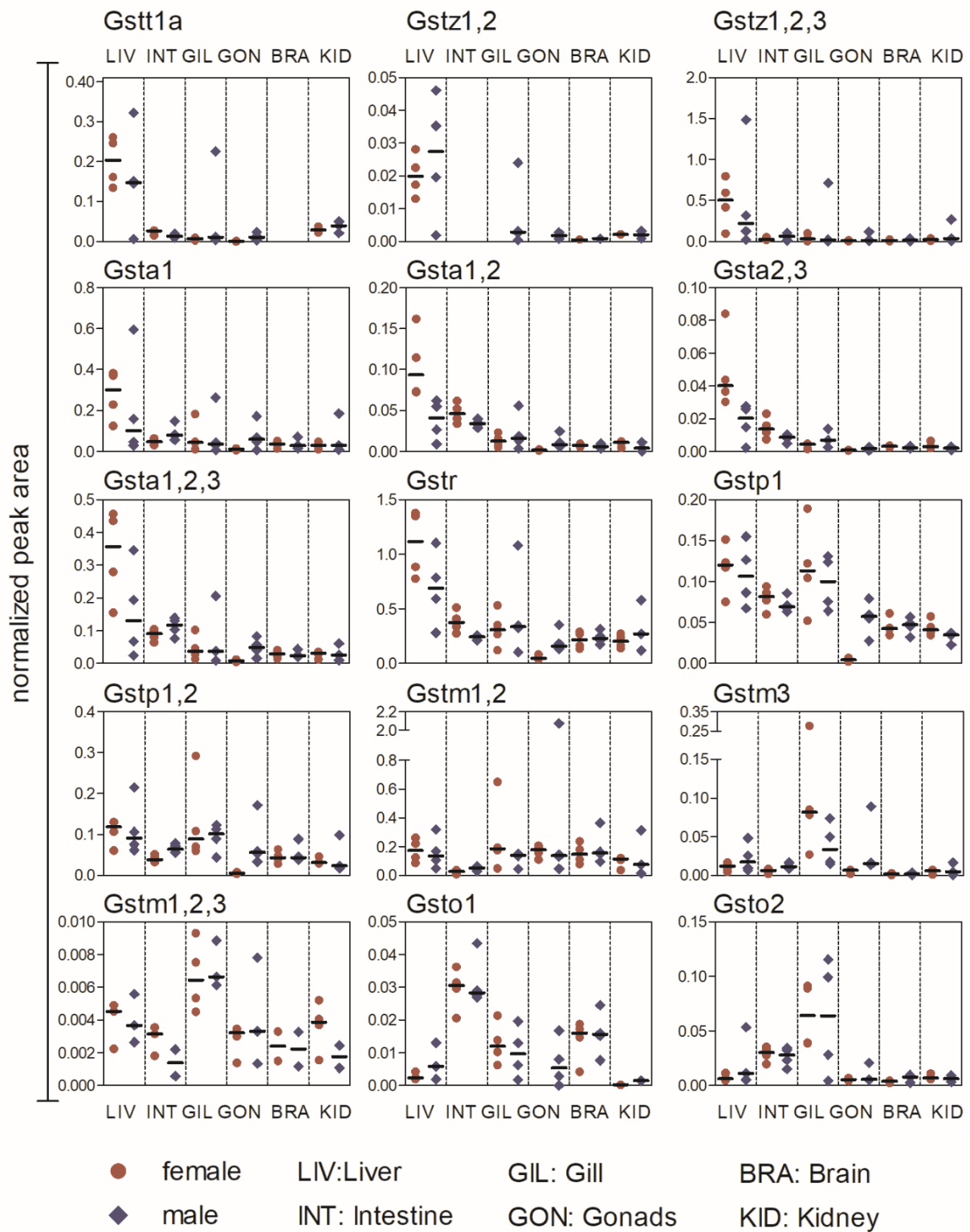


Figure 12: GST expression in different organs (liver, intestine, gill, gonads, brain, and kidney) of adult female and male zebrafish. Data are shown as peak area normalized to the spiked synthetic standard apomyoglobin. Each replicate (a sample of organs pooled from 4 fish) is shown in addition to the median (black line). For visualization, the normalized peak area of peptides belonging to the same enzyme (in case of proteotypic peptides) or several isoenzymes from the same class (in case of shared peptides) were cumulated. The number and characteristics of the cumulated peptides is summarized in SI Table 2 and 6.

2.5 Discussion

We present the protein expression of cytosolic GSTs during zebrafish development and in organs of adult zebrafish. With the use of targeted proteomics, we are now able to distinguish selected GST isoenzymes despite their high sequence identity. By monitoring conserved protein regions, we can also analyze the cumulative expression of enzymes belonging to the same GST class.

Some cytosolic GST family members are involved in the inactivation of endogenous compounds and cell signaling processes (Adler et al. 1999; Cho et al. 2001; Singhal et al. 2015); their expression might be relevant for embryogenesis and post hatching development. Considering that GSTs have a broad and overlapping substrate specificity (Glisic et al. 2015; Mannervik and Danielson 1988), GST family members with a putative role in endogenous processes may also accept xenobiotics as substrates and be of significance for the protection of the embryo against natural toxins and xenobiotics. Using recombinant enzymes, a previous study demonstrated that cytosolic GST classes catalyze the GSH conjugation with model substrates CDNB and monochlorobimane (MCB), although at different turnover rates (Glisic et al. 2015). The class pi enzymes (Gstp1, Gstp2) and Gstt1a showed the highest enzyme efficiencies towards CDNB and MCB, respectively. However, to conclude on the role each isoenzyme plays in xenobiotic defense processes, not only the enzyme efficiency, but also its expression level at the respective life stage needs to be considered. Therefore, mapping of GST expression during embryogenesis as well as in tissues of adults is necessary in order to ascribe GST isoforms to the biotransformation of xenobiotics.

2.5.1 GST expression in early life stages of zebrafish reflects important developmental events

Prior to the activation of the embryonic genome, the embryo completely relies on the maternally deposited gene products. In zebrafish, maternal mRNA drives cellular processes within the first three hours after fertilization (Tadros and Lipshitz 2009). Maternal deposition of GST mRNA transcripts and the presence of all cytosolic GST classes within the first four hours post fertilization have been demonstrated in previous studies (Glisic et al. 2016; Timme-Laragy et al. 2013). Our study on the protein level confirms the expression of GST classes alpha, mu, pi and rho as early as 4 hpf. GST enzymatic activity was also detected within the first four hours of zebrafish development (Notch et al. 2011; Otte et al. 2017; Wiegand et al. 2000). These findings indicate that GST enzymes are not only expressed but also active and capable of catalyzing GSH conjugation

reactions with xenobiotic compounds already within the first hours of embryogenesis. Apart from GSH conjugation reactions, GSTs have been shown to interact non-catalytically with different ligands such as kinases (Akhdar et al. 2012; Sheehan et al. 2001) and perform isomerase and peroxidase reactions (Hurst et al. 1998; Johansson and Mannervik 2001) which may be of importance for early developmental processes.

During zebrafish embryogenesis, the heart forms as the first organ. The zebrafish heart tube starts to beat by 22 hpf and after 24 hpf blood circulation begins (Stainier et al. 1993). At this stage, enzymes of the classes alpha, mu, pi and rho are expressed, but only Gsta1 shows an increase in the expression. Interestingly, Brox et al. (2016) reported a potential GST biotransformation product of clofibric acid at 28 hpf indicating that, GSTs expressed by the first day of zebrafish development are already active.

The majority of cytosolic GSTs were first observed after 72 hpf followed by a slight increase in expression level. In agreement with this, cytosolic GST enzyme activity experiences an increase after 72 hpf (Otte et al. 2017; Wiegand et al. 2000). Within the first 72 hours, the major organ patterning has been completed (Kimmel et al. 1995). Thus, during the major organ development, only four GST classes (alpha, mu, pi and rho) catalyze the endogenous reactions and protect the embryo from environmental stressors. After 72 hpf, organs, such as liver and intestine, enter the growth phase and continue to develop into fully vascularized and functional organs (Field et al. 2003; Kimmel et al. 1995; Ng et al. 2005). The development of liver and intestine thus clearly correlates with an increase in the expression of most GST isoenzymes and classes.

The 72 hpf also marks the end of the hatching period (42-72 hpf) and the transition of the zebrafish embryo to the free swimming stage (eleutheroembryo) (Kimmel et al. 1995). Timme-Laragy et al. (2013) show that hatching is associated with changes in the balance of reduced and oxidized glutathione (GSH and GSSG, respectively) resulting in a more negative, i.e. more reducing, redox potential. It is thus possible that the increase in post-hatch GSH levels are linked to the increase in expression levels of some GST family members. It is conceivable that the interplay of GST expression and change in redox state of the organism is important in the protection of the organism from an increase in aerobic metabolism as the embryo enters a period of dynamic growth with an increase in cell proliferation.

One enzyme class, the pi-class, is constantly expressed throughout early zebrafish development. However, we were only able to detect isoenzyme Gstp1 as well as shared peptides for the class pi enzymes. Although Glisic et al. (2015) showed that Gstp2 biotransforms CDNB with the highest enzyme efficiency compared to

other analyzed GSTs, its constitutive expression is low during zebrafish development. In contrast, Gstp1, the enzyme with the second highest efficiency for CDNB (Glisic et al. 2015), is present in all analyzed zebrafish life stages and might be dominating the activity assays.

Finally, Gstm1,2 showed a highly variable expression pattern. However, as this dynamic trend could only be observed for one peptide, we cannot distinguish if the observed pattern reflects changes in the enzyme expression or if it is caused by changes in post translational modifications over time.

2.5.2 GST expression in adult organs is organ-specific and variable among individuals

Knowledge regarding the organ-specific expression pattern of cytosolic GSTs is of importance, as the lack of individual GST classes can result in a predisposition of specific organs to damage by electrophilic compounds. Additionally, the expression level of specific GSTs in barrier tissues and principal organs of biotransformation provides information regarding the involvement of specific GST enzymes in xenobiotic defense mechanisms. Our study shows a constitutive expression of GST enzymes in all examined organs of zebrafish, indicating that GSH-conjugation is a xenobiotic defense mechanism functioning in all tissues. Nonetheless, some organs show a higher expression of selected GST family members in relation to others. Liver – the presumed main organ responsible for biotransformation – shows the highest protein expression of the alpha-class, zeta-class, Gstm1a and Gstr. Gills, barrier tissues directly exposed to chemicals at the water interface, show an elevated expression of Gstm3, Gstm1,2,3 and Gsto2. Overall, these expression patterns are comparable to those reported on the mRNA level by Glisic et al. (2015), with one exception: class alpha GSTs were present at low mRNA levels in the liver.

Although in some GST classes, such as in class alpha and zeta, the isoenzymes show consistent trends in tissue expression, this is not true for all GSTs. Gsto1 is predominately expressed in intestine and brain whereas Gsto2 expression is highest in the gills. A comparable expression pattern for Gsto1 was observed on the mRNA level (Glisic et al. 2015). Furthermore, Gstp1 is expressed in all analyzed organs and follows pattern (iii) during embryo development, while Gstp2 was not detected. The expression pattern of Gstp1 is potentially indicative of constitutive expression of this isoenzyme. Consistent with this observation, mRNA analysis identified gstp1 as the predominant isoenzyme of the pi-class and its constitutive gene expression was demonstrated to be high in all zebrafish tissues (Glisic et al. 2015).

The expression of many GST classes is low in female gonads, which can be explained by the structure of the organ. A large proportion of the zebrafish ovarian proteome consists of vitellogenins, precursor proteins of egg yolk (Groh et al. 2011). Hence, other proteins are underrepresented in relation to egg yolk and thus, due to limited sensitivity, appear to be expressed at low levels with respect to other organs. In contrast to the sex dependent mRNA expression of most GST enzymes (Glisic et al. 2015), no further gender differences are apparent within our dataset.

The variability in GST expression is more pronounced in sample replicates of adult zebrafish as compared to the expression data obtained from early life stages. For a better representation of the biological diversity within zebrafish, we chose a wild-type mix over an inbred strain. The wild-type mix chosen for its genetic diversity might explain the higher variability in the adults when compared to the embryos, also because of the limited pool involved (pool of four adults vs pool of 60 embryos).

2.5.3 GSTs expressed in zebrafish show similarities to humans

Being able to study the expression of GST classes and isoenzymes is of great value because some of their polymorphic variations may be informative about an individual's susceptibility to develop diseases, such as cancer. In addition, information about GST expression can help to predict a patient's ability to respond to certain drug treatments (Hollman et al. 2016; McIlwain et al. 2006). Among all members of the GST family, four cytosolic classes (GST class alpha, theta, mu and pi) have been in the center of attention for the last decade, due to their role in anti-oxidation processes and detoxification of therapeutic drugs, carcinogens as well as environmental pollutants (Hollman et al. 2016). Therefore, it is important to compare the known expression of human GSTs with that determined in zebrafish.

In human embryogenesis, cytosolic classes, alpha, mu and pi are already expressed (Raijmakers et al. 2001). Similar to human data, GST classes alpha, mu and pi were expressed very early during zebrafish embryogenesis, indicating that those classes may be most critical for the protection and functioning of cells during early phases of vertebrate development. In addition to the human orthologues, zebrafish embryos express a GST enzyme designated to the class rho. Class rho is an evolutionarily distinct member of the GST family that is present in teleosts and cephalo-chordate (Glisic et al. 2015). It is assumed to play a role in microcystin toxicity and shows reactivity towards some model substrates (Glisic et al. 2015; Hao et al. 2008; Liang et al. 2007).

In human adult liver, GSTA1 is the dominant form. In addition, class mu and class theta are reported to be expressed in the liver of healthy adults (Coles and Kadlubar 2003; Mainwaring et al. 1996; Rowe et al. 1997). Similarly, class alpha and theta in zebrafish have a pronounced expression in the liver, indicating conserved roles of these GST-classes in fish and mammals. GSTP1 is expressed in most adult human tissues including digestive, urinary and respiratory organs (Schnekenburger et al. 2014). Similarly, class pi was expressed in all zebrafish organs with an elevated level in the liver, intestine and gill.

All cytosolic GST classes are present on the protein level during zebrafish development and in organs of adults. The early expression of GSTs during zebrafish embryogenesis and the similarities to humans support the use of zebrafish as model in research applications that depend on functional biotransformation pathways. The targeted proteomics methods developed within this study allow to determine specific isoenzymes of the GST classes, thereby opening new avenues for understanding the role of GSTs in endogenous processes and upon exposure to chemicals.

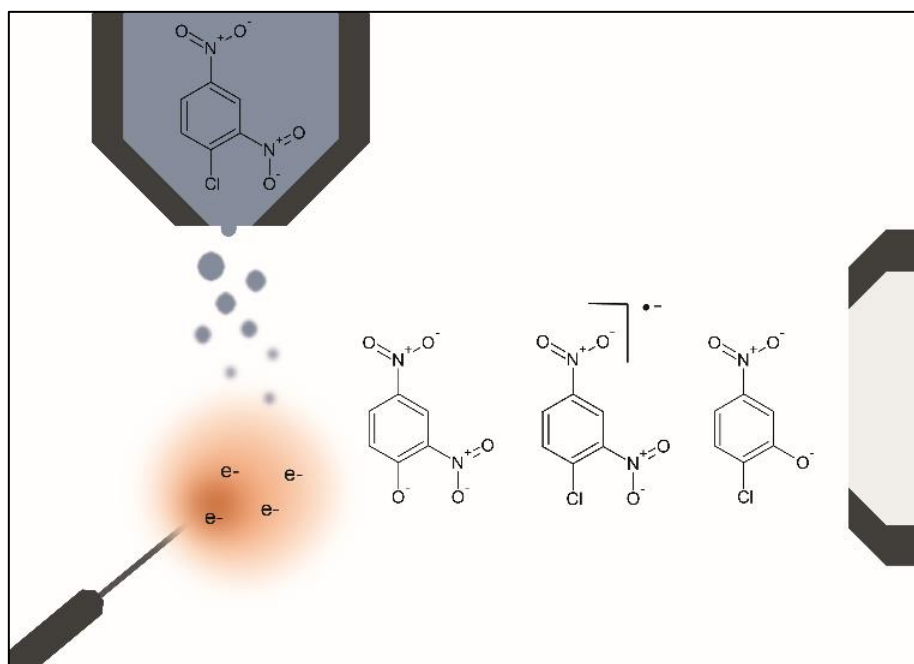
Chapter 3 LC-APCI(-)-MS determination of 1-chloro-2,4-dinitrobenzene, a model substrate for glutathione S-transferases

Alena Tierbach, Ksenia J Groh, René Schönenberger, Kristin Schirmer, Marc J-F Suter

Published in *Journal of the American Society for Mass Spectrometry*

<https://doi.org/10.1021/jasms.9b00116>

Publishing date: 24 January 2020



Contributions

I was supported within this project in the following ways:

- Technical assistance in mass spectrometric analysis: René Schönenberger
- Experimental design and discussions: Ksenia J Groh, Kristin Schirmer, Marc J-F Suter
- Reviewing & editing: Ksenia J Groh, Kristin Schirmer, Marc J-F Suter

3.1 Abstract

1-Chloro-2,4-dinitrobenzene (CDNB) is widely used as a model substrate for measuring enzyme activity of glutathione S-transferases in toxicity studies and in studies focusing on the metabolic capacity of different test systems. To allow the quantification of CDNB at low, non-toxic concentrations, we developed a sensitive liquid chromatography-mass spectrometry (LC-MS) technique, which is based on electron capture ionization using atmospheric pressure chemical ionization (APCI) in negative ion mode. Gas phase reactions occurring under atmospheric pressure produce specific ions that allow direct CDNB quantification down to 17 ng/ml in water. Using the new technique, we were able to verify CDNB exposure concentrations applied in two typical toxicity studies with early life stages of the common model organisms, zebrafish (*Danio rerio*) and a zebrafish embryonic cell line (PAC2).

3.2 Introduction

The electrophilic compound 1-chloro-2,4-dinitrobenzene (CDNB) is used among others as a chemical reagent during the manufacturing of azo dyes, and as an algaecide in the coolant water of air-conditioning systems. In contact with skin, CDNB induces allergic contact dermatitis. Relatedly, it was shown to be effective as an immunostimulant and in treatment of viral warts (HSDB 2019). The compound is also widely used as a model substrate for activity studies of glutathione S-transferases (GSTs). The GSTs are a family of enzymes that plays a major role in detoxification of electrophilic compounds, such as drugs and environmental pollutants, by catalyzing the conjugation reaction of the electrophilic moiety with glutathione (GSH). Connected to this major role in phase II metabolism, the level of GST activity is frequently used to define the biotransformation capacity of biological test systems (Hinchman et al. 1991; Otte et al. 2017).

However, *in vivo* studies that focus on biotransformation (e.g. phase II metabolism) require a substrate concentration that does not induce toxicity in the test organism - otherwise the biotransformation enzymes might be adversely affected. Therefore, when using CDNB as a substrate for GSTs, it is frequently required to measure CDNB at low, non-toxic concentrations in biological matrices or exposure solutions in order to verify and monitor the chemical load. Traditionally, high-performance liquid chromatography (HPLC) with ultraviolet (UV) detection has been used to measure CDNB concentrations (Hinchman et al. 1991). This technique exploits the fact that biotransformation of CDNB by GSTs results in the formation of a GSH-conjugate (DNP-SG, $\lambda_{\text{max}}=340$ nm) which can be spectrophotometrically distinguished from the parent compound (CDNB, $\lambda_{\text{max}}=280$ nm) (Habig et al. 1974; Vaidya and Gerk 2007). However, the lowest limit of quantification (LOQ) for CDNB with this technique was reported to be 200 ng/ml (Vaidya and Gerk 2007).

Available toxicity data on aquatic organisms, such as guppy (*Poecilia reticulata*) and rotifers (*Brachionus calyciflorus*), report a half-maximal lethal (LC_{50}) CDNB concentration of 200-1'300 ng/ml (HSDB 2019). The HPLC-UV LOQ of 200 ng/ml (Vaidya and Gerk 2007) is very close to the CDNB LC_{50} . As the non-toxic concentration is significantly lower than the LC_{50} , a more sensitive technique is needed to be able to quantify the frequently used CDNB at low, non-toxic concentrations. For this reason, we were interested in developing a more sensitive method for its quantification. While GC-MS has traditionally been used for halogenated aromatic compounds, the most powerful technique to access chemical compounds in biological matrices and environmental samples, without major sample preparation, is HPLC coupled to a high-resolution mass spectrometer

(HR-MS). Currently, electrospray ionization (ESI) and atmospheric pressure chemical ionization (APCI) sources are the predominantly used interfaces. Both techniques enable the ionization and transfer of the analytes into the gas phase. Typically, ionization occurs based on acid/base reactions (protonation and deprotonation in the positive and negative ion mode, respectively), either in the liquid (ESI) or the gas phase (APCI). Thus, the ionization efficiencies for non-polar molecules that are not prone to protonation/deprotonation reaction, such as CDNB, are usually poor with both interfaces. However, nonpolar nitroaromatic compounds have been shown to undergo dissociative and non-dissociative electron-capture (EC) ionization with APCI in the negative ion mode (Hayen et al. 2002). We demonstrate that this feature can be exploited for the quantification of CDNB down to the 17 ng/ml range, without enrichment.

As representative model systems for toxicity studies, we focus on zebrafish early life stages and zebrafish cell lines (PAC2), due to their versatile application possibilities in life and environmental sciences. In both exposure systems, this technique allows measuring the whole range of exposure concentrations in a typical toxicity study, down to non-toxic concentrations.

3.3 Materials and methods

3.3.1 Chemicals and reagents

1-Chloro-2,4-dinitrobenzene (CDNB) and ammonia were purchased from Sigma Aldrich (United States) with $\geq 99\%$ purity, and methanol and ethanol (for HPLC, gradient grade, $\geq 99.8\%$) from Fisher Scientific (United States). Nanopure water was obtained from Barnstead Nanopure, Fisher Scientific (United States). Dimethyl sulfoxide (DMSO) was purchased from Sigma Aldrich (United States). Reconstituted water (294.0 mg/l $\text{CaCl}_2 \cdot 2\text{H}_2\text{O}$, 123.2 mg/l $\text{MgSO}_4 \cdot 7\text{H}_2\text{O}$, 64.7 mg/l NaHCO_3 , and 5.7 mg/l KCl; ISO 15088:2007(E); 2007) and Leibovitz L-15 medium (Invitrogen, United States) supplemented with 5% fetal bovine serum (FBS; PAA Laboratories, Switzerland) were prepared freshly.

3.3.2 Mass spectrometry

For method development, CDNB was directly infused into the mass spectrometer at a concentration of 1 $\mu\text{g/ml}$ and a flow rate of 15 $\mu\text{l/min}$. The measurements were performed on a quadrupole orbitrap mass spectrometer (Q Exactive Plus, Thermo Fisher Scientific Inc.) using an APCI source, operated in negative ion mode

(APCI(-)). Full scan data were acquired over a mass range of 50-300 m/z with a resolving power of 30'000 at m/z 200. Capillary temperature was set to 250 °C, APCI vaporizer temperature to 250 °C, sheath gas flow to 30, aux gas flow to 10.

To evaluate the method, two 13 point calibration series were prepared over a concentration range of 0 (blank) to 2'000 ng/ml (0, 1, 5, 10, 125, 250, 500, 750, 1'000, 1'250, 1'500, 1'750 and 2'000 ng/ml) in five replicates, which covered the fish LC₅₀ from literature (200-1'300 ng/ml (HSDB 2019)). The first calibration curve was prepared in reconstituted water with 0.01% ethanol to mimic the condition of a typical assay with zebrafish. For this, CDNB stock solutions were prepared in warm ethanol and then spiked into samples of reconstituted water. The second calibration curve was prepared in L15 medium supplemented with 5% FBS and end concentration of 0.5% DMSO to mimic the condition of a typical cell line assay. To prepare the samples, CDNB stock solutions were prepared in DMSO and then spiked into samples of L15 medium with 5% FBS. A slightly larger concentration range was chosen for the calibration curve in L15 medium with 5% FBS because we assumed a higher non-toxic concentration and LC₅₀ in cell lines, as indicated by preliminary toxicity tests.

3.3.3 Chromatography

The samples were injected onto a Poroshell 120 EC - C18 column (2.7 µm particle size, 2.1x100 mm – Agilent, Switzerland) and separated at a flow rate of 200 µl/min using a 2 min linear gradient from 80% solvent A (10% methanol in water, 0.1% ammonia) to 100% solvent B (100% methanol, 0.1% ammonia) followed by a washing step (2 min, 100% solvent B) and a re-equilibration step (4 min, 80% solvent A), giving a total runtime of 8 min.

3.3.4 Verification of exposure levels in CDNB toxicity studies

To verify CDNB concentrations used in a typical CDNB toxicity study with zebrafish early life stages, working solutions with the concentrations of 3.0, 2.0, 1.2, 1.0, 0.7, 0.5 and 0.25 µg/ml were prepared in ethanol. The working solutions were then diluted by a factor of 10⁴ with reconstituted water to obtain the nominal exposure concentrations of 300.0, 200.0, 120.0, 100.0, 50.0 and 25.0 ng/ml and a final ethanol content of 0.01%. To verify CDNB concentrations used in a typical CDNB toxicity study with zebrafish cell lines (PAC2), working solutions with the concentrations of 320.0, 256.0, 204.8, 163.8, 131.1 and 83.9 µg/ml were prepared in DMSO,

and then diluted by a factor of 200 with L15 medium supplemented with 5% FBS, to obtain the nominal exposure concentrations of 1'600.0, 1'280.0, 1'024.0, 819.2, 655.7 and 419.4 ng/ml and a final DMSO content of 0.5%.

The exposure concentrations were chosen to cover the range between the LC₅₀ and non-toxic concentrations, by considering data from literature (HSDB 2019) and running range finding experiments. For the quantification of CDNB in the respective exposure medium, 1 ml of medium was sampled at the beginning of each experiment and stored at 4 °C until further processing.

3.3.5 Data processing and evaluation

Method development, generation of theoretical isotope patterns and evaluation of the mass spectrometric data was done using Thermo Xcalibur 3.0.63 (Thermo Fisher Scientific Inc.). Following the measurements, peak areas were extracted from the datasets, using a mass tolerance of 5 ppm. The integrated peaks (unsmoothed) were manually reviewed. The sum of all peak areas corresponding to the dissociative and non-dissociative EC ions (Figure 13, A, B, C, D and E) were used for the linear regression. For this, the CDNB concentration (x) was fitted against the peak area (y) and a regression was performed without forcing the line to go through zero (SI Figure 1). The LOD and LOQ were calculated based on the linear calibration curve ($y=a+bx$) according to the following equations: $LOD=3S_a/b$ and $LOQ=10S_a/b$, where x is the concentration, y is the peak area, S_a is the standard deviation of the y -intercepts of the regression lines ($n=5$) and b is the slope of the calibration curve.

3.3.6 Supplementary information Chapter 3

Measured and predicted mass-to-charge ratios (m/z) of the electron capture ions and the relative intensities of the respective isotopes are summarized in SI Table 8. SI Figure 1 shows the calibration curves prepared in reconstituted water and L15 medium with 5% FBS in addition to the calculated LOQ and LOD. The calibration curves were used to calculate the measured CDNB concentrations used in toxicity studies (SI Table 9).

3.4 Results and discussion

CDNB is a nonpolar compound that lacks proton-accepting and proton-donating functional groups. Thus, ionization of this molecule via acid/base reactions is not likely to occur. However, we were able to exploit the fact that CDNB undergoes electron capture processes in the APCI interface, thus allowing the determination of CDNB in liquid media. Electrons from the corona discharge in the APCI interface can interact with the nebulizer gas producing gas-phase low-energy electrons. Electron-affine molecules in the gas phase capture those low-energy electrons and form negative ions. This electron capture mechanism allows the measurement of electron-affine compounds in APCI(-) with high sensitivity (Higashi et al. 2002; Lee et al. 2003).

3.4.1 CDNB undergoes dissociative and non-dissociative EC in APCI(-)

It has been reported previously that aromatic compounds containing a halogen and/or a nitro-group can undergo dissociative electron capture in APCI(-) (Gudlawar and Dwivedi 2014; Hayen et al. 2002). An interaction of the analyte ion or the neutral analyte with an oxygen or a superoxide ion can lead to a substitution of the halogen and/or the nitro-group by oxygen (Gudlawar and Dwivedi 2014). Indeed, we observed dissociative EC ions at $m/z=183.00$ and 171.98 that showed a substitution of the chloride and nitro-group, respectively (Figure 13A, E). The good agreement between the measured and theoretically generated isotope profiles (Figure 14A, E) supports the proposition that CDNB undergoes dissociative electron capture in APCI(-), forming the predicted ions (Figure 13A, E).

Since the nitroaromatic system of CDNB has electron accepting capabilities, non-dissociative electron capture ionization should be possible (Hayen et al. 2002). Indeed, we observed a peak at $m/z=201.98$, which corresponds to the negatively charged molecular radical ion $[M]^{-\bullet}$ (Figure 13D, Figure 14D). However, the isotopic distribution of the measured ion does not agree with the theoretically generated isotope profile. In addition, a further ion $[M-H]^{-}$ with the $m/z=200.97$ is present in our measurements (Figure 13C, Figure 14C). Its isotopic distribution clearly overlaps with the isotopic pattern of the molecular radical ion. By subtracting the theoretical isotope intensities of the $[M-H]^{-}$ from the measured isotope pattern, a pattern emerges that agrees with the theoretical isotope distribution of the $[M]^{-\bullet}$ (SI Table 8). Additionally, we observed a solvent (methanol) cluster $[M+\text{solvent}-H]^{-}$ with an $m/z=233.00$, whose identity was confirmed by the theoretically generated isotope profile (Figure 13B, Figure 14B).

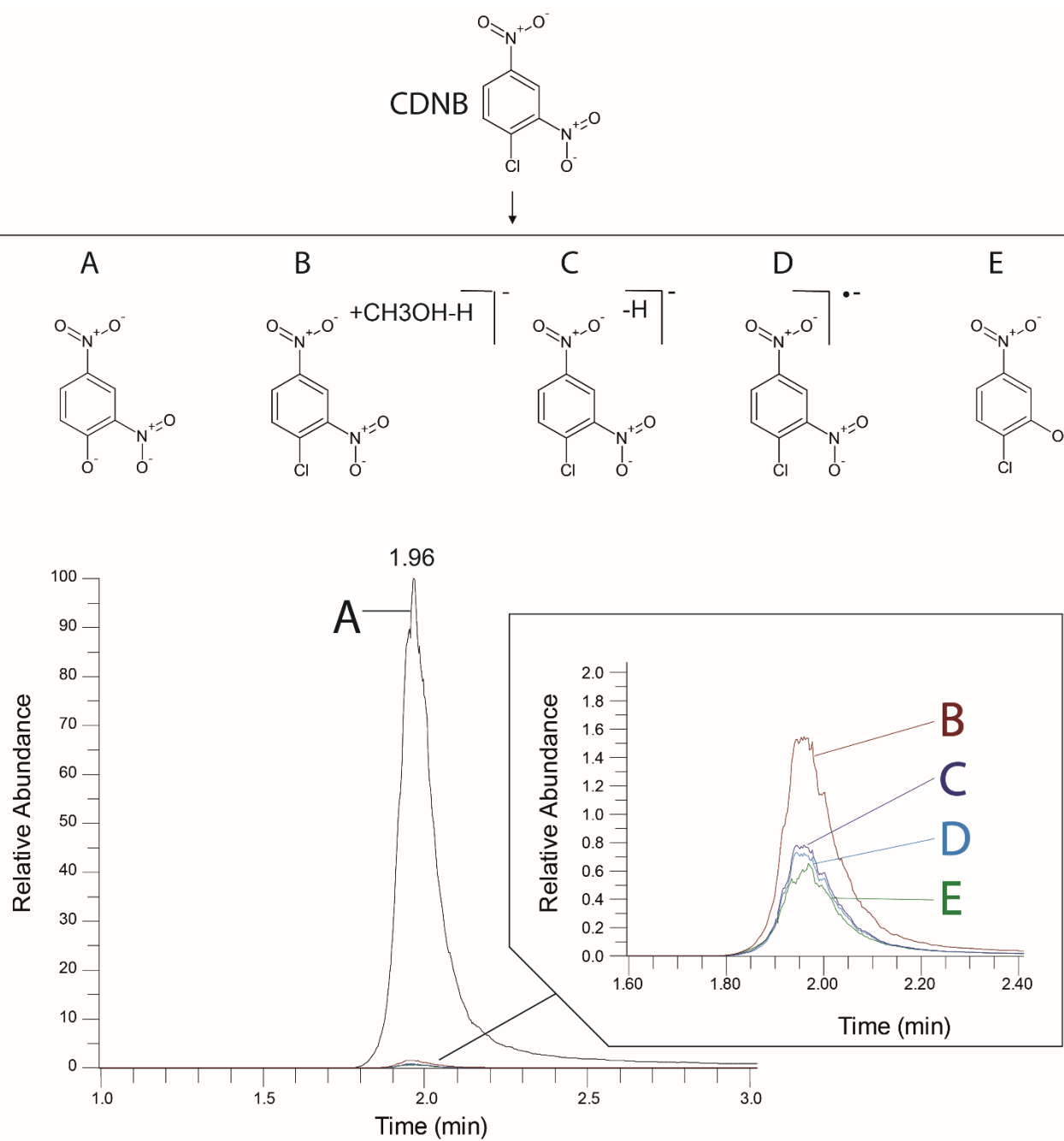


Figure 13: Structural formula of 1-chloro-2,4-dinitrobenzene (CDNB) and proposed chemical formula of ions produced with APCI(-)-MS electron capture (A, B, C, D and E). Below, the relative abundance of the ions (A, B, C, D and E) is shown including an in-frame zoom on the low abundance ions.

The dissociative substitution of the chloride group by oxygen is the predominant reaction within the APCI source producing by far the strongest ion. The remaining ions contribute only little to the overall signal. Nonetheless, as ion formation in the APCI interface is a chemical gas phase reaction, the ratio of the ions produced might vary depending on the pressure gradient and source settings of the MS and the concentration used.

3.4.2 Dissociative EC in APCI(-) allows to measure CDNB load in common toxicity studies

Having successfully ionized CDNB by electron capture in APCI(-), we investigated whether this approach would be suitable and sensitive enough to identify and measure CDNB in two typical toxicity studies with different exposure media. CDNB is a lipophilic compound ($\log K_{ow}=2.17$) (Debnath et al. 1991) which can be dissolved in organic solvents but is poorly soluble in water. However, in toxicity studies with aquatic organisms or cells, aqueous solutions are predominantly used as exposure medium.

First, to separate the analyte from other components present in the exposure medium, an 8 min HPLC method was established. In this gradient separation, CDNB elutes at 2 min. No carryover of the analyte was observed in blank samples. Second, to test if our method is suitable for toxicity studies, we measured CDNB dilution series in reconstituted water and L15 medium substituted with 5% FBS.

In both media, peak areas and concentrations showed a linear relationship within the analyzed concentration range (1-2'000 ng/ml) (SI Figure 1). In reconstituted water, we were able to detect CDNB down to the concentration of 5 ng/ml (LOD) and to quantify it down to the concentration of 17 ng/ml (LOQ). The LOQ of our method is 11 times lower than the previously reported LC_{50} for fish (200 ng/ml) (Vaidya and Gerk 2007) which implies that we should be able to monitor the CDNB concentration in the exposure medium down to the non-toxic concentrations. Considering literature on CDNB toxicity in different aquatic organisms (HSDB 2019), we have chosen an exposure concentration range of 300 to 25 ng/ml for toxicity studies with zebrafish early life stages. By using the developed method, we determined the actual CDNB concentrations prior to the exposure experiments (SI Table 9A), which allows a better interpretation of toxicity results.

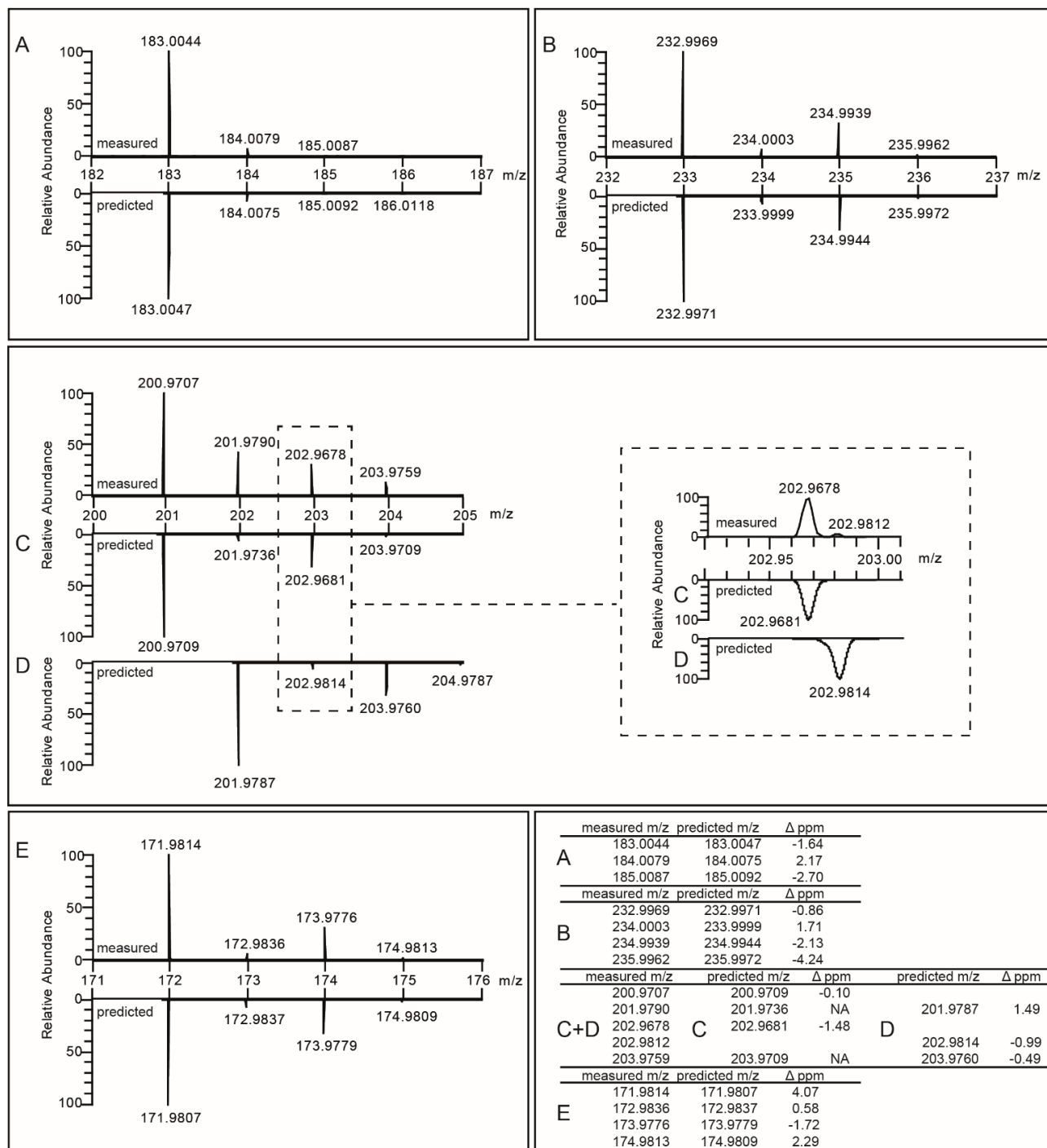


Figure 14: Mass spectra of ions produced with APCI(-)-MS electron capture A, B, C, D and E (structural formula shown in Figure 13), and a table with the parts per million (ppm) difference (Δ) between the measured and predicted mass-to-charge ratio (m/z). The measured isotopic distribution is shown on top of the predicted isotopic distribution in case of A, B and E. In case of C and D, the overlapping isotope pattern of the ions is shown at the top and the theoretical isotope distributions for ions C and D, respectively, is shown at the bottom. An in-frame zoom on m/z of 202.95-203.00 is shown to emphasize the presence of both, C and D, isotope patterns within the measurements.

In L15 medium substituted with 5% FBS, we were able to detect CDNB down to the concentration of 17 ng/ml (LOD) and to quantify it down to the concentration of 57 ng/ml (LOQ). Preliminary range finding experiments indicated that the CDNB toxic range for PAC2 cell lines is higher as compared to the fish embryos. For this reason, we selected a higher exposure concentration range of 1'600 to 420 ng/ml. The calibration curve was suitable to verify the concentrations in this typical cell toxicity assay (SI Table 9B).

During the toxicity study, the actual CDNB concentration deviated by up to 33% in water and up to 27% in L15 medium with 5% FBS from the nominal concentration in both exposure media due to handling. Through the correction of the nominal concentration, the toxic effects can be better correlated with the toxicants concentration and facilitate the design of further experiments.

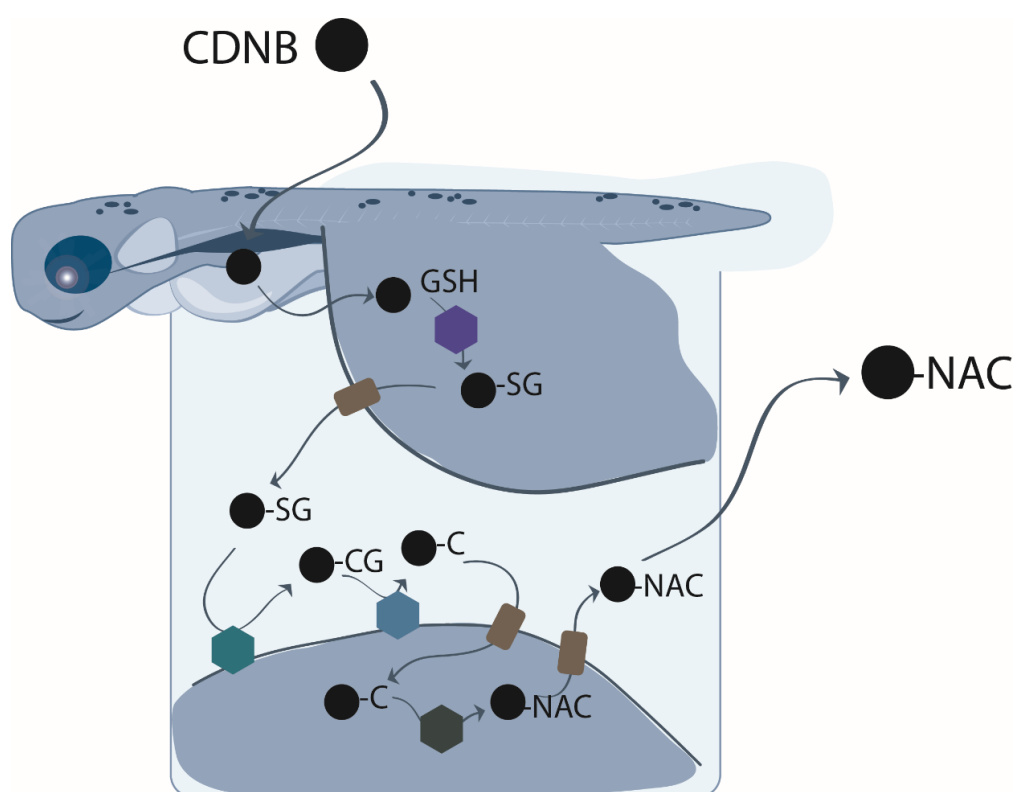
3.5 Conclusion

We showed that APCI(-) is a powerful technique which can be applied to quantify nonpolar, nitroaromatic compounds, such as CDNB, through solvent adduct formation, dissociative and non-dissociative electron capture ionization. Considering that CDNB is widely used in toxicity research, especially as a model substrate for GST activity studies, a sensitive technique for compound quantification is of high importance to allow for a high degree of flexibility in experimental design.

Chapter 4 Biotransformation capacity of zebrafish (*Danio rerio*) early life stages: Functionality of the mercapturic acid pathway

Alena Tierbach, Ksenia J Groh, René Schönenberger, Kristin Schirmer, Marc J-F Suter

Under review at *Toxicological Sciences*



Contributions

I was supported within this project in the following ways:

- Technical assistance in mass spectrometric analysis: René Schönenberger
- Experimental design and discussions: Ksenia J Groh, Kristin Schirmer, Marc J-F Suter
- Reviewing & editing: Ksenia J Groh, Kristin Schirmer, Marc J-F Suter

4.1 Abstract

Zebrafish (*Danio rerio*) early life stages, offer a versatile model system to study the efficacy and safety of drugs or other chemicals with regard to human and environmental health. This is because, aside from the well-characterized genome of zebrafish and the availability of a broad range of experimental and computational research tools, they are exceptionally well suited for high-throughput approaches. Yet, one important pharmacokinetic aspect is thus far only poorly understood in zebrafish embryo and early larvae: their biotransformation capacity. Especially biotransformation of electrophilic compounds is a critical pathway because such chemicals easily react with nucleophile molecules, such as DNA or proteins, potentially inducing adverse health effects. To combat such adverse effects, conjugation reactions with glutathione and further processing within the mercapturic acid pathway have evolved. We here explore the functionality of this pathway in zebrafish early life stages using a reference substrate (1-chloro-2,4-dinitrobenzene, CDNB).

With this work, we show that zebrafish embryos can biotransform CDNB to the respective glutathione conjugate as early as 4 hours post fertilization. At all examined life stages, the glutathione conjugate is further biotransformed to the last metabolite of the mercapturic acid pathway, the mercapturate, which is slowly excreted.

Being able to biotransform electrophiles within the mercapturic acid pathway shows that zebrafish early life stages possess the potential to process xenobiotic compounds through glutathione conjugation and the formation of mercapturates. The presence and functionality of this chemical biotransformation and clearance route in zebrafish early life stages supports the application of this model in toxicology and chemical hazard assessment.

4.2 Introduction

Fast and reliable screening of drug candidates and environmental pollutants for their efficacy and safety demands suitable and well-characterized test systems. Many compounds undergo biotransformation reactions, which can alter the compounds' reactivity and body clearance. Therefore, characterization of biotransformation processes within a biological test system is fundamental in order to establish it as a reliable risk assessment model. One test system of growing attraction in this regard is zebrafish at early life stages. Indeed, zebrafish embryos and early larvae combine the advantages of a multicellular organism with high-throughput capability, making it a popular model in numerous research fields, including environmental sciences and biomedical research (Dai et al. 2014; Perkins et al. 2013). However, a remaining hurdle for an even wider application spectrum is the incomplete understanding of the biotransformation processes in zebrafish early life stage development.

A major biotransformation route for electrophilic compounds, be they drugs, environmental pollutants, reactive intermediates, or endogenous molecules, is conjugation with glutathione and further processing to mercapturic acids (Figure 15) (Armstrong et al. 2018; Cooper and Hanigan 2018). In this route, electrophilic compounds are conjugated with the sulfhydryl group of the nucleophile glutathione (GSH) by the enzyme family glutathione S-transferases (GSTs) to produce glutathione-conjugates (Armstrong 1997; Habig et al. 1974). Although non-catalytic conjugation can also occur, the GST-catalyzed conjugation reaction is predominant (Higgins and Hayes 2011; Stoelting and Tjeerdema 2000). Members of the ATP-binding cassette/multidrug resistance-associated protein transporter family (ABCC/MRP) actively transport the glutathione-conjugate to the cell surface (Ballatori et al. 2009; Ursic et al. 2009). On the cell surface, the membrane-bound γ -glutamyl transferase converts the glutathione-conjugate to a cysteinylglycine S-conjugate by removing the γ -glutamyl group (Cooper and Hanigan 2018; Pompella et al. 2006). This product is then further processed to the cysteine S-conjugate through removal of the glycyl group by peptidases, including aminopeptidase N, cysteinylglycine dipeptidase, and leucyl dipeptidase (Cooper and Hanigan 2018). Finally, the cysteine S-conjugate re-enters the cell *via* transporters and is acetylated to the *N*-acetyl-L-cysteine S-conjugate, the mercapturic acid form of the chemical compound, by *N*-acetyl transferases (Cooper and Hanigan 2018; Dilda et al. 2008; Garnier et al. 2014; Hinchman et al. 1998). The mercapturic acid metabolite is usually non-toxic and more hydrophilic and thus excreted by the cells and generally eliminated from the body through healthy kidneys (Cooper and Hanigan 2018; Monks et al. 1990).

The use of zebrafish early life stages to assess the toxicity of drugs or environmental pollutants requires information about the mercapturic acid pathway's functionality. Protein expression analysis of the cytosolic GSTs showed that some enzyme classes are expressed as early as 4 hours post fertilization (hpf), while others are present only after hatching (72 hpf) (Tierbach et al. 2018). By means of a common *in vitro* assay (Habig et al. 1974), GST enzymatic activity could also be detected early in the zebrafish development (Notch et al. 2011; Otte et al. 2017; Wiegand et al. 2000). The mRNA expression of γ -glutamyl transferases was reported to be low during the first 48 hpf (Timme-Laragy et al. 2013). At later developmental stages, however, γ -glutamyl transferase activity was detected in the head and digestive system of ~73 hpf old larvae (Li et al. 2016), and in the liver and digestive system of ~121 hpf larvae (Li et al. 2018; Zhang et al. 2016). The developmental expression of peptidases involved in the mercapturic acid pathway remains largely unknown, while *N*-acetyl transferase activity was detected already at 2.5 hpf, though the activity stayed low until 48 hpf (Otte et al. 2017).

Although the studies mentioned above contribute valuable information about the mercapturic acid pathway's most important players, the analysis of one pathway segment at a time cannot provide a complete picture of an organism's biotransformation capacity. As the developing embryo is subject to constant change in the tissue and organ structure, it is important to know at which life stage the chain of reactions within the mercapturic acid pathway is complete. To fill the existing knowledge gaps, we analyzed biotransformation products of the mercapturic acid pathway in zebrafish embryos and early larvae using a model substrate for GST activity, 1-chloro-2,4-dinitrobenzene (CDNB).

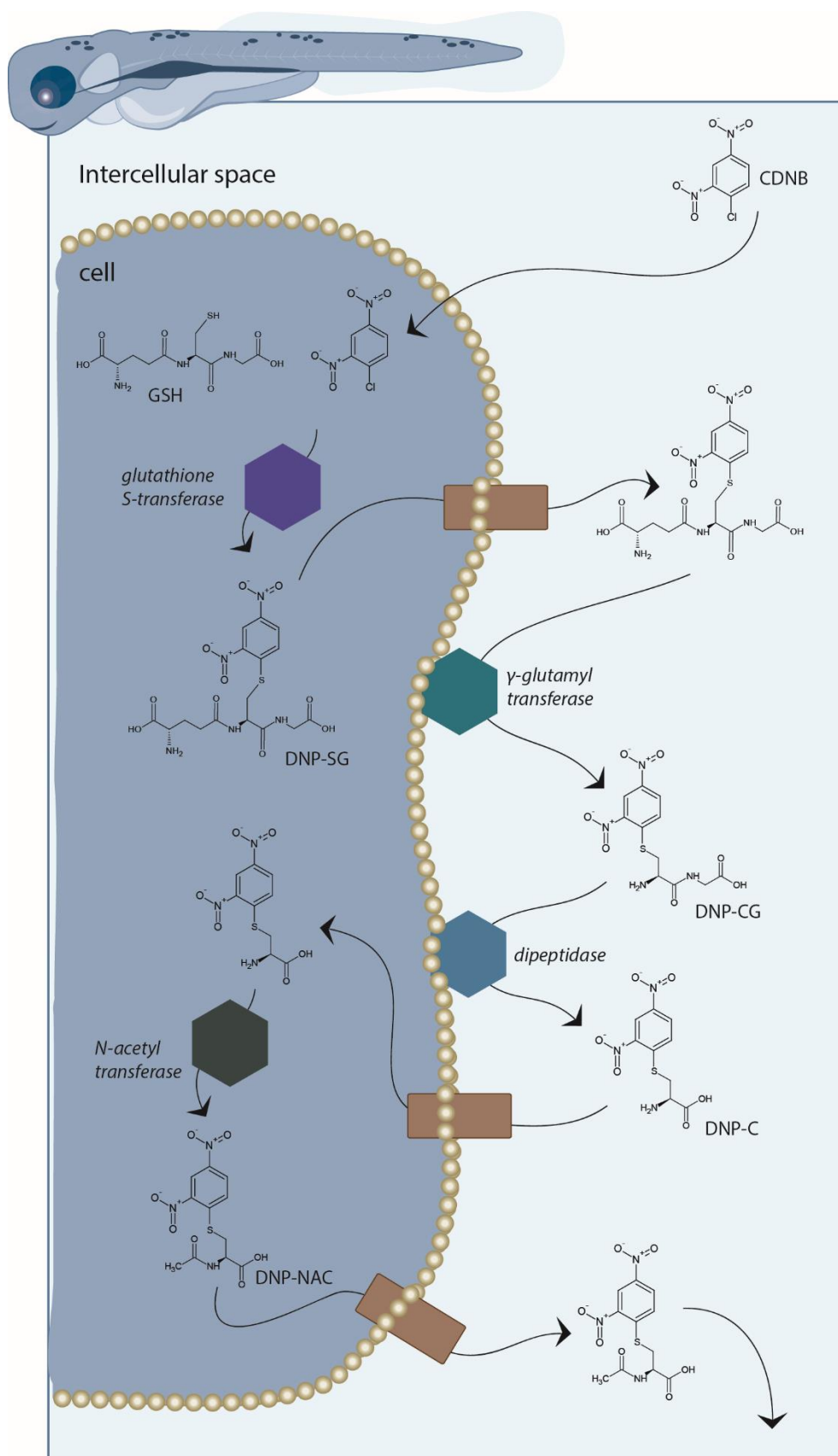


Figure 15: The biotransformation of 1-chloro-2,4-dinitrobenzene (CDNB) through the mercapturic acid pathway; glutathione (GSH); 2,4-dinitrophenyl-S-glutathione (DNP-SG); 2,4-dinitrophenyl cysteinylglycine (DNP-CG); 2,4-dinitrophenyl cysteine (DNP-C); 2,4-dinitrophenyl N-acetylcysteine (DNP-NAC) – the mercapturate form. For details on this pathway, see Introduction.

4.3 Materials and methods

4.3.1 Chemicals and reagents

Nanopure water was obtained from Barnstead Nanopure, Fisher Scientific (United States). Methanol and ethanol, for HPLC, gradient grade, $\geq 99.8\%$ and formic acid were purchased from Fisher Scientific (United States). 3,4-dichloroaniline, 1-chloro-2,4-dinitrobenzene (CDNB), and 5-chloro-2,4-dinitrotoluene (CDNT) were purchased from Sigma Aldrich (United States). The Glutathione S-Transferase (GST) Assay Kit (CS0410) was purchased from Sigma Aldrich (United States).

4.3.2 Zebrafish maintenance and breeding

Wild-type zebrafish with a mixed genetic background were maintained and bred in the fish facility according to procedures recommended by Nüsslein-Volhard (2002). The mixed genetic background was obtained by rearing wild type fish from WiK (Max Planck Institute for Developmental Biology, Tuebingen, Germany), OBI (Helmholtz Centre for Environmental Research, established from OBI Baumarkt, Leipzig, Germany) and Qualipet (pet shop, Dietlikon, Switzerland) together in a flow-through system at a light/dark cycle of 14/10 h. The flow-through system was filled with a 1:2 mixture of reconstituted water (294.0 mg/l $\text{CaCl}_2 \cdot 2\text{H}_2\text{O}$, 123.2 mg/l $\text{MgSO}_4 \cdot 7\text{H}_2\text{O}$, 64.7 mg/l NaHCO_3 , and 5.7 mg/l KCl; ISO 15088:2007(E); 2007), and tap water. Water temperature ranged from 26 to 28 °C. Zebrafish were fed twice daily with dry vitamin flakes (TetraMin, USA) and live food (*Artemia nauplia*). Zebrafish eggs were obtained from group crosses. Eggs were collected and washed with reconstituted water 1 h after the light in the facility was switched on.

4.3.3 CDNB toxicity study

The CDNB standard solution of 10 mg/ml was prepared by weighing CDNB powder and ethanol at 25 °C. To dissolve CDNB, the standard solution was heated to 40 °C under continuous stirring and cooled back to room temperature (25 °C). To find the toxic range of CDNB, working solutions with the concentrations of 300, 200, 100, 50 and 25 µg/ml were prepared in ethanol by diluting the CDNB standard solution. The working solutions were further diluted by a factor of 10^4 with reconstituted water to obtain the nominal exposure concentrations of 300, 200, 100, 50 and 25 ng/ml and a final concentration of 0.01% ethanol (v/v). For measuring the actual exposure concentration used in the toxicity studies, 1 ml of medium was sampled at the beginning of each

experiment and stored at -20 °C until further processing. The method for the analysis of CDNB in aqueous solutions and the verification of the exposure concentrations is described in Tierbach et al. (2020), (Chapter 3).

The impact of CDNB on zebrafish development was evaluated with the zebrafish embryo acute toxicity test (zFET) in triplicates, following the OECD guideline 236 (OECD 2013), with some modifications. The positive control (3,4-dichloroaniline at 4 µg/ml) was included only during range finding experiments. The lethal (increased coagulation, lack of heart beat, lack of somite formation, non-detachment of the tail, non-hatching) and sub-lethal (spinal curvature, deformation of the tail, pericardial edema, yolk sac edema) effects observed at 96 hours post fertilization (hpf) were used to calculate the half-maximal lethal concentration (LC₅₀), the half-maximal effective concentration (EC₅₀) and the concentration that did not cause a toxic effect significantly different from the control (non-toxic concentration, NtC, according to Stadnicka-Michalak et al. (2018)).

4.3.4 CDNB exposure experiments for biotransformation analysis

In a previous study by Tierbach et al. (2018), (Chapter 2) it was shown that a repertoire of cytosolic GSTs is already present at 4 hpf, indicating maternal transfer of the enzymes. However, the zebrafish express members of all cytosolic GST classes only after hatching. Based on the constitutive GST expression, we selected two exposure time frames of 24 h each, one starting at 2 hpf (embryo) and one starting at 74 hpf (early larvae). Zebrafish embryos were raised as mentioned above until the age of 2 or 74 hpf. At 2 or 74 hpf, the embryos / larvae were exposed to CDNB at the NtC of 25 ng/ml in paraffin-sealed glass Petri dishes. For this exposure, the working solution with the concentration of 250 µg/ml was diluted by a factor of 10⁴ with reconstituted water to obtain the nominal exposure concentration of 25 ng/ml and a final concentration of 0.01% ethanol (v/v). Per one Petri dish, 30 embryos were exposed in 30 ml of exposure medium (one ml exposure medium per embryo), meaning that three Petri dishes were used per replicate and time point.

After 2, 6 and 24 h of exposure, 90 embryos per sample were collected and snap-frozen in liquid nitrogen. In parallel, 90 embryos per control sample were raised in reconstituted water until the age of 26 hpf or 74 hpf (schematic representation of the experiments is shown in SI Figure 2, top panel). The samples were stored at -80 °C until further use. Additionally, 10 ml of exposure medium were sampled at each time point for chemical analysis and stored at -20 °C.

4.3.5 Metabolite depuration analysis

To study the clearance of CDNB metabolites, zebrafish embryos (5 samples with 90 embryos per sample) were exposed at 2 hpf to CDNB at the NtC of 25 ng/ml in paraffin-sealed glass Petri dishes. In parallel, 90 embryos were raised in reconstituted water until the age of 26 hpf to be used as control. After 24 h of CDNB exposure, one of the five experimental samples was collected and snap-frozen in liquid nitrogen. The remaining samples were washed three times with reconstituted water and transferred to CDNB-free reconstituted water. At 24, 48, 72 and 94 h of depuration, samples were collected and snap-frozen in liquid nitrogen (schematic representation of the experiments is shown in SI Figure 2, middle panel). The samples were stored at -80 °C.

4.3.6 Preparation of standards for method development and normalization

The high-resolution mass spectrometry method (HR-MS) was developed with the use of an *in vitro* synthesized CDNB glutathione-conjugate, 2,4-dinitrophenyl-S-glutathione (DNP-SG). The conjugate was synthesized with the use of the Glutathione S-Transferase (GST) Assay Kit according to the procedure for positive control as described in the assay kit. Briefly, 980 µl phosphate buffer saline, 10 µl GSH reduced (200 mM), 10 µl CDNB (100 mM in 100% ethanol) and 4 µl human GST solution were mixed and incubated for 3 h at room temperature. The enzymatic reaction was terminated through the addition of 3 µl formic acid. For method development, the DNP-SG solution was injected into the HR-MS after liquid chromatographic (LC) separation.

To account for variations during sample preparation and for variations between injections, the signal intensities of targets were normalized to the internal standard, 2,4-dinitrotoluene-S-glutathione (DNT-SG), which is the glutathione-conjugate of 2,4-dinitrotoluene. DNT-SG was produced by reacting CDNT with glutathione using the GST Assay Kit. Details of the procedure are described in the assay protocol of the GST Assay Kit (provided by Sigma Aldrich, United States); incubation duration was 24 hours. The DNT-SG was synthesized once and immediately spiked into all samples prior to sample preparation for relative quantification.

4.3.7 Extraction of CDNB metabolites from tissue

The homogenization and extraction of internal metabolites from the whole body was performed as described in Rosch et al. (2016), with some modifications. The samples were thawed at 4 °C for 15 min. Subsequently, 2.5 µl of DNT-SG were added to each sample as internal standard. The samples were taken up in 500 µl methanol and homogenized with the soft tissue homogenizing kit with 1.4 mm ceramic beads (zirconium oxide; Bertin Instruments, France) and a FastPrep-24 Homogenizer (MP Biomedicals, United States) in two cycles with 15 s at 6 m/s. In between the cycles, samples were chilled on ice for 5 min. The sample lysate was centrifuged (6 min, 10'000 rcf, RT), the supernatant was filtered through Amicon Ultrafree centrifugal filters, 0.45 µm cut-off (Millipore, United States), and filters were washed with 400 µl methanol. The filtrates and the wash were merged, evaporated using a vacuum centrifuge at 30 °C, and re-dissolved in 800 µl nanopure water with 0.1% formic acid. For sample cleanup and enrichment, embryo extracts and water samples (10 ml) were loaded onto reversed-phase cartridges (Sep-Pak Vac tC18, Waters, United States), eluted in 800 µl of 80% acetonitrile solution with 0.1% formic acid, evaporated using a vacuum centrifuge at 30 °C, re-dissolved in 50 µl nanopure water with 0.1% formic acid, and stored at 4 °C.

To analyze the loss of metabolites during the sample preparation, DNP-SG was synthesized with the use of the Glutathione S-Transferase (GST) Assay Kit as described above. Subsequently, 2.5 µl of freshly synthesized DNP-SG and the DNT-SG standard were spiked into 50 µl (final volume) of nanopure water with 0.1% formic acid (n=3). The water samples were stored at 4°C for 24 h. In parallel, 2.5 µl of the DNP-SG solution and the standard were spiked into samples of unexposed zebrafish embryos (age 24 hpf, 90 embryos/replicate, n=2) and larvae (age 96 hpf, n=2). The zebrafish samples were processed as described above. DNP-SG recovery was calculated by comparing the DNP-SG amount in water samples and embryo/larvae samples after sample preparation.

4.3.8 LC-HRMS analysis of CDNB metabolites

Samples were injected onto a Poroshell 120 EC-C18 column (2.7 μ m particle size, 2.1 \times 100 mm column, Agilent, USA) and separated at a flow rate of 100 μ l/min using a 10 min linear gradient from 90% solvent A (10% methanol in water, 0.1% formic acid) to 100% solvent B (90% methanol, 0.1% formic acid), followed by a washing step (5 min with 100% solvent B) and a re-equilibration step (4 min with 90% solvent A). To control for carry over, a blank sample (nanopure water) was injected between all samples.

The measurements were performed on a quadrupole orbitrap mass spectrometer (Q Exactive Plus, Thermo Fisher Scientific Inc.) using electrospray ionization (ESI) in positive ion mode. Full scans were acquired with a resolution of 140'000 (at m/z 200) over a mass range of 50 to 600 m/z . The full scan was followed by data-dependent MS/MS scans with an isolation window of 1.0 Da and a resolution of 17'500 (at m/z 200). Capillary temperature was set to 150 $^{\circ}$ C, sheath gas flow to 15, auxiliary gas flow to 5 and the spray voltage to + 4 kV. An inclusion list with the masses of the suspected CDNB biotransformation products and the spiked-in standards was created for triggering data-dependent MS/MS acquisition. The identity of CDNB biotransformation products was verified through characteristic fragments produced by higher energy collisional dissociation (HCD 30). The masses of the expected CDNB biotransformation products and spiked-in standards are summarized in SI Table 10.

4.3.9 Protein expression analysis

Freshly collected zebrafish embryos were raised to an age of 2 or 74 hpf as described above. Zebrafish embryos (2 hpf) were exposed to the CDNB NtC of 25 ng/ml for 24 h whereas zebrafish larvae (74 hpf) were exposed for 6 or 24 h. After the respective exposure duration, 120 embryos per sample were collected, washed in ice-cold phosphate-buffered saline and snap-frozen in liquid nitrogen (schematic representation of the experiments is shown in SI Figure 2, bottom panel). The samples were stored at -80 $^{\circ}$ C until protein extraction. Protein extraction and trypsin digestion were performed as reported previously (Tierbach et al. 2018), (Chapter 2). The prepared protein samples were stored at 4 $^{\circ}$ C until analysis. Liquid chromatography and peptide measurement were performed as reported previously (Tierbach et al. 2018), (Chapter 2). The targeted proteomics method showed to be reproducible, with the control embryos expressing all previously measured enzymes at

the respective life stage, with one exception: the enzyme Gstt1b, which showed the weakest signals in the previous study, was not detected in this experiment.

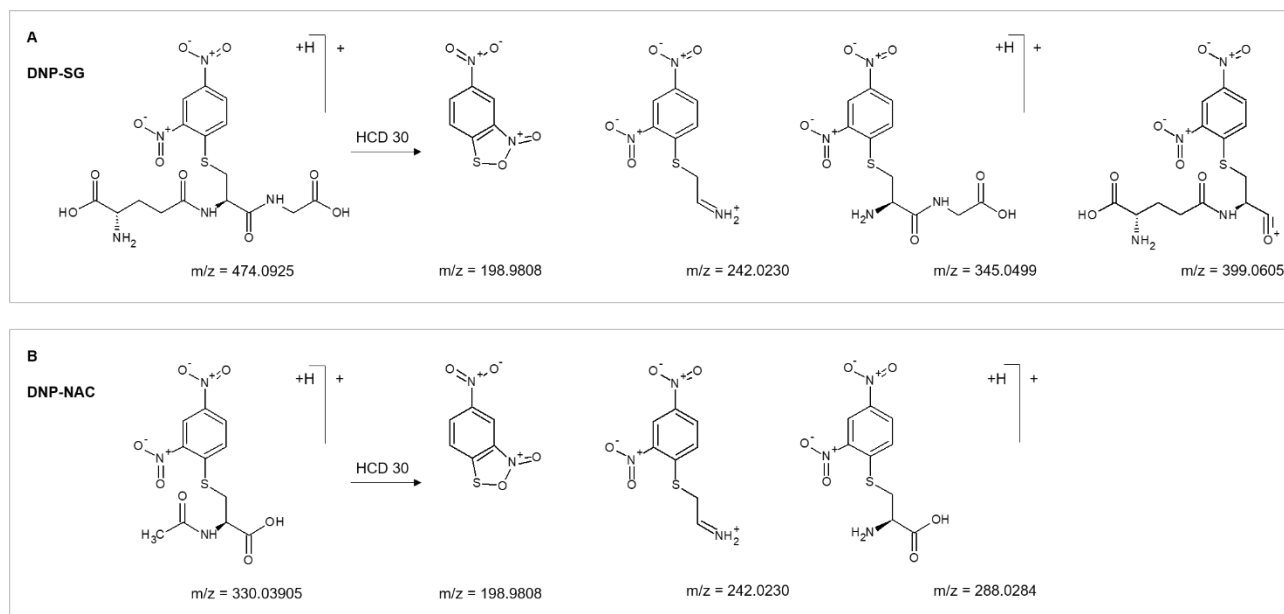


Figure 16: Precursor ions of 2,4-dinitrophenyl-S-glutathione (DNP-SG) (A) and 2,4-dinitrophenyl N-acetylcysteine (DNP-NAC) (B) are shown in combination with the proposed structures of the fragment ions produced by higher energy collisional dissociation (HCD) of 30. 2,4-dinitrophenyl cysteinylglycine (DNP-CG) and 2,4-dinitrophenyl cysteine (DNP-C) were not detected. m/z =mass-to-charge ratio.

4.3.10 Data evaluation

The LC_{50} , EC_{50} and NtC were calculated with an algorithm described by Stadnicka-Michalak et al. (2018). The analysis of mass spectrometric data of CDNB biotransformation products was performed with Thermo Xcalibur 3.0.63 (Thermo Fisher Scientific Inc.): method development and generation of theoretical isotope patterns were performed with the Qual browser; Quan browser was used to extract peak areas from datasets by using a mass tolerance of 5 ppm. The integrated peaks were manually reviewed. Only chromatographic peaks with a minimum of three data points per peak were accepted. Targeted proteomics data were evaluated with Skyline (MacLean et al. 2010). Data visualization and t-test were performed using GraphPad Prism version 7.00 for Windows (GraphPad Software, La Jolla California USA, www.graphpad.com). Values were considered as significantly different if $p < 0.01$.

4.3.11 Supplementary information Chapter 4

The Supplemental Information (Chapter 4) contains a graphical overview of the experimental procedure used within the current study (SI Figure 2), a graph depicting the results from DNP-SG recovery experiments (SI Figure 3), dose response curves for lethal and sub lethal effects (SI Figure 4 and 5) and a table summarizing physico-chemical calculations/predictions for DNT and DNP conjugates (SI Table 10). In addition, the Supplemental Information provides chromatograms and mass spectra of DNP-SG and DNP-NAC (SI Figure 6 and 7) and difference (ppm) between the measured and predicted masses of parent and fragment ions (SI Table 11 and 12). Furthermore, it contains a note about the generation of DNP-C through gas-phase reactions in the ESI source. This gas-phase reaction needs to be considered during data evaluation in order to avoid false-positive identification of the biotransformation product DNP-C.

Supplemental Information (Chapter 4) also contains information about sample name and identifiers, peak area of the analytes and the peak area of analytes normalized to the standard DNT-SG collected during CDNB exposure experiments (SI Table 13) and depuration experiments (SI Table 14). In addition, the second part (B) contains data on the cytosolic GST expression in zebrafish embryos and larvae exposed to CDNB non-toxic concentration (NtC) (SI Table 15).

4.4 Results

4.4.1 LC-MS can be used to analyze CDNB biotransformation products

With the use of *in vitro* synthesized DNP-SG, we established a sample preparation protocol and an LC-MS method to analyze CDNB biotransformation products. The DNP-SG molecule could be identified by its mass-to-charge ratio (m/z) and its characteristic isotope pattern. The MS/MS spectra of the parent molecule showed fragment ions with the dinitrophenyl (DNP) moiety (Figure 16A). Those specific fragment ions can be used to differentiate the xenobiotic from endogenous glutathione conjugates. Being able to measure DNP-SG, we estimated the metabolite losses during extraction from zebrafish samples. Through the comparison of unprocessed water samples and processed embryo samples, we calculated a recovery for DNP-SG of 67.5% (SI Figure 3). We assume that the sample preparation and LC-MS parameters optimized for DNP-SG are also suitable to cover the whole pathway, as DNP-conjugates of the mercapturic acid pathway have overall similar physico-chemical properties (SI Table 10).

4.4.2 CDNB induces toxicity in zebrafish early life stages at concentrations higher than 25 ng/ml

We performed the zFET to define the toxic range and the NtC of CDNB. Through evaluation of lethal effects, we calculated an LC_{50} of 107 ng/ml (SI Figure 4) which is in good agreement with previously published LC_{50} data in fish (*Brachionus calyciflorus*, LC_{50} =200 ng/ml) (HSDB 2019). To analyze the functionality of the mercapturic acid pathway during zebrafish development, we decided to use a CDNB concentration that does not exceed the capacity of the detoxification system. For this, we monitored sub-lethal effects for the calculation of the NtC. At concentrations higher than 25 ng/ml, spinal curvature, deformation of the tail, pericardial edema, and yolk sac edema were observed in zebrafish early larvae (96 hpf). Based on the sub-lethal effects, we calculated an EC_{50} of 56 ng/ml and an NtC of 25 ng/ml (SI Figure 5).

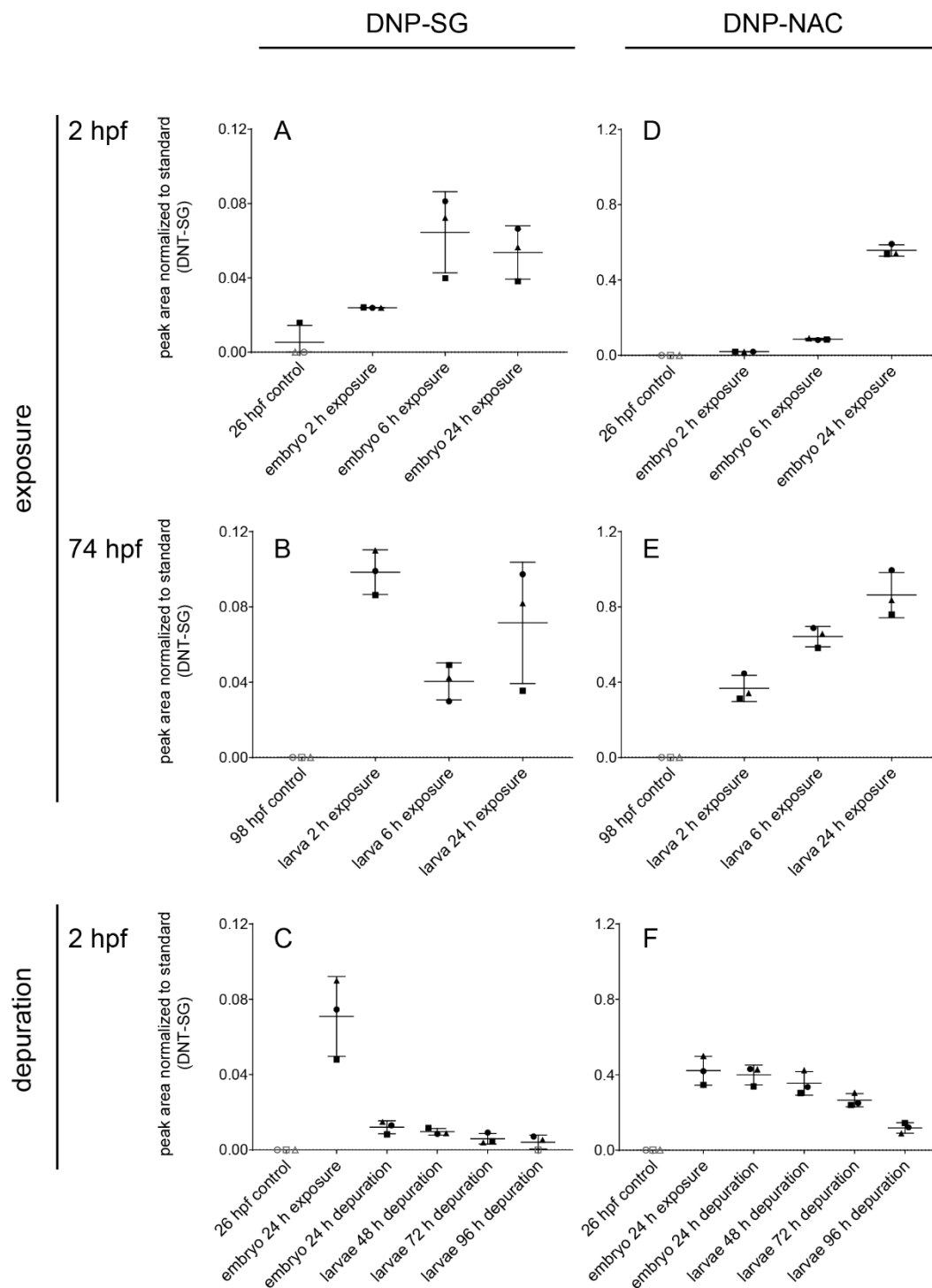


Figure 17: Formation (A, B, D, E) and depuration (C, F) of biotransformation products during zebrafish exposure to the non-toxic concentration (NtC=25 ng/ml) of 1-chloro-2,4-dinitrobenzene (CDNB) and during a subsequent depuration period of 96 h. Exposure: zebrafish were exposed at 2 hours post fertilization (hpf) (A) and 74 hpf (B) for 2, 6, and 24 h. Control zebrafish (not exposed) were sampled at 26 and 98 hpf. Depuration: zebrafish were exposed at 2 hpf for 24 h and raised in clean medium for 24, 48, 72 and 96 h. Control zebrafish (not exposed) were sampled at 26 hpf. 2,4-dinitrophenyl-S-glutathione (DNP-SG) is shown in the first column (A, B, C) and the 2,4-dinitrophenyl N-acetylcysteine (DNP-NAC) in the second column (D, E, F). The 2,4-dinitrophenyl cysteinylglycine (DNP-CG) and 2,4-dinitrophenyl cysteine (DNP-C) were not detected. In one of six control samples (unexposed control embryos), a small amount of DNP-SG was detected, which could be attributed to contamination during sample preparation. In addition to zebrafish embryos and early larvae, also the respective water samples were screened for CDNB metabolites of the mercapturic acid pathway. However, none of the CDNB metabolites could be observed in the water samples. Data represents the peak area normalized to the standard 2,4-dinitrotoluene-S-glutathione (DNT-SG). Each replicate is shown (replicate 1=circle; replicate 2=square; replicate 3=triangle) in addition to the mean and standard deviation. White symbols represent samples where the respective metabolite was not detected. For further information, please refer to supporting information chapter 4 B.

4.4.3 Metabolites of the mercapturic acid pathway are formed upon exposure to the NtC of CDNB

Upon exposure to the CDNB NtC, zebrafish embryos and larvae were screened for CDNB metabolites of the mercapturic acid pathway (Figure 15). DNP-SG was detected in all samples exposed to CDNB for 2 h or longer. The identity of the molecule was confirmed by the retention time, isotopic pattern and the characteristic fragment ions (Figure 16A, SI Figure 6 and 7, SI Table 11 and 12). In particular, the typical y_2 and b_2 peptide fragments, m/z 345 and 399, respectively, were visible (Figure 16, SI Figure 6D). In zebrafish embryos exposed at 2 hpf, the DNP-SG concentration was the lowest after 2 h of exposure, increased after 6 h of exposure, and stayed similar thereafter (Figure 17A). In zebrafish larva exposed at 74 hpf, the DNP-SG concentration was similar at all exposure durations (Figure 17B). In direct comparison of the two life stages, we observed a higher amount of DNP-SG after 2 h of exposure in larvae. At longer exposure duration, no difference in DNP-SG concentration between the embryo and larva was detected (Figure 17). We did not detect the 2,4-dinitrophenyl cysteinylglycine (DNP-CG) and the 2,4-dinitrophenyl cysteine (DNP-C) in any of the life stages and exposure durations. However, we did identify the N-acetylcysteine S-conjugate of CDNB (DNP-NAC) in exposed embryos by its isotopic ratios and fragmentation pattern (Figure 16B, SI Figure 7). DNP-NAC was detected in all embryos and larvae exposed to CDNB and its concentration increased noticeably with the exposure duration (Figure 17D, E). In direct comparison of zebrafish embryo and larva, the DNP-NAC concentration was higher in larvae than in embryos exposed to CDNB for the same exposure duration (Figure 17D, E).

4.4.4 Zebrafish embryo and larvae excrete mercapturic acid metabolites

To analyze the depuration of mercapturic acid metabolites, we raised zebrafish embryos in clean medium after exposure to the CDNB NtC for 94 hours. Within 24 h of depuration, the concentration of the DNP-SG conjugate decreased rapidly by around 80% and continued to decrease slowly during the subsequent depuration period. In contrast, the DNP-NAC metabolite concentration decreased constantly and slowly over the entire duration of the depuration experiment (Figure 17C, F).

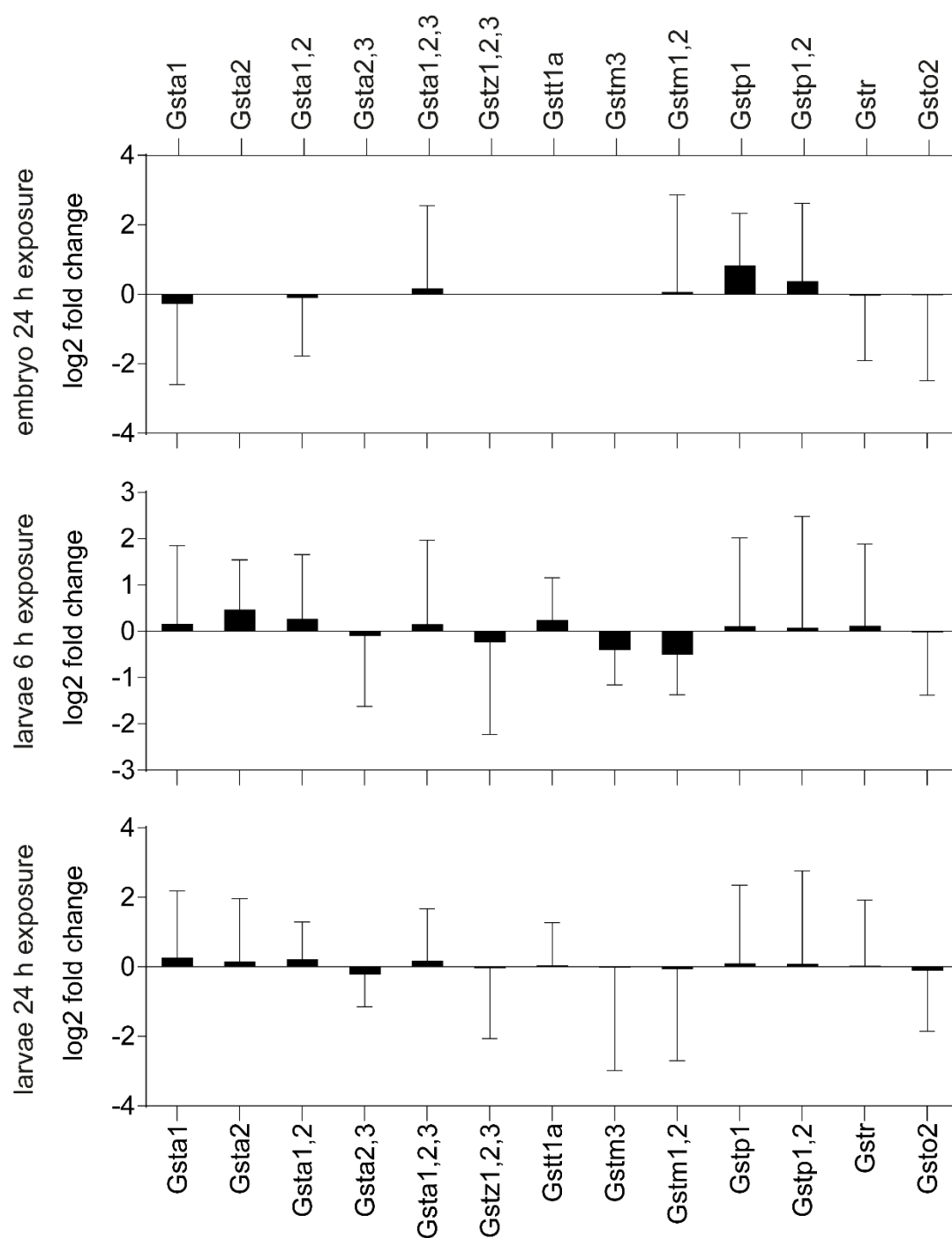


Figure 18: Expression of cytosolic GSTs in zebrafish early life stages exposed to the non-toxic concentration (NtC=25 ng/ml) of 1-chloro-2,4-dinitrobenzene (CDNB). Zebrafish embryos were exposed at 2 hpf for 24 h. Zebrafish larvae were exposed at 74 hpf for 6 and 24 h. Data is normalized to the housekeeping protein GAPDH and shown as log₂ fold change to the respective control. The mean of four replicates (60 pooled embryos/replicate) and standard error are shown. For expression analysis, the normalized peak area of peptides belonging to the same enzyme or several isoenzymes from the same class were cumulated. No significant differences between exposure and control samples were observed ($p > 0.01$, unpaired t-test). For further information, please refer to supporting information chapter 4 B.

4.4.5 Exposure to the non-toxic concentration of CDNB does not affect GST protein expression

The protein expression of cytosolic GSTs was measured upon exposure to the CDNB NtC in zebrafish embryo and larvae in order to investigate if formation of biotransformation products was associated with increased levels of GST protein expression. Exposure of zebrafish embryos (2 hpf) and larvae (74 hpf) to the NtC of CDNB had no significant effects on the protein expression of cytosolic GSTs (Figure 18).

4.5 Discussion

Electrophiles are detoxified, and in rare cases activated, through conjugation with glutathione and the subsequent biotransformation to mercapturic acids (Armstrong et al. 2018; Cooper and Hanigan 2018; Hinchman and Ballatori 1994). Consequently, the formation of mercapturates has become an important biomarker for evaluation of environmental exposure and potential health risks (Haufrond and Lison 2005; Mathias and B'Hymer 2014; Park et al. 2015). With the aim to broaden knowledge of this pathway in zebrafish early life stages, we now characterized the mercapturic acid pathway during zebrafish development with the use of the model substrate CDNB.

At the early stages of development, the zebrafish embryo is surrounded by the chorion, an acellular membrane with pores that can act as a protective molecular sieve. Due to the low molecular weight ($\leq 4'000$ Da) of CDNB, its uptake is not expected to be impaired by the chorion. The uptake of CDNB into the body is expected to occur *via* simple diffusion (Elferink et al. 1993). Within the organism, GSTs catalyze a nucleophilic aromatic substitution between CDNB and glutathione, releasing a chloride ion as the leaving group (Habig et al. 1974; Van der Aar et al. 1996). Previous *in vitro* tests showed that also zebrafish GSTs accept CDNB as a substrate (Glisic et al. 2015; Otte et al. 2017), making it an optimal model chemical for our study.

4.5.1 Mercapturic acid pathway is functional in zebrafish early life stages

Studies in mammalian systems report a fast uptake and a rapid biotransformation of CDNB (Hinchman et al. 1991; Jewell et al. 2000; Villanueva et al. 2006; Wahllander and Sies 1979). Similarly, we observed the first metabolite of the mercapturic acid pathway (DNP-SG) already after 2 hours of exposure in both life stages, zebrafish embryo (4 hpf) and larvae (74 hpf), pointing to sufficient constitutive levels. From an early stage of

embryogenesis, zebrafish express some members of the GSTs enzyme family, including enzymes of the class pi (Tierbach et al. 2018), (Chapter 2). Class pi enzymes were identified as the zebrafish GSTs that biotransform CDNB with the highest enzyme efficiencies (Glisic et al. 2015). As no adverse developmental effects were observed, it can be assumed that the early expressed GSTs already have the capacity to be simultaneously involved in biotransformation of both xenobiotic and endogenous compounds, provided that the glutathione pool is not depleted.

After formation of the first product of the mercapturic acid pathway, DNP-SG, this product is transported to the cell surface. The respective transporters (ABCC/MRP) are present in the embryo from the onset (Long et al. 2011). The further biotransformation of DNP-SG to DNP-CG and DNP-C occurs in close proximity to the extracellular membrane, by membrane-associated enzymes (Cooper and Hanigan 2018; Pompella et al. 2006). In our study, those intermediate products of the mercapturic acid pathway could not be detected. Though never tested before in zebrafish, some previous studies describe the formation of DNP-CG and DNP-C in different systems, such as isolated liver perfusions and mollusks (Hinchman et al. 1991; Simmons et al. 1991; Trevisan et al. 2016; Vaidya and Gerk 2007). Those studies, however, used higher CDNB concentrations and different dosing systems. DNP-C is reabsorbed by cells and further metabolized to the mercapturic acid form (DNP-NAC) (Cooper and Hanigan 2018; Dilda et al. 2008; Garnier et al. 2014; Hinchman et al. 1998). The formation of the mercapturate was observed in previous studies focusing on the metabolic capacity of rodents, fish and mollusk (Hinchman et al. 1991; Simmons et al. 1991; Trevisan et al. 2016). Considering the fact that we observed DNP-NAC in our study suggests that the intermediate products have been formed as well, but evaded detection due to their low concentration or short-lived nature.

Although the first and last metabolite of the mercapturic acid pathway were observed at all tested life stages, the total amount of the biotransformation products was higher in zebrafish larvae compared to the embryo: after 2 hours of exposure, total amount of products was 4 times and 18 times higher for DNP-SG and DNP-NAC, respectively (Figure 17A, B). Nonetheless, during longer exposure periods, the DNP-SG levels became similar in both life stages and the difference in DNP-NAC levels less pronounced. Data collected in other species indicate that the rate-limiting factor for DNP-SG formation at low CDNB concentrations is the CDNB uptake (Stoelting and Tjeerdema 2000; Wahllander and Sies 1979). Since the chorion does not form a barrier for CDNB, the uptake should be similar between embryo and larvae. As we did not observe toxicity in our

study, the amount and activity of GSTs expressed at any developmental stage seems to be sufficient to counteract the CDNB infusion and keep the concentration of the reactive substrate low. This raises the question why the initial amount of biotransformation products differs between embryo and larvae (Figure 17). We assume that those variations originate from morphological differences. At 4 hpf, the embryo is mostly composed of yolk, whereas at later developmental stages, the protein content (including biotransformation enzymes) increases as the organism becomes more differentiated (Hachicho et al. 2015). These differences in proportion of metabolically active tissue to overall biomass might result in lower metabolite production at early stages of development.

In mammals, the mercapturic acid pathway is considered an inter-organ process characterized by an interplay between liver and kidney. The liver is the major organ responsible for glutathione conjugation while the conversion of glutathione conjugates to cysteine conjugates occurs predominantly in the kidney. The reason for this circumstance is the organ specific distribution of mercapturic acid pathway enzymes, especially of γ -glutamyl transferase, the only enzyme capable of initiating further biotransformation of glutathione-conjugates (Hinchman and Ballatori 1994). However, the γ -glutamyl transferase activity and organ distribution vary considerably between species thereby influencing whether the formed glutathione conjugate is biotransformed on-site to mercapturic acid or transported further *via* circulatory systems (Hinchman and Ballatori 1994). Furthermore, the proportion of each biotransformation product in relation to the overall chemical load depends on the parent compound itself and the concentration applied (Hinchman et al. 1991). At comparable concentrations (61 and 101 ng/ml CDNB), skate and rat livers excreted > 50% of total hepatic biotransformation products as DNP-SG, whereas in guinea pigs DNP-NAC represented the highest proportion of hepatic DNP-conjugates (Hinchman et al. 1991; Simmons et al. 1991). In mollusks, the concentrations of DNP-conjugates varied between organs, with DNP-NAC being the most abundant excreted form (Trevisan et al. 2016).

In order to account for the excretion of mercapturic acids, we enriched and analyzed water samples taken during the experiments, but could not detect any DNP-conjugates. We assume that the excreted conjugates stayed below the detection limit because we used a lower CDNB concentration and a lower ratio of biomass to exposure medium as compared to the studies described above. Since the water samples did not provide any information on the excretion of the biotransformation products, we performed additional exposure and

depuration experiments. The amount of DNP-SG decreased strongly already during the first 24 h of depuration, while the amount of DNP-NAC decreased slowly, but continuously within the timeframe of the experiment. Thus, our data suggest that CDNB is biotransformed within the mercapturic acid pathway and slowly excreted.

4.6 Exposure to the non-toxic concentration of a model electrophile does not affect GST protein expression

It was postulated that, due to their highly reactive nature, electrophilic substances require a detoxification system with a large overcapacity (Rinaldi et al. 2002). In other words, the constituent expression of GSTs is sufficiently high, so that, unless the glutathione pool becomes depleted, a fraction of enzymes is always available to bind the substrate and carry out the conjugation reaction. Therefore, at toxic chemical concentrations, not the GSTs, but the glutathione levels within the organism are the most relevant factor for toxicity (Rinaldi et al. 2002). For this reason, we deliberately used the NtC within this study. Nonetheless, even at low chemical concentrations, a small fraction of chemical can escape the conjugation (Rinaldi et al. 2002). This small, not detoxified amount of chemical is unlikely to cause acute toxic effects but can lead to, e.g., DNA damage and development of cancer in the long term.

Electrophiles that escape conjugation are known to affect the expression of genes involved in cellular defense mechanisms, including GSTs, regulated through the nuclear factor-like 2 (Nrf2) transcription factor (Chanas et al. 2002; Knight et al. 2008; Ma 2013). To analyze whether the non-detoxified CDNB fraction affects the protein expression of GSTs in zebrafish embryo and larvae, we characterized the GST expression with the use of a targeted proteomics method established in Tierbach et al. (2018), (Chapter 2). Our results demonstrate that a single exposure to the NtC of CDNB does not affect GST protein expression. It is plausible that at low concentrations only a few CDNB molecules escape conjugation, remaining below the threshold that triggers an immediate defense mechanism on the protein expression level.

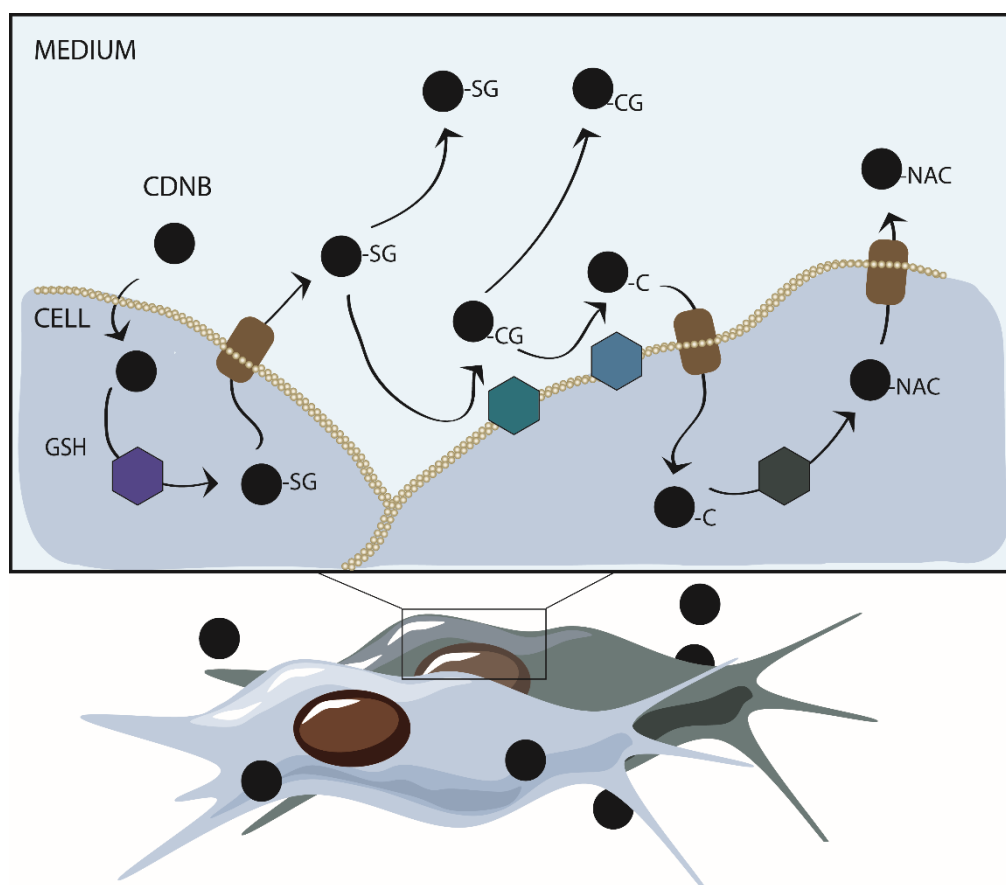
4.6.1 Functionality of mercapturic acid pathway has consequences for the manifestation of toxicity

The mercapturic acid pathway is considered a detoxification mechanism leading to elimination of reactive compounds from the body (Townsend and Tew 2003). However, in some cases, glutathione conjugation can also lead to the formation of toxic metabolites. For instance, 1,2-dihaloalkanes (e.g. 1,2-dibromoethane) can be bioactivated, i.e. increased in toxicity, via glutathione conjugation leading to sulfur mustards, which may

rearrange to reactive episulfonium ions (Armstrong et al. 2018; Bakke and Gustafsson 1984; Monks et al. 1990; Vamvakas and Anders 1991). In this work, we demonstrate that the mercapturic acid pathway is active in zebrafish early life stages; hence, this convenient model has the potential to detoxify or activate drug candidates and environmental pollutants. The results of our study confirm the suitability of this model to not only study detoxification of chemicals but as well the biotransformation-dependent toxicity mechanisms.

Chapter 5 Expression of cytosolic glutathione S-transferases and performance of the mercapturic acid pathway in the zebrafish embryo cell line, PAC2

Alena Tierbach, Ksenia J Groh, René Schönenberger, Kristin Schirmer, Marc J -F Suter



Contributions

I was supported within this project in the following ways:

- Technical assistance in mass spectrometric analysis: René Schönenberger
- Experimental design and discussions: Ksenia J Groh, Kristin Schirmer, Marc J-F Suter
- Reviewing & editing: Ksenia J Groh, Kristin Schirmer, Marc J-F Suter

5.1 Abstract

In view of the steadily increasing number of chemical compounds synthesized for various products and applications, only high throughput toxicity screening techniques can meet the needs of 21st century risk assessment. Zebrafish (*Danio rerio*), especially its early life stages, are increasingly used in such screening efforts. In contrast, cell lines derived from this model, though avoiding the need for animals and being even simpler to maintain and use, have received less attention thus far. One reason is the limited knowledge about their overall capacity to biotransform chemicals and the spectrum of expressed biotransformation pathways.

One important biotransformation pathway is the mercapturic acid pathway, which protects organisms from harmful electrophilic compounds. To be fully functional, it requires a succession of several enzymatic reactions. We analyzed the biotransformation products of the mercapturic acid pathway in the PAC2 cell line, which originates from zebrafish embryo, upon exposure to non-toxic concentrations of the reference substrate 1-chloro-2,4-dinitrobenzene (CDNB). Additionally, we used targeted proteomics to monitor the abundance of classes of cytosolic glutathione S-transferases (GST), the enzyme family catalyzing the first reaction of the pathway.

Our results reveal that the PAC2 cell line expresses a fully functional mercapturic acid pathway. All but one intermediate biotransformation product were identified. We suspect that the 2D cell culture setup and dilution in the culture medium prevented the analysis of the non-detectable intermediate. The presence of the functional mercapturic acid pathway was further supported by the discovery of a large palette of GST classes in the cell line, namely enzymes belonging to the classes zeta, theta, mu, pi, rho and omega. Interestingly, enzymes of the class alpha, one of the dominant GST classes in the zebrafish embryo, were not identifiable; yet this did not seem to affect the capacity of the PAC2 cells to biotransform CDBN. As has previously been shown in zebrafish embryos, the protein expression of the cytosolic GSTs remained unaffected upon exposure to the model electrophile.

The presence of the functional mercapturic acid pathway along with a wide range of classes of GSTs in the PAC2 cell line supports its use in toxicology and chemical hazard assessment. Exploring 3D instead of 2D cultures could be a promising next step as this may facilitate efficient transfer of intermediates within the confines of the cell culture.

5.2 Introduction

State-of-the-art approaches in drug discovery and environmental risk assessment rely on high-throughput technologies that enable affordable screening of large chemical libraries. To make them amenable to high-throughput approaches, test systems have progressively been miniaturized and automated. Cell-based systems are especially suitable for the development of simple and resource-efficient technologies. They can be used in multiwell plate-based assays, with fully automated readout of effects, indicated for instance by changes in color, fluorescence or luminescence of an indicator dye or reporter molecule (Vega-Avila and Pugsley 2011).

The model organism zebrafish is very popular in life sciences and toxicology, and one of the best-researched vertebrates, with well-described morphology, genetics and molecular disease pathways. Surprisingly, zebrafish cell lines are still scarce, and the ones available are not well characterized (He et al. 2006). One issue limiting their application in pharmacological and toxicological studies is the lack of knowledge regarding their biotransformation potential. One such zebrafish cell line is the embryonic PAC2 line, which was derived from 24 hours post fertilization old embryos (Lin et al. 1994). The cell line has previously been successfully applied to cytotoxicity assessment of antibiotics, flame-retardants and model genotoxics (Klobucar et al. 2013; Srut et al. 2015; van Boxtel et al. 2008; van Boxtel et al. 2010).

Many potential drug candidates and environmental pollutants are electrophiles or obtain an electrophilic group during phase I metabolism within the organism. Those electrophiles can undergo reactions with nucleophilic sites in DNA and proteins, and induce long lasting cellular damages. A major detoxification route for electrophilic substances is the mercapturic acid pathway, with the glutathione S-transferase (GST) enzyme family playing the principal role (Armstrong et al. 2018; Cooper and Hanigan 2018) (Figure 19). GSTs catalyze the first reaction of the mercapturic acid pathway, which is the conjugation of the nucleophile glutathione with the electrophilic group of the foreign or endogenous target compound (Armstrong 1997; Habig et al. 1974). The initial conjugation reaction occurs within the cells and subsequently, members of the ATP-binding cassette/multidrug resistance-associated protein transporter family (ABCC/MRP) transport the glutathione conjugate to the cell surface (Ballatori et al. 2009; Ursic et al. 2009). On the cell surface, the conjugate is further biotransformed by membrane-bound γ -glutamyl transferases and peptidases, which results in the one by one removal of the γ -glutamyl and glycyl group from the glutathione conjugate (Cooper and Hanigan 2018; Pompella et al. 2006). The cysteine conjugate produced this way re-enters the cell *via* transporters and is acetylated

to the *N*-acetyl-L-cysteine S-conjugate by *N*-acetyl transferases (Cooper and Hanigan 2018; Dilda et al. 2008; Garnier et al. 2014; Hinchman et al. 1998). The *N*-acetyl-L-cysteine S-conjugate, or rather the mercapturic acid form of the chemical compound, is the final product of the pathway and usually excreted by the cells and eliminated from the body (Cooper and Hanigan 2018; Monks et al. 1990).

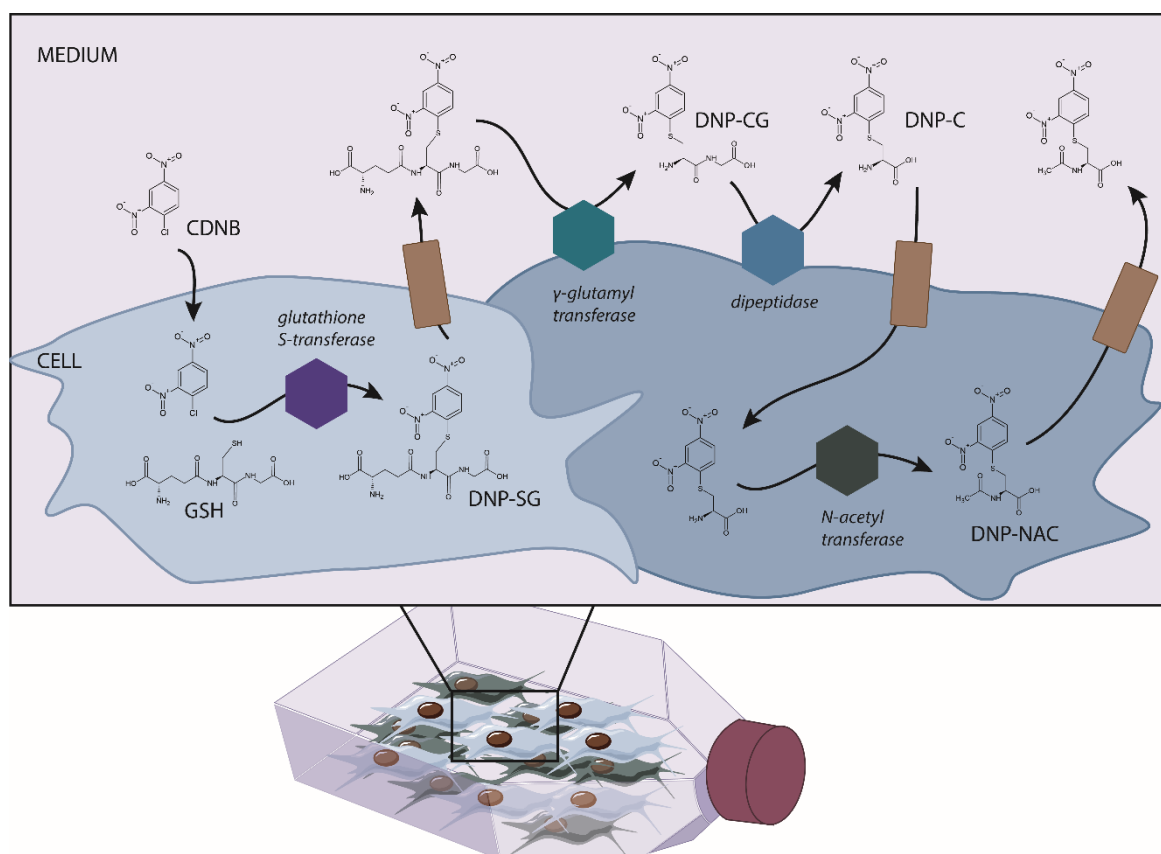


Figure 19: The biotransformation of 1-chloro-2,4-dinitrobenzene (CDNB) through the mercapturic acid pathway in cell lines; CDNB enters the cell and is conjugated with glutathione (GSH) to 2,4-dinitrophenyl-S-glutathione (DNP-SG) which is further biotransformed to 2,4-dinitrophenyl cysteinylglycine (DNP-CG), 2,4-dinitrophenyl cysteine (DNP-C), and 2,4-dinitrophenyl *N*-acetylcysteine (DNP-NAC) – the mercapturate. See Introduction for details on this pathway.

Although the biotransformation of chemicals within the mercapturic acid pathway is generally considered a detoxification route, some chemical groups, including isocyanates and haloalkenes, can be bio-activated to toxic transformation products within the pathway, or through a branching pathway (Armstrong et al. 2018; Bakke and Gustafsson 1984; Monks et al. 1990; Vamvakas and Anders 1991). Therefore, for an accurate interpretation of toxicity data, knowledge about the functionality of the mercapturic acid pathway in cell-based systems is of importance.

Considering the relevance of cell cultures as a replacement for *in vivo* vertebrate models in toxicity testing, we aim to extend the knowledge about the biotransformation capacity of the PAC2 cell line in order to broaden its application field. For the analysis of biotransformation processes within the cells, we used a model substrate, 1-chloro-2,4-dinitrobenzene (CDNB), and measured biotransformation products of the mercapturic acid pathway under typical cell culture conditions with the use of liquid chromatography high-resolution mass spectrometry (LC-HRMS). We moreover monitored the abundance of cytosolic glutathione S-transferases (GST), the enzyme family catalyzing the first reaction of the mercapturic acid pathway.

5.3 Materials and methods

5.3.1 Chemicals and reagents

Nanopure water was obtained from Barnstead Nanopure, Fisher Scientific (United States). Methanol and ethanol for HPLC (gradient grade, $\geq 99.8\%$), formic acid, Versene, Alamer Blue and CFDA-AM were from Fisher Scientific (United States). Dimethyl sulfoxide (DMSO), 3,4-dichloroaniline, 1-chloro-2,4-dinitrobenzene (CDNB), 5-chloro-2,4-dinitrotoluene (CDNT), the Glutathione S-Transferase (GST) Assay Kit (CS0410), and Neutral Red were from Sigma Aldrich (United States). Leibovitz L-15 medium was obtained from Invitrogen (United States) and fetal bovine serum (FBS) from PAA Laboratories (Switzerland). Trypsin was purchased from Biowest (France).

5.3.2 Routine PAC2 cell culture

The PAC2 fibroblast cell line was kindly provided to the Schirmer group by Dr. Nick Foulkes (Max-Planck-Institute for Developmental Biology, Tübingen, Germany). The adherence-dependent cell line was derived from 24 hours post fertilization (hpf) zebrafish embryos (*Danio rerio*) via spontaneous immortalization (Lin et

al. 1994). The cells were routinely cultured in Leibovitz L-15 medium supplemented with 10% FBS at 26 ± 2 °C in ambient atmosphere in an incubator in the dark. The cells were sub-cultured every 5 to 10 days at a ratio of 1:2 to 1:3 after the formation of a confluent monolayer. For subcultivation, cells were washed twice with Versene and detached from the culture surface with trypsin.

5.3.3 CDNB toxicity study

The analysis of CDNB biotransformation products requires the selection of a suitable CDNB exposure concentration such that the products are well detectable with the analytical method while not being cytotoxic. Thus, we defined the non-toxic CDNB concentration (NtC) within our test system by using a modified version of the RTgill-W1 cell line assay (Fischer et al. 2019; Tanneberger et al. 2013).

Preparation of exposure media: A CDNB stock solution with a concentration of 3.2 mg/ml was prepared freshly in DMSO on the day of exposure. A dilution series of CDNB was established in DMSO such that a 200-fold dilution in the final exposure medium yielded nominal concentrations of 1'600, 1'280, 1'024, 819.2, 655.36 and 419.43 ng/ml with a final DMSO content throughout of 0.5% (v/v). The exposure dilutions were well mixed by inverting and 10 min shaking on a horizontal shaker. 1 ml of each exposure medium was sampled and stored at -20 °C for the verification of exposure concentrations.

Exposure experiments: PAC2 cells were seeded in L-15 medium supplemented with 10% FBS at a cell seeding density of 30'000 cells/ml into 24-well plates (approximately 316'000 cells/cm²). After 24 h, the attached cells were washed with 2 ml L-15 medium supplemented with 5% FBS to match the exposure medium. Subsequently, the cells were exposed in paraffin-sealed plates for 24 h in the dark at 26 °C to different CDNB concentrations in 2 mL exposure dilutions as explained above.

Cell viability assessment: The cell responses to different CDNB concentrations were tested in three independent biological replicates with cells originating from different passage numbers (passage 69 to 71). To assess the cell viability, tests with three fluorescent dyes were performed on the same set of cells, where Alamar Blue was used to measure metabolic activity, 5-carboxyfluorescein diacetate acetoxy-methyl ester (CFDA-AM) to assess cell membrane integrity and Neutral Red to measure lysosomal integrity (Fischer et al. 2019; Tanneberger et al. 2013).

Verification of CDNB exposure concentration: CDNB concentrations in the exposure dilutions were determined using a quadrupole-orbitrap mass spectrometer (QExactive Plus, Thermo Scientific, United States) and atmospheric pressure chemical ionization in negative ion mode (APCI(-)). CDNB was quantified with the method developed in Tierbach et al. (2020), (Chapter 3), with a limit of quantitation of ≥ 17 ng/ml without enrichment, using dissociative and non-dissociative electron capture ions originating from the CDNB precursor under APCI.

5.3.4 Exposure experiments for the analysis of CDNB biotransformation and GST expression

To investigate the performance of the mercapturic acid pathway within the PAC2 embryonic cell line, we analyzed the formation of CDNB biotransformation products after the exposure to a non-toxic CDNB concentration. In addition, we investigated the regulation of GST enzymes on the protein level during the exposure. Both exposures, for the analysis of biotransformation products and the protein expression, were run in parallel in four independent biological replicates with the passage numbers 71 to 74.

Preparation of exposure media: A CDNB stock solution with a concentration of 7.4 mg/ml was prepared freshly in DMSO at the day of exposure. Subsequently, a dilution was prepared in DMSO such that a 200-fold dilution in the final exposure medium yielded nominal concentrations of 368 ng/ml with a final DMSO content of 0.5% (v/v).

Exposure experiments: Prior to exposure, cells were seeded in L-15 medium supplemented with 10% FBS at a cell seeding density of 60'000 cells/cm² into T-75 cell culture flasks. After 24 h, the attached cells were washed with 10 ml of the exposure medium, i.e. L-15 supplemented with 5% FBS. Subsequently, the cells were exposed to the CDNB non-toxic concentration for 24 h at 26 °C in the dark. In parallel, control samples were prepared by cultivating cells in CDNB-free medium under the same conditions. The sampling was performed according to the following procedure: at the respective time-point, the exposure medium (10 ml from each of the two flasks) was removed from the cells, transferred to clean sampling glass vials and stored at -20 °C. The cells were washed once with L-15 medium supplemented with 5% FBS, then twice with Versene, and detached from the flask surface through trypsinization, and centrifuged down for 3 min at 1000 rcf. The pellet was re-suspended in 1 ml phosphate-buffered saline (pH 7), transferred to a clean 1.5 ml Eppendorf tube, and centrifuged down for 5 min at 10'000 rcf. After the supernatant was removed, the samples were snap-frozen in liquid nitrogen and stored at -80 °C. Samples were taken after exposure durations of 1, 3, 6

and 24 h. Unexposed cells were sampled at the 24 h time point as control for CDNB biotransformation and at the 1, 3, 6 and 24 h time points as control for the GST protein levels.

5.3.5 Analysis of CDNB biotransformation products in PAC2 cells and exposure medium

Prior to all sample preparations, cell and medium samples were spiked with 2.5 µl of a reference standard, 2,4-dinitrotoluene-S-glutathione (DNT-SG), as described in Chapter 4. The extraction of CDNB biotransformation products from the cells was performed according to the method established in Chapter 4, with some modifications. Briefly, the samples were thawed, taken up in 500 µl methanol and homogenized. Subsequently, the sample lysate was centrifuged (6 min, 10'000 rcf, RT), the supernatant filtered, evaporated and re-dissolved in 25 µl nanopure water with 0.1% formic acid.

Exposure medium was collected at each time point from cells exposed to CDNB for GST protein and CDNB biotransformation analysis. The exposure medium collected at the same time point was subsequently pooled, resulting in a total volume of 20 ml. To clean and enrich the CDNB biotransformation products, the samples were acidified through addition of 0.1% formic acid and 15 ml were loaded onto reversed-phase cartridges (Sep-Pak Vac tC18, Waters, United States). The samples were eluted with 800 µl of 80% aqueous acetonitrile solution with 0.1% formic acid, evaporated using a vacuum centrifuge at 30 °C, re-dissolved in 25 µl nanopure water with 0.1% formic acid, and stored at 4 °C. The LC-HRMS analysis of CDNB biotransformation products in cells and in medium samples was performed as described in detail in Chapter 4.

5.3.6 Protein expression analysis

Protein extraction and trypsin digestion were performed as described in Chapter 2 (Tierbach et al. 2018). Briefly, the collected cells were homogenized in lysis buffer and the proteins precipitated using the methanol/chloroform method. Subsequently, proteins within each sample were digested with trypsin at 37 °C for 16 h. The samples were desalted using reversed-phase cartridges (Sep-Pak Vac tC18, Waters, USA) and stored at 4 °C or immediately measured on the TSQ Vantage (Thermo Scientific, United States).

5.3.7 Data evaluation

Data presentation and statistics: Data visualization, t-test (to analyze changes in protein expression upon exposure to CDNB) and one-way ANOVA (to analyze differences in EC₅₀/NtC calculated based on different fluorescent dyes) were performed using GraphPad Prism version 7.05 for Windows (GraphPad Software, La Jolla California USA, www.graphpad.com). Values were considered significantly different if $p < 0.01$.

Cell viability assessment: The background fluorescence of CDNB was subtracted from data obtained with the three fluorescent dyes (Alamar Blue, CFDA-AM and Neutral Red) and normalized to a CDNB-free solvent control. The EC₅₀ and NtC were calculated based on the nominal and measured concentrations with an algorithm described by Stadnicka-Michalak et al. (2018).

Analysis of biotransformation products: The analysis of mass spectrometric data of CDNB biotransformation products was performed with Thermo Xcalibur 3.0.63 (Thermo Fisher Scientific Inc.) as described in Chapter 4.

Analysis of GST expression: The analysis of targeted proteomics data was performed with Skyline (MacLean et al. 2010) as described in Chapter 2 (Tierbach et al. 2018).

5.3.8 Supplementary information Chapter 5

The Supplemental Information (Chapter 5) provides data on the nominal and measured CDNB concentrations at the beginning (SI Table 16) and at the end of the toxicity experiments (SI Table 17). This data was used to verify the exposure concentrations and to calculate the geometric mean. SI Figure 8 shows the dose response curves representing cell viability measured with the use of three fluorescent dyes, Alamar Blue, CFDA-AM, and Neutral Red based on the nominal-, measured- and the geometric data. The mean EC₅₀ and NtC values of the three dyes modelled based on the nominal-, measured- and the geometric data are summarized in SI Table 18. In addition, the Supplemental Information provides chromatograms and mass spectra of the analytes DNT-SG (standard, SI Figure 9), DNP-SG, DNP-CG and DNP-NAC (SI Figure 10), and the difference (ppm) between the measured and predicted isotopes of the respective analytes (SI Table 19). SI Figure 11 shows the chromatogram and the MS2 fragmentation pattern of the analyte DNP-SG. The basal expression of cytosolic GSTs in PAC2 cells cultured in L15 medium supplemented with 5% FBS is shown in SI Figure 12 and the kinetic model output of the CDNB concentration in T75 cell culture flasks in a cell-free system (Fischer et

al. 2018) is shown in SI Figure 13. Furthermore, the first part (A) provides a short note about the generation of DNP-CG through gas-phase reactions in the ESI source.

Supplemental Information (Chapter 5) also contains data about sample name and identifiers, peak area of the analytes and the peak area of analytes normalized to the standard DNT-SG measured during CDNB exposure experiments in PAC2 cells (SI Table 20) and in the medium (SI Table 21). In addition, it contains data on the cytosolic GST expression in PAC2 cells exposed to CDNB non-toxic concentration (NtC) (SI Table 22) and raw data on CDNB measurements during the exposure experiments in presence and in absence of cells (SI Table 23).

5.4 Results

5.4.1 Determination of EC₅₀ and non-toxic CDNB concentrations

To define the toxic range and the non-toxic concentration (NtC) of CDNB, we assessed the cell viability of PAC2 cells by using fluorescent dyes that reflect the state of metabolic activity (Alamar-Blue), cell membrane integrity (CFDA-AM) and lysosomal integrity (Neutral Red) (SI Figure 8).

We calculated the median effect concentration (EC₅₀) and the NtC based on 3 datasets; the first calculations were based on the nominal concentrations EC₅₀ (nominal) / NtC (nominal), the second calculations were based on measured CDNB starting concentrations EC₅₀ (measured)/NtC (measured) (SI Table 16), and the third calculations were based on the geometric mean of concentrations measured at the beginning and at the end of the exposure (C_{0h} and C_{24h}) EC₅₀ (geomean)/NtC (geomean) (SI Table 17). We did not observe a significant difference between EC₅₀/NtC values calculated based on different fluorescent dyes (Alamar Blue, CFDA-AM and Neutral Red). Therefore, average numbers (\bar{x}) were used for toxicity assessment. Within the experiments, we observed an EC₅₀ (\bar{x} nominal) of 886 ng/ml and NtC (\bar{x} nominal) of 398 ng/ml, an EC₅₀ (\bar{x} measured) of 482 ng/ml and NtC (\bar{x} measured) of 181 ng/ml and an EC₅₀ (\bar{x} geomean) of 220 ng/ml and NtC (\bar{x} geomean) of 86 ng/ml (SI Figure 8, SI Table 18). The discrepancy between nominal vs measured values reflects the fact that the measured CDNB concentration was lower than the nominal concentration by an average value of 42% (SI Table 16). However, the relative standard deviation between the media prepared for different replicates was acceptable ($\leq 17\%$).

For biotransformation studies, it is important to use a substrate concentration that does not yield an effect significantly different from the control, and thus is not expected to exceed the capacity of the detoxification system. To account for possible effects caused by the medium preparation and to avoid toxicity, we have chosen the lowest NtC_(nominal) of 368 ng/ml (SI Figure 8D, CFDA-AM) for biotransformation studies.

5.4.2 Kinetics of CDNB in the culture system

Throughout the entire duration of the biotransformation experiments, the CDNB concentration in the exposure medium was measured in two different experimental setups: in cell-free and cell-containing culture systems. In the cell-free culture system, the CDNB concentration decreased continuously until, after 24 hours of incubation, only 22% of the initial CDNB load remained in the medium (Figure 20).

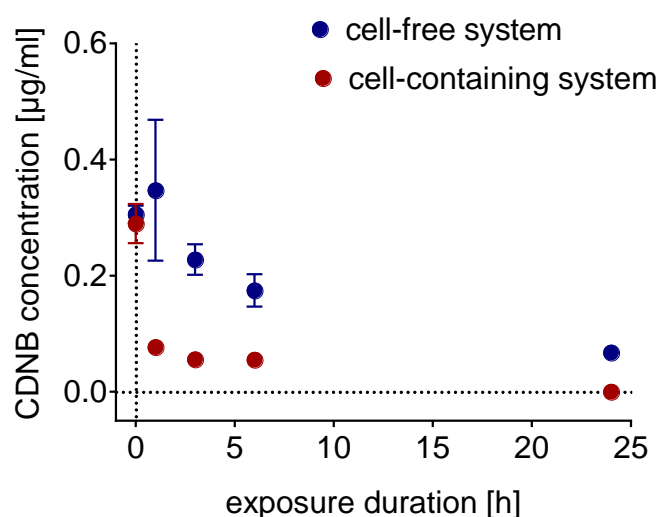


Figure 20: Measured 1-chloro-2,4-dinitrobenzene (CDNB) medium concentrations in cell-free (blue) and cell-containing (red) systems. The data is shown as mean of 4 replicates from cell-containing systems and 3 replicates from cell-free systems. Vertical lines indicate the standard deviation.

In the cell-containing system, the CDNB concentration decreased rapidly within the first hours of exposure and continued to decrease slowly thereafter. At the end of the experiment (24 hours of exposure), no CDNB could be detected in the medium in the cell-containing culture setup (Figure 20).

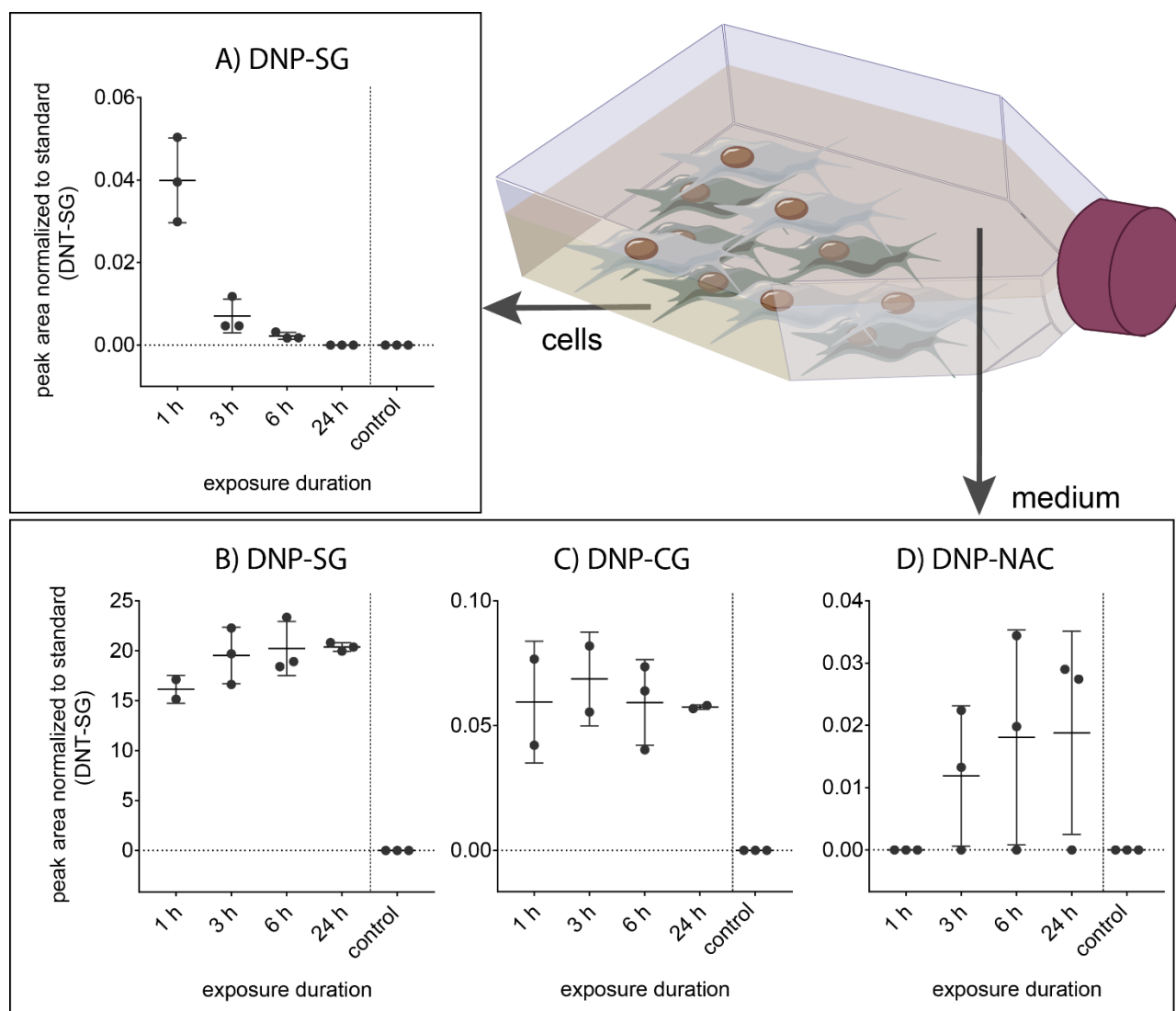


Figure 21: Biotransformation products present in PAC2 cell lines (A) and medium (B, C, and D) upon cell exposure to the non-toxic concentration of 1-chloro-2,4-dinitrobenzene (CDNB). Cells (1 confluent T75 culture flask/replicate) and medium (15 ml) were sampled after 1, 3, 6, and 24 exposure hours. Control cells (not exposed) were sampled at the 24 hour time point. A) and B) 2,4-dinitrophenyl-S-glutathione (DNP-SG) measured in cells and medium, respectively. C) 2,4-dinitrophenyl cysteinylglycine (DNP-CG) measured in medium and D) 2,4-dinitrophenyl N-acetylcysteine (DNP-NAC) measured in medium. 2,4-dinitrophenyl cysteinylglycine (DNP-CG) was not detected. Data represents the peak area normalized to the standard 2,4-dinitrotoluene-S-glutathione (DNT-SG). Each replicate is shown in addition to the mean and standard deviation. For further information, please refer to Supplemental Information 5 B.

5.4.3 Identification of biotransformation products of the mercapturic acid pathway

All but one of the four biotransformation products of the mercapturic acid pathway were identified in cells and/or the exposure medium. Their identity was confirmed by the excellent fit of the mass determined, the characteristic isotope ratios and fragmentation pattern as described in Chapter 4 (Figure 21, SI Figure 9, SI Figure 10, SI Figure 11, SI Table 10 and 19). Within PAC2 cells, the highest concentration of the first mercapturic acid pathway biotransformation product, 2,4-dinitrophenyl-S-glutathione (DNP-SG), was detected at the earliest sampling point (1 h of exposure). Subsequently, its concentration decreased continuously in the cells and reached a value below the limit of detection at 24 hours of exposure. No further biotransformation products of the mercapturic acid pathway could be detected in the PAC2 cells (Figure 21A).

In addition, analysis of the exposure medium revealed the presence of DNP-SG. DNP-SG was detected already after 1 hour of exposure and its concentration increased thereafter (Figure 21B). Additionally, we detected two further 2,4-dinitrophenol conjugates, 2,4-dinitrophenyl cysteinylglycine (DNP-CG) and 2,4-dinitrophenyl N-acetylcysteine (DNP-NAC). These CDNB biotransformation products were detected after 1 (in case of DNP-CG), 3, 6 and 24 exposure hours in more than one replicate. However, compared to DNP-SG, their signal intensity was rather low (Figure 21C, D). One biotransformation product of the mercapturic acid pathway, 2,4-dinitrophenyl cysteine (DNP-C), was neither detected in cells nor medium samples.

5.4.4 Analysis of GST protein expression upon exposure to CDNB

The cytosolic GST family contains isoenzymes that are grouped into different classes: alpha, zeta, theta, mu, pi, rho and omega. Within the PAC2 cells, we could detect the expression of enzymes belonging to the classes zeta, theta, mu, pi, rho and omega while members of the class alpha were not detected (Figure 22, SI Figure 12). While some slight changes in expression levels were detected in CDNB-free medium (SI Figure 12) no changes in response to CDNB exposure occurred (Figure 22).

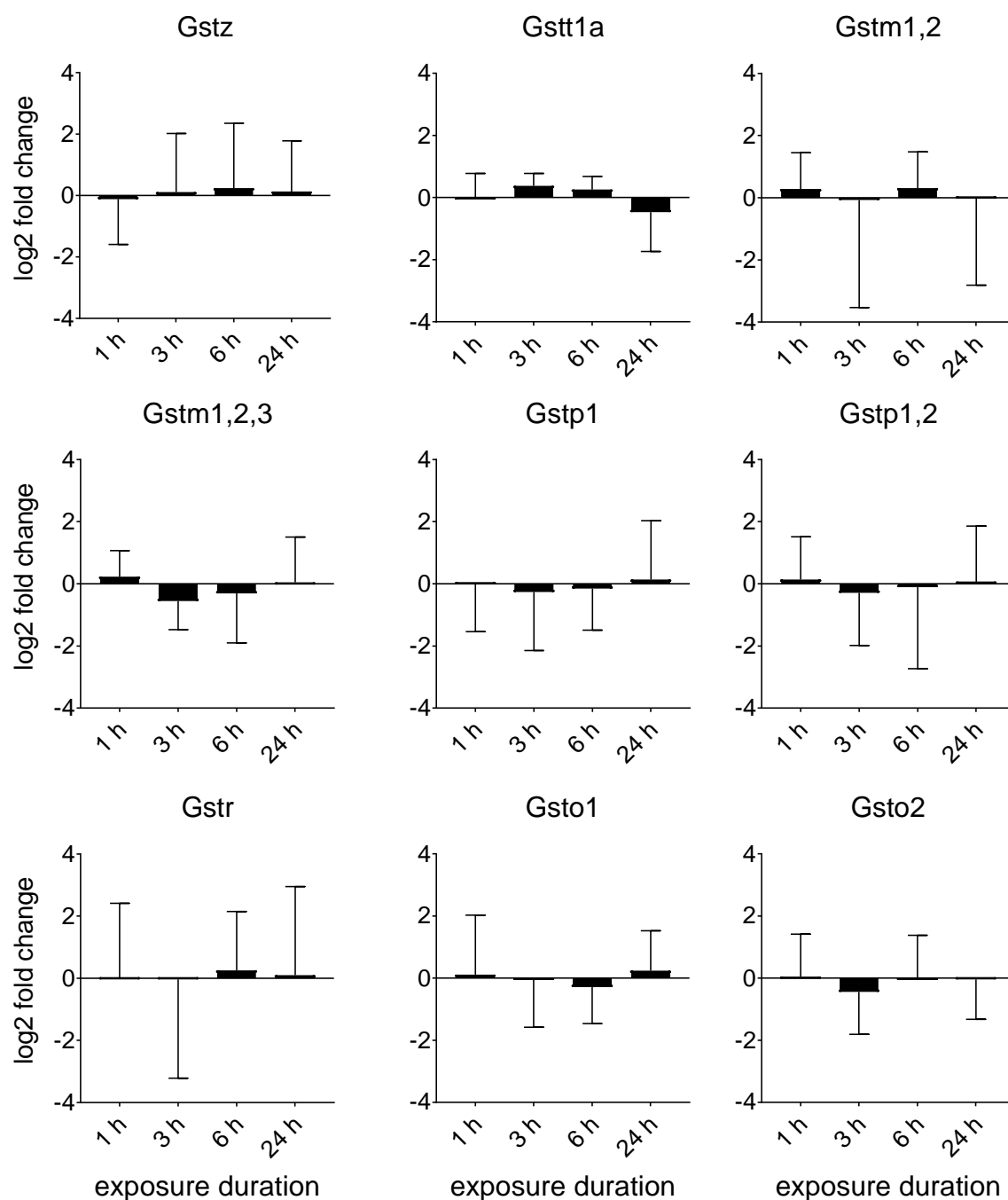


Figure 22: Expression of cytosolic GSTs in the PAC2 cell line exposed to the non-toxic concentration of 1-chloro-2,4-dinitrobenzene (CDNB) for 1, 3, 6, and 24 hours. Data is normalized to the housekeeping proteins β -actin and 40S ribosomal protein S18 and shown as log₂ fold change to the respective CDNB-free control taken at the same time point. The mean of four replicates (1 T75 cell culture flask) and standard error are shown. For expression analysis, the normalized peak area of peptides belonging to the same enzyme or several isoenzymes from the same class were cumulated. No significant differences between exposure and control samples taken at the same time point were observed ($p > 0.01$, unpaired t-test). For further information, please refer to Supplemental Information 5 B.

5.5 Discussion

Knowledge about active biotransformation pathways in model systems, such as cell cultures, and their consequences for the manifestation of toxicity is required for understanding and predicting toxicity. With the aim to shed some light on an important phase II biotransformation route, we characterized the mercapturic acid pathway in the zebrafish embryonic cell line PAC2 with the use of a model compound, CDNB.

5.5.1 CDNB concentrations in cell-free and cell-containing systems show different kinetics

Within the timeframe of our biotransformation experiments (24 h), the CDNB concentration considerably decreased in cell-free systems. Abiotic degradation of CDNB due to light exposure or hydrolysis is unlikely to cause a reduction in the CDNB starting concentration because the culture plates were incubated in the dark, and the compound lacks functional groups susceptible to abiotic hydrolysis (HSDB 2019). Sorption of CDNB to the polystyrene of cell culture flasks is possible, but explains only a small fraction of CDNB loss over time. A loss of 4% only can be predicted by diffusion into plastic (SI Figure 13) based on a kinetic model by Fischer et al. (2018). The model takes into account the log K_{ow} (CDNB log K_{ow} =2.89 (Debnath et al. 1991)), the amount of FBS% in the medium, the medium volume and the polystyrene area in contact with the exposure solution. The comparison of CDNB log K_{ow} with two chemicals analyzed in a previous study by Stadnicka-Michalak et al. (2014) (malathion with log K_{ow} of 2.36 and cyproconazole with log K_{ow} of 2.9), also suggests a low partitioning into plastic. The Henry's Law constant (CDNB k_H = 2×10^{-6} [m³·atm/mol], (HSDB 2019)), which is in the same order of magnitude as ethanol (k_H = 5×10^{-6} [m³·atm/mol], (Sander 2011)), on the other hand indicates that evaporation from the medium surface could occur and contribute to CDNB loss over time (HSDB 2019). However, CDNB showed a more rapid disappearance in cell-containing systems, most prominently during the first hours of exposure. The clear divergence between cell-free and cell-containing culture systems strongly indicates that CDNB is taken up and biotransformed by PAC2 cells.

5.5.2 CDNB acute toxicity in PAC2 cells is similar to acute toxicity in other aquatic organisms

For a wide range of chemicals, the highest agreement between *in vivo* and *in vitro* toxicological data was found when the EC₅₀ values were based on the geometric mean of concentrations measured at the beginning and at the end of the exposure (c_{0h} and c_{24h}) (Tanneberger et al. 2013). Therefore, for the comparison of CDNB

toxicity in PAC2 cells with other aquatic organisms, we use EC₅₀ (\bar{x} geomean) and NtC (\bar{x} geomean) values. The toxicity study with the PAC2 cell line yielded an EC₅₀ (\bar{x} geomean) of 220 ng/ml, which is 4 times higher than the EC₅₀ of zebrafish early life stages (*Danio rerio*, 96 h zFET, EC₅₀=56 ng/ml, Chapter 4). However, the PAC2 EC₅₀ is still within the same range of median lethal concentrations (LC₅₀) previously published for other aquatic organisms, such as fish (*Poecilia reticulata*, LC₅₀ (14 d)=200 ng/ml), water flea (*Daphnia magna*, LC₅₀ (48 h)=800 ng/ml and LC₅₀ (21 d)=430 ng/ml) and rotifer (*Brachionus calyciflorus* LC₅₀ (24 h)=1300 ng/ml) (HSDB 2019). The NtC (\bar{x} geomean) was calculated to be 86 ng/ml, which is again roughly 4 times higher than the NtC of zebrafish early life stages (*Danio rerio*, 96 h zFET, NtC=25 ng/ml, Chapter 4). One apparent difference between the cell-based assay and the zFET is the exposure medium composition. It is possible that CDNB adsorbs onto proteins and lipids present in the cell exposure medium, which may result in a reduced free substance concentration and thus to a reduced toxicity.

5.5.3 All but one cytosolic GST class is detectable in the PAC2 cell line

The GST enzyme family catalyzes the initial reaction of the mercapturic acid pathway. This important group of enzymes has previously been characterized in zebrafish early life stages (age 4 to 168 hpf) and organs of adult zebrafish (Tierbach et al. 2018), (Chapter 2). It was shown that only enzymes belonging to the cytosolic GST classes alpha, mu, pi, rho and omega are expressed in zebrafish embryos (age 4 to 48 hpf), while in free swimming larvae (75 to 168 hpf) and in adult fish all cytosolic GST classes are present (Tierbach et al. 2018), (Chapter 2). The PAC2 cell line was derived from 24 hpf old embryos. It shows a large overlapping expression of GSTs, but also some differences compared to the donor organism. In addition to mu, pi, rho and omega, the GST classes zeta and theta were identified in the embryonic cell line, while the class alpha was missing. Similar to our findings, microarray data provided by He et al. (He et al. 2006) revealed the expression of GST classes mu, pi, rho, omega, and theta in PAC2 cells, while no information was provided on the GST classes alpha and zeta (He et al. 2006). Based on these data, it might be argued that the GST class alpha is absent in PAC2 cells. However, an alternative explanation would be that the enzymes are regulated in the cell line by posttranslational modifications. Modified peptides would then not be detected by our targeted proteomics method. It is not surprising that cultured cells have a protein expression pattern or posttranslational regulation distinct from the donor organism, which may e.g. be due to adaptations to cell culture conditions. Based on microarray data, it was previously concluded that the gene expression of PAC2 cells differs to some extent

from 24 hpf old zebrafish embryo (He et al. 2006). Especially for fish cells, adaptations are expected, since no culture medium can truly mimic all physiological conditions of a fish.

It has been hypothesized that the GST class alpha plays an important role in detoxification of therapeutic drugs, carcinogens and environmental pollutants (Hollman et al. 2016). This assumption is supported by the fact that, in adult human liver, GSTA1 is the most abundant cytosolic GST isoenzyme (Coles and Kadlubar 2003; Mainwaring et al. 1996; Rowe et al. 1997). In zebrafish as well, the class alpha showed strong hepatic expression (Tierbach et al. 2018), (Chapter 2). Nevertheless, based on the fact that GSTs have overlapping substrate specificities (Glisic et al. 2015; Mannervik and Danielson 1988), we think that a possible lack of GST class alpha has no substantial consequences for the biotransformation capacity of PAC2 cells.

5.5.4 Cytosolic GST protein expression is not affected by low concentrations of a model substrate

Upon a single exposure to the non-toxic concentration of the model electrophile, CDNB, the protein expression of cytosolic GSTs was not affected. These results are in agreement with a study performed with zebrafish early life stages (Chapter 4) where it was shown that exposure to a low CDNB concentration does not alter cytosolic GST expression.

GSTs are known to be regulated by several responsive elements involved in xenobiotic defense, including antioxidant or electrophile responsive element (ARE/EpRE), (Knight et al. 2008; van Bladeren 2000) aryl hydrocarbon receptor (AhR) (Higgins and Hayes 2011; Knight et al. 2008) and nuclear factor-like 2 (Nrf2) transcription factor (Chanas et al. 2002; Knight et al. 2008; Ma 2013). It is probable that the cellular damage caused by low CDNB concentrations remains below the level necessary to activate a cellular defense mechanism on the protein level.

5.5.5 Mercapturic acid pathway is functional in PAC2 cells

Based on the identification of all but one biotransformation product of the mercapturic acid pathway, the pathway appears fully available in the PAC2 cell line. In agreement with our observations, raw microarray data provided by He et al. (2006) reports expression of GSTs, one γ -glutamyl transferase, several dipeptidases and N-acetyltransferases within PAC2 cells, thus indicating the pathways availability. However, in direct comparison to zebrafish embryo and larvae, it becomes apparent that the transfer of biotransformation products along

the pathway is less efficient in the cell line as compared to the full organism, since DNP-SG is the only detected transformation product in the cells and the most intense in the medium (Figure 19).

In a complex organism, such as a zebrafish embryo, the intracellular space is limited. Therefore, DNP-SG transported out of a cell stays in close proximity to cell surfaces, where it is further biotransformed to DNP-CG and DNP-C. The DNP-C produced close to the cell surface is transported into the cell, where it can be acetylated to DNP-NAC (Figure 19). The biotransformation of DNP-SG to DNP-NAC is fast and efficient, so that the intermediate products do not reach a concentration detectable by available LC-MS techniques (Chapter 4). The study described in Chapter 4 showed that this complex chain of biochemical reactions is complete in zebrafish embryos with DNP-NAC being the excreted form. However, under cell culture conditions, particular factors appear to impede this smooth process. The cells are in contact with the medium volume of 10 cm³. Here, DNP-SG transported out of the cell is diluted in the culture medium, which results in a reduced likelihood of the DNP-SG conjugate reaching the membrane-bound γ -glutamyl transferases. Therefore, only a few molecules get further biotransformed by γ -glutamyl transferases to DNP-CG. A fraction of the produced DNP-CG becomes attenuated in the exposure medium while the remaining molecules are further biotransformed to DNP-C. We propose that not all DNP-CG molecules were efficiently further biotransformed so that we were able to detect this intermediate product in the exposure medium. Once DNP-C is formed, it is transported into the cell and acetylated to DNP-NAC. DNP-NAC is the final product of the mercapturic acid pathway, which is efficiently excreted into the surrounding medium (Figure 19).

We conclude that, although PAC2 cells express all enzymes involved in the mercapturic acid pathway and have the potential to perform all reactions of the mercapturic acid pathway, the two dimensional nature of traditional cell cultures appears to impair the pathways efficiency. We therefore suggest the use of 3D cultures as one avenue to overcome limitations of the conventional cell culture setup. We show that the GST expression of the PAC2 cell line differs from the expression pattern of zebrafish early life stages and adult fish. However, this does not affect the cell line's potential to biotransform the model compound CDNB to the respective glutathione conjugate.

Chapter 6 Conclusion and outlook

In this thesis, I characterized the mercapturic acid pathway within zebrafish early life stages and the zebrafish embryo-derived PAC2 cell line with a particular focus on the cytosolic enzyme family, glutathione S-transferases (GSTs), which catalyzes its first step, the conjugation with glutathione. The presence and functionality of this important phase II transformation pathway in both examined test systems highlights the value of zebrafish early life stages and PAC2 cells for toxicological investigations and emphasizes their potential to refine and replace animal experimentations.

The key conclusions of this thesis are:

- A wide range of CDNB exposure concentrations for zebrafish embryo and PAC2 toxicity studies could be verified with the use of HPLC-APCI(-)-MS. In addition, CDNB biotransformation products could be successfully analyzed *via* HPLC-ESI(+)-MS.
- GST expression in early life stages of zebrafish is dynamic and reflects important developmental events, e.g. hatching and liver development.
- In adult zebrafish, GST expression is organ-dependent, with most of the GST classes showing the highest expression in the liver.
- PAC2 cells express all classes of cytosolic GSTs, with the exception of GST class alpha.
- The protein expression of cytosolic GSTs in zebrafish early life stages and the PAC2 cell line is not affected by non-toxic CDNB concentrations.
- The mercapturic acid pathway is present and functional in zebrafish early life stages and the PAC2 cell line.

This thesis contributes valuable information regarding the biotransformation potential of zebrafish early life stages and the PAC2 cell line. However, further effort is needed to evaluate these alternatives to animal testing and improve chemical risk assessment. In the following part, I will set the key outcomes of my thesis into perspective for future research.

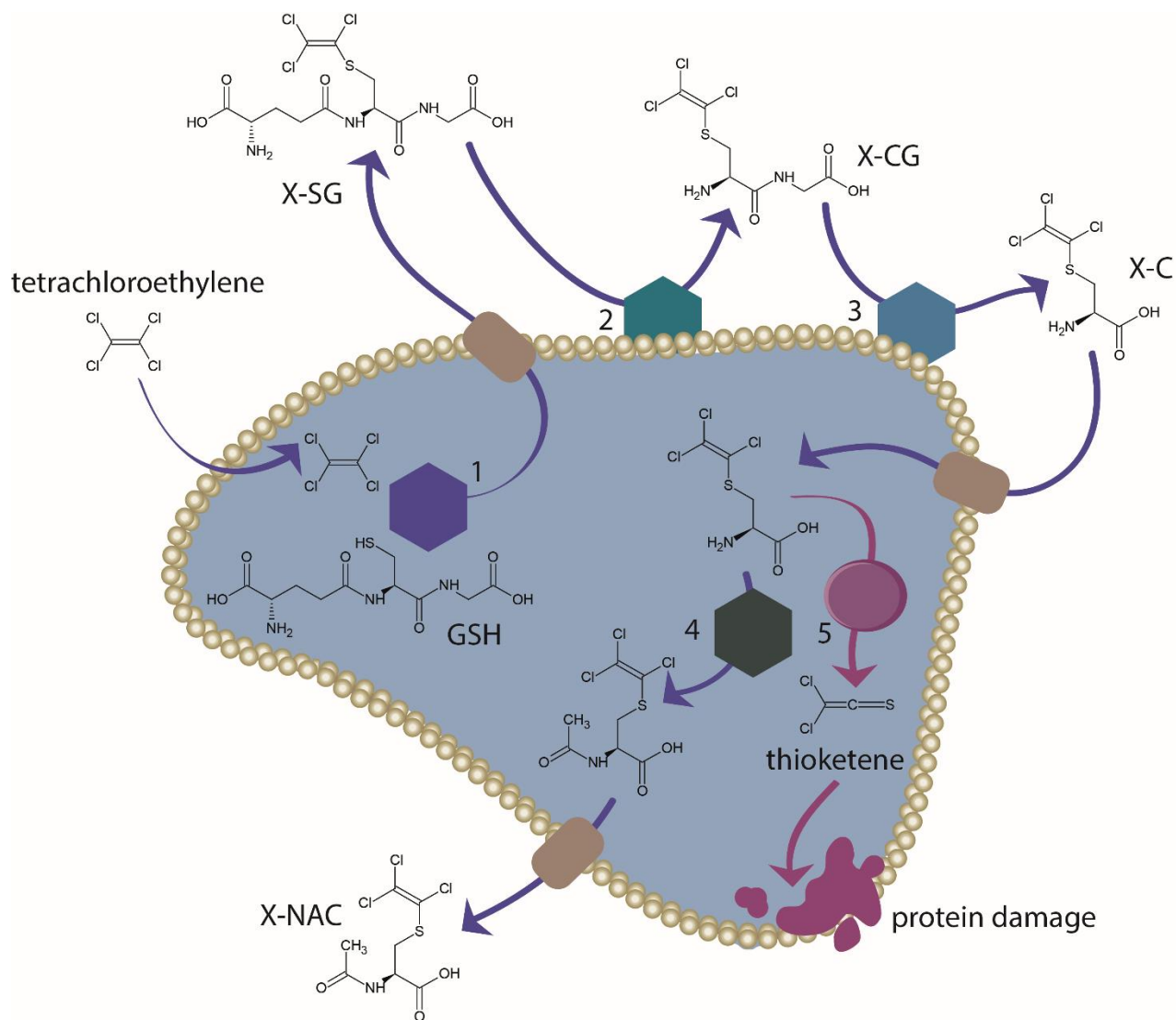


Figure 23: Schematic representation of the mercapturic acid pathway. The electrophilic compound (tetrachloroethylene) is conjugated to the glutathione conjugate (X-SG) by glutathione S-transferases (1) and is further biotransformed to cysteinylglycine (X-CG) by γ -glutamyl transferases (2), cysteine (X-C) conjugate by peptidases (3) and to mercapturic acid (X-NAC) by N-acetyl transferases (4). As tetrachloroethylene has a good leaving group in the β -position to the cysteine conjugate (Cl) it can be biotransformed by β -lyase (5), which results in activation of the chemical compound by production of thioketene, which induces protein damage (shown in purple). The enzymes are represented as circles while rounded rectangles represent different types of transporters. Adapted from (Anders 2004).

6.1 Future directions in the study of glutathione S-transferases

Since the publication of Chapter 2 that focuses on the protein expression of cytosolic GSTs in zebrafish (Tierbach et al. 2018), multiple studies were published describing functional characterizations of specific GST isoenzymes, analysis of interactions between zebrafish GSTs and environmentally relevant organotin compounds, and mapping of organ-specific GST activity (Basica et al. 2019; Mihaljevic et al. 2020; Rastogi et al. 2019). These efforts reflect the interest of the research community in GSTs and their importance in xenobiotic biotransformation. However, the following knowledge gaps need to be addressed for a more complete characterization of this enzyme family.

Now that we have described the dynamics of GST expression during early zebrafish development and the differences in GST expression in organs of adult fish (Tierbach et al. 2018), (Chapter 2), it would be of interest to quantitatively compare the expression of the different GST isoenzymes in zebrafish early life stages, adults and cell lines. Quantitative proteomics information would provide valuable insight into the expression ratios between enzyme classes. In addition, it would allow a direct comparison of expression levels between zebrafish early life stages, adults and cell lines. This can be achieved using isotope-labelled standard peptides, in combination with the targeted proteomics technique presented in Chapter 2 (Tierbach et al. 2018). In addition, established labelling techniques such as isobaric tag for relative and absolute quantitation, iTRAQ (Ross et al. 2004), or stable isotope labeling by amino acids in cell culture, SILAC (Ong et al. 2003), can provide valuable relative quantification data.

In addition to the cytosolic GST classes, the zebrafish genome contains the enzyme classes kappa (located in the mitochondria) and MAPEG (membrane-associated enzymes located in the endoplasmic reticulum). These enzyme classes perform biotransformation reactions and contribute to the overall biotransformation capacity. The sample preparation routine presented in Chapter 2 (Tierbach et al. 2018) however is optimized for the detection of soluble, cytosolic proteins. Thus, proteins expressed in organelles and hydrophilic membrane proteins will most likely be missed. However, for a complete picture of zebrafish GSTs it is of interest to also analyze the expression of these additional GST classes. Nowadays, several techniques are available for organelle enrichment and proteomics techniques particularly optimized for the study of membrane proteins have been established (Palmfeldt and Bross 2017; Prados-Rosales et al. 2019). These techniques can be adapted for zebrafish, providing great potential to increase the GST family coverage and close the knowledge

gap regarding the protein expression of non-cytosolic GSTs in zebrafish and zebrafish based alternative test systems.

From our study dealing with cytosolic GST classes, we know that their expression remains unaffected upon exposure to low concentrations of model substrates (Chapter 3 and 4). This is not surprising, since the expression of GSTs is high enough at all stages to empty the GSH pool within seconds (Rinaldi et al. 2002). Therefore, not the GST expression level but the GSH concentration is the most important factor affecting acute toxicity (Rinaldi et al. 2002). However, it cannot be excluded that repeated dosing of a chemical at low concentration could lead to GST regulations (Spriggs et al. 2016) indicating cell adaptation to chronic toxicity. Studies of cellular adaptation to repeated exposures to low chemical concentrations are of great value for regulatory authorities, because they more closely represent the environmental exposure scenario.

6.2 Further analysis of the mercapturic acid pathway and its branches

A large fraction of electrophile parent compounds and phase I activated metabolites are biotransformed within the mercapturic acid pathway. My thesis research has shown that this important biotransformation route is complete and functional in zebrafish early life stages and PAC2 cell lines. As the methods developed in Chapter 3 and 4 are transferable to other organisms and their cell lines, it would be of interest to investigate similarities and differences in the efficiency of the mercapturic acid pathway between different organisms and cell lines. This could help to explain species sensitivity differences and, by using cell lines derived from multiple organs, indicate main sites of chemical biotransformation within the mercapturic acid pathway. In addition, ^{14}C -labelling would allow CDNB mass balances and thus help to identify potential sinks and unexpected transformation products.

Furthermore, although the mercapturic acid pathway is the major biotransformation route for electrophiles, it also contains some branching pathways (Figure 23). Although not relevant for CDNB, these side reactions are of great importance for the manifestation of toxicity of some groups of chemicals, such as halogenated alkenes, as they are often responsible for the activation of non-reactive conjugates. Instead of being acetylated by N-acetyltransferases within the mercapturic acid pathway, biotransformation products that possess a good leaving group in the β -position to the cysteine conjugate can be transformed by cysteine S-conjugate β -lyases, which can lead to bioactivation and increase in toxicity (Figure 23), (Cooper and Pinto 2006; Cooper et al.

2011). This biochemical activation event can also be exploited for the development of β -lyase activated prodrugs, e.g. in cancer therapy (Cooper et al. 2011). In light of the significance of β -lyase activity for the toxicity of chemical compounds and the efficacy of potential drug candidates, knowledge about this important branching pathway in toxicological test systems is needed.

The necessary data could be obtained through a screening of biotransformation products within a test system under the application of an appropriate model substance (e.g. a prodrug).

This thesis was conducted in the laboratory with the application of CDNB as single stressor only and at low concentrations. However, in the environment, organisms are exposed to a mixture of natural and anthropogenic substances that might impair the functionality of the mercapturic acid pathway. Therefore, in future studies it would be important to investigate to what extent xenobiotics can affect the activity of glutathione S-transferases and the efficacy of the mercapturic acid pathway. To address this issue, it would be beneficial to consider compounds that 1) selectively inhibit specific GST isoforms, 2) affect all GSTs simultaneously via inhibition or GSH depletion, and 3) inhibit N-acetyltransferases and thus favor the β -lyase pathway for compounds with a good leaving group that can undergo β -elimination. For instance, fluoxetine has been shown to selectively inhibit GST pi in human placenta (Dalmizrak et al. 2012) whereas buthionine sulfoximine (BSO) causes GSH deficiency through an interference with GSH synthesis (Sevgiler and Uner 2010). In addition, some effort has been invested into identifying selective N-acetyltransferase inhibitors, such as rhodanine and thiazolidin-2,4-dione derivatives (Russell et al. 2009).

6.3 Innovations in cell culture technologies to mimic certain *in vivo* conditions

Clearly, the field of toxicology and chemical risk assessment has moved a large step forward with the implementation of cell culture techniques. Cell cultures are very beneficial due to their reduced complexity as compared to an organism, especially because the culture techniques can be optimized for the question at hand. This thesis demonstrates that, although both zebrafish embryos and PAC2 cells possess a functional mercapturic acid pathway, the biotransformation of the glutathione conjugate to the respective mercapturic acid appears to be more efficient in embryos as compared to the cell line. Within a complex organism, such as a zebrafish embryo, the cells are embedded in a three-dimensional (3D) microenvironment, with efficient nutrient supply and continuous metabolite elimination. The imitation of this 3D *in vivo* condition is beneficial for the study of selected research topics, such as cell differentiation and tissue organization, which is reflected in the

effort invested into the development and optimization of 3D cell systems and Organ-on-Chip technologies (Lammel et al. 2019; Lee and Sung 2018). It is possible that cells cultured in such a 3D manner would biotransform chemicals within the mercapturic acid pathway with a similar efficiency as the donor organism. Thus, the analysis of the mercapturic acid pathway in 3D cell culture systems is an important future research topic that would increase our knowledge about similarities and differences of available cell culture techniques.

6.4 Concluding statement

In accordance with the consequentialist approach, the scientific community has the duty, in keeping with its principle to minimize suffering in all sentient life, to refine and replace animal experimentation. In view of the increasing need for toxicological risk assessment of environmental pollutants and potential drug candidates, this goal can only be achieved with the use of less sentient animal life stages and alternative techniques to animal testing. However, in order to fulfil the requirements of a comprehensive cost-benefit analysis, the refinement/replacement of animal experimentation should not be implemented at the expense of higher uncertainties of toxicological studies and thus increased risk for humans and the environment. Thus, refinement/replacement methodologies need to be extensively validated in order to define their advantages and limitations. By focusing on zebrafish early life stages and the zebrafish PAC2 cell line as promising systems for the refinement and replacement of animal experimentation, this thesis closes knowledge gaps regarding the biotransformation capacity of these systems, in particular the functionality of the mercapturic acid pathway. Both, zebrafish early life stages and PAC2 cells express multiple classes of GSTs and have the potential to biotransform electrophilic compounds within the mercapturic acid pathway. The functionality of this important phase II detoxification route supports the use of zebrafish early life stages and PAC2 cells in chemical risk assessment.

Bibliography

- Abreu RD, Penalva LO, Marcotte EM, Vogel C. 2009. Global signatures of protein and mrna expression levels. *Mol Biosyst* 5:1512-1526.
- Abunnaja MS, Kurogi K, Mohammed YI, Sakakibara Y, Suiko M, Hassoun EA, et al. 2017. Identification and characterization of the zebrafish glutathione s-transferase pi-1. *J Biochem Mol Toxicol*. 31:e 21948
- Adler V, Yin Z, Fuchs SY, Benezra M, Rosario L, Tew KD, et al. 1999. Regulation of jnk signaling by gstp. *EMBO J* 18:1321-1334.
- Akhdar H, Legendre C, Aninat C, More F. 2012. Anticancer drug metabolism: Chemotherapy resistance and new therapeutic approaches In: Topics on drug metabolism, (Paxton J, ed):InTech.
- Anders MW. 2004. Glutathione-dependent bioactivation of haloalkanes and haloalkenes. *Drug Metab Rev* 36:583-594.
- Armstrong RN. 1997. Structure, catalytic mechanism, and evolution of the glutathione transferases. *Chem Res Toxicol* 10:2-18.
- Armstrong RN, Morgenstern R, Board PG. 2018. Glutathione transferases. In: *Comprehensive toxicology*, 328-362.
- Authority EFS. 2005. Opinion of the scientific panel on animal health and welfare (ahaw) on a request from the commission related to the aspects of the biology and welfare of animals used for experimental and other scientific purposes. *EFSA Journal* 3:292.
- Bailey J, Oliveri A, Levin ED. 2013. Zebrafish model systems for developmental neurobehavioral toxicology. *Birth Defects Res C Embryo Today* 99:14-23.
- Bakke J, Gustafsson JA. 1984. Mercapturic acid pathway metabolites of xenobiotics - generation of potentially toxic metabolites during enterohepatic circulation. *Trends Pharmacol Sci* 5:517-521.
- Ballatori N, Krance SM, Marchan R, Hammond CL. 2009. Plasma membrane glutathione transporters and their roles in cell physiology and pathophysiology. *Mol Aspects Med* 30:13-28.
- Bambino K, Chu J. 2017. Zebrafish in toxicology and environmental health. *Curr Top Dev Biol* 124:331-367.
- Basica B, Mihaljevic I, Marakovic N, Kovacevic R, Smital T. 2019. Molecular characterization of zebrafish gstr1, the only member of teleost-specific glutathione s- transferase class. *Aquat Toxicol* 208:196-207.
- Belanger SE, Rawlings JM, Carr GJ. 2013. Use of fish embryo toxicity tests for the prediction of acute fish toxicity to chemicals. *Environ Toxicol Chem* 32:1768-1783.
- Bereman MS, MacLean B, Tomazela DM, Liebler DC, MacCoss MJ. 2012. The development of selected reaction monitoring methods for targeted proteomics via empirical refinement. *Proteomics* 12:1134-1141.
- Best JH, Pflugmacher S, Wiegand C, Eddy FB, Metcalf JS, Codd GA. 2002. Effects of enteric bacterial and cyanobacterial lipopolysaccharides, and of microcystin-Lr, on glutathione s-transferase activities in zebra fish (danio rerio). *Aquat Toxicol* 60:223-231.
- Breithaupt H. 2006. The costs of reach. Reach is largely welcomed, but the requirement to test existing chemicals for adverse effects is not good news for all. *EMBO Rep* 7:968-971.
- Brox S, Seiwert B, Haase N, Kuster E, Reemtsma T. 2016. Metabolism of clofibric acid in zebrafish embryos (danio rerio) as determined by liquid chromatography-high resolution-mass spectrometry. *Comp Biochem Physiol C Toxicol Pharmacol* 185-186:20-28.

- Busquet F, Strecker R, Rawlings JM, Belanger SE, Braunbeck T, Carr GJ, et al. 2014. Oecd validation study to assess intra- and inter-laboratory reproducibility of the zebrafish embryo toxicity test for acute aquatic toxicity testing. *Regul Toxicol Pharmacol* 69:496-511.
- Chanas SA, Jiang Q, McMahon M, McWalter GK, McLellan LI, Elcombe CR, et al. 2002. Loss of the nrf2 transcription factor causes a marked reduction in constitutive and inducible expression of the glutathione s-transferase gsta1, gsta2, gstm1, gstm2, gstm3 and gstm4 genes in the livers of male and female mice. *Biochem J* 365:405-416.
- Cho SG, Lee YH, Park HS, Ryoo K, Kang KW, Park J, et al. 2001. Glutathione s-transferase mu modulates the stress-activated signals by suppressing apoptosis signal-regulating kinase 1. *J Biol Chem* 276:12749-12755.
- Christen V, Fent K. 2014. Tissue-, sex- and development-specific transcription profiles of eight udp-glucuronosyltransferase genes in zebrafish (*danio rerio*) and their regulation by activator of aryl hydrocarbon receptor. *Aquat Toxicol* 150:93-102.
- Coles BF, Kadlubar FF. 2003. Detoxification of electrophilic compounds by glutathione s-transferase catalysis: Determinants of individual response to chemical carcinogens and chemotherapeutic drugs? (reprinted from thiol metabolism and redox regulation of cellular functions). *Biofactors* 17:115-130.
- Cooper AJ, Pinto JT. 2006. Cysteine s-conjugate beta-lyases. *Amino Acids* 30:1-15.
- Cooper AJ, Krasnikov BF, Niatetskaya ZV, Pinto JT, Callery PS, Villar MT, et al. 2011. Cysteine s-conjugate beta-lyases: Important roles in the metabolism of naturally occurring sulfur and selenium-containing compounds, xenobiotics and anticancer agents. *Amino Acids* 41:7-27.
- Cooper AJL, Hanigan MH. 2018. Metabolism of glutathione s-conjugates – multiple pathways☆. In: *Comprehensive Toxicology*, 363-406.
- Dahm R, Geisler R. 2006. Learning from small fry: The zebrafish as a genetic model organism for aquaculture fish species. *Mar Biotechnol* 8:329-345.
- Dai YJ, Jia YF, Chen N, Bian WP, Li QK, Ma YB, et al. 2014. Zebrafish as a model system to study toxicology. *Environ Toxicol Chem* 33:11-17.
- Dalmizrak O, Kulaksiz-Erkmen G, Ozer N. 2012. Evaluation of the in vitro inhibitory impact of hypericin on placental glutathione s-transferase pi. *Protein J* 31:544-549.
- Debnath AK, Lopez Decompadre RL, Debnath G, Shusterman AJ, Hansch C. 1991. Structure activity relationship of mutagenic aromatic and heteroaromatic nitro-compounds - correlation with molecular-orbital energies and hydrophobicity. *J Med Chem* 34:786-797.
- Di Paolo C, Seiler T-B, Keiter S, Hu M, Muz M, Brack W, et al. 2015. The value of zebrafish as an integrative model in effect-directed analysis - a review. *Environ Sci Europe* 27.
- Dilda PJ, Ramsay EE, Corti A, Pompella A, Hogg PJ. 2008. Metabolism of the tumor angiogenesis inhibitor 4-(n-(s-glutathionylacetyl)amino) phenylarsonous acid. *J Biol Chem* 283:35428-35434.
- Dooley K, Zon LI. 2000. Zebrafish: A model system for the study of human disease. *Curr Opin Genet Dev* 10:252-256.
- Elferink RPJO, Bakker CTM, Jansen PLM. 1993. Glutathione-conjugate transport by human colon adenocarcinoma cells (caco-2 cells). *Biochem J* 290:759-764.
- Embry MR, Belanger SE, Braunbeck TA, Galay-Burgos M, Halder M, Hinton DE, et al. 2010. The fish embryo toxicity test as an animal alternative method in hazard and risk assessment and scientific research. *Aquat Toxicol* 97:79-87.

- EuropeanCommission. 2010. Directive 2010/63/eu of the eu-ropean parliament and of the council of 22 september 2010 and of the council of 22 september 2010 on the protection of animals used for scientific purposes. Official Journal of the European Union.
- FederalLawGazette. 2005. Announcement of the amendment of the wastewater charges act on the 18th january 2005.
- Field HA, Ober EA, Roeser T, Stainier DY. 2003. Formation of the digestive system in zebrafish. I. Liver morphogenesis. *Dev Biol* 253:279-290.
- Fischer FC, Cirpka OA, Goss KU, Henneberger L, Escher BI. 2018. Application of experimental polystyrene partition constants and diffusion coefficients to predict the sorption of neutral organic chemicals to multiwell plates in vivo and in vitro bioassays. *Environ Sci Technol* 52:13511-13522.
- Fischer M, Belanger SE, Berckmans P, Bernhard MJ, Bláha L, Coman Schmid DE, et al. 2019. Repeatability and reproducibility of the rtgill-w1 cell line assay for predicting fish acute toxicity. *Toxicol Sci* 169:353-364.
- Garnier N, Redstone GGJ, Dahabieh MS, Nichol JN, del Rincon SV, Gu YX, et al. 2014. The novel arsenical darinaparsin is transported by cystine importing systems. *Mol Pharmacol* 85:576-585.
- Glisic B, Mihaljevic I, Popovic M, Zaja R, Loncar J, Fent K, et al. 2015. Characterization of glutathione-s-transferases in zebrafish (*danio rerio*). *Aquat Toxicol* 158:50-62.
- Glisic B, Hrubik J, Fa S, Dopudj N, Kovacevic R, Andric N. 2016. Transcriptional profiles of glutathione-s-transferase isoforms, cyp, and aoe genes in atrazine-exposed zebrafish embryos. *Environ Toxicol* 31:233-244.
- Goldsmith JR, Jobin C. 2012. Think small: Zebrafish as a model system of human pathology. *J Biomed Biotechnol*.
- Goldstone JV, McArthur AG, Kubota A, Zanette J, Parente T, Jonsson ME, et al. 2010. Identification and developmental expression of the full complement of cytochrome p450 genes in zebrafish. *Bmc Genomics* 11.
- Graham P, Cheng K. 2009. Ants use the panoramic skyline as a visual cue during navigation. *Curr Biol* 19:R935-937.
- Groh KJ, Nesatyy VJ, Segner H, Eggen RIL, Suter MJF. 2011. Global proteomics analysis of testis and ovary in adult zebrafish (*danio rerio*). *Fish Physiol Biochem* 37:619-647.
- Groh KJ, Schonenberger R, Eggen RIL, Segner H, Suter MJF. 2013. Analysis of protein expression in zebrafish during gonad differentiation by targeted proteomics. *Gen Comp Endocr* 193:210-220.
- Gudlawar SK, Dwivedi J. 2014. Substitution reactions in apci negative mass spectrometry: Analysis of 1-chloro-2-nitrobenzene in quetiapine fumarate. *J Liq Chromatogr R T* 37:2131-2141.
- Habig WH, Pabst MJ, Jakoby WB. 1974. Glutathione s-transferases. The first enzymatic step in mercapturic acid formation. *J Biol Chem* 249:7130-7139.
- Hachicho N, Reithel S, Miltner A, Heipieper HJ, Kuster E, Luckenbach T. 2015. Body mass parameters, lipid profiles and protein contents of zebrafish embryos and effects of 2,4-dinitrophenol exposure. *PLoS One* 10:e0134755.
- Hao L, Xie P, Fu J, Li GY, Xiong Q, Li HY. 2008. The effect of cyanobacterial crude extract on the transcription of *gst mu*, *gst kappa* and *gst rho* in different organs of goldfish (*carassius auratus*). *Aquat Toxicol* 90:1-7.
- Haufroid V, Lison D. 2005. Mercapturic acids revisited as biomarkers of exposure to reactive chemicals in occupational toxicology: A minireview. *Int Arch Occ Env Hea* 78:343-354.
- Hayen H, Jachmann N, Vogel M, Karst U. 2002. Lc-electron capture apci-ms for the determination of nitroaromatic compounds. *Analyst* 127:1027-1030.

- Hayes JD, Pulford DJ. 1995. The glutathione s-transferase supergene family: Regulation of *gst* and the contribution of the isoenzymes to cancer chemoprotection and drug resistance. *Crit Rev Biochem Mol Biol* 30:445-600.
- Hayes JD, Flanagan JU, Jowsey IR. 2005. Glutathione transferases. *Annu Rev Pharmacol* 45:51-88.
- He S, Salas-Vidal E, Rueb S, Krens SF, Meijer AH, Snaar-Jagalska BE, et al. 2006. Genetic and transcriptome characterization of model zebrafish cell lines. *Zebrafish* 3:441-453.
- Higashi T, Takido N, Yamauchi A, Shimada K. 2002. Electron-capturing derivatization of neutral steroids for increasing sensitivity in liquid chromatography/negative atmospheric pressure chemical ionization-mass spectrometry. *Anal Sci* 18:1301-1307.
- Higgins LG, Hayes JD. 2011. Mechanisms of induction of cytosolic and microsomal glutathione transferase (*gst*) genes by xenobiotics and pro-inflammatory agents. *Drug Metab Rev* 43:92-137.
- Hill AJ, Teraoka H, Heideman W, Peterson RE. 2005. Zebrafish as a model vertebrate for investigating chemical toxicity. *Toxicol Sci* 86:6-19.
- Hinchman CA, Matsumoto H, Simmons TW, Ballatori N. 1991. Intrahepatic conversion of a glutathione conjugate to its mercapturic acid. Metabolism of 1-chloro-2,4-dinitrobenzene in isolated perfused rat and guinea pig livers. *J Biol Chem* 266:22179-22185.
- Hinchman CA, Ballatori N. 1994. Glutathione conjugation and conversion to mercapturic acids can occur as an intrahepatic process. *J Toxicol Env Health* 41:387-409.
- Hinchman CA, Rebbeor JF, Ballatori N. 1998. Efficient hepatic uptake and concentrative biliary excretion of a mercapturic acid. *Am J Physiol-Gastr L* 275:G612-G619.
- Hollman AL, Tchounwou PB, Huang HC. 2016. The association between gene-environment interactions and diseases involving the human *gst* superfamily with *snp* variants. *Int J Environ Res Public Health* 13:379.
- Howe K, Clark MD, Torroja CF, Torrance J, Berthelot C, Muffato M, et al. 2013. The zebrafish reference genome sequence and its relationship to the human genome. *Nature* 496:498-503.
- Howe K, Clark MD, Torroja CF, Torrance J, Berthelot C, Muffato M, et al. 2014. The zebrafish reference genome sequence and its relationship to the human genome (vol 496, pg 498, 2013). *Nature* 505:248-248.
- HSDB. 2019. Hazardous substances data bank [internet]. Bethesda (md): National library of medicine (us); [5/17/2012; cited 2019]. 1-chloro-2,4-dinitrobenzene; hazardous substances databank number: 5306. Available from: <http://toxnet.nlm.nih.gov/cgi-bin/sis/htmlgen?Hsdb>.
- Hurst R, Bao Y, Jemth P, Mannervik B, Williamson G. 1998. Phospholipid hydroperoxide glutathione peroxidase activity of human glutathione transferases. *Biochem J* 332 (Pt 1):97-100.
- Jakobsson PJ, Morgenstern R, Mancini J, Ford-Hutchinson A, Persson B. 1999. Common structural features of mapeg - a widespread superfamily of membrane associated proteins with highly divergent functions in eicosanoid and glutathione metabolism. *Protein Sci* 8:689-692.
- Jewell C, Heylings J, Clowes HM, Williams FM. 2000. Percutaneous absorption and metabolism of dinitrochlorobenzene in vitro. *Arch Toxicol* 74:356-365.
- Johansson AS, Mannervik B. 2001. Human glutathione transferase $\alpha 3-3$, a highly efficient catalyst of double-bond isomerization in the biosynthetic pathway of steroid hormones. *J Biol Chem* 276:33061-33065.
- Kimmel CB, Ballard WW, Kimmel SR, Ullmann B, Schilling TF. 1995. Stages of embryonic-development of the zebrafish. *Dev Dynam* 203:253-310.

- Klobucar RS, Brozovic A, Stambuk A. 2013. Ecotoxicological assessment of nitrofurantoin in fish cell lines, unicellular algae *desmodesmus subspicatus*, and bacterial strains of *salmonella typhimurium*. *Fresen Environ Bull* 22:2669-2675.
- Kluver N, Ortmann J, Paschke H, Renner P, Ritter AP, Scholz S. 2014. Transient overexpression of *adh8a* increases allyl alcohol toxicity in zebrafish embryos. *PLoS One* 9:e90619.
- Knight TR, Choudhuri S, Klaassen CD. 2008. Induction of hepatic glutathione s-transferases in male mice by prototypes of various classes of microsomal enzyme inducers. *Toxicol Sci* 106:329-338.
- Knobel M, Busser FJ, Rico-Rico A, Kramer NI, Hermens JL, Hafner C, et al. 2012. Predicting adult fish acute lethality with the zebrafish embryo: Relevance of test duration, endpoints, compound properties, and exposure concentration analysis. *Environ Sci Technol* 46:9690-9700.
- Krewski D, Acosta D, Jr., Andersen M, Anderson H, Bailar JC, 3rd, Boekelheide K, et al. 2010. Toxicity testing in the 21st century: A vision and a strategy. *J Toxicol Environ Health B Crit Rev* 13:51-138.
- Kumagai Y, Abiko Y. 2017. Environmental electrophiles: Protein adducts, modulation of redox signaling, and interaction with persulfides/polysulfides. *Chem Res Toxicol* 30:203-219.
- Lammel T, Tsoukatou G, Jellinek J, Sturve J. 2019. Development of three-dimensional (3d) spheroid cultures of the continuous rainbow trout liver cell line rtl-w1. *Ecotoxicol Environ Saf* 167:250-258.
- Lange V, Picotti P, Domon B, Aebersold R. 2008. Selected reaction monitoring for quantitative proteomics: A tutorial. *Mol Syst Biol* 4.
- Langheinrich U. 2003. Zebrafish: A new model on the pharmaceutical catwalk. *Bioessays* 25:904-912.
- Lee SH, Williams MV, DuBois RN, Blair IA. 2003. Targeted lipidomics using electron capture atmospheric pressure chemical ionization mass spectrometry. *Rapid Commun Mass Sp* 17:2168-2176.
- Lee SH, Sung JH. 2018. Organ-on-a-chip technology for reproducing multiorgan physiology. *Adv Healthc Mater* 7.
- Li HD, Yao QC, Xu F, Xu N, Duan R, Long SR, et al. 2018. Imaging gamma-glutamyltranspeptidase for tumor identification and resection guidance via enzyme-triggered fluorescent probe. *Biomaterials* 179:1-14.
- Li JJ, Bickel PJ, Biggin MD. 2014. System wide analyses have underestimated protein abundances and the importance of transcription in mammals. *PeerJ* 2:e270.
- Li LH, Shi W, Wu XF, Gong QY, Li XH, Ma HM. 2016. Monitoring gamma-glutamyl transpeptidase activity and evaluating its inhibitors by a water-soluble near-infrared fluorescent probe. *Biosens Bioelectron* 81:395-400.
- Liang XF, Li GG, He S, Huang Y. 2007. Transcriptional responses of alpha- and rho-class glutathione s-transferase genes in the liver of three freshwater fishes intraperitoneally injected with microcystin-Lr: Relationship of inducible expression and tolerance. *J Biochem Mol Toxic* 21:289-298.
- Lin S, Gaiano N, Culp P, Burns JC, Friedmann T, Yee JK, et al. 1994. Integration and germ-line transmission of a pseudotyped retroviral vector in zebrafish. *Science* 265:666-669.
- Long Y, Li Q, Cui ZB. 2011. Molecular analysis and heavy metal detoxification of *abcc1/mrp1* in zebrafish. *Mol Biol Rep* 38:1703-1711.
- Ma Q. 2013. Role of *nrf2* in oxidative stress and toxicity. *Annu Rev Pharmacol Toxicol* 53:401-426.
- MacLean B, Tomazela DM, Shulman N, Chambers M, Finney GL, Frewen B, et al. 2010. Skyline: An open source document editor for creating and analyzing targeted proteomics experiments. *Bioinformatics* 26:966-968.

- Mainwaring GW, Williams SM, Foster JR, Tugwood J, Green T. 1996. The distribution of theta-class glutathione s-transferases in the liver and lung of mouse, rat and human. *Biochem J* 318 (Pt 1):297-303.
- Mannervik B, Danielson UH. 1988. Glutathione transferases--structure and catalytic activity. *CRC critical reviews in biochemistry* 23:283-337.
- Mathias PI, B'Hymer C. 2014. A survey of liquid chromatographic-mass spectrometric analysis of mercapturic acid biomarkers in occupational and environmental exposure monitoring. *J Chromatogr B* 964:136-145.
- McGrath P, Li CQ. 2008. Zebrafish: A predictive model for assessing drug-induced toxicity. *Drug Discov Today* 13:394-401.
- McIlwain CC, Townsend DM, Tew KD. 2006. Glutathione s-transferase polymorphisms: Cancer incidence and therapy. *Oncogene* 25:1639-1648.
- Mihaljevic I, Basica B, Marakovic N, Kovacevic R, Smital T. 2020. Interaction of organotin compounds with three major glutathione s-transferases in zebrafish. *Toxicol In Vitro* 62:104713.
- Mitchell AE, Morin D, Lakritz J, Jones AD. 1997. Quantitative profiling of tissue- and gender-related expression of glutathione s-transferase isoenzymes in the mouse. *Biochem J* 325 (Pt 1):207-216.
- Monks TJ, Anders MW, Dekant W, Stevens JL, Lau SS, Bladeren PJv. 1990. Contemporary issues in toxicology. Glutathione conjugate mediated toxicities. *Toxicol Appl Pharm* 106:1-19.
- Ng AN, de Jong-Curtain TA, Mawdsley DJ, White SJ, Shin J, Appel B, et al. 2005. Formation of the digestive system in zebrafish: Iii. Intestinal epithelium morphogenesis. *Dev Biol* 286:114-135.
- Notch EG, Miniutti DM, Berry JP, Mayer GD. 2011. Cyanobacterial lps potentiates cadmium toxicity in zebrafish (danio rerio) embryos. *Environ Toxicol* 26:498-505.
- Nüsslein-Volhard CaD, R. 2002. Zebrafish: A practical approach. New York: Oxford University Press:303.
- OECD. 2013. Test no. 236: Fish embryo acute toxicity (fet) test.
- Ong SE, Kratchmarova I, Mann M. 2003. Properties of c-13-substituted arginine in stable isotope labeling by amino acids in cell culture (silac). *J Proteome Res* 2:173-181.
- Otte JC, Schultz B, Fruth D, Fabian E, van Ravenzwaay B, Hidding B, et al. 2017. Intrinsic xenobiotic metabolizing enzyme activities in early life stages of zebrafish (danio rerio). *Toxicol Sci* 159:86-93.
- Palmfeldt J, Bross P. 2017. Proteomics of human mitochondria. *Mitochondrion* 33:2-14.
- Park SL, Carmella SG, Chen ML, Patel Y, Stram DO, Haiman CA, et al. 2015. Mercapturic acids derived from the toxicants acrolein and crotonaldehyde in the urine of cigarette smokers from five ethnic groups with differing risks for lung cancer. *PLoS One* 10.
- Pavagadhi S, Gong Z, Hande MP, Dionysiou DD, de la Cruz AA, Balasubramanian R. 2012. Biochemical response of diverse organs in adult danio rerio (zebrafish) exposed to sub-lethal concentrations of microcystin-lr and microcystin-rr: A balneation study. *Aquat Toxicol* 109:1-10.
- Perkins EJ, Ankley GT, Crofton KM, Garcia-Reyero N, LaLone CA, Johnson MS, et al. 2013. Current perspectives on the use of alternative species in human health and ecological hazard assessments. *Environ Health Persp* 121:1002-1010.
- Picotti P, Aebersold R. 2012. Selected reaction monitoring-based proteomics: Workflows, potential, pitfalls and future directions. *Nat Methods* 9:555-566.

- Pompella A, De Tata V, Paolicchi A, Zunino F. 2006. Expression of gamma-glutamyltransferase in cancer cells and its significance in drug resistance. *Biochem Pharmacol* 71:231-238.
- Prados-Rosales RC, Aragonese-Cazorla G, Estevez H, Garcia-Calvo E, Machuca A, Luque-Garcia JL. 2019. Strategies for membrane protein analysis by mass spectrometry. *Adv Exp Med Biol* 1140:289-298.
- Raijmakers MT, Steegers EA, Peters WH. 2001. Glutathione s-transferases and thiol concentrations in embryonic and early fetal tissues. *Hum Reprod* 16:2445-2450.
- Ramsay EE, Dilda PJ. 2014. Glutathione s-conjugates as prodrugs to target drug-resistant tumors. *Front Pharmacol* 5.
- Rastogi A, Clark CW, Conlin SM, Brown SE, Timme-Laragy AR. 2019. Mapping glutathione utilization in the developing zebrafish (*danio rerio*) embryo. *Redox Biol* 26:101235.
- Rennekamp AJ, Peterson RT. 2015. 15 years of zebrafish chemical screening. *Curr Opin Chem Biol* 24:58-70.
- Rinaldi R, Eliasson E, Swedmark S, Morgenstern R. 2002. Reactive intermediates and the dynamics of glutathione transferases. *Drug Metab Dispos* 30:1053-1058.
- Rosch A, Anliker S, Hollender J. 2016. How biotransformation influences toxicokinetics of azole fungicides in the aquatic invertebrate *gammarus pulex*. *Environ Sci Technol* 50:7175-7188.
- Ross PL, Huang YLN, Marchese JN, Williamson B, Parker K, Hattan S, et al. 2004. Multiplexed protein quantitation in *saccharomyces cerevisiae* using amine-reactive isobaric tagging reagents. *Mol Cell Proteomics* 3:1154-1169.
- Rovida C, Hartung T. 2009. Re-evaluation of animal numbers and costs for in vivo tests to accomplish reach legislation requirements for chemicals - a report by the transatlantic think tank for toxicology (t(4)). *ALTEX* 26:187-208.
- Rowe JD, Nieves E, Listowsky I. 1997. Subunit diversity and tissue distribution of human glutathione s-transferases: Interpretations based on electrospray ionization ms and peptide sequence-specific antisera. *Biochem J* 325:481-486.
- Russell AJ, Westwood IM, Crawford MH, Robinson J, Kawamura A, Redfield C, et al. 2009. Selective small molecule inhibitors of the potential breast cancer marker, human arylamine n-acetyltransferase 1, and its murine homologue, mouse arylamine n-acetyltransferase 2. *Bioorg Med Chem* 17:905-918.
- Ruzza P, Calderan A. 2013. Glutathione transferase (gst)-activated prodrugs. *Pharmaceutics* 5:220-231.
- Sander SP, Abbatt, J., Barker, J. R., Burkholder, J. B., Friedl, R. R., Golden, D. M., Huie, R. E., Kolb, C. E., Kurylo, M. J., Moortgat, G. K., Orkin, V. L., and Wine, P. H. 2011. Chemical kinetics and photochemical data for use in atmospheric studies, evaluation no. 17, jpl publication 10-6, jet propulsion laboratory, pasadena, <http://jpldataeval.jpl.nasa.gov>.
- Sau A, Tregno FP, Valentino F, Federici G, Caccuri AM. 2010. Glutathione transferases and development of new principles to overcome drug resistance. *Arch of Biochem Biophys* 500:116-122.
- Schnekenburger M, Karius T, Diederich M. 2014. Regulation of epigenetic traits of the glutathione s-transferase p1 gene: From detoxification toward cancer prevention and diagnosis. *Front Pharmacol* 5.
- Scholz S, Fischer S, Gundel U, Kuster E, Luckenbach T, Voelker D. 2008. The zebrafish embryo model in environmental risk assessment--applications beyond acute toxicity testing. *Environ Sci Pollut Res Int* 15:394-404.
- Schwanhaussner B, Busse D, Li N, Dittmar G, Schuchhardt J, Wolf J, et al. 2011. Global quantification of mammalian gene expression control. *Nature* 473:337-342.
- Senghaas N, Koster RW. 2009. Culturing and transfecting zebrafish pac2 fibroblast cells. *Cold Spring Harb Protoc* 2009:prot5235.

- Sevgiler Y, Uner N. 2010. Tissue-specific effects of fenthion on glutathione metabolism modulated by nac and bso in *oreochromis niloticus*. *Drug Chem Toxicol* 33:348-356.
- Sheehan D, Meade G, Foley VM, Dowd CA. 2001. Structure, function and evolution of glutathione transferases: Implications for classification of non-mammalian members of an ancient enzyme superfamily. *Biochem J* 360:1-16.
- Simmons TW, Hinchman CA, Ballatori N. 1991. Polarity of hepatic glutathione and glutathione s-conjugate efflux, and intraorgan mercapturic acid formation in the skate. *Biochem Pharmacol* 42:2221-2228.
- Singhal SS, Singh SP, Singhal P, Horne D, Singhal J, Awasthi S. 2015. Antioxidant role of glutathione s-transferases: 4-hydroxynonenal, a key molecule in stress-mediated signaling. *Toxicol Appl Pharmacol* 289:361-370.
- Spriggs S, Sheffield D, Olayanju A, Kitteringham NR, Naisbitt DJ, Aleksic M. 2016. Effect of repeated daily dosing with 2,4-dinitrochlorobenzene on glutathione biosynthesis and nrf2 activation in reconstructed human epidermis. *Toxicol Sci* 154:5-15.
- Srut M, Bourdineaud JP, Stambuk A, Klobucar GI. 2015. Genomic and gene expression responses to genotoxic stress in pac2 zebrafish embryonic cell line. *J Appl Toxicol* 35:1381-1389.
- Stadnicka-Michalak J, Tanneberger K, Schirmer K, Ashauer R. 2014. Measured and modeled toxicokinetics in cultured fish cells and application to in vitro-in vivo toxicity extrapolation. *PLoS One* 9:e92303.
- Stadnicka-Michalak J, Knobel M, Zupanec A, Schirmer K. 2018. A validated algorithm for selecting non-toxic chemical concentrations. *ALTEX* 35:37-50.
- Stainier DY, Lee RK, Fishman MC. 1993. Cardiovascular development in the zebrafish. I. Myocardial fate map and heart tube formation. *Development* 119:31-40.
- Stoelting MS, Tjeerdema RS. 2000. Glutathione-dependent biotransformation of 1-chloro-2,4-dinitrobenzene in arterial and venous blood of the striped bass (*morone saxatilis*). *Aquat Toxicol* 50:177-187.
- Strahle U, Scholz S, Geisler R, Greiner P, Hollert H, Rastegar S, et al. 2012. Zebrafish embryos as an alternative to animal experiments--a commentary on the definition of the onset of protected life stages in animal welfare regulations. *Reprod Toxicol* 33:128-132.
- Surinova S, Huttenhain R, Chang CY, Espona L, Vitek O, Aebersold R. 2013. Automated selected reaction monitoring data analysis workflow for large-scale targeted proteomic studies. *Nat Protoc* 8:1602-1619.
- Tadros W, Lipshitz HD. 2009. The maternal-to-zygotic transition: A play in two acts. *Development* 136:3033-3042.
- Tanneberger K, Knobel M, Busser FJ, Sinnige TL, Hermens JL, Schirmer K. 2013. Predicting fish acute toxicity using a fish gill cell line-based toxicity assay. *Environ Sci Technol* 47:1110-1119.
- Testa B. 2009. Drug metabolism for the perplexed medicinal chemist. *Chem Biodivers* 6:2055-2070.
- Testa B, Pedretti A, Vistoli G. 2012. Reactions and enzymes in the metabolism of drugs and other xenobiotics. *Drug Discov Today* 17:549-560.
- Thomson RE, Bigley AL, Foster JR, Jowsey IR, Elcombe CR, Orton TC, et al. 2004. Tissue-specific expression and subcellular distribution of murine glutathione s-transferase class kappa. *J Histochem Cytochem* 52:653-662.
- Tierbach A, Groh KJ, Schonenberger R, Schirmer K, Suter MJF. 2018. Glutathione s-transferase protein expression in different life stages of zebrafish (*danio rerio*). *Toxicol Sci* 162:702-712.
- Tierbach A, Groh KJ, Schonenberger R, Schirmer K, Suter MJ. 2020. Lc-apci(-)-ms determination of 1-chloro-2,4-dinitrobenzene, a model substrate for glutathione s-transferases. *J Am Soc Mass Spectrom*.

- Timme-Laragy AR, Goldstone JV, Imhoff BR, Stegeman JJ, Hahn ME, Hansen JM. 2013. Glutathione redox dynamics and expression of glutathione-related genes in the developing embryo. *Free Radic Biol Med* 65:89-101.
- Townsend DM, Tew KD. 2003. The role of glutathione-s-transferase in anti-cancer drug resistance. *Oncogene* 22:7369-7375.
- Trevisan R, Mello DF, Delapiedra G, Silva DGH, Arl M, Danielli NM, et al. 2016. Gills as a glutathione-dependent metabolic barrier in pacific oysters *crassostrea gigas*: Absorption, metabolism and excretion of a model electrophile. *Aquat Toxicol* 173:105-119.
- Ursic D, Berginc K, Zakelj S, Kristl A. 2009. Influence of luminal monosaccharides on secretion of glutathione conjugates from rat small intestine in vitro. *Int J Pharmaceut* 381:199-204.
- Vaidya SS, Gerk PM. 2007. Simultaneous determination of 1-chloro-2,4-dinitrobenzene, 2,4-dinitrophenyl-s-glutathione and its metabolites for human placental disposition studies by high-performance liquid chromatography. *J Chromatogr B Analyt Technol Biomed Life Sci* 859:94-102.
- Vamvakas S, Anders MW. 1991. Formation of reactive intermediates by phase ii enzymes: Glutathione-dependent bioactivation reactions. *Adv Exp Med Biol* 283:13-24.
- van Bladeren PJ. 2000. Glutathione conjugation as a bioactivation reaction. *Chem Biol Interact* 129:61-76.
- van Boxtel AL, Kamstra JH, Cenijn PH, Pieterse B, Wagner JM, Antink M, et al. 2008. Microarray analysis reveals a mechanism of phenolic polybrominated diphenylether toxicity in zebrafish. *Environ Sci Technol* 42:1773-1779.
- van Boxtel AL, Pieterse B, Cenijn P, Kamstra JH, Brouwer A, van Wieringen W, et al. 2010. Dithiocarbamates induce craniofacial abnormalities and downregulate sox9a during zebrafish development. *Toxicol Sci* 117:209-217.
- Van der Aar EM, Bouwman T, Commandeur JN, Vermeulen NP. 1996. Structure-activity relationships for chemical and glutathione s-transferase-catalysed glutathione conjugation reactions of a series of 2-substituted 1-chloro-4-nitrobenzenes. *Biochem J* 320 (Pt 2):531-540.
- Vega-Avila E, Pugsley MK. 2011. An overview of colorimetric assay methods used to assess survival or proliferation of mammalian cells. *Proc West Pharmacol Soc* 54:10-14.
- Veldman MB, Lin S. 2008. Zebrafish as a developmental model organism for pediatric research. *Pediatr Res* 64:470-476.
- Villanueva SSM, Ruiz ML, Soroka CJ, Cai SY, Luquita MG, Torres AM, et al. 2006. Hepatic and extrahepatic synthesis and disposition of dinitrophenyl-s-glutathione in bile duct-ligated rats. *Drug Metab Dispos* 34:1301-1309.
- Villeneuve D, Volz DC, Embry MR, Ankley GT, Belanger SE, Leonard M, et al. 2014. Investigating alternatives to the fish early-life stage test: A strategy for discovering and annotating adverse outcome pathways for early fish development. *Environ Toxicol Chem* 33:158-169.
- Vogel C, Marcotte EM. 2012. Insights into the regulation of protein abundance from proteomic and transcriptomic analyses. *Nat Rev Genet* 13:227-232.
- Volz DC, Belanger S, Embry M, Padilla S, Sanderson H, Schirmer K, et al. 2011. Adverse outcome pathways during early fish development: A conceptual framework for identification of chemical screening and prioritization strategies. *Toxicol Sci* 123:349-358.
- Wahllander A, Sies H. 1979. Glutathione s-conjugate formation from 1-chloro-2,4-dinitrobenzene and biliary s-conjugate excretion in the perfused rat liver. *Eur J Biochem* 96:441-446.
- Wiegand C, Pflugmacher S, Oberemm A, Steinberg C. 2000. Activity development of selected detoxication enzymes during the ontogenesis of the zebrafish (*danio rerio*). *Int Rev Hydrobiol* 85:413-422.

Zhang PS, Jiang XF, Nie XZ, Huang Y, Zeng F, Xia XT, et al. 2016. A two-photon fluorescent sensor revealing drug-induced liver injury via tracking gamma-glutamyltranspeptidase (ggt) level in vivo. *Biomaterials* 80:46-56.

Glossary

3RCC	3R Swiss Competence Centre
ABCC/MRP	ATP-binding cassette/multidrug resistance-associated protein transporter family
ADH	alcohol dehydrogenases
AFT	acute fish toxicity test
AOP	adverse outcome pathway
APCI	atmospheric pressure chemical ionization
ATCC	american type culture collection
au	arbitrary units
CDNB	1-chloro-2,4-dinitrobenzene
CDNT	5-chloro-2,4-dinitrotoluene
CFDA-AM	5-carboxyfluorescein diacetate
CYP450	cytochrome P450
DMSO	dimethyl sulfoxide
DNP	dinitrophenyl
DNP-C	2,4-dinitrophenyl cysteine
DNP-CG	2,4-dinitrophenyl cysteinylglycine
DNP-NAC	2,4-dinitrophenyl N-acetylcysteine
DNP-SG	2,4-dinitrophenyl-S-glutathione
DNT-SG	2,4-dinitrotoluene-S-glutathione
EC	electron capture
EC ₅₀	median effect concentration
ECHA	european chemicals agency
EH	epoxide hydrolases
ESI	electrospray ionization
GAPDH	glyceraldehyde 3-phosphate dehydrogenase
GSH	glutathione reduced
GSSG	glutathione oxidized
GST	glutathione S-transferases
HCD	higher-energy collisional dissociation
hpf	hours post fertilization
HPLC	high-performance liquid chromatography
HRMS	high-resolution mass spectrometry
iRT	indexed retention time
ISO	international organization for standardization
iTRAQ	isobaric tag for relative and absolute quantitation
k _H	Henry's Law constant
K _{ow}	octanol/water partition coefficient
LC	liquid chromatography

LC ₅₀	median lethal concentration
LOD	limit of detection
LOQ	limit of quantification
m/z	mass-to-charge ratios
MCB	monochlorobimane
MGST/MAPEG	membrane-associated proteins in eicosanoid and glutathione metabolism
MRM	multiple reaction monitoring
MS	mass spectrometry
MS222	tricaine methanesulfonate
Nrf2	nuclear factor-like 2
NtC	non-toxic concentration
rcf	relative centrifugal force
S/N	signal-to-noise ratio
SILAC	stable isotope labeling by amino acids in cell culture
SULT	sulfotransferases
UGT	uridine 5'-diphospho-glucuronosyltransferases
UV	ultraviolet
zFET	zebrafish embryo acute toxicity test

Supplementary information Chapter 2

SI Table 1: Summary of the GST family classes, nomenclature of the isoforms and gene and protein reference sequences obtained from NCBI Reference Sequence Database.

GST Class	Nomenclature	Protein Name	NCBI Reference Sequence: Gene	NCBI Reference Sequence: Protein
Alpha	Gsta1	glutathione S-transferase, alpha tandem duplicate 1	NM_213394	NP_998559.1
	Gsta2	glutathione S-transferase, alpha tandem duplicate 2	NM_001102648	NP_001096118.1
	Gsta3	uncharacterized protein LOC799288	NM_001109731	NP_001103201.1
Zeta	Gstz1	maleylacetoacetate isomerase isoform 1	NM_001030271	NP_001025442.2
	Gstz2	maleylacetoacetate isomerase isoform 2	NM_001002481	NP_001002481.1
	Gstz3	maleylacetoacetate isomerase isoform 3	NM_001319834	NP_001306763.1
Theta	Gstt1a	glutathione S-transferase theta 1a	NM_001327762	NP_001314691.1
	Gstt1b	glutathione S-transferase theta 1b	NM_200584	NP_956878.1
	Gstt2	glutathione S-transferase theta 2	NM_200521	NP_956815.1
Mu	Gstm1	glutathione S-transferase mu, tandem duplicate 1	NM_212676	NP_997841.1
	Gstm2	glutathione S-transferase mu 3	NM_001110116	NP_001103586.1
	Gstm3	glutathione S-transferase mu tandem duplicate 3	NM_001162851	NP_001156323.1
Pi	Gstp1	glutathione S-transferase pi	NM_131734	NP_571809.1
	Gstp2	glutathione S-transferase pi 2	NM_001020513	NP_001018349.1
Rho	Gstr1	glutathione S-transferase rho	NM_001045060	NP_001038525.1
Omega	Gsto1	glutathione S-transferase omega 1	NM_001002621	NP_001002621.1
	Gsto2	uncharacterized protein LOC492500	NM_001007372	NP_001007373.1

SI Table 2: Summary of synthetic peptides that have been purchased from JPT, Innovative Peptide Solutions, Germany.

#	DrGst class	DrGst isoenzyme	peptide sequence and position within the protein	Note	Zebrafish embryo and larvae	Organs of adult zebrafish
1	Alpha	Gsta1	R.WLLAVAGVQFEEVFLTEK.E [20, 37]	N/D		
2		Gsta1	K.IQAFQEQMK.A [178, 186]		+	+
3		Gsta1	K.IQAFQEQMK.A [178, 186]			
4		Gsta1	K.AVLSHLFK.- [215, 222]		+	+
5		Gsta2	R.WLLAAAGVQFEEVFFTK.K [20, 36]	N/D		
6		Gsta2	K.TYSSIEEK.A [119, 126]		+	+
7		Gsta3	R.WLLAAAGVQFEEVFLTEK.E [20, 37]	N/D		
8		Gsta3	K.ALANSFFLVGK.Q [138, 148]			
9		Gsta1,2	K.ALANSFFLVGK.Q [138, 148]		+	+
10		Gsta2,3	K.IQAFQEQMK.A [178, 186]		+	+
11		Gsta2,3	K.IQAFQEQMK.A [178, 186]			
12		Gsta1,2,3	K.AILNYIAGK.Y [69, 77]		+	+
13		Gsta1,2,3	K.FLQPGSAR.K [194, 201]		+	+
14		Gsta1,2,3	K.VVLHYFNKR.G [4, 12]		+	+
15		Gsta1,2,3	R.KPPPDEEYVR.T [202, 211]		+	+
16	Zeta	Gstz1,2	K.DGGQQLTDQFK.A [41, 51]/[45, 55]			+

17		Gstz1,2,3	R.LLPADPMQR.A [88, 96]/[92, 100]/[32, 40]		+	+
18		Gstz1,2,3	R.LLPADPMQR.A [88, 96]/[92, 100]/[32, 40]			
19		Gstz1,2,3	R.IICDIIASGIQPLQNLVYLQK.I [101, 121]/[103, 125]/[45, 65]			+
20		Gstz1,2,3	K.VQWAQHFINR.G [127, 136]/[131, 140]/[71, 80]			
21		Gstz1,2,3	R.LNQTLVEIEAFK.A [188, 199]/[192, 203]/[132, 143]			+
22	Theta	Gstt1a	K.DGDFLLTESIAILLYLAGK.H [58, 76]	N/D		
23		Gstt1a	R.AQVDEFLSWQHTNIR.S [92, 106]		+	+
24		Gstt1a	K.GVLPVAVTGAPVPK.E [117, 129]		+	+
25		Gstt1a	K.MDSALEDLNMSLK.I [132, 144]		+	+
26		Gstt1a	K.MDSALEDLNMSLK.I [132, 144]			
27		Gstt1a	K.FLQSRPFIIGDK.I [150, 161]			
28		DrGstt1b	K.ISLFEGYQYGEEFGK.I [32, 46]			
29		Gstt1b	K.DGDFCLAESVAIMIYLADK.F [58, 76]	N/D		
30		Gstt1b	K.DGDFCLAESVAIMIYLADK.F [58, 76]	N/D		
31		Gstt1b	K.ILIPVGLGAIEVPK.E [117, 129]			
32		Gstt1b	K.MENAEENLNVALQLFQDK.F [132, 149]		+	+
33		Gstt1b	K.MENAEENLNVALQLFQDK.F [132, 149]			
34		Gstt2	K.IPHTVEQIAIR.K [29, 39]			
35		Gstt2	K.VPVEDNGFVLTESDAIK.Y [57, 75]			
36		Gstt2	K.VPDHWYPK.L [83, 90]			
37		Gstt2	K.ALSDLSGTLDK.L [139, 149]			
38	Mu	Gstm1	K.FYT _C GEAPNYDK.S [31, 42]			
39		Gstm1	K.HNL _C GETEEEQMR.V [83, 95]			
40		Gstm1	R. _C FLDHFESLEK.I [181, 191]			
41		Gstm2	K.LYS _C GEAPNYDR.S [31, 42]			
42		Gstm2	K.HNL _C GETEEEQIR.V [83, 95]			
43		Gstm2	R.NGFVQL _C YFDFDK.N [108, 120]			
44		Gstm2	R. _C FLDHFENLEK.I [181, 191]			
45		Gstm3	K.VVQSNAIR.Y [69, 77]		+	+
46		Gstm3	K.NNL _C GETEEEQTR.V [83, 95]			
47		Gstm3	K.NKPC _C YCEK.L [121, 128]			
48		Gstm1,2	R.MFEPAC _L DDFK.N [167, 177]		+	+
49		Gstm1,2	R.MFEPAC _L DDFK.N [167, 177]			
50		Gstm1,2	K.IVQSNAIMR.Y [69, 77]		+	+
51		Gstm1,2	K.IVQSNAIMR.Y [69, 77]			
52		Gstm1,2,3	R.LLLEYTGTK.Y [18, 26]			
53		Gstm1,2,3	R.VDILENQAMDFR.N [96, 107]			+
54		Gstm1,2,3	R.VDILENQAMDFR.N [96, 107]			
55		Gstm1,2,3	K.QFSDFLGDR.K [135, 143]			+
56	Pi	Gstp1	K.ENLVTFEEWMK.G [30, 40]			+
57		Gstp1	K.ENLVTFEEWMK.G [30, 40]			
58		Gstp1	K.AT _C VFGQLPK.F [45, 54]		+	+
59		Gstp1	K.FEDGDLVLFQSNAMLR.H [55, 70]		+	+
60		Gstp1	K.FEDGDLVLFQSNAMLR.H [55, 70]			

61		Gstp1	K. <u>C</u> FENVLAK.N [128, 135]		+	+
62		Gstp2	K.ENVVTVQDWMK.G [30, 40]			
63		Gstp2	K.ENVVTVQDWM <u>M</u> K.G [30, 40]			
64		Gstp2	R.AT <u>C</u> LFGLPK.F [45, 54]			
65		Gstp2	K.FEDGDLVLYQSNAILR.H [55, 70]			
66		Gstp1,2	K.LIQEYETGK.E [106, 115]			+
67		Gstp1,2	K.ALLE <u>C</u> ENFK.K [189, 197]		+	+
68		Gstp1,2	K.LPINGNGK.Q [199, 206]			
69	Rho	Gstr	R.LMIALEEK.Q [18, 25]		+	+
70		Gstr	R. <u>M</u> IALEEK.Q [18, 25]			
71		Gstr	R.LIPDNPAEMALVYQR.M [87, 101]		+	+
72		Gstr	R.LIPDNPAEMALVYQR.M [87, 101]			
73		Gstr	R.MFETENLQQK.M [102, 111]		+	+
74		Gstr	R. <u>M</u> FETENLQQK.M [102, 111]			
75		Gstr	R.LMEYYEMVK.D [191, 199]			+ (**)
76		Gstr	R.L <u>M</u> EYYE <u>M</u> VK.D [191, 199]			
77	Omega	Gsto1	K.GSPAPGPVPK.D [10, 19]			
78		Gsto1	K.YDTININLK.N [47, 55]			+
79		Gsto1	K.NKPDWFLEK.N [56, 64]			
80		Gsto1	R.MLLELFISK.V [113, 120]		+	+
81		Gsto1	R. <u>M</u> LLELFISK.V [113, 120]			
82		Gsto1	K.GEDVSALETELK.D [135, 146]			
83		Gsto2	K.E <u>C</u> SAPGPVPNGQIR.L [10, 23]			
84		Gsto2	K.LLPSPFER.A [100, 108]		+	+
85		Gsto2	R.GEDVSTAEAEFTEK.L [135, 148]			
86		Gsto2	K.LLQLNEALANK.K [149, 159]			

- + detected in biological sample
 N/D not detected synthetic standard
C carbamidomethyl (C)
M oxidation (M)
 (**) detected but excluded due to 2 methionin and low intensity

SI Table 3: Summary of proteotypic peptides (PP) and shared peptides (SP), detected (+) in zebrafish embryos and in organs of adult zebrafish. Carbamidomethyl (C) cysteine is indicated as C, the position of the peptide in the protein (first and last amino acids) is indicated in square brackets.

class	isoenzyme	peptide type	number of peptides	peptide sequence and position in the protein	detection of corresponding endogenous peptides	
					zebrafish embryo and larvae	organs of adult zebrafish
Alpha	Gsta1	PP	Peptide # 1	K.IQAFQE ^C QMK.A [178, 186]	+	+
	Gsta1	PP	Peptide # 2	K.AVLSHLFK.- [215, 222]	+	+
	Gsta2	PP	Peptide # 1	K.TYSSIEEK.A [119, 126]	+	+
	Gsta1,2	SP	Peptide # 1	K.ALANSSFLVGK.Q [138, 148]	+	+
	Gsta2,3	SP	Peptide # 1	K.IQAFQE ^C QMK.A [178, 186]	+	+
	Gsta1,2,3	SP	Peptide # 1	K.AILNYIAGK.Y [69, 77]	+	+
	Gsta1,2,3	SP	Peptide # 2	K.FLQPGSAR.K [194, 201]	+	+
	Gsta1,2,3	SP	Peptide # 3	K.VVLHYFNGR.G [4, 12]	+	+
	Gsta1,2,3	SP	Peptide # 4	R.KPPPDEEYVR.T [202, 211]	+	+
Zeta	Gstz1,2	SP	Peptide # 1	K.DGGQQLTDQFK.A [41, 51]/[45, 55]		+
	Gstz1,2,3	SP	Peptide # 1	R.LLPADPMQR.A [88, 96]/[92, 100]/[32, 40]	+	+
	Gstz1,2,3	SP	Peptide # 2	R.II <u>C</u> DIASGIQPLQNLVYLQK.I [101, 121]/[103, 125]/[45, 65]		+
	Gstz1,2,3	SP	Peptide # 3	R.LNQTLVEIEAFK.A [188, 199]/[192, 203]/[132, 143]		+
Theta	Gstt1a	PP	Peptide # 1	R.AQVDEFLSWQHTNIR.S [92, 106]	+	+
	Gstt1a	PP	Peptide # 2	K.GVLPAVTGAPVPK.E [117, 129]	+	+
	Gstt1a	PP	Peptide # 3	K.MDSALEDLNMSLK.I [132, 144]	+	+
	Gstt1b	PP	Peptide # 1	K.MENAEENLNVALQLFQDK.F [132, 149]	+	+
Mu	Gstm3	PP	Peptide # 1	K.VVQSNAILR.Y [69, 77]	+	+
	Gstm1,2	SP	Peptide # 1	R.MFEPA <u>C</u> LDDFK.N [167, 177]	+	+
	Gstm1,2	SP	Peptide # 2	K.IVQSNAIMR.Y [69, 77]	+	+
	Gstm1,2,3	SP	Peptide # 1	R.VDILENQAMDFR.N [96, 107]		+
	Gstm1,2,3	SP	Peptide # 2	K.QFSDFLGDR.K [135, 143]		+
Pi	Gstp1	PP	Peptide # 1	K.ENLVTFE ^C WMK.G [30, 40]		+
	Gstp1	PP	Peptide # 2	K.ATC <u>V</u> F ^C GPLPK.F [45, 54]	+	+
	Gstp1	PP	Peptide # 3	K.FEDGDLVLFQSNAMLR.H [55, 70]	+	+
	Gstp1	PP	Peptide # 4	K. <u>C</u> FENVLAK.N [128, 135]	+	+
	Gstp1,2	SP	Peptide # 1	K.LIQEYETGK.E [106, 115]		+
	Gstp1,2	SP	Peptide # 2	K.ALLE <u>C</u> ENFK.K [189, 197]	+	+
Rho	Gstr	PP	Peptide # 1	R.LMIALEEK.Q [18, 25]	+	+
	Gstr	PP	Peptide # 2	R.LIPDNPAEMALVYQR.M [87, 101]	+	+
	Gstr	PP	Peptide # 3	R.MFETENLQ ^C QK.M [102, 111]	+	+
Omega	Gsto1	PP	Peptide # 1	K.YDTININLK.N [47, 55]		+
	Gsto1	PP	Peptide # 2	R.MLLELF ^C SK.V [113, 120]	+	+
	Gsto2	PP	Peptide # 1	K.LLPSPD ^C FER.A [100, 108]	+	+

SI Table 4: CLUSTAL O (1.2.4) multiple sequence alignments of isoenzymes belonging to the same class.

PEPTIDE proteotypic peptides
PEPTIDE peptides characteristic for part of the class
PEPTIDE peptides characteristic for all members of the class

Gst class Alpha

Gsta1 MSGKVVLHYFNGRGKMESIRWLLAVAGVQFEEVFLTEKEQFDKLLSDGALTFQQVPLVEI
 Gsta2 MSGKVVLHYFNGRGKMESIRWLLAAAGVQFEEVFFTKKEQFDKLLNDGVLTFQQVPLVEI
 Gsta3 MSEKVVLHYFNGRMESIRWLLAAAGVQFEEVFLTEKEQFDKLLNDGALTFQQVPLVEI

Gsta1 DGMKLVQSKAILNYIAGKYNLYGKDLKERAMIDIYSEGLIDLMEMIMVSPFPAENKEKV
 Gsta2 DGMKLVQSKAILNYIAGKYNLYGKDLKERAMIDIYSEGLIDLMGMIIMAPLGAENKEKT
 Gsta3 DGMKLVQCRAILNYIAGKYNLYGKDLKERAMIDIYSEGLIDLMGMIIMSPFPAENKEET

Gsta1 FSNIEEKAKVRFLPVFEKALANSSFLVGKQLSRADVHLLEATLMLQELFPSILATFPKIQ
 Gsta2 YSSIEEKAKVRFLPVFEKALANSSFLVGKQLSRADVHLLEATLMLQELFPSILATFPKIQ
 Gsta3 FRNIEEKAKVRFLPVFEKALANSSFLVGKQLSRADVHLLEATLMLQELFPSILATFPKIQ

Gsta1 AFQEQMKALPAISKFLQPGSAR KPPPDEEYVRTVKAVLSHLFK
 Gsta2 AFQDQMKALPAISKFLQPGSAR KPPPDEEYVRTVKSVLPHLFK
 Gsta3 AFQDQMKALPAISKFLQPGSAR KPPPDEEYVRTVKSVLPHRFK

Gst class Zeta

Gstz2 MSATVARLIKPVLYGYRSSCSWRVRIAFALKGIEYEQKPINLIKDGGQQLTDQFKAINP
 Gstz1 ----MAAQTKPVLYGYRSSCSWRVRIAFALKGIEYEQKPINLIKDGGQQLTDQFKAINP
 Gstz3 -----

Gstz2 MQQVPAVSIDGITLSQSLAIQYIEETRPEPRLLPADPMQRAHVRIICDIIASGIQPLQN
 Gstz1 MQQVPAVSIDGITLSQSLAIQYIEETRPEPRLLPADPMQRAHVRIICDIIASGIQPLQN
 Gstz3 MQQVPAVSIDGITLSQSLAIQYIEETRPEPRLLPADPMQRAHVRIICDIIASGIQPLQN

Gstz2 LYVLQKIGEDKVQWAQHFINRGFQALEPVLKETAGKYCVGDEISMADICLVPQVYNADRF
 Gstz1 LYVLQKIGEDKVQWAQHFINRGFQALEPVLKETAGKYCVGDEISMADICLVPQVYNADRF
 Gstz3 LYVLQKIGEDKVQWAQHFINRGFQALEPVLKETAGKYCVGDEISMADICLVPQVYNADRF

Gstz2 KVDMTQYPTIRRLNQTLVEIEAFKASHPSRQPDTPDDLRL
 Gstz1 KVDMTQYPTIRRLNQTLVEIEAFKASHPSRQPDTPDDLRL
 Gstz3 KVDMTQYPTIRRLNQTLVEIEAFKASHPSRQPDTPDDLRL

Gst class Theta

Gstt2 MTGRQAVKAYLDLMSQPCRAVLIFLKHNPHTVEQIAIRKGEQKTPEFTKLNPMQKVPV
 Gstt1a ----MPLELYLDLHSQPCRSVFIFAKINKIPFEYKAVDLSAGEQYGDEFGKVSIRKVPV
 Gstt1b ----MTLEIYLDLFSQPCRSVYIFAKNNIQFDYKKISLFEGYQYGEEFGKINPLRKFT

Gstt2 LEDNGFVLTESDAILKYLATTYKVPDHWYPKLPEKRARVDEYTAWHHMNTRMHAATVFWQ
 Gstt1a LKDGDFLLTESIAILLYLAGKHSTPDHWYPADLQKRAQVDEFLSWQHTNIRSHGSKVFWF
 Gstt1b IKDGDFLCLAESVAIMIYLADKFHTPDHWFPADLQKRARVNEYSWQHTSIRMHGAKIWF

Gstt2 EVLLPLMTGQPANTAKLEKALSDLSGTLDKLENMFLKRQAFLCGDDISLADLLAICELMQ
 Gstt1a KGVLPVAVTGAPVPKEKMDSLEDLNMSLKIFEDKFLQSRPFIIGDKISLADIVAIVEMMQ
 Gstt1b KILIPVVGAEVPKEKMENAEENLNVALQLFQDKFLQDKPFIVGDQISLADLVAIVEIMQ

Gstt2 PMSSGRDILKDRPKLMSWRSRVQSALS-DSFDEAHTIVYRLRDKFTAKLRKITGQGVSA
 Gstt1a PVATGVDVFEGRPALSAWRDRVKKEVGVELFDEAHKVIMNVESLPQ----TFENKGLPEF
 Gstt1b PFAAGMDVFENRPKLKAWKDRVRVAIGAKLFDEAHQATMSLRDQAK----IIDPKGLSPL

Gstt2 DLV-----
 Gstt1a FKLKIQKMFN
 Gstt1b KDKILKYFLS

Gst class Mu

Gstm3 MAMKLAYWDIRGIAQPVRLLEFTGTYEEKFYSCGEAPDYDKSCWFNEKNKLGLAFPNL
 Gstm1 MAMKLAYWDIRGLAQPIRLLEFTGTYEEKFYTCGEAPNYDKSCWFNEKSKLGMDFPNL
 Gstm2 MAMKLVYWDIRGLAQPIRLLEFTGTYEEKLYSCGEAPNYDRSCWLNDKSKLGMDFPNL

Gstm3 PYLEGDGDKVVSQSNAILRYIARKNNLCGETEEEEQTRVDILENQAMDFRNGFIQLCYGDFD
 Gstm1 PYLEGDGDKIVQSNAIMRYIARKHNLGGETEEEEQMRVDILENQAMDFRNGFVQLCYLDFD
 Gstm2 PYLEGDGDKIVQSNAIMRYIARKHNLGGETEEEEQIRVDILENQAMDFRNGFVQLCYDFD

Gstm3 KNKPCYCEKLPGLSKQFSDFLGDRKWFAGDKITFVDFIMYDLLDLHRLHPECLDDYRNL
 Gstm1 KNKSSYCEKLSGTLKQFSDFLGDRKWFAGDKITFVDFIMYELLDQHRMFEPACLDDEFKNL
 Gstm2 KNKSSYCEKLPGLTKQFSDFLGDRKWFAGDKITFVDFIMYELLDQHRMFEPACLDDEFKNL

Gstm3 RSFLDHFESLEKIVAYMKS NKYMKTPVNNKMAKWGNKKE
 Gstm1 RCFLDHFESLEKIAEYMKS NRFMETPVNNKMAKWGNKKE
 Gstm2 RCFLDHFENLEKIAEYMKS NRFMKTPVNSKMAKWGNKKE

Gst class Pi

Gstp1 MAPYTLTYFAVKGRCGALKIMLADKDQQLKENLVTFEEWMKGDLKATCVFGQLPK FEDGD
 Gstp2 MAPYTLTYFAIKGRAGPLKILLADKEQQLKENVVTVQDWMKGDIRATCLFGQLPK FEDGD

Gstp1 LVLFQSNAMLRHLGRKHAAYGKNDSEASLIDVMNDGVEDLRLKYIK LIYQEYETGKEAFI
 Gstp2 LVLYQSNAILRHLGRKHGAYGKNDCEASLIDMMNDAAQDLRQKYIK LIYQEYETGKEAFI

Gstp1 KDLPNHLKCFENVLAKNKTGFLVGDQISFADYNLFDLLLNLKVLSPSCLDSFPSLKSFVD
 Gstp2 KDLPNEFKPFENILAKSKTGFLVGDQISLADYNLFDLLLNLKVLSPSCLDSFPSLKSFVD

Gstp1 KISARPKVK ALLECENFKKLPINGNGKQ
 Gstp2 KISARPKVK ALLECENFKKLPINGNGKQ

Gst class Rho

MAQNMLLYWGTGSPPCWRL MIALEEKQLQGYKHKLLSFDKKEHQSPVKALNPRAQLPTFKH-
 GEIVVNES
 FAACLYLESVFKSQGTRLIPDNPAEMALVYQR MFETENLQQKMYEVAFYDWLVPEGERLESALKRN-
 KEKL
 IEELKLWEGYLEKMGKGSYLAGKNFSMADVVCFPVIAYFPRLQCPKERCPR-
 MEYYEMVKDRPSIKASWP
 PEWLEKPVGEDILKSL

Gst class Omega

Gsto1 MAASQKCLGKGSPAPGPVPKDHIRLYSMRFCPFAQRTRLVLNAKGIKYDTININLKNKPD
 Gsto2 MASSPKCLGKECSAPGPVPNGQIRLYSMRFCPFAQRTRLVLTAKGVKHDIIININLVSKPD

Gsto1 WFLEKNPLGLVPVLETQSGQVIYESPITCEYLDEVYPEKKLLPFDPFERAQQRM LLELFS
 Gsto2 WFLKKNPFGTVPVLETSSGQVIYESPITCEYLDEVYPEKK LLPSDPFERAQQKM LLELYS

Gsto1 KVTPYFYKIPVNRTKGEDVSALETELKD KLSQFNEILLKKKSKFFGGDSITMIDYMMWPW
 Gsto2 KVIPYFYKISMGKKRGEDVSTAEAEFTEKLLQLNEALANKTKYFGGDSITMIDYLIWPW

Gsto1 FERLETMNLKHCLDGTPELKKWTERMMEDPTVKATMFSTETYMVFYKSYMEGNPNYDYGL
 Gsto2 FERAEMMGVKHCLAKTPELKRKWIELMFEDPVVKATMFNTDVHKVFFDSYMDGKPNYDYGL

SI Table 5: Peak area (normalized to the internal standard GAPDH) of proteotypic peptides (PP) and shared peptides (SP) detected in zebrafish embryo. Carbamidomethyl (C) cysteine is indicated as C, the position of the peptide in the protein (first and last amino acids) is indicated in square brackets.

peptide type	isoenzyme	number of peptides	peptide sequence and position in the protein	age		replicates			
						1	2	3	4
PP	Gsta1	Peptide # 1	K.IQAFQE ^C QMK.A [178, 186]	4	hpf	0	0	0	0
				8	hpf	0	0	0	0
				24	hpf	0	0	0.009223	0
				48	hpf	0.009873	0	0	0
				72	hpf	0.011269	0.020108	0.01878	0
				96	hpf	0.03562	0.035504	0.030817	0.031798
				120	hpf	0.05377	0.080302	0.077774	0.0488
				168	hpf	0.056913	0.108245	0.089863	0.077368
PP	Gsta1	Peptide # 2	K.AVL ^C SHLFK.- [215, 222]	4	hpf	0	0	0.00844	0.014125
				8	hpf	0	0	0.020419	0
				24	hpf	0.024168	0.037587	0.023822	0.034565
				48	hpf	0.049716	0.059597	0.039621	0.053435
				72	hpf	0.056955	0.061142	0.060639	0.071369
				96	hpf	0.103528	0.090738	0.109958	0.078872
				120	hpf	0.140703	0.131272	0.115601	0.097589
				168	hpf	0.151416	0.20355	0.131525	0.143939
PP	Gsta2	Peptide # 1	K.TYSSIEEK.A [119, 126]	4	hpf	0	0	0	0
				8	hpf	0	0	0	0
				24	hpf	0	0	0	0
				48	hpf	0	0	0	0
				72	hpf	0	0	0.005638	0
				96	hpf	0.006288	0.009033	0.007733	0.00851
				120	hpf	0.005869	0.011735	0.012234	0.009734
				168	hpf	0.00836	0.015421	0.016561	0.015829
SP	Gsta1,2	Peptide # 1	K.ALANSSFLVGK.Q [138, 148]	4	hpf	0	0	0	0
				8	hpf	0	0	0	0
				24	hpf	0	0	0.013747	0
				48	hpf	0.016865	0.007782	0.013938	0.009797
				72	hpf	0.02167	0.034068	0.025204	0
				96	hpf	0.052274	0.052559	0.04569	0.039285
				120	hpf	0.073891	0.101169	0.103279	0.063182
				168	hpf	0.092054	0.149235	0.130129	0.105611
SP	Gsta2,3	Peptide # 1	K.IQAFQE ^C QMK.A [178, 186]	4	hpf	0	0	0	0
				8	hpf	0	0	0	0
				24	hpf	0	0	0	0
				48	hpf	0	0	0	0
				72	hpf	0.006111	0	0.008079	0
				96	hpf	0.009883	0.014124	0.012457	0.013202
				120	hpf	0.019044	0.022862	0.026368	0.018301
				168	hpf	0.027202	0.035684	0.044933	0.035307

SP	Gsta1,2,3	Peptide # 1	K.AILNYIAGK.Y [69, 77]	4	hpf	0	0	0	0
				8	hpf	0	0	0	0
				24	hpf	0	0	0	0
				48	hpf	0	0	0	0
				72	hpf	0	0	0	0
				96	hpf	0	0.007667	0.005899	0
				120	hpf	0.015493	0.024043	0.025225	0.015794
				168	hpf	0.021082	0.027715	0.037103	0.022264
SP	Gsta1,2,3	Peptide # 2	K.FLQPGSAR.K [194, 201]	4	hpf	0	0.003889	0.012248	0
				8	hpf	0.011658	0	0.013988	0.007384
				24	hpf	0.026304	0.022623	0.033242	0.022762
				48	hpf	0.039671	0.053723	0.051515	0.05787
				72	hpf	0.0568	0.099367	0.078347	0.026179
				96	hpf	0.110061	0.140941	0.131202	0.118604
				120	hpf	0.151116	0.247144	0.227936	0.174522
				168	hpf	0.173239	0.341183	0.2619	0.264217
SP	Gsta1,2,3	Peptide # 3	K.VVLHYFNGR.G [4, 12]	4	hpf	0	0	0	0
				8	hpf	0	0	0	0
				24	hpf	0	0	0	0
				48	hpf	0	0	0	0
				72	hpf	0	0	0	0
				96	hpf	0.00295	0.002879	0.002261	0.002277
				120	hpf	0.009586	0.009315	0.01232	0.009602
				168	hpf	0.009835	0.009122	0.011351	0.010231
SP	Gsta1,2,3	Peptide # 4	R.KPPPDEEYVR.T [202, 211]	4	hpf	0	0	0	0
				8	hpf	0	0	0	0
				24	hpf	0	0	0	0
				48	hpf	0	0	0	0
				72	hpf	0	0	0	0
				96	hpf	0	0.003806	0.003773	0.005154
				120	hpf	0.005062	0.006396	0.005912	0.006478
				168	hpf	0.008892	0.008383	0.009655	0.009684
SP	Gstz1,2,3	Peptide # 1	R.LLPADPMQR.A [88, 96]/[92, 100]/[32, 40]	4	hpf	0	0	0	0
				8	hpf	0	0	0	0
				24	hpf	0	0	0	0
				48	hpf	0	0	0	0
				72	hpf	0.002581	0	0.003757	0
				96	hpf	0.003485	0.005239	0.008296	0.008598
				120	hpf	0.011259	0.013113	0.013189	0.012972
				168	hpf	0.018859	0.026421	0.021913	0.023355
PP	Gstt1a	Peptide # 1	R.AQVDEFLSWQHT- NIR.S [92, 106]	4	hpf	0	0	0	0
				8	hpf	0	0	0	0
				24	hpf	0	0	0	0

				48	hpf	0	0	0	0
				72	hpf	0	0	0	0
				96	hpf	0.006645	0.008294	0.006203	0.0052
				120	hpf	0.00811	0.011153	0.010793	0.009078
				168	hpf	0.007829	0.01703	0.010542	0.007675
PP	Gstt1a	Peptide # 2	K.GVLPAVTGAPVPK.E [117, 129]	4	hpf	0	0	0	0
				8	hpf	0	0	0	0
				24	hpf	0	0	0	0
				48	hpf	0	0	0	0
				72	hpf	0	0	0	0
				96	hpf	0.0128	0.011654	0.005918	0.00753
				120	hpf	0.010703	0.014054	0.016597	0.011935
				168	hpf	0.016435	0.023122	0.025053	0.01729
PP	Gstt1a	Peptide # 3	K.MDSALEDLNMSLK.I [132, 144]	4	hpf	0	0	0	0
				8	hpf	0	0	0	0
				24	hpf	0	0	0	0
				48	hpf	0	0	0	0
				72	hpf	0.004594	0	0	0
				96	hpf	0	0.002909	0.001909	0.001937
				120	hpf	0.004075	0.003759	0.004694	0.003913
				168	hpf	0.004992	0.006205	0.005797	0.00486
PP	Gstt1b	Peptide # 1	K.MENAEENLN-VALQLFQDK.F [132, 149]	4	hpf	0	0	0	0
				8	hpf	0	0	0	0
				24	hpf	0	0	0	0
				48	hpf	0	0	0	0
				72	hpf	0.006053	0.004747	0.004238	0
				96	hpf	0.006188	0.004887	0.001701	0.003326
				120	hpf	0	0.003554	0.003637	0.002347
				168	hpf	0.003432	0.006034	0.004782	0.003216
PP	Gstm3	Peptide # 1	K.VVQSNAILR.Y [69, 77]	4	hpf	0	0	0	0
				8	hpf	0	0	0	0
				24	hpf	0	0	0	0
				48	hpf	0	0	0	0
				72	hpf	0.011851	0.026692	0.016899	0.008683
				96	hpf	0.022696	0.02775	0.021792	0.022409
				120	hpf	0.021894	0.034468	0.029053	0.027516
				168	hpf	0.030167	0.046257	0.043761	0.036233
SP	Gstm1,2	Peptide # 1	R.MFEPACLDLDFK.N [167, 177]	4	hpf	0	0	0	0
				8	hpf	0	0	0	0
				24	hpf	0	0	0	0
				48	hpf	0	0	0	0
				72	hpf	0	0	0	0
				96	hpf	0	0.003499	0	0

				120	hpf	0	0	0.003694	0
				168	hpf	0.00251	0.005445	0.007809	0.003114
SP	Gstm1,2	Peptide # 2	K.IVQSNAMR.Y [69, 77]	4	hpf	0.165557	0.190287	0.213133	0.168693
				8	hpf	0.188224	0.210489	0.194797	0.192736
				24	hpf	0.212527	0.201469	0.210974	0.187383
				48	hpf	0.163102	0.191	0.188908	0.198743
				72	hpf	0.127716	0.154336	0.152049	0.104792
				96	hpf	0.09819	0.127211	0.118129	0.119432
				120	hpf	0.086919	0.117174	0.120951	0.10735
				168	hpf	0.10645	0.142888	0.137631	0.122741
PP	Gstp1	Peptide # 2	K.ATCVFGQLPK.F [45, 54]	4	hpf	0	0	0.005799	0
				8	hpf	0	0	0	0
				24	hpf	0	0	0.021396	0
				48	hpf	0	0	0	0
				72	hpf	0	0	0.005857	0
				96	hpf	0.008853	0.007017	0	0.005666
				120	hpf	0.00383	0.008193	0.007978	0
				168	hpf	0.006961	0.014336	0.018594	0.010805
PP	Gstp1	Peptide # 4	K.QFENVLAK.N [128, 135]	4	hpf	0.027999	0.021317	0.075369	0.028789
				8	hpf	0.080906	0.034429	0.042391	0.045862
				24	hpf	0.071794	0.026585	0.101037	0.025067
				48	hpf	0.053467	0.038357	0.058414	0.039249
				72	hpf	0.059236	0.083377	0.070069	0.013546
				96	hpf	0.062751	0.078466	0.055123	0.058175
				120	hpf	0.051631	0.09247	0.096634	0.076739
				168	hpf	0.073438	0.103341	0.128532	0.088642
PP	Gstp1	Peptide # 3	K.FEDGDLVLFQS- NAMLH.H [55, 70]	4	hpf	0.006786	0	0	0
				8	hpf	0.007695	0	0	0.005029
				24	hpf	0	0.016351	0.010503	0
				48	hpf	0.004226	0.025576	0.00486	0
				72	hpf	0.031385	0.005045	0.013234	0.020487
				96	hpf	0.006449	0.002583	0.004906	0.003086
				120	hpf	0	0.00338	0.006631	0.003556
				168	hpf	0.007552	0.005976	0.006354	0.004679
SP	Gstp1,2	Peptide # 2	K.ALLECEENFK.K [189, 197]	4	hpf	0.114517	0.107933	0.165946	0.10143
				8	hpf	0.220412	0.112743	0.120858	0.121024
				24	hpf	0.18903	0.120828	0.220886	0.100399
				48	hpf	0.145027	0.112366	0.113795	0.097631
				72	hpf	0.136616	0.150441	0.123251	0.061867
				96	hpf	0.140891	0.138709	0.107382	0.112562
				120	hpf	0.098234	0.130743	0.129793	0.111521
				168	hpf	0.147157	0.154087	0.184459	0.140462
PP	Gstr	Peptide # 1	R.LMIALEEK.Q [18, 25]	4	hpf	0.018458	0	0.04323	0.018061

				8	hpf	0.039044	0.02456	0.023324	0.026428
				24	hpf	0.033624	0.040936	0.047066	0.023278
				48	hpf	0.027825	0.03808	0.026585	0.029724
				72	hpf	0.038669	0.043478	0.040306	0.027714
				96	hpf	0.036356	0.047756	0.03168	0.032215
				120	hpf	0.038784	0.06955	0.062168	0.043908
				168	hpf	0.078923	0.121288	0.115621	0.076211
PP	Gstr	Peptide # 2	R.LIPDNPAE- MALVYQR.M [87, 101]	4	hpf	0	0	0	0
				8	hpf	0	0	0	0
				24	hpf	0	0	0	0
				48	hpf	0	0	0	0
				72	hpf	0	0	0	0
				96	hpf	0.002817	0.003881	0.002773	0.003963
				120	hpf	0.004701	0.005527	0.005417	0.005398
				168	hpf	0.011272	0.01117	0.012099	0.009566
PP	Gstr	Peptide # 3	R.MFETENLQQK.M [102, 111]	4	hpf	0	0	0	0
				8	hpf	0	0	0	0
				24	hpf	0	0	0	0
				48	hpf	0	0	0	0
				72	hpf	0.004518	0.005957	0.004473	0
				96	hpf	0.006654	0.007346	0.008004	0.00729
				120	hpf	0.010451	0.013221	0.014478	0.009475
				168	hpf	0.014768	0.026422	0.029209	0.023231
SP	Gsto1	Peptide # 2	R.MLLEFSK.V [113, 120]	4	hpf	0	0	0	0
				8	hpf	0	0	0	0
				24	hpf	0	0	0	0
				48	hpf	0	0	0	0
				72	hpf	0	0	0	0
				96	hpf	0	0	0	0
				120	hpf	0	0.002866	0.003087	0
				168	hpf	0.004238	0.006727	0.008157	0.006358
SP	Gsto2	Peptide # 1	K.LLPSPFER.A [100, 108]	4	hpf	0	0	0.02067	0
				8	hpf	0	0	0	0
				24	hpf	0	0	0.036215	0
				48	hpf	0	0	0.014079	0
				72	hpf	0.01866	0.022652	0.015402	0
				96	hpf	0.020211	0.020886	0.012018	0.012238
				120	hpf	0.01682	0.031506	0.029515	0.023572
				168	hpf	0	0.05093	0.056395	0.040791

SI Table 6: Peak area (normalized to the internal standard Myoglobin) of proteotypic peptides (PP) and shared peptides (SP) detected in organs of adult zebrafish. Carbamidomethyl (C) cysteine is indicated as C, the position of the peptide in the protein (first and last amino acid) is indicated in square brackets. Blank boxes represent missing replicate.

peptide type	isoenzyme	number of peptides	peptide sequence and position in the protein	organ	replicates			
					1	2	3	4
PP	Gsta1	Peptide # 1	K.IQAFQEQMK.A [178, 186]	Female Liver	0.083671	0.027153	0.052556	0.055256
				Male Liver	0.007856	0.010518	0.024042	0.043945
				Female Intestine	0.015396	0.034093	0.025065	0.024913
				Male Intestine	0.019203	0.026517	0.020865	0.024388
				Female Gill	0.005165	0.003043	0.01358	0.013507
				Male Gill	0.043803	0.002411	0.0113	0.010678
				Female Gonads	0	0.001125	0.001318	0.001988
				Male Gonads	0.007406	0.02453		0.006917
				Female Brain	0.003602	0.003652	0.006669	0.008103
				Male Brain	0.003521	0.004875	0.003739	0.002623
				Female Kidney	0.008168	0.002799	0.011581	0.011114
				Male Kidney	0.00861	0.00288	0	
				Female Liver	0.287001	0.096998	0.32969	0.174222
				Male Liver	0.020965	0.034398	0.571691	0.113797
PP	Gsta1	Peptide # 2	K.AVLSHLFK.- [215, 222]	Female Intestine	0.014324	0.012911	0.022226	0.03944
				Male Intestine	0.06219	0.029664	0.126739	0.053401
				Female Gill	0.037606	0.007718	0.169229	0.032536
				Male Gill	0.219501	0.004304	0.032516	0.01932
				Female Gonads	0.010158	0.004099	0.009647	0.0127
				Male Gonads	0.061849	0.024368	0.172699	0
				Female Brain	0.024912	0.00909	0.044769	0.036806
				Male Brain	0.026501	0.010793	0.066762	0.023978
				Female Kidney	0.020487	0.007842	0.035028	0.018184
				Male Kidney	0.021082	0.005327	0.18508	
				Female Liver	0	0	0	0
				Male Liver	0.002564	0	0	0
				Female Intestine	0.00038	0.00075	0	0
				Male Intestine	0	0.000637	0	0.001868
PP	Gsta2	Peptide # 1	K.TYSSIEEK.A [119, 126]	Female Gill	0	0.000236	0	0.003037
				Male Gill	0	0.000247	0.002098	0.001626
				Female Gonads	0	0	0	0
				Male Gonads	0	0.000152	0	0
				Female Brain	0	0	0	0
				Male Brain	0	0	0	0
				Female Liver	0	0	0	0
				Male Liver	0	0	0	0
				Female Intestine	0	0	0	0
				Male Intestine	0	0	0	0

				Female Kidney	0.001681	0.000137	0.001512	0.00248
				Male Kidney	0.001394	0	0	
SP	Gsta1,2	Peptide # 1	K.ALANSSFLVGK.Q [138, 148]	Female Liver	0.16171	0.072595	0.114422	0.073287
				Male Liver	0.009088	0.026815	0.055032	0.061997
				Female Intestine	0.040256	0.06184	0.052183	0.034034
				Male Intestine	0.029035	0.039703	0.032837	0.035115
				Female Gill	0.009448	0.005431	0.023118	0.015794
				Male Gill	0.056045	0.003643	0.01872	0.013252
				Female Gonads	0.00164	0.001481	0.001873	0.002648
				Male Gonads	0.010897	0.024761	0.005643	0.005762
				Female Brain	0.007676	0.007259	0.009617	0.005458
				Male Brain	0.005769	0.009526	0.006474	0.004013
				Female Kidney	0.01035	0.00454	0.011312	0.012242
				Male Kidney	0.011258	0.004066	0	
SP	Gsta2,3	Peptide # 1	K.IQAFQEQMK.A [178, 186]	Female Liver	0.084015	0.036731	0.043663	0.030382
				Male Liver	0.002381	0.014892	0.025876	0.027459
				Female Intestine	0.015831	0.023069	0.011694	0.007455
				Male Intestine	0.004798	0.008126	0.00937	0.010349
				Female Gill	0.004323	0.00153	0	0.004714
				Male Gill	0.013874	0	0.006917	0.002674
				Female Gonads	0.000939	0.000623	0	0
				Male Gonads	0.002688	0.001807	0	0.000667
				Female Brain	0.003608	0.003156	0	0.00254
				Male Brain	0.001922	0.00334	0	0.002258
				Female Kidney	0.006566	0.002082	0.003258	0.002616
				Male Kidney	0.003026	0.000967	0	
SP	Gsta1,2,3	Peptide # 1	K.AILNYIAGK.Y [69, 77]	Female Liver	0.023061	0.01573	0.048684	0.01156
				Male Liver	0.001248	0.014641	0.003352	0.007663
				Female Intestine	0.017436	0.0247	0.018825	0.011471
				Male Intestine	0.005178	0.010929	0.006973	0.007241
				Female Gill	0	0.005321	0	0
				Male Gill	0.009367	0.003731	0.002384	0.002702
				Female Gonads	0	0	0	0
				Male Gonads	0.001222	0.010397	0	0.001902
				Female Brain	0	0.002687	0	0
				Male Brain	0	0.002988	0	0
				Female Kidney	0.001723	0.004721	0.001029	0.001995

				Male Kidney	0.001466	0.003241	0	
SP	Gsta1,2,3	Peptide # 2	K.FLQPGSAR.K [194, 201]	Female Liver	0.367241	0.119332	0.353017	0.239782
				Male Liver	0.021321	0.046139	0.323518	0.162877
				Female Intestine	0.038566	0.068045	0.053246	0.078801
				Male Intestine	0.091563	0.05742	0.124336	0.109756
				Female Gill	0.026387	0.00793	0.102629	0.044193
				Male Gill	0.183689	0.00504	0.032703	0.031674
				Female Gonads	0.007548	0.004101	0.007576	0.012437
				Male Gonads	0.037975	0.042215	0.083089	0.012421
				Female Brain	0.020356	0.010212	0.037117	0.038339
				Male Brain	0.021818	0.014834	0.041889	0.023017
				Female Kidney	0.024435	0.007705	0.032261	0.030216
				Male Kidney	0.023092	0.00616	0.060921	
SP	Gsta1,2,3	Peptide # 3	K.VVLHYFNGR.G [4, 12]	Female Liver	0.030366	0.010164	0.010526	0.011686
				Male Liver	0.000909	0.003946	0	0.009641
				Female Intestine	0.006064	0.009641	0.006051	0.006683
				Male Intestine	0.002284	0.00619	0.002505	0.005445
				Female Gill	0	0.000551	0	0
				Male Gill	0.004072	0.000545	0.002073	0.002038
				Female Gonads	0.000515	0.000438	0	0
				Male Gonads	0	0.003652	0	0.001648
				Female Brain	0	0.000895	0	0
				Male Brain	0	0.00123	0	0
				Female Kidney	0.000964	0.00037	0	0.001954
				Male Kidney	0.000631	0.000234	0	
SP	Gsta1,2,3	Peptide # 4	R.KPPPDEEYVR.T [202, 211]	Female Liver	0.034935	0.009892	0.022804	0.016147
				Male Liver	0.000614	0.002923	0.018541	0.012807
				Female Intestine	0.002146	0.002313	0.00333	0.003783
				Male Intestine	0.004956	0.00225	0.005285	0.008258
				Female Gill	0.001735	0.000338	0	0.00216
				Male Gill	0.009427	0.000129	0.001117	0.001246
				Female Gonads	0.000321	0	0	0
				Male Gonads	0.002053	0.00043	0	0
				Female Brain	0.001319	0.000551	0	0.002643
				Male Brain	0.001057	0.000733	0.00178	0.001939
				Female Kidney	0.001496	0.000403	0.000876	0.000907
				Male Kidney	0.000889	0.000216	0	

SP	Gstz1,2	Peptide # 1	K.DGGQQLTDQFK.A [41, 51]/[45, 55]	Female Liver	0.022506	0.013023	0.01728	0.028114
				Male Liver	0.00188	0.019556	0.046098	0.03523
				Female Intestine	0	0	0	0
				Male Intestine	0	0	0	0
				Female Gill	0	0	0	0
				Male Gill	0.024009	0.000474	0.003174	0.002635
				Female Gonads	0	0	0	0
				Male Gonads	0	0.000834	0	0.002745
				Female Brain	0	0.000534	0	0
				Male Brain	0	0.000852	0	0
				Female Kidney	0	0	0	0.002151
				Male Kidney	0.003206	0.000933	0	
SP	Gstz1,2,3	Peptide # 1	R.LLPADPMQR.A [88, 96]/[92, 100]/[32, 40]	Female Liver	0.590563	0.093647	0.791046	0.414861
				Male Liver	0.022296	0.11933	1.473951	0.310987
				Female Intestine	0.021713	0.017715	0.026137	0.052904
				Male Intestine	0.072214	0.012248	0.103524	0.057704
				Female Gill	0.034926	0.005959	0.098469	0.032004
				Male Gill	0.709413	0.003243	0.023305	0.017885
				Female Gonads	0.00971	0.003945	0.008549	0.012471
				Male Gonads	0.009889	0.006946	0.117795	0.016979
				Female Brain	0.015253	0.003534	0.023698	0.012636
				Male Brain	0.017713	0.005135	0.035162	0.015411
				Female Kidney	0.033458	0.007345	0.027326	0.022717
				Male Kidney	0.034705	0.005106	0.267674	
SP	Gstz1,2,3	Peptide # 2	R.IICDIASGIQPLQN- LYVLQK.I [101, 121]/[103, 125]/[45, 65]	Female Liver	0	0.002111	0	0.001676
				Male Liver	0	0	0	0
				Female Intestine	0	0	0	0
				Male Intestine	0	0	0	0
				Female Gill	0.002539	0	0	0
				Male Gill	0	0	0	0
				Female Gonads	0	0	0	0
				Male Gonads	0	0	0	0
				Female Brain	0	0	0	0
				Male Brain	0	0	0	0
				Female Kidney	0.000401	0.000121	0	
				Male Kidney				

SP	Gstz1,2,3	Peptide # 3	R.LNQTLVEIEAFK.A [188, 199]/[192, 203]/[132, 143]	Female Liver	0.004142	0.002605	0.00509	0.002766
				Male Liver	0	0.003764	0.010475	0.003269
				Female Intestine	0.000591	0.000575	0	0
				Male Intestine	0	0	0	0
				Female Gill	0	0.000245	0	0
				Male Gill	0.00318	0	0	0
				Female Gonads	0	0	0	0
				Male Gonads	0	0	0	0
				Female Brain	0	0	0	0
				Male Brain	0	0	0	0
				Female Kidney	0.000573	0.000193	0	0
				Male Kidney	0	0	0	
PP	Gstt1a	Peptide # 1	R.AQVDEFLSWQHT-NIR.S [92, 106]	Female Liver	0.083523	0.034576	0.144085	0.049681
				Male Liver	0.002233	0.0268	0.229569	0.042132
				Female Intestine	0.007662	0.005745	0.010532	0.00617
				Male Intestine	0.003654	0.001864	0.012573	0.005004
				Female Gill	0.002179	0.000825	0.007805	0.002033
				Male Gill	0.122819	0.000697	0.002475	0.002056
				Female Gonads	0.001268	0	0.00057	0
				Male Gonads	0.003047	0.001874	0.012942	0.00381
				Female Brain	0	0	0	0
				Male Brain	0	0	0	0
				Female Kidney	0.013692	0.003148	0.011575	0.006048
				Male Kidney	0.014901	0.003344	0.050035	
PP	Gstt1a	Peptide # 2	K.GVLPVAVTGAPVPK.E [117, 129]	Female Liver	0.124758	0.096257	0.095708	0.06612
				Male Liver	0.003015	0.093071	0.060289	0.075437
				Female Intestine	0.016035	0.017977	0.013145	0.007834
				Male Intestine	0.007152	0.006293	0.006833	0.007887
				Female Gill	0	0.003771	0	0.004789
				Male Gill	0.079927	0.002155	0.004987	0.006567
				Female Gonads	0	0	0	0
				Male Gonads	0	0.00539	0	0.013113
				Female Brain	0	0	0	0
				Male Brain	0	0	0	0
				Female Kidney	0.018577	0.015626	0.010941	0.018335
				Male Kidney	0.018902	0.013994	0	
PP	Gstt1a	Peptide # 3	K.MDSALEDLNMSLK.I [132, 144]	Female Liver	0.037959	0.030121	0.021074	0.018827

				Male Liver	0.000932	0.024163	0.031313	0.033184
				Female Intestine	0.003824	0.003341	0.002286	0.001308
				Male Intestine	0.001343	0.001696	0	0.001761
				Female Gill	0	0.000952	0	0.001878
				Male Gill	0.022725	0.000671	0.002431	0.002682
				Female Gonads	0	0	0	0
				Male Gonads	0	0.001378	0	0.006243
				Female Brain	0	0	0	0
				Male Brain	0	0	0	0
				Female Kidney	0.005029	0.003705	0.003805	0.006828
				Male Kidney	0.00575	0.003653	0	
PP	Gstt1b	Peptide # 1	K.MENAEENLN-VALQLFQDK.F [132, 149]	Female Liver	0.003059	0.001483	0.00138	0.001133
				Male Liver	0	0.000384	0	0.001402
				Female Intestine	0.001741	0.003078	0.003756	0.001376
				Male Intestine	0.000633	0.001658	0	0.000943
				Female Gill	0	0	0	0.000805
				Male Gill	0	0	0	0.001251
				Female Gonads	0	0	0	0
				Male Gonads	0.000627	0.000817	0	0.001068
				Female Brain	0	0.00025	0	0
				Male Brain	0	0.000372	0	0
				Female Kidney	0.00065	0	0	0.00131
				Male Kidney	0.000506	0	0	
PP	Gstm3	Peptide # 1	K.VVQSNAILR.Y [69, 77]	Female Liver	0.015498	0.004769	0.016796	0.008719
				Male Liver	0.048241	0.006661	0.025566	0.009449
				Female Intestine	0.006757	0.002134	0.00578	0.008409
				Male Intestine	0.010487	0.00905	0.012162	0.016514
				Female Gill	0.078376	0.027095	0.276649	0.084892
				Male Gill	0.015205	0.017672	0.073863	0.049872
				Female Gonads	0.00654	0.001932	0.006967	0.006665
				Male Gonads	0.016718	0.013894	0.089127	0.014167
				Female Brain	0.001414	0.00064	0.001763	0.002969
				Male Brain	0.000797	0.000589	0.002482	0.004
				Female Kidney	0.006963	0.001513	0.005099	0.006606
				Male Kidney	0.00467	0.00082	0.016482	
SP	Gstm1,2	Peptide # 1	R.MFEPACLDLDFK.N [167, 177]	Female Liver	0	0.002655	0	0.002987
				Male Liver	0.005564	0.007551	0	0.004164

				Female Intestine	0.002495	0.001948	0.001421	0
				Male Intestine	0	0.002218	0	0
				Female Gill	0.003147	0.0101	0	0.005764
				Male Gill	0.001458	0.008879	0.005611	0.011178
				Female Gonads	0	0.001303	0.000888	0
				Male Gonads	0.001927	0.005052	0	0.013334
				Female Brain	0.004406	0.006347	0	0
				Male Brain	0.001633	0.004746	0	0
				Female Kidney	0.004576	0.00954	0.002086	0.007868
				Male Kidney	0.002856	0.003749	0	
SP	Gstm1,2	Peptide # 2	K.IVQSNAIMR.Y [69, 77]	Female Liver	0.221983	0.085341	0.261932	0.123454
				Male Liver	0.163291	0.04093	0.320033	0.101143
				Female Intestine	0.026839	0.007587	0.022366	0.035795
				Male Intestine	0.053091	0.028729	0.062623	0.050104
				Female Gill	0.172908	0.038418	0.650214	0.18823
				Male Gill	0.134665	0.036371	0.142561	0.140433
				Female Gonads	0.208072	0.108726	0.15715	0.197895
				Male Gonads	0.1422	0.040887	2.07001	0.118489
				Female Brain	0.176172	0.073039	0.23677	0.112367
				Male Brain	0.161637	0.090976	0.365568	0.148816
				Female Kidney	0.116982	0.02768	0.10766	0.109376
				Male Kidney	0.072303	0.011718	0.3141	
SP	Gstm1,2,3	Peptide # 1	R.VDILENQAMDFR.N [96, 107]	Female Liver	0.004522	0.003233	0	0.002239
				Male Liver	0.003732	0.002224	0	0.002035
				Female Intestine	0.000598	0	0	0
				Male Intestine	0	0.001088	0	0.000577
				Female Gill	0.003278	0.006285	0.005339	0.004698
				Male Gill	0	0.004293	0.003698	0.004932
				Female Gonads	0.00295	0.001398	0.003005	0.003451
				Male Gonads	0.001344	0.001664	0	0.004404
				Female Brain	0.001503	0.001892	0	0
				Male Brain	0.001169	0.002036	0	0
				Female Kidney	0.002576	0.002211	0.00155	0.003045
				Male Kidney	0.001275	0.000475	0	
SP	Gstm1,2,3	Peptide # 2	K.QFSDFLGDR.K [135, 143]	Female Liver	0	0.001663	0	0
				Male Liver	0.001842	0.001446	0	0.000606
				Female Intestine	0.00295	0.003148	0.001812	0

				Male Intestine	0	0.001111	0	0
				Female Gill	0.001228	0.003011	0	0.002831
				Male Gill	0	0.001831	0.002932	0.003903
				Female Gonads	0.000512	0	0	0
				Male Gonads	0	0.001651	0	0.003397
				Female Brain	0	0.0014	0	0
				Male Brain	0	0.001238	0	0
				Female Kidney	0.001481	0.001478	0	0.002166
				Male Kidney	0.001181	0.000603	0	
PP	Gstp1	Peptide # 1	K.ENLVTFEEWMK.G [30, 40]	Female Liver	0.002622	0.004089	0	0.001598
				Male Liver	0	0.005038	0	0.001962
				Female Intestine	0.003913	0.001835	0.001308	0.000564
				Male Intestine	0	0.001625	0	0
				Female Gill	0	0.014272	0	0.002039
				Male Gill	0	0.009445	0.002629	0.003671
				Female Gonads	0	0	0	0
				Male Gonads	0	0.002223	0	0.00188
				Female Brain	0	0.001384	0	0
				Male Brain	0	0.001296	0	0
				Female Kidney	0.000674	0.006025	0	0.001638
				Male Kidney	0	0.003112	0	0
PP	Gstp1	Peptide # 2	K.ATCVFGQLPK.F [45, 54]	Female Liver	0.008373	0.010981	0.005138	0.008096
				Male Liver	0.005599	0.024049	0	0.009893
				Female Intestine	0.010534	0.011577	0.006232	0.00404
				Male Intestine	0.002509	0.012818	0	0.003606
				Female Gill	0.002784	0.041432	0	0.006877
				Male Gill	0.004386	0.02349	0.012852	0.015781
				Female Gonads	0	0	0	0
				Male Gonads	0.001283	0.01243	0	0.007122
				Female Brain	0.00235	0.007202	0	0
				Male Brain	0.002179	0.00677	0	0
				Female Kidney	0.00322	0.015717	0	0.006844
				Male Kidney	0.002642	0.007231	0	
PP	Gstp1	Peptide # 3	K.FEDGDLVLFQS-NAMLR.H [55, 70]	Female Liver	0.020559	0.013008	0.014419	0.009943
				Male Liver	0.005912	0.009508	0.012939	0.007871
				Female Intestine	0.00701	0.00176	0.004657	0.005015
				Male Intestine	0.005271	0.006245	0.005854	0.004369

				Female Gill	0.007611	0.016282	0.016477	0.007425
				Male Gill	0.008009	0.011137	0.010196	0.011124
				Female Gonads	0	0	0	0
				Male Gonads	0.002741	0.005762	0	0.005915
				Female Brain	0.003246	0.003788	0.003732	0.008448
				Male Brain	0.003079	0.004065	0	0
				Female Kidney	0.002829	0.007954	0.002169	0.004661
				Male Kidney	0.003205	0.004727	0	0
PP	Gstp1	Peptide # 4	K.CFENVLAK.N [128, 135]	Female Liver	0.091723	0.047172	0.097694	0.131614
				Male Liver	0.055697	0.04797	0.142086	0.10661
				Female Intestine	0.064686	0.061968	0.081935	0.050342
				Male Intestine	0.059874	0.065047	0.057302	0.062708
				Female Gill	0.041821	0.032568	0.172326	0.105793
				Male Gill	0.0634	0.020273	0.105258	0.093252
				Female Gonads	0.002436	0.002737	0.006888	0.006266
				Male Gonads	0.023634	0.039239	0.079404	0.040326
				Female Brain	0.036421	0.031171	0.057407	0.026207
				Male Brain	0.02692	0.03714	0.056618	0.045331
				Female Kidney	0.03142	0.01459	0.032505	0.04425
				Male Kidney	0.028881	0.007708	0.037256	0
SP	Gstp1,2	Peptide # 1	K.LIQEYETGK.E [106, 115]	Female Liver	0	0.00125	0	0
				Male Liver	0.001131	0.00178	0	0.001347
				Female Intestine	0.002863	0.002138	0.001729	0
				Male Intestine	0	0.000986	0	0
				Female Gill	0	0.002726	0	0
				Male Gill	0	0.001495	0	0.001637
				Female Gonads	0	0	0	0
				Male Gonads	0.000343	0.001077	0	0.000951
				Female Brain	0	0.000648	0	0
				Male Brain	0	0.000788	0	0
				Female Kidney	0.000752	0.00137	0	0
				Male Kidney	0.000588	0.000866	0	
SP	Gstp1,2	Peptide # 2	K.ALLECENFK.K [189, 197]	Female Liver	0.130496	0.059578	0.130162	0.107127
				Male Liver	0.060371	0.073859	0.214878	0.105404
				Female Intestine	0.029828	0.041939	0.050158	0.032752
				Male Intestine	0.056839	0.070634	0.078489	0.055653
				Female Gill	0.060069	0.067487	0.291546	0.108572

				Male Gill	0.089809	0.042622	0.123138	0.111864
				Female Gonads	0.00522	0.004217	0.007877	0.006161
				Male Gonads	0.033234	0.052456	0.171353	0.058539
				Female Brain	0.047965	0.03792	0.063907	0.028728
				Male Brain	0.038629	0.044913	0.088627	0.040633
				Female Kidney	0.028938	0.031084	0.030204	0.046411
				Male Kidney	0.023083	0.0171	0.098583	0
PP	Gstr	Peptide # 1	R.LMIALEEK.Q [18, 25]	Female Liver	0.648246	0.525475	0.664212	0.407018
				Male Liver	0.131682	0.39905	0.468053	0.389563
				Female Intestine	0.280158	0.369276	0.222158	0.130976
				Male Intestine	0.073858	0.159481	0.120219	0.110785
				Female Gill	0.115367	0.083543	0.223692	0.192682
				Male Gill	0.441834	0.073658	0.198869	0.202042
				Female Gonads	0.039574	0.025052	0.019365	0.021608
				Male Gonads	0.049965	0.085494	0.147956	0.117963
				Female Brain	0.11478	0.102096	0.121026	0.055427
				Male Brain	0.104718	0.129411	0.1198	0.069398
				Female Kidney	0.132031	0.095151	0.070666	0.142166
				Male Kidney	0.12437	0.083945	0.174138	
PP	Gstr	Peptide # 2	R.LIPDNPAE-MALVYQR.M [87, 101]	Female Liver	0.294815	0.08567	0.388981	0.253173
				Male Liver	0.073663	0.080102	0.408878	0.195824
				Female Intestine	0.037755	0.024888	0.042321	0.072672
				Male Intestine	0.089897	0.03737	0.076556	0.072001
				Female Gill	0.083796	0.01605	0.189201	0.081587
				Male Gill	0.370264	0.012647	0.06379	0.058155
				Female Gonads	0.024278	0.007493	0.014386	0.017589
				Male Gonads	0.052	0.019655	0.139472	0.020719
				Female Brain	0.08511	0.026193	0.093346	0.051015
				Male Brain	0.083421	0.035022	0.117809	0.063195
				Female Kidney	0.065279	0.019016	0.047972	0.045848
				Male Kidney	0.072111	0.014463	0.288087	
PP	Gstr	Peptide # 3	R.MFETENLQQK.M [102, 111]	Female Liver	0.434015	0.164409	0.29549	0.224494
				Male Liver	0.074705	0.114081	0.226152	0.201361
				Female Intestine	0.091986	0.11664	0.073042	0.072429
				Male Intestine	0.04924	0.059173	0.051771	0.058038
				Female Gill	0.067846	0.0225	0.12091	0.078136
				Male Gill	0.268033	0.018123	0.085016	0.066227

				Female Gonads	0.018404	0.008446	0.00929	0.011893
				Male Gonads	0.036875	0.02912	0.068293	0.043063
				Female Brain	0.069565	0.036032	0.076109	0.029467
				Male Brain	0.06009	0.048068	0.075553	0.040874
				Female Kidney	0.075067	0.02615	0.045365	0.052061
				Male Kidney	0.074783	0.020805	0.118266	
SP	Gsto1	Peptide # 1	K.YDTININLK.N [47, 55]	Female Liver	0	0	0	0
				Male Liver	0	0	0	0
				Female Intestine	0.001461	0.001102	0	0
				Male Intestine	0.000464	0.001212	0	0.000454
				Female Gill	0	0.000544	0	0
				Male Gill	0	0.000479	0	0
				Female Gonads	0	0	0	0
				Male Gonads	0	0.000467	0	0
				Female Brain	0	0.000351	0	0
				Male Brain	0	0.000596	0	0
				Female Kidney	0	0	0	0
				Male Kidney	0	0	0	
SP	Gsto1	Peptide # 2	R.MLLELFISK.V [113, 120]	Female Liver	0.004262	0.001982	0	0.002396
				Male Liver	0.013041	0.001947	0	0.005846
				Female Intestine	0.028128	0.030257	0.036224	0.020597
				Male Intestine	0.026481	0.042169	0.028988	0.027156
				Female Gill	0.010268	0.00569	0.021351	0.01386
				Male Gill	0.001763	0.005803	0.019591	0.013027
				Female Gonads	0	0	0	0
				Male Gonads	0.008008	0.01631	0	0.002864
				Female Brain	0.014764	0.016904	0.018699	0.004227
				Male Brain	0.01604	0.023919	0.015136	0.007692
				Female Kidney	0	0	0	0.00023
				Male Kidney	0.001442	0	0	
SP	Gsto2	Peptide # 1	K.LLPSPDPER.A [100, 108]	Female Liver	0.011476	0.004632	0.00655	0.005683
				Male Liver	0.053379	0.00536	0	0.011372
				Female Intestine	0.027861	0.035392	0.032708	0.019657
				Male Intestine	0.032551	0.034384	0.014995	0.023284
				Female Gill	0.038698	0.039395	0.09128	0.088896
				Male Gill	0.004427	0.028367	0.099151	0.115306
				Female Gonads	0.006141	0.006793	0.004491	0.004954

				Male Gonads	0.005268	0.020876	0	0.005689
				Female Brain	0.004406	0.002439	0.004486	0.003811
				Male Brain	0.00959	0.007891	0	0.002572
				Female Kidney	0.006951	0.0059	0.006746	0.011084
				Male Kidney	0.009127	0.003479	0	

SI Table 7: Indexed retention time (iRT) values for the respective peptides.

Peptide Sequence	iRT
AILNYIAGK	43.15
ALANSSFLVGK	40.27
ALLECFNK	28.22
AQVDEFLSWQHTNIR	65.34
ATCVFGQLPK	42.77
AVLSHLFK	32.65
CFENVLAK	27.39
CFLDHFENLEK	60.56
CFLDHFESLEK	71.08
DGGQQLTDQFK	17.89
ECSAPGPVPNGQIR	5.12
FEDGDLVLFQSNAMLR	91.57
FLQPGSAR	-0.93
FYTCGEAPNYDK	6.27
GVLPAVTGAPVPK	48.61
IICDIIASGIQPLQNLVYLQK	101.24
IQAFQDQMK	13.48
IQAFQEQQMK	12.41
IVQSNAIMR	4.82
KPPPDEEYVR	-5.26
LIPDNPAEMALVYQR	72.51
LIYQEYETGK	15.97
LLPADPMQR	25.17
LLPSDPFER	51.18
LMEYYEMVK	44.85
LMIALEEK	41.17
LNQTLVEIEAFK	78.74
LYSCGEAPNYDR	1.2
MDSALEDLNMSLK	78.25
MENAEENLNVALQLFQDK	99.18
MFEPACLDDEFK	67.59
MFETENLQQK	14.26
MLLELFSK	83.3
NKPCYCEK	-13.91
QFSDFLGDR	47.52
TYSSIEEK	-6.5
VDILENQAMDFR	66.77

VRFLPVFEK	55.15
VVLHYFNGR	17.13
VVQSNAILR	9.59
YDTININLK	49.53

Supplementary information Chapter 3

SI Table 8: Measured and predicted mass-to-charge ratio (m/z), the intensities and the relative intensities of isotopes corresponding to the ions A, B, C, D and E. The structural formula is shown in figure 13.

A) $[C_6H_3N_2O_5]^-$

measured				predicted		
	m/z	intensity	relative intensity	m/z	intensity	relative intensity
1	183.0	4.38E+08	100.0	183.0047	9.19E+05	100.0
2	184.0	2.86E+07	6.5	184.0081	5.96E+04	6.5
3	185.0	4.68E+06	1.1	185.009	9.44E+03	1.0

B) $[C_6H_3ClN_2O_4+CH_3OH-H]^-$

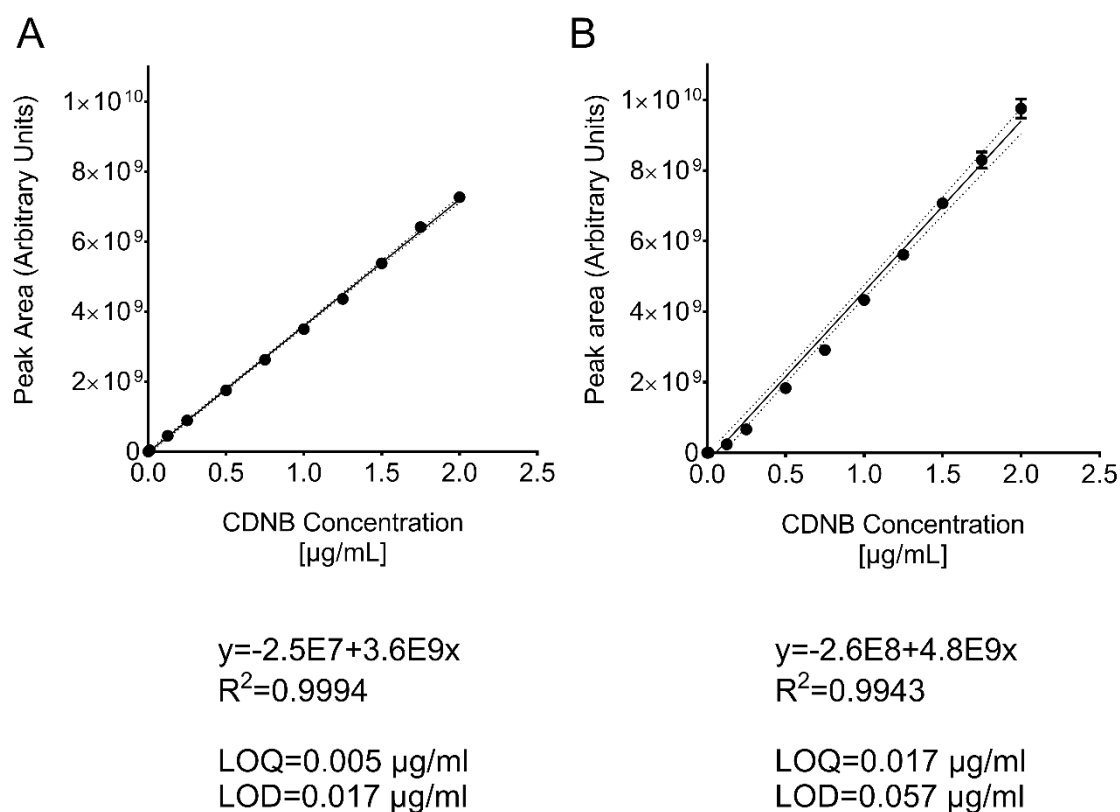
measured				predicted		
	m/z	intensity	relative intensity	m/z	intensity	relative intensity
1	232.9969	6.88E+06	100.0	232.9971	6.89E+05	100.0
2	234.0003	5.19E+05	7.5	234.0004	5.21E+04	7.6
3	234.9939	2.19E+06	31.8	234.9941	2.20E+05	32.0
4	235.9962	1.57E+05	2.3	235.9975	1.67E+04	2.4

C) $[C_6H_3ClN_2O_4-H]^-$ and D) $[C_6H_3ClN_2O_4]^{\bullet-}$

measured				I) predicted			II) predicted			measured - predicted (I)	
	m/z	intensity	relative intensity	m/z	intensity	relative intensity	m/z	intensity	relative intensity	intensity	relative intensity
1	200.9707	1.07E+07	100.0	200.9709	6.98E+05	100.0	201.9787	6.98E+05	100	3.86E+06	100
2	201.979	4.55E+06	42.7	201.9742	4.53E+04	6.5					
3	202.9678	3.25E+06	30.5	202.9679	2.23E+05	32.0					
4	202.9812	2.49E+05	2.3	203.9713	1.45E+04	2.1	202.982	4.53E+04	6.49	2.49E+05	6.5
5	203.9759	1.45E+06	13.6				203.9757	2.23E+05	31.96	1.23E+06	31.8

D) $[C_6H_3ClNO_3]^-$

measured				predicted		
	m/z	intensity	relative intensity	m/z	intensity	relative intensity
1	171.9814	2.82E+06	100.0	171.9807	7.02E+05	100.0
2	172.9836	1.81E+05	6.4	172.984	4.56E+04	6.5
3	173.9776	8.59E+05	30.5	173.9777	2.25E+05	32.0
4	174.9813	5.73E+04	2.0	174.9811	1.46E+04	2.1

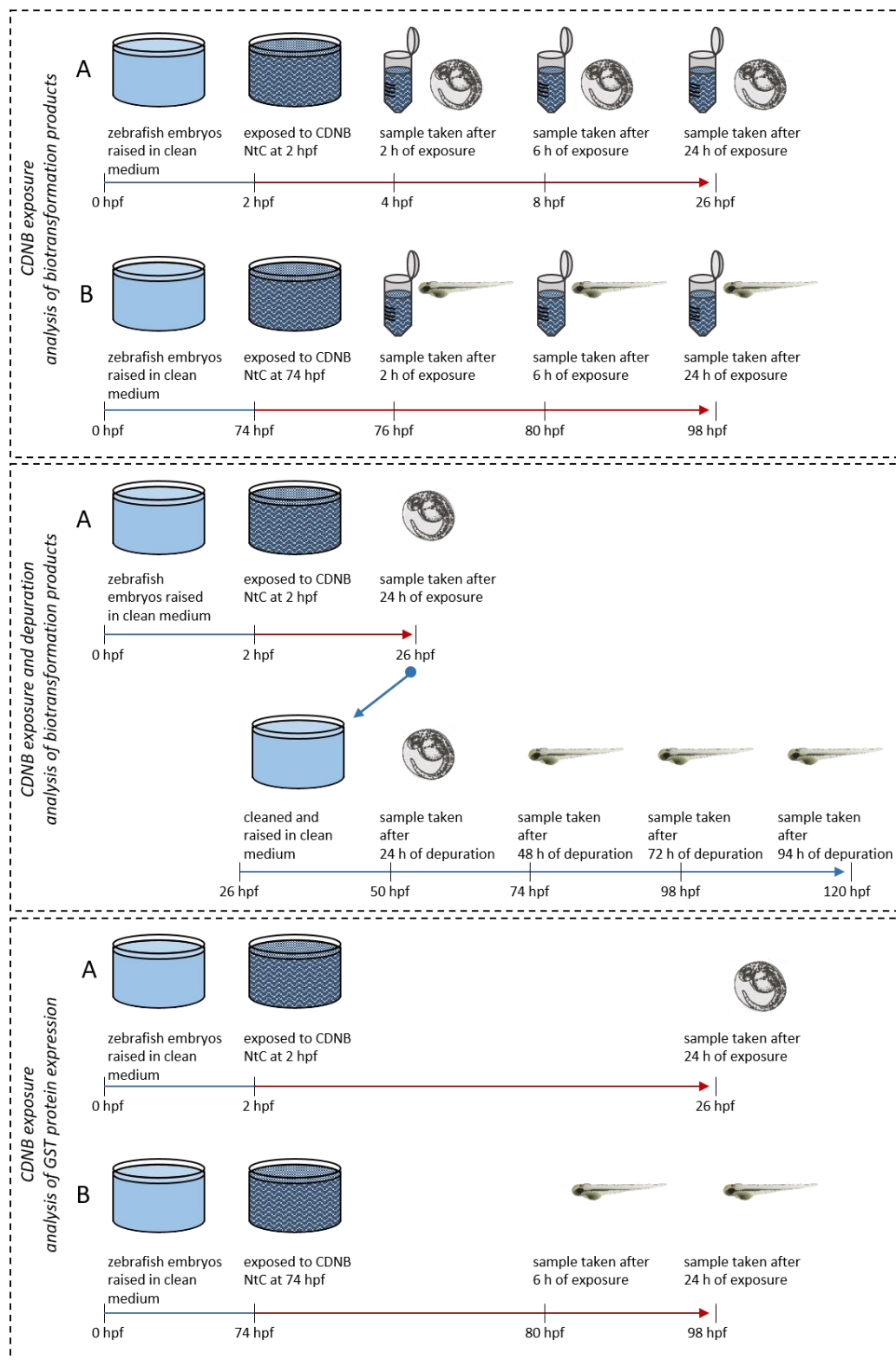


SI Figure 1: Calibration series over the concentration range of 0 to 2 µg/ml in reconstituted water (A) and L15 medium with 5% FBS (B). The mean peak area of five replicates is shown in addition to the 95% confidence interval. The formula ($y=a+bx$), the R square (R^2), Limit of detection (LOD) and limit of quantification (LOQ) are shown below the calibration graph.

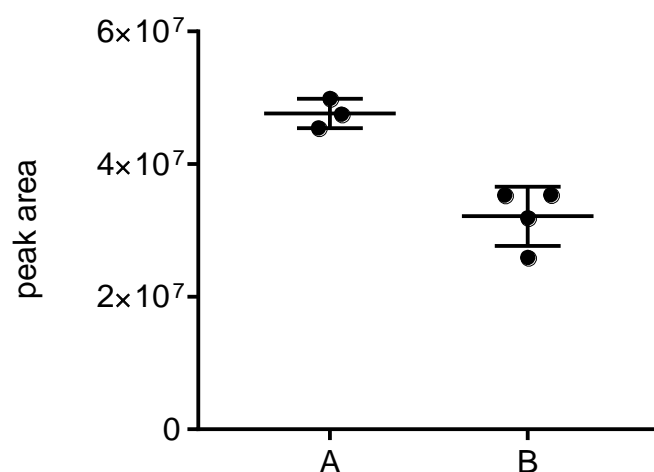
SI Table 9: Nominal and measured 1-chloro-2,4-dinitrobenzene (CDNB) concentrations used for toxicity studies in reconstituted water (A) and L15 medium with 5% FBS (B).

	A: reconstituted water		B: L15 medium with 5%FBS	
	nominal concentration [µg/ml]	measured concentration [µg/ml]	nominal concentration [µg/ml]	measured concentration [µg/ml]
1	0.3	0.2	1.6	0.35
2	0.2	0.14	1.28	0.54
3	0.12	0.11	1.02	0.66
4	0.1	0.08	0.82	0.79
5	0.07	0.06	0.66	0.95
6	0.05	0.04	0.42	0.35
7	0.025	0.03		

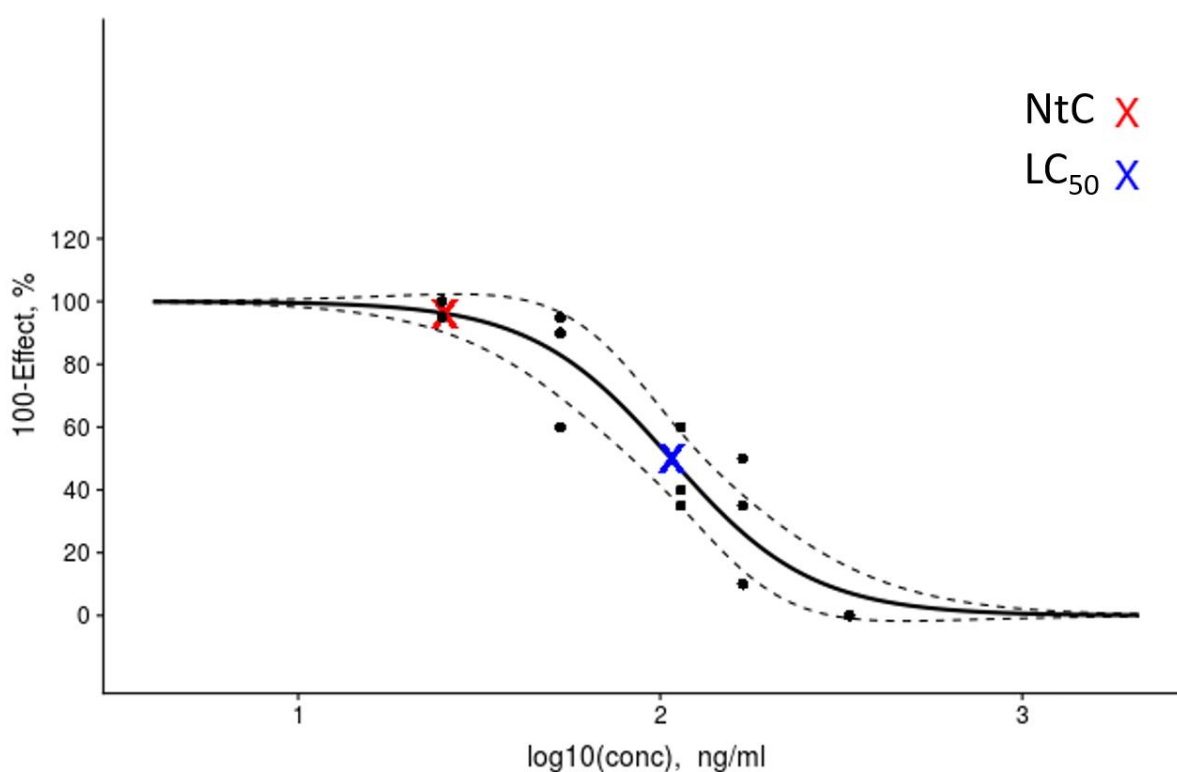
Supplementary information Chapter 4



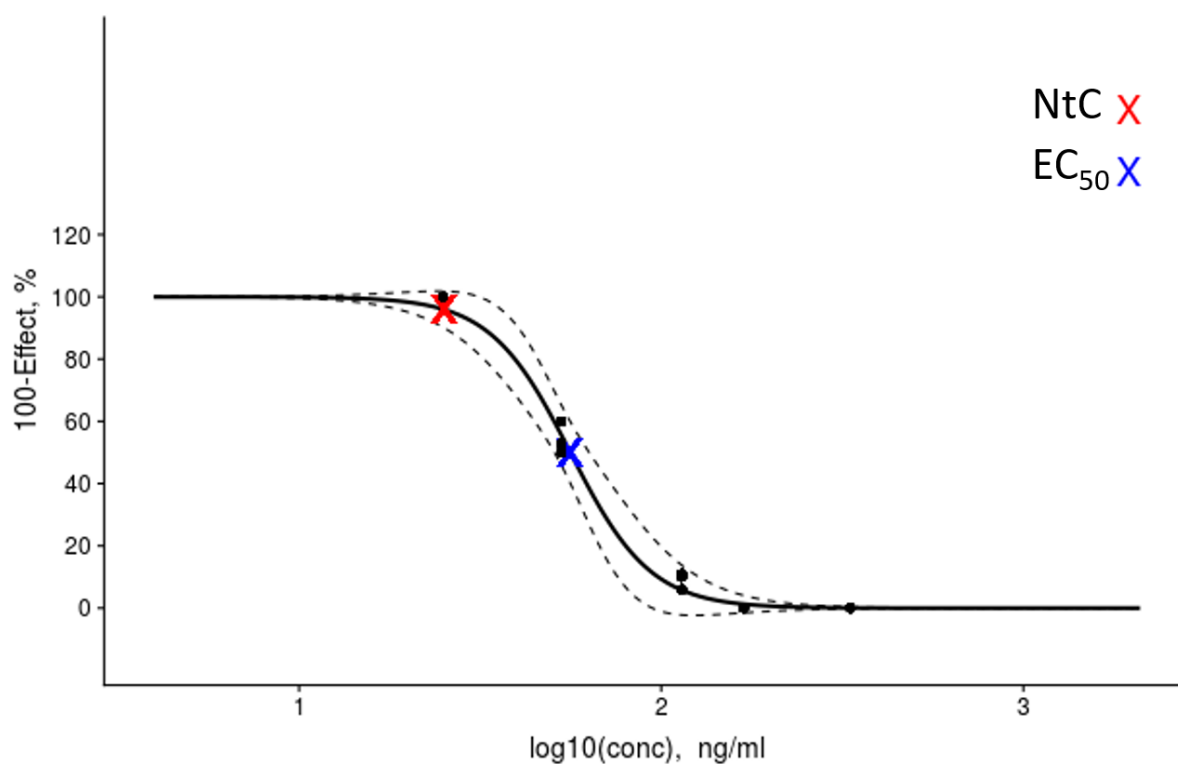
SI Figure 2: Experimental workflow Chapter 4: zebrafish embryos were exposed to the non-toxic concentration (NtC=25 ng/ml) of 1-chloro-2,4-dinitrobenzene (CDNB) at 2 hours post fertilization (hpf) (A) or 74 hpf (B). During the CDNB exposure for the analysis of biotransformation products (top panel), 90 embryos/larvae and 10 ml exposure medium were sampled after 2, 6 and 24 exposure hours. For the investigation of biotransformation products in the CDNB exposure and depuration study (middle panel), 90 embryos were sampled after 24 exposure hours while the remaining organisms were transferred into clean medium. Subsequently 90 embryos/larvae were sampled after 24, 48, 72 and 94 hours of depuration. During the CDNB exposure for the analysis of glutathione S-transferase (GST) protein expression (bottom panel), 120 embryos/larvae were sampled after 24 (embryos) or 6 and 24 (larvae) exposure hours. Each experiment was performed in triplicates. Blue lines represent clean medium and red lines represent medium with 25 ng/ml CDNB.



SI Figure 3: Recovery of 2,4-dinitrophenyl-S-glutathione (DNP-SG) measured through the comparison of A: unprocessed samples ($n=3$, average peak area=47 617 263, arbitrary units) and B: processed embryo samples ($n=4$, average peak area = 32 125 031, arbitrary units). Calculated recovery of 67.5%.

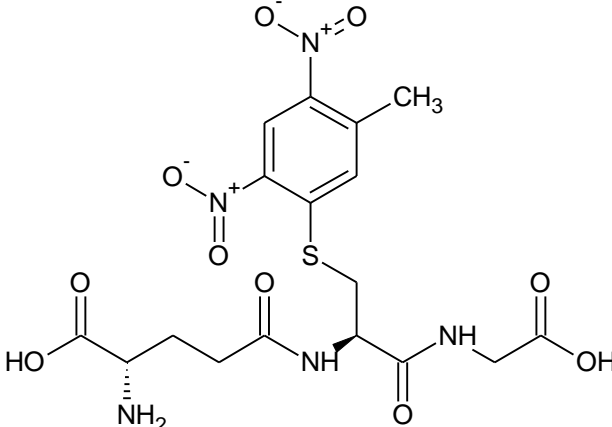
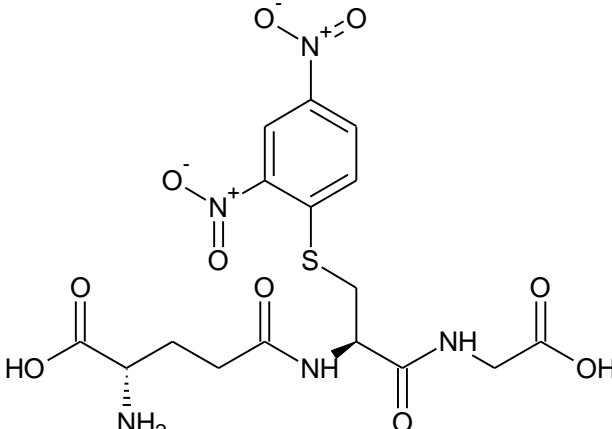


SI Figure 4: Dose-response curve for lethal effects of 1-chloro-2,4-dinitrobenzene (CDNB). The toxic range of CDNB was investigated by monitoring lethal effects at CDNB measured concentrations of 333, 196, 114, 53 and 25 ng/ml in three independent biological replicates. The curve fit and the calculation of the non-toxic concentration ($NtC=25$ ng/ml) and the half-maximal lethal concentration ($LC_{50}=107$ ng/ml) were performed with the use of an algorithm developed by Stadnicka-Michalak et al. (2018). The figure shows the fitted sigmoidal curve together with 95% confidence intervals and measured data where each dot represents the mean of 20 embryos assessed in one independent experiment. The NtC and LC_{50} values are indicated as a red and a blue cross, respectively. The LC_{50} confidence interval is [83, 132] ng/ml.

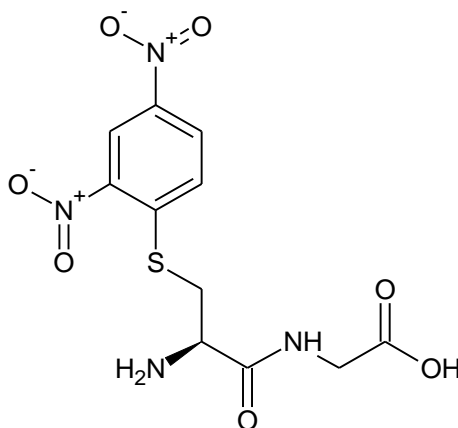


SI Figure 3: Dose-response curve for sublethal effects of 1-chloro-2,4-dinitrobenzene (CDNB). The toxic range of CDNB was investigated by monitoring sublethal effects at CDNB measured concentrations of 333, 196, 114, 53 and 25 ng/ml in three independent biological replicates. The curve fit and the calculation of the non-toxic concentration ($NtC=25$ ng/ml) and the half-maximal effective concentration ($EC_{50}=56$ ng/ml) were performed with the use of an algorithm developed by Stadnicka-Michalak et al. (2018). The figure shows the fitted sigmoidal curve together with 95% confidence intervals and measured data where each dot represents the mean of 20 embryos assessed in one independent experiment. The NtC and EC_{50} values are indicated as a red and a blue cross, respectively. The EC_{50} confidence interval is [51, 63] ng/ml.

SI Table 10: Physico-chemical calculations and predictions for 2,4-dinitrotoluene-S-glutathione (DNT-SG); 2,4-dinitrophenyl-S-glutathione (DNP-SG); 2,4-dinitrophenyl cysteinylglycine (DNP-CG); 2,4-dinitrophenyl cysteine (DNP-C); 2,4-dinitrophenyl N-acetylcysteine (DNP-NAC), performed with the use of the software Chemicalize (june, 2019, <https://chemicalize.Com/> developed by chemaxon, <http://www.Chemaxon.Com>).

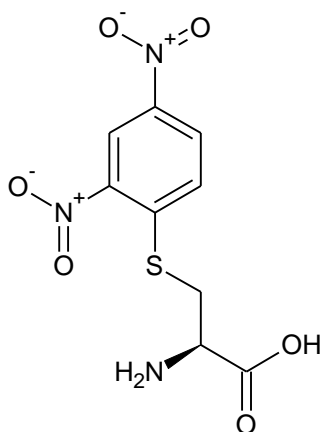
DNT-SG	
	
Formula	C ₁₇ H ₂₁ N ₅ O ₁₀ S
Molar mass	487.44 g/mol
Exact mass	487.1009 Da
InChI	InChI=1/C17H21N5O10S/c1-8-4-13(12(22(31)32)5-11(8)21(29)30)33-7-10(16(26)19-6-15(24)25)20-14(23)3-2-9(18)17(27)28/h4-5,9-1OH,2-3,6-7,1BH2,1H3,(H,19,26)(H,20,23)(H,24,25)(H,27,28)
InChIKey	SJZUDKZPSQBPHZ-UHFFFAOYNA-N
Isoelectric point	2.22
logP	-2.78
Intrinsic solubility	0.0194 mg/ml
Solubility category	Moderate
DNP-SG	
	
Formula	C ₁₆ H ₁₉ N ₅ O ₁₀ S
Molar mass	473.41 g/mol
Exact mass	473.0852 Da
InChI	InChI=1S/C16H19N5O10S/c17-9(16(26)27)2-4-13(22)19-10(15(25)18-6-14(23)24)7-32-12-3-1-8(20(28)29)5-11(12)21(30)31/h1,3,5,9-1OH,2,4,6-7,17H2,(H,18,25)(H,19,22)(H,23,24)(H,26,27)/t9-,10-/m0/s1
Isoelectric point	3.92
logP	-1.71
Intrinsic solubility	1.07 mg/ml
Solubility category	High

DNP-CG



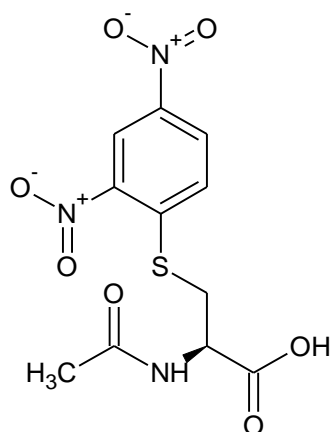
Formula	C ₁₁ H ₁₂ N ₄ O ₇ S
Molar mass	344.3 g/mol
Exact mass	344.0426 Da
InChI	InChI=1/ C11H12N4O7S/c12-7(11(18)13-4 -10(16)17)5-23- 9-2-1-6(14(19)20)3-8(9)15(21)22/h1-3,7H,4-5,12H2, (H,13,18)(H,16,17)
Isoelectric point	5.23
logP	-2.25
Intrinsic solubility	0.0280 mg/ml
Solubility category	Moderate

DNP-C

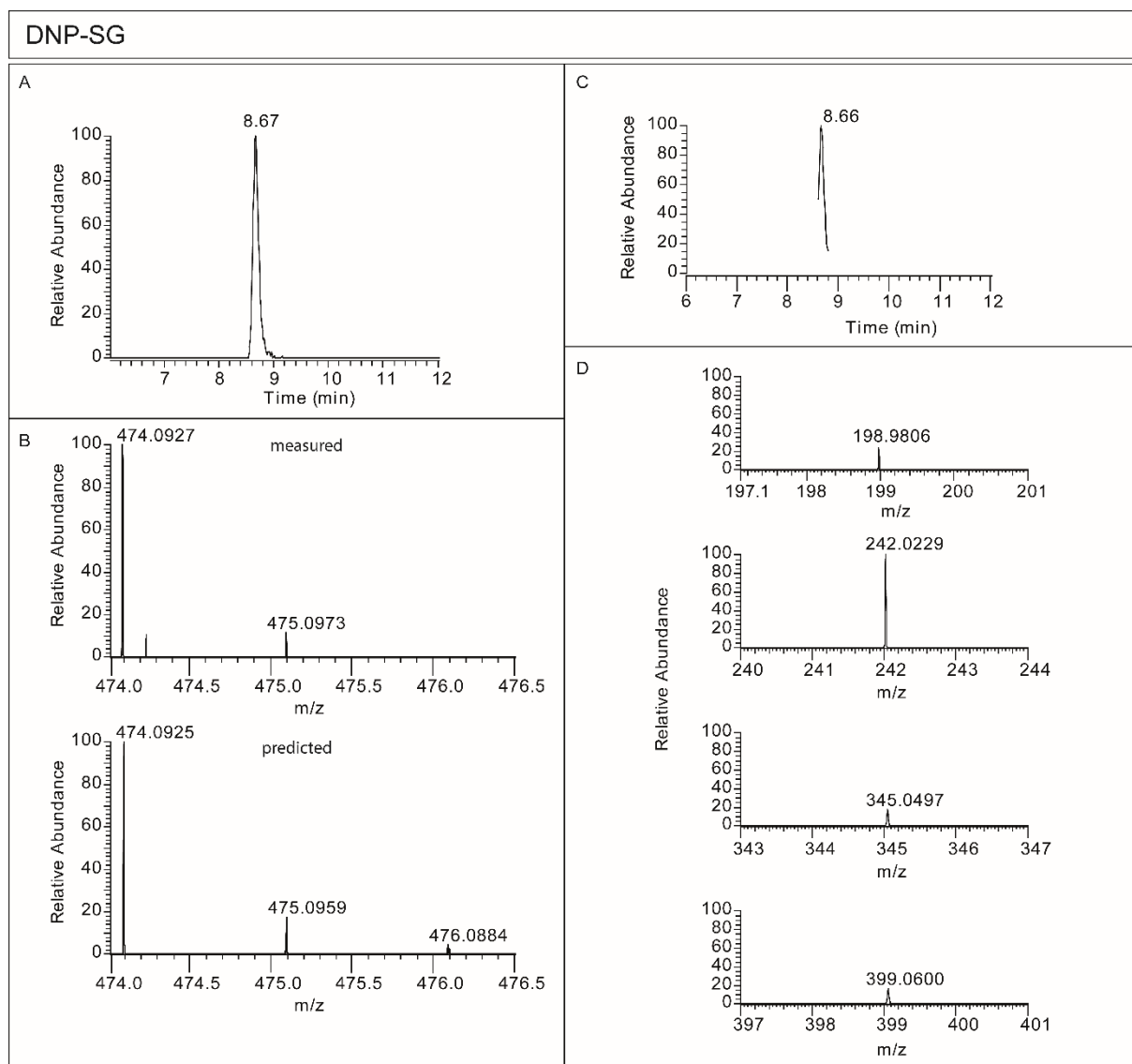


Formula	C ₉ H ₉ N ₃ O ₆ S
Molar mass	287.25 g/mol
Exact mass	287.0212 Da
InChI	InChI=1/C9H9N3O6S/c10-6(9(13)14)4-19-8-2-1-5(11(15)16)3-7(8)12(17)18/h1-3,6H,4,10H2,(H,13,14)
Isoelectric point	5.36
logP	-1.15
Intrinsic solubility	0.0421 mg/ml
Solubility category	Moderate

DNP-NAC



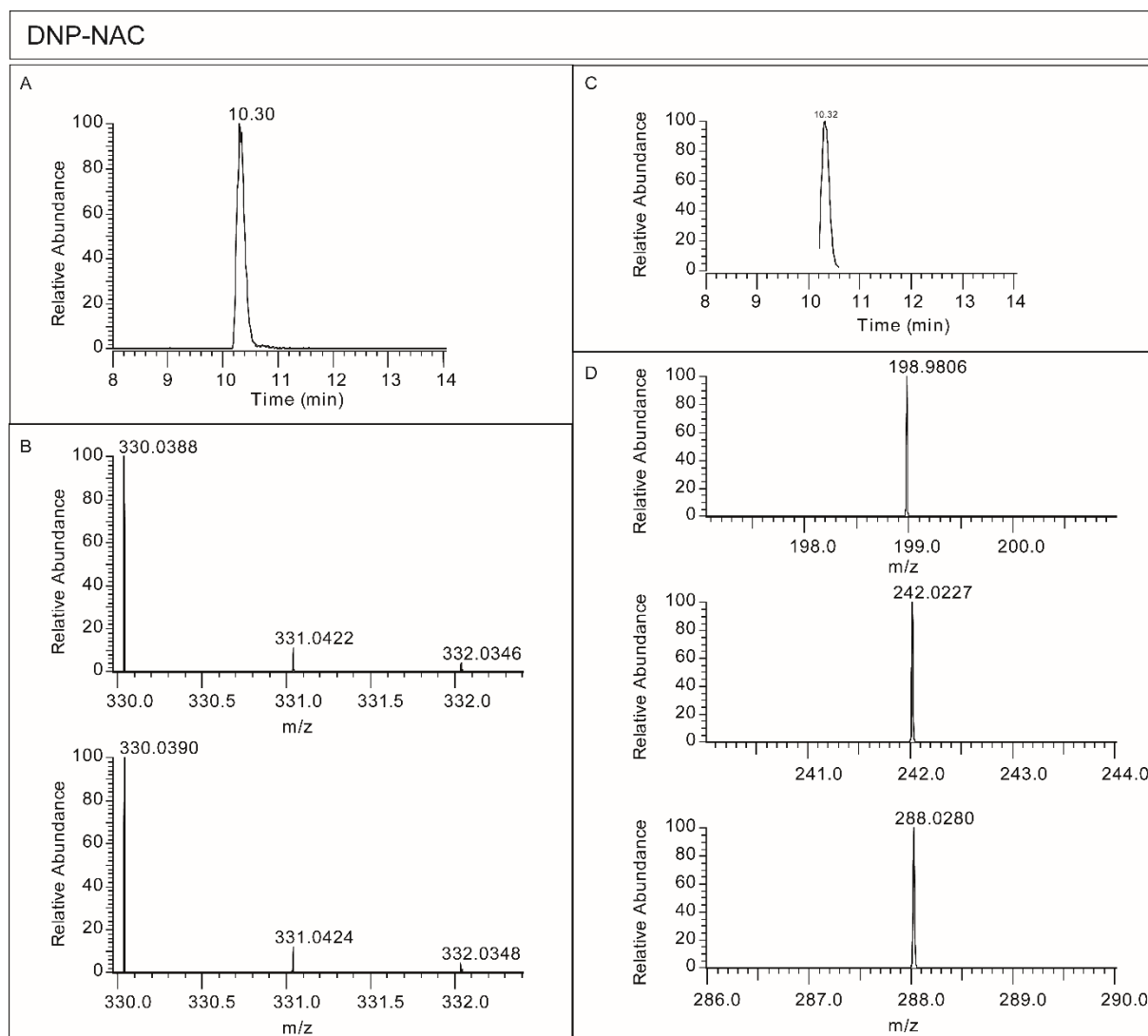
Formula	C ₁₁ H ₁₁ N ₃ O ₇ S
Molar mass	329.28 g/mol
Exact mass	329.0317 Da
InChI	InChI=1/C11H11N3O7S/c1-6{15}12-8{11(16)17}5-22-10-3- 2-7(13(18)19)4-9(10)14(20)21/h2-4,8H,5H2,1H3,(H,12,15)(H,16,17)
Isoelectric point	N/A
logP	0.93
Intrinsic solubility	0.0216
Solubility category	Moderate



SI Figure 4: Chromatogram and mass spectra of 2,4-dinitrophenyl-S-glutathione (DNP-SG). A: Chromatographic peak of the precursor ion ($m/z=474.09$) in full scan mode, B: measured and predicted isotope distribution of the molecular ion DNP-SG, C: MS2 chromatogram of the $m/z=474.09$ precursor ion and D: MS2 accurate mass spectra of the monoisotopic fragment ions. m/z : mass-to-charge ratio.

SI Table 11: Difference (ppm) between the measured and predicted masses of the precursor ion 2,4-dinitrophenyl-S-glutathione (DNP-SG) in full scan (MS) and of the fragment ions (MS2).

MS			MS2		
predicted m/z	measured m/z	ppm difference	predicted m/z	measured m/z	ppm difference
474.0925	474.0927	0.4219	198.9808	198.9806	-1.0051
475.0959	475.0973	2.9468	242.0230	242.0229	-0.4132
476.0884	ND	ND	345.0499	345.0497	-0.5796
			399.0605	399.0600	-1.2529



SI Figure 5: Chromatogram and mass spectra of 2,4-dinitrophenyl N-acetylcysteine (DNP-NAC). A: Chromatographic peak of the precursor ion ($m/z=330.04$) in full scan mode, B: measured and predicted isotope distribution of the molecular ion DNP-NAC, C: MS2 chromatogram of the $m/z=330.04$ precursor ion, D: MS2 accurate mass spectra of the monoisotopic fragment ions. m/z : mass-to-charge ratio.

SI Table 12: Difference (ppm) between the measured and predicted masses of the precursor ion 2,4-dinitrophenyl N-acetylcysteine (DNP-NAC) in full scan (MS) and of the fragment ions (MS2).

MS			MS2		
predicted m/z	measured m/z	ppm difference	predicted m/z	measured m/z	ppm difference
330.0390	330.0388	-0.6060	198.9808	198.9806	-1.0051
331.0424	331.0422	-0.6042	242.0230	242.0227	-1.2396
332.0348	332.0346	-0.6023	288.0284	288.0280	-1.3888

Generation of DNP-C through gas-phase reactions in the ESI source

During the sample run we observed a peak with the mass $m/z = 288.0285$ at a retention time of 10.3 min in some samples. This m/z corresponds to the 1-chloro-2,4-dinitrobenzene (CDNB) biotransformation product 2,4-dinitrophenyl cysteine (DNP-C). However, the CDNB biotransformation product 2,4-dinitrophenyl N-acetylcysteine (DNP-NAC) elutes at exactly the same retention time (RT), while, based on the predicted properties, DNP-C is expected to elute before DNP-NAC. Therefore, we conclude that the $m/z = 288.0285$ signal detected at RT of 10.3 min corresponds to a DNP-NAC fragment (loss of the acetyl group) artificially produced within the ESI source.

SI Table 13: Analysis of biotransformation products in 1-chloro-2,4-dinitrobenzene (CDNB) exposure experiments.

2,4-dinitrotoluene-S-glutathione (DNT-SG); 2,4-dinitrophenyl-S-glutathione (DNP-SG); 2,4-dinitrophenyl N-acetylcysteine (DNP-NAC)
Zebrafish were exposed at 2 hpf (embryo) and 74 hpf (larva) for 2, 6, and 24 h. Embryos/larvae were sampled after 2, 6, and 24 exposure hours. Control zebrafish (not exposed) were sampled at 26 and 98 hpf.

NF = not found

RT = retention time

S/N = signal-to-noise ratio

INF = infinite

au = arbitrary units

Content:

A	Sample	Sample name and identifiers
B	DNT-SG	Peak area of the standard DNT-SG
C	DNP-SG	Peak area of biotransformation products
D	DNP-NAC	Peak area of biotransformation products
E	Normalization	Data normalization to standard DNT-SG

A

Sample name	Sample identification	
Sample_1	Control Replicate 1	zebrafish embryo not exposed age 26 hpf
Sample_2	Control Replicate 2	zebrafish embryo not exposed age 26 hpf
Sample_3	Control Replicate 3	zebrafish embryo not exposed age 26 hpf
Sample_4	Exposure duration 2 h; Replicate 1	zebrafish embryo exposed at 2 hpf
Sample_5	Exposure duration 2 h; Replicate 2	zebrafish embryo exposed at 2 hpf
Sample_6	Exposure duration 2 h; Replicate 3	zebrafish embryo exposed at 2 hpf
Sample_7	Exposure duration 6 h; Replicate 1	zebrafish embryo exposed at 2 hpf
Sample_8	Exposure duration 6 h; Replicate 2	zebrafish embryo exposed at 2 hpf
Sample_9	Exposure duration 6 h; Replicate 3	zebrafish embryo exposed at 2 hpf
Sample_10	Exposure duration 24 h; Replicate 1	zebrafish embryo exposed at 2 hpf
Sample_11	Exposure duration 24 h; Replicate 2	zebrafish embryo exposed at 2 hpf
Sample_12	Exposure duration 24 h; Replicate 3	zebrafish embryo exposed at 2 hpf
Sample_13	Control Replicate 1	zebrafish larva not exposed age 98 hpf
Sample_14	Control Replicate 2	zebrafish larva not exposed age 98 hpf
Sample_15	Control Replicate 3	zebrafish larva not exposed age 98 hpf
Sample_16	Exposure duration 2 h; Replicate 1	zebrafish larva exposed at 74 hpf
Sample_17	Exposure duration 2 h; Replicate 2	zebrafish larva exposed at 74 hpf
Sample_18	Exposure duration 2 h; Replicate 3	zebrafish larva exposed at 74 hpf
Sample_19	Exposure duration 6 h; Replicate 1	zebrafish larva exposed at 74 hpf
Sample_20	Exposure duration 6 h; Replicate 2	zebrafish larva exposed at 74 hpf
Sample_21	Exposure duration 6 h; Replicate 3	zebrafish larva exposed at 74 hpf
Sample_22	Exposure duration 24 h; Replicate 1	zebrafish larva exposed at 74 hpf
Sample_23	Exposure duration 24 h; Replicate 2	zebrafish larva exposed at 74 hpf
Sample_24	Exposure duration 24 h; Replicate 3	zebrafish larva exposed at 74 hpf

Sample measurement order

1	Sample_1
2	Sample_2
3	Sample_3
4	Sample_13
5	Sample_14
6	Sample_15
7	Sample_7
8	Sample_8
9	Sample_9
10	Sample_4
11	Sample_5
12	Sample_6
13	Sample_16
14	Sample_17
15	Sample_18
16	Sample_19
17	Sample_20
18	Sample_21
19	Sample_10
20	Sample_11
21	Sample_12
22	Sample_22
23	Sample_23
24	Sample_24

B DNT-SG

Sample Name	Area (au)	Height (au)	RT (min)	S/N
Sample_1	176401379.36	22088032.00	9.59	6254.65
Sample_2	277033632.64	31810652.86	9.59	11942.34
Sample_3	237450450.18	29722679.23	9.60	INF
Sample_4	264285648.80	35578512.12	9.57	3071.28
Sample_5	252069502.27	32804089.82	9.56	INF
Sample_6	293289611.40	34319750.35	9.58	INF
Sample_7	284986195.12	34758216.24	9.57	18052.21
Sample_8	268281595.51	33052022.57	9.58	14795.77
Sample_9	270893747.55	34184470.32	9.56	17821.31
Sample_10	241248848.88	30644521.46	9.55	12526.29
Sample_11	252322403.56	32016768.17	9.59	INF
Sample_12	229177061.57	27726088.67	9.56	INF
Sample_13	319997367.25	42159900.98	9.58	INF
Sample_14	323989050.63	37771944.00	9.59	8670.79
Sample_15	320966568.40	37155705.28	9.60	INF
Sample_16	270804897.80	33830790.31	9.56	6858.99
Sample_17	341063094.82	42591665.09	9.58	INF
Sample_18	297432108.49	35488474.35	9.61	INF
Sample_19	268496151.38	33314433.74	9.57	INF
Sample_20	312590096.84	37814492.83	9.59	INF
Sample_21	273913188.36	35906341.59	9.57	INF
Sample_22	277175019.90	32193434.19	9.60	6211.81
Sample_23	257323347.88	32538350.00	9.58	16346.42
Sample_24	241905865.52	31125773.12	9.58	INF

C DNP-SG

Sample Name	Area (au)	Height (au)	RT (min)	S/N
Sample_1	NF	NF	NF	NF
Sample_2	4404568.73	989221.75	8.64	INF
Sample_3	NF	NF	NF	NF
Sample_4	6319272.55	1453755.50	8.63	INF
Sample_5	6089934.45	1161673.75	8.64	INF
Sample_6	7026208.51	1503775.13	8.65	INF
Sample_7	23166066.57	4371847.50	8.67	INF
Sample_8	10694528.11	2272512.75	8.63	INF
Sample_9	19600160.91	3421804.00	8.65	INF
Sample_10	16020296.57	3315186.50	8.64	INF
Sample_11	9623346.54	1866380.88	8.64	INF
Sample_12	12949695.58	2789283.75	8.66	1867.67
Sample_13	NF	NF	NF	NF
Sample_14	NF	NF	NF	NF
Sample_15	NF	NF	NF	NF
Sample_16	26829556.30	3973489.75	8.66	9755.74
Sample_17	29431487.69	4092988.25	8.66	INF
Sample_18	32714256.56	4437298.50	8.66	2308.54
Sample_19	8005772.32	1647130.38	8.63	4647.08
Sample_20	15370747.04	3388585.00	8.66	3173.32
Sample_21	11611759.72	2295785.00	8.66	INF
Sample_22	26980377.46	4681071.00	8.64	2831.93
Sample_23	9107036.14	2098748.00	8.65	INF
Sample_24	19817684.14	2841165.25	8.67	INF

D DNP-NAC

Sample Name	Area (au)	Height (au)	RT (min)	S/N
Sample_1	NF	NF	NF	NF
Sample_2	NF	NF	NF	NF
Sample_3	NF	NF	NF	NF
Sample_4	5278440.47	936157.81	10.34	INF
Sample_5	5250666.89	673212.44	10.36	254.40
Sample_6	5715719.84	867893.25	10.33	INF
Sample_7	23340643.87	2896258.25	10.34	8851.53
Sample_8	22571199.65	3020502.00	10.33	INF
Sample_9	24754913.61	3320534.75	10.33	935.98
Sample_10	142953042.61	15464152.08	10.34	INF
Sample_11	135975813.73	16309612.59	10.33	INF
Sample_12	124056742.09	12915247.22	10.34	23881.53
Sample_13	NF	NF	NF	NF
Sample_14	NF	NF	NF	NF
Sample_15	NF	NF	NF	NF
Sample_16	120918796.29	14141789.00	10.32	INF
Sample_17	106860880.40	11593978.00	10.32	INF
Sample_18	101494368.51	12095359.41	10.32	INF
Sample_19	184647544.77	18808797.24	10.32	3287.50
Sample_20	181858431.64	19653312.99	10.36	5012.61
Sample_21	179916044.32	18707327.10	10.34	INF
Sample_22	275725076.23	26421994.59	10.29	9822.64
Sample_23	195188244.70	20390920.58	10.33	900.18
Sample_24	202261650.39	23054312.46	10.30	55895.50

E					
Sample Name	Measured peak area (au)			Peak area normalized to DNT-SG	
	DNT-SG	DNP-SG	DNP-NAC	DNP-SG/DNT-SG	DNP-NAC/DNT-SG
Sample_1	176401379.36	NF	NF	NF	NF
Sample_2	277033632.64	4404568.73	NF	0.02	NF
Sample_3	237450450.18	NF	NF	NF	NF
Sample_4	264285648.80	6319272.55	5278440.47	0.02	0.02
Sample_5	252069502.27	6089934.45	5250666.89	0.02	0.02
Sample_6	293289611.40	7026208.51	5715719.84	0.02	0.02
Sample_7	284986195.12	23166066.57	23340643.87	0.08	0.08
Sample_8	268281595.51	10694528.11	22571199.65	0.04	0.08
Sample_9	270893747.55	19600160.91	24754913.61	0.07	0.09
Sample_10	241248848.88	16020296.57	142953042.61	0.07	0.59
Sample_11	252322403.56	9623346.54	135975813.73	0.04	0.54
Sample_12	229177061.57	12949695.58	124056742.09	0.06	0.54
Sample_13	319997367.25	NF	NF	NF	NF
Sample_14	323989050.63	NF	NF	NF	NF
Sample_15	320966568.40	NF	NF	NF	NF
Sample_16	270804897.80	26829556.30	120918796.29	0.10	0.45
Sample_17	341063094.82	29431487.69	106860880.40	0.09	0.31
Sample_18	297432108.49	32714256.56	101494368.51	0.11	0.34
Sample_19	268496151.38	8005772.32	184647544.77	0.03	0.69
Sample_20	312590096.84	15370747.04	181858431.64	0.05	0.58
Sample_21	273913188.36	11611759.72	179916044.32	0.04	0.66
Sample_22	277175019.90	26980377.46	275725076.23	0.10	0.99
Sample_23	257323347.88	9107036.14	195188244.70	0.04	0.76
Sample_24	241905865.52	19817684.14	202261650.39	0.08	0.84

SI Table 14: Analysis of biotransformation products in 1-chloro-2,4-dinitrobenzene (CDNB) depuration experiments.

2,4-dinitrotoluene-S-glutathione (DNT-SG); 2,4-dinitrophenyl-S-glutathione (DNP-SG); 2,4-dinitrophenyl N-acetylcysteine (DNP-NAC)

Zebrafish were exposed at 2 hpf for 24 h. Embryos/larvae were sampled after 24 h of exposure and after 24, 48, 72 and 96 h of depuration. Control zebrafish (not exposed) were sampled at 26 hpf.

Content:

A	Sample	Sample name and identifiers
B	DNT-SG	Peak area of the standard DNT-SG
C	DNP-SG	Peak area of biotransformation products
D	DNP-NAC	Peak area of biotransformation products
E	Normalization	Data normalization to standard DNT-SG

A

Sample name	Sample identification
Control_R1	zebrafish embryo not exposed age 26 hpf
Control_R2	zebrafish embryo not exposed age 26 hpf
Control_R3	zebrafish embryo not exposed age 26 hpf
Exposure_R1	Exposure duration 24 h; Replicate 1
Exposure_R2	Exposure duration 24 h; Replicate 2
Exposure_R3	Exposure duration 24 h; Replicate 3
Clean_24_R1	Depuration duration 24 h; Replicate 1
Clean_24_R2	Depuration duration 24 h; Replicate 2
Clean_24_R3	Depuration duration 24 h; Replicate 3
Clean_48_R1	Depuration duration 48 h; Replicate 1
Clean_48_R2	Depuration duration 48 h; Replicate 2
Clean_48_R3	Depuration duration 48 h; Replicate 3
Clean_72_R1	Depuration duration 72 h; Replicate 1
Clean_72_R2	Depuration duration 72 h; Replicate 2
Clean_72_R3	Depuration duration 72 h; Replicate 3
Clean_96_R1	Depuration duration 94 h; Replicate 1
Clean_96_R2	Depuration duration 94 h; Replicate 2
Clean_96_R3	Depuration duration 94 h; Replicate 3

Sample measurement order

1	Control_R1
2	Control_R2
3	Control_R3
4	Clean_94_R1
5	Clean_24_R2
6	Clean_24_R3
7	Clean_72_R2
8	Clean_48_R2
9	Clean_72_R1
10	Exposure_R2
11	Clean_94_R2
12	Clean_48_R3
13	Clean_72_R3
14	Clean_24_R1
15	Clean_48_R1
16	Exposure_R3
17	Clean_94_R3
18	Exposure_R1

B DNT-SG

Sample Name	Area (au)	Height (au)	RT (min)	S/N
Control_R1	265690218.04	25100735.42	11.15	3868.09
Control_R2	302508837.96	30057508.97	11.13	INF
Control_R3	322846157.44	32393789.47	11.14	19158.65
Exposure_R1	343150023.59	33279445.06	11.16	18146.23
Exposure_R2	347239349.23	31026847.98	11.15	25893.44
Exposure_R3	354153689.87	33063095.50	11.17	14096.77
Clean_24_R1	192334428.24	18408370.92	11.16	INF
Clean_24_R2	188000112.76	18955878.00	11.16	35841.27
Clean_24_R3	214598274.00	20948334.18	11.15	INF
Clean_48_R1	289473553.63	28647778.09	11.16	INF
Clean_48_R2	235330405.66	21673757.16	11.23	INF
Clean_48_R3	323341861.09	28870751.79	11.12	INF
Clean_72_R1	350640970.80	32913961.12	11.18	5847.62
Clean_72_R2	298184860.97	26820586.60	11.14	9408.10
Clean_72_R3	356943898.78	35766958.15	11.16	INF
Clean_94_R1	317650919.97	29074754.25	11.14	14474.09
Clean_94_R2	313486657.42	30906185.00	11.17	INF
Clean_94_R3	338025355.78	32510424.93	11.19	4640.89

C DNP-SG

Sample Name	Area (au)	Height (au)	RT (min)	S/N
Control_R1	NF	NF	NF	NF
Control_R2	NF	NF	NF	NF
Control_R3	NF	NF	NF	NF
Exposure_R1	25608747.68	2606416.75	10.06	INF
Exposure_R2	16701112.45	1709493.63	10.09	1496.31
Exposure_R3	31890488.32	2910613.25	10.09	427.44
Clean_24_R1	2504271.88	377971.31	10.08	93.70
Clean_24_R2	1550476.29	306881.34	10.07	INF
Clean_24_R3	3196451.38	435156.72	10.07	INF
Clean_48_R1	2473705.90	372415.75	10.08	INF
Clean_48_R2	2087058.91	280609.09	10.20	INF
Clean_48_R3	3781390.58	520346.59	10.06	INF
Clean_72_R1	3231992.81	504456.00	10.11	306.84
Clean_72_R2	1403872.78	355046.13	10.06	INF
Clean_72_R3	1414761.92	287538.19	10.07	INF
Clean_94_R1	2260053.03	405738.03	10.05	143.95
Clean_94_R2	NF	NF	NF	NF
Clean_94_R3	1822119.89	319762.41	10.09	206.68

D DNP-NAC

Sample Name	Area (au)	Height (au)	RT (min)	S/N
Control_R1	NF	NF	NF	NF
Control_R2	NF	NF	NF	NF
Control_R3	NF	NF	NF	NF
Exposure_R1	143790544.67	12230224.30	11.96	4942.03
Exposure_R2	120270432.12	10452490.55	11.92	INF
Exposure_R3	177086075.35	15821855.78	11.92	4898.21
Clean_24_R1	82867353.13	7953181.29	11.92	INF
Clean_24_R2	63672989.88	5865331.71	11.96	2413.17
Clean_24_R3	92006432.55	8684061.90	11.91	3629.65
Clean_48_R1	97026039.74	9615181.03	11.93	1842.61
Clean_48_R2	71496487.51	6728219.08	11.98	INF
Clean_48_R3	137229630.05	13564234.04	11.91	INF
Clean_72_R1	87652004.93	8767404.47	11.93	INF
Clean_72_R2	71491486.87	7376132.03	11.92	INF
Clean_72_R3	108920292.10	10891375.30	11.90	INF
Clean_94_R1	38260066.38	3603978.00	11.94	2768.40
Clean_94_R2	45004220.10	4393292.50	11.92	INF
Clean_94_R3	30017134.67	3289657.75	11.93	1568.09

E

Sample Name	Measured peak area			Peak area normalized to	
	DNT-SG	DNP-SG	DNP-NAC	DNP-SG/DNT-SG	DNP-NAC/DNT-SG
Control_R1	265690218.04	NF	NF	NF	NF
Control_R2	302508837.96	NF	NF	NF	NF
Control_R3	322846157.44	NF	NF	NF	NF
Exposure_R1	343150023.59	25608747.68	143790544.67	0.07	0.42
Exposure_R2	347239349.23	16701112.45	120270432.12	0.05	0.35
Exposure_R3	354153689.87	31890488.32	177086075.35	0.09	0.50
Clean_24_R1	192334428.24	2504271.88	82867353.13	0.01	0.43
Clean_24_R2	188000112.76	1550476.29	63672989.88	0.01	0.34
Clean_24_R3	214598274.00	3196451.38	92006432.55	0.01	0.43
Clean_48_R1	289473553.63	2473705.90	97026039.74	0.01	0.34
Clean_48_R2	235330405.66	2087058.91	71496487.51	0.01	0.30
Clean_48_R3	323341861.09	3781390.58	137229630.05	0.01	0.42
Clean_72_R1	350640970.80	3231992.81	87652004.93	0.01	0.25
Clean_72_R2	298184860.97	1403872.78	71491486.87	0.00	0.24
Clean_72_R3	356943898.78	1414761.92	108920292.10	0.00	0.31
Clean_94_R1	317650919.97	2260053.03	38260066.38	0.01	0.12
Clean_94_R2	313486657.42	NF	45004220.10	NF	0.14
Clean_94_R3	338025355.78	1822119.89	30017134.67	0.01	0.09

SI Table 15: Cytosolic GST expression in zebrafish embryos and larvae exposed to 1-chloro-2,4-dinitrobenzene (CDNB) non-toxic concentration (NtC).

Content:

GST-Family	Summary of the GST family classes, nomenclature of the isoforms and gene and protein reference sequences obtained from NCBI Reference Sequence Database
Embryo exposure	Peak area of proteotypic peptides (PP) and shared peptides (SP) detected in zebrafish embryo exposed at 2 hpf to CDNB NtC .
Larvae exposure	Peak area of proteotypic peptides (PP) and shared peptides (SP) detected in zebrafish larva exposed at 74 hpf to CDNB NtC .

A

Summary of the GST family classes, nomenclature of the isoforms and gene and protein reference sequences obtained from NCBI Reference Sequence Database

GST Class	Nomenclature	Protein Name	NCBI Reference Sequence: Gene	NCBI Reference Sequence: Protein
Alpha	DrGsta1	glutathione S-transferase, alpha tandem duplicate 1	NM_213394	NP_998559.1
	DrGsta2	glutathione S-transferase, alpha tandem duplicate 2	NM_001102648	NP_001096118.1
	DrGsta3	uncharacterized protein LOC799288	NM_001109731	NP_001103201.1
Zeta	DrGstz1	maleylacetoacetate isomerase isoform 1	NM_001030271	NP_001025442.2
	DrGstz2	maleylacetoacetate isomerase isoform 2	NM_001002481	NP_001002481.1
	DrGstz3	maleylacetoacetate isomerase isoform 3	NM_001319834	NP_001306763.1
Theta	DrGstt1a	glutathione S-transferase theta 1a	NM_001327762	NP_001314691.1
	DrGstt1b	glutathione S-transferase theta 1b	NM_200584	NP_956878.1
	DrGstt2	glutathione S-transferase theta 2	NM_200521	NP_956815.1
Mu	DrGstm1	glutathione S-transferase mu, tandem duplicate 1	NM_212676	NP_997841.1
	DrGstm2	glutathione S-transferase mu 3	NM_001110116	NP_001103586.1
	DrGstm3	glutathione S-transferase mu tandem duplicate 3	NM_001162851	NP_001156323.1
Pi	DrGstp1	glutathione S-transferase pi	NM_131734	NP_571809.1
	DrGstp2	glutathione S-transferase pi 2	NM_001020513	NP_001018349.1
Rho	DrGstr1	glutathione S-transferase rho	NM_001045060	NP_001038525.1
Omega	DrGsto1	glutathione S-transferase omega 1	NM_001002621	NP_001002621.1
	DrGsto2	uncharacterized protein LOC492500	NM_001007372	NP_001007373.1

B Embryo exposure

Peak area normalized to GAPDH of proteotypic peptides (PP) and shared peptides (SP) detected in zebrafish embryos exposed at 2 hpf to CDNB NtC. Carbamidomethyl (C) cysteine is indicated as C, the position of the peptide in the protein (first and last amino acids) is indicated in square brackets

Zebrafish embryos were exposed at 2 hpf for 24 h.

Replicate (normalized peak area)

peptide type	isoenzyme	peptide sequence and position in the protein	Sample	exposure duration	1	2	3	4
PP	Gsta1	K.AVLSHLFK.- [215, 222]	Control	24h		0.03577	0.03576	0.04601
			CDNB-exposure	24h	0.02838	0.02951	0.03615	0.03611
SP	Gsta1,2	K.ALANSSFLVGK. Q [138, 148]	Control	24h		0.00913	0.01133	0.016
			CDNB-exposure	24h	0.01255	0.01048	0.00958	0.01243
SP	Gsta1,2,3	K.FLQPGSAR.K [194, 201]	Control	24h		0.02155	0.02363	0.02874
			CDNB-exposure	24h	0.02893	0.02598	0.02427	0.03188
SP	Gstm1,2	K.IVQSNAMR.Y [69, 77]	Control	24h		0.17941	0.19796	0.16612
			CDNB-exposure	24h	0.19601	0.20437	0.19815	0.1572
PP	Gstp1	K.CFENVLAK.N [128, 135]	Control	24h		0.0256	0.03064	0.02014
			CDNB-exposure	24h	0.0592	0.0463	0.02786	0.04722
SP	Gstp1,2	K.ALLECENFK.K [189, 197]	Control	24h		0.0686	0.06877	0.05433
			CDNB-exposure	24h	0.10358	0.07785	0.07832	0.0728
PP	Gstr	R.LMIALEEK.Q [18, 25]	Control	24h		0.02135	0.02035	0.01724
			CDNB-exposure	24h	0.02043	0.02514	0.01661	0.01751
PP	Gstr	R.LIPDNPAE- MALVYQR.M [87, 101]	Control	24h		0.00572	0.00761	0.00515
			CDNB-exposure	24h	0.00529	0.00587	0.00501	0.00604
PP	Gstr	R.MFETENLQKK.M [102, 111]	Control	24h		0.00559	0.0094	0.00625
			CDNB-exposure	24h	0.00779	0.00908	0	0.00878
SP	Gsto2	K.LLPSPDPER.A [100, 108]	Control	24h		0.01385	0.01729	0.0154
			CDNB-exposure	24h	0.01538	0.01537	0.01239	0.01779

C Larvae Exposure

Peak area normalized to GAPDH of proteotypic peptides (PP) and shared peptides (SP) detected in zebrafish larva exposed at 74 hpf to CDNB NtC. Carbamidomethyl (C) cysteine is indicated as C, the position of the peptide in the protein (first and last amino acids) is indicated in square brackets.

Zebrafish larva were exposed at 74 hpf for 6 and 24 h .

Replicate (normalized peak area)

pep- tide type	isoenzyme	peptide sequence and position in the protein	Sample	expo- sure dura- tion	1	2	3	4
PP	Gsta1	K.IQAFQEQMK.A [178, 186]	Control	6h	0.01163	0.01222	0.00531	0.00748
			Control	24h	0.02098	0.0214	0.00844	0.01673
			CDNB-exposure	6h	0.01286	0.01007	0.01636	0.00908
			CDNB-exposure	24h	0.02465	0.02015	0.01319	0.01562
PP	Gsta1	K.AVLSHLFK.- [215, 222]	Control	6h	0.03453	0.03631	0.05008	0.0325
			Control	24h	0.04427	0.05832	0.04415	0.04656
			CDNB-exposure	6h	0.03965	0.03625	0.05778	0.03063
			CDNB-exposure	24h	0.07162	0.06279	0.06464	0.04206
PP	Gsta2	K.TYSSIEEK.A [119, 126]	Control	6h	0.00223	0.00213	0.00113	0.00101
			Control	24h	0.00265	0.00228	0.00211	0.00174
			CDNB-exposure	6h	0.00268	0.00266	0.00224	0.00141
			CDNB-exposure	24h	0.00295	0.0028	0.00175	0.00225
SP	Gsta1,2	K.ALANSSFLVGK.Q [138, 148]	Control	6h	0.01946	0.02178	0.01094	0.01358
			Control	24h	0.03257	0.03224	0.01356	0.02136
			CDNB-exposure	6h	0.02162	0.01903	0.02453	0.01393
			CDNB-exposure	24h	0.03889	0.03272	0.02102	0.0226
SP	Gsta2,3	K.IQAFQEQMK.A [178, 186]	Control	6h	0.00418	0.0059	0	0.00449
			Control	24h	0.01036	0.00756	0.00421	0.005
			CDNB-exposure	6h	0.00428	0.00447	0.00631	0.00311
			CDNB-exposure	24h	0.00757	0.00737	0.00439	0.004
SP	Gsta1,2,3	K.AILNYIAGK.Y [69, 77]	Control	6h	0.00192	0.00169	0.00042	0.00094
			Control	24h	0.00546	0.00402	0	0.00226
			CDNB-exposure	6h	0.00199	0.0014	0.00178	0
			CDNB-exposure	24h	0.00407	0.0037	0.00183	0.00206
SP	Gsta1,2,3	K.FLQPGSAR.K [194, 201]	Control	6h	0.0413	0.03738	0.0367	0.03014
			Control	24h	0.05445	0.06425	0.03713	0.04477
			CDNB-exposure	6h	0.03986	0.03799	0.05191	0.02876
			CDNB-exposure	24h	0.0739	0.06627	0.04775	0.04364
SP	Gsta1,2,3	K.VVLHYFNNGR.G [4, 12]	Control	6h	0.00141	0.00112	0	0
			Control	24h	0.004	0.00271	0.00192	0.00197
			CDNB-exposure	6h	0.00181	0.00124	0.0022	0.00105
			CDNB-exposure	24h	0.00366	0.00272	0.00196	0.00191
SP	Gsta1,2,3	R.KPPPDEEYVR.T [202, 211]	Control	6h	0.00192	0.0022	0.00184	0.0021
			Control	24h	0.00325	0.00285	0.003	0.00303
			CDNB-exposure	6h	0.00214	0.0021	0.00286	0.0019

			CDNB-exposure	24h	0.00352	0.0029	0.00228	0.00251
SP	Gstz1,2,3	R.LLPADPMQR.A [88, 96]/[92, 100]/[32, 40]	Control	6h	0.00423	0.00484	0.00633	0.00393
			Control	24h	0.00471	0.00552	0.006	0.00394
			CDNB-exposure	6h	0.0041	0.00398	0.00474	0.00352
			CDNB-exposure	24h	0.00564	0.0056	0.00408	0.00431
PP	Gstt1a	R.AQVDEFLSWQHT-NIR.S [92, 106]	Control	6h	0.00106	0.0016	0	0.00079
			Control	24h	0.00216	0.00192	0.00085	0.00142
			CDNB-exposure	6h	0.00122	0.00199	0.00151	0.00073
			CDNB-exposure	24h	0.00193	0.00188	0.00114	0.0016
PP	Gstm3	K.VVQSNAILR.Y [69, 77]	Control	6h	0.00806	0.00743	0.00832	0.01016
			Control	24h	0.01016	0.00992	0.00933	0.0095
			CDNB-exposure	6h	0.00957	0.0069	0.00806	0.0011
			CDNB-exposure	24h	0.01028	0.00989	0.00785	0.01033
SP	Gstm1,2	R.MFEPACLDLDFK.N [167, 177]	Control	6h	0.00169	0.00204	0	0
			Control	24h	0.00272	0.00191	0.00193	0.00177
			CDNB-exposure	6h	0.00138	0	0	0.0013
			CDNB-exposure	24h	0.00165	0	0	0.002
SP	Gstm1,2	K.IVQSNAIMR.Y [69, 77]	Control	6h	0.07348	0.08272	0.07946	0.07627
			Control	24h	0.05639	0.05923	0.07775	0.05638
			CDNB-exposure	6h	0.07744	0.07512	0.0564	0.01133
			CDNB-exposure	24h	0.06021	0.06067	0.06015	0.06222
PP	Gstp1	K.ATCVFGQLPK.F [45, 54]	Control	6h	0.00289	0.0023	0	0
			Control	24h	0.00443	0.00231	0.00205	0.00189
			CDNB-exposure	6h	0.00232	0.00317	0	0.00139
			CDNB-exposure	24h	0.00252	0.00322	0.00138	0.00174
PP	Gstp1	K.CFENVLAK.N [128, 135]	Control	6h	0.02747	0.02735	0.0165	0.02185
			Control	24h	0.0317	0.02697	0.02493	0.02355
			CDNB-exposure	6h	0.02822	0.02686	0.02331	0.01956
			CDNB-exposure	24h	0.0352	0.0286	0.02864	0.02419
PP	Gstp1	K.FEDGDLVLFQS-NAMLR.H [55, 70]	Control	6h	0.0019	0.00212	0.00226	0.00193
			Control	24h	0.00189	0.00206	0.00165	0.002
			CDNB-exposure	6h	0	0.00199	0.00213	0.00603
			CDNB-exposure	24h	0.00189	0.00247	0.00182	0.00217
SP	Gstp1,2	K.ALLECENFK.K [189, 197]	Control	6h	0.0446	0.04145	0.03289	0.03375
			Control	24h	0.04855	0.03984	0.03972	0.03601
			CDNB-exposure	6h	0.04498	0.04281	0.03657	0.03592
			CDNB-exposure	24h	0.04764	0.04343	0.04528	0.03854
PP	Gstr	R.LMIALEEK.Q [18, 25]	Control	6h	0.01785	0.0148	0.01035	0.01146
			Control	24h	0.01876	0.01668	0.01059	0.01118
			CDNB-exposure	6h	0.01703	0.01675	0.01311	0.0113
			CDNB-exposure	24h	0.01777	0.01743	0.01225	0.01262
PP	Gstr	R.LIPDNPAE-MALVYQR.M [87, 101]	Control	6h	0.00426	0.00499	0	0.00614
			Control	24h	0.00464	0.00533	0.00415	0.00466
			CDNB-exposure	6h	0.00421	0.00538	0.00478	0.00367
			CDNB-exposure	24h	0.00481	0.00513	0.00431	0.00451

PP	Gstr	R.MFETENLQQK.M [102, 111]	Control	6h	0.00557	0.00561	0.00402	0.00586
			Control	24h	0.00723	0.00678	0.00474	0.00569
			CDNB-exposure	6h	0.00674	0.00503	0.00548	0.00527
			CDNB-exposure	24h	0.00691	0.00616	0.00539	0.00501
SP	Gsto2	K.LLPSPFER.A [100, 108]	Control	6h	0.01163	0.0117	0.00566	0.01078
			Control	24h	0.01534	0.01092	0.00917	0.00989
			CDNB-exposure	6h	0.01152	0.01167	0.00962	0.00615
			CDNB-exposure	24h	0.01194	0.01196	0.00829	0.0098

Supplementary information Chapter 5

SI Table 16: Nominal and measured 1-chloro-2,4-dinitrobenzene (CDNB) concentrations in the medium at the beginning of each toxicity study. R1-3 are the replicates 1 to 3, SD is the standard deviation, RSD the relative standard deviation and Δ% the difference between the nominal and measured concentration in percent.

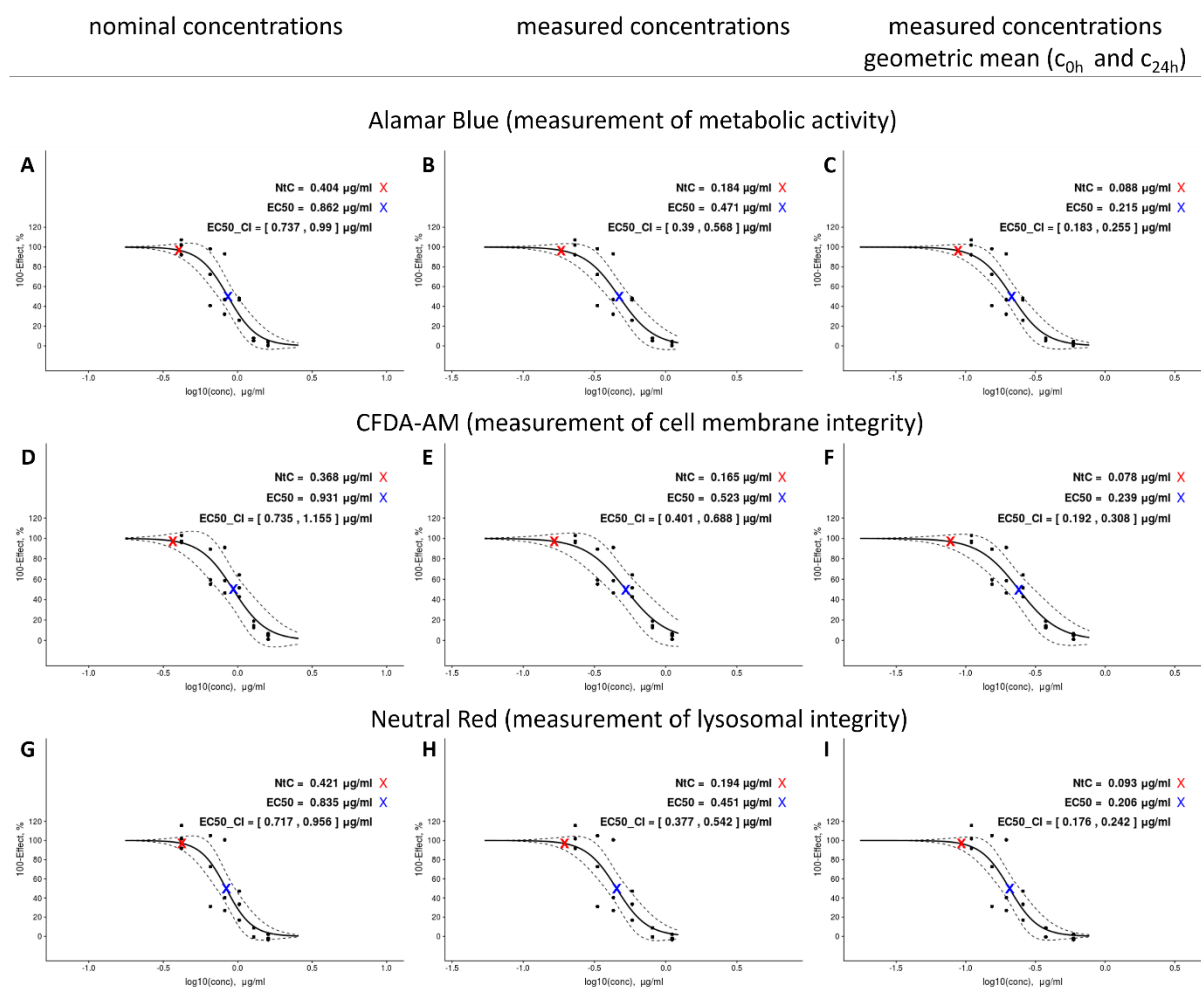
concentration	nominal concentration [μg/ml]	measured concentration [μg/ml]						
		R1	R2	R3	average	SD	RSD	Δ%
C1	1.6	0.956	1.056	1.314	1.109	0.151	13.579	30.715
C2	1.28	0.761	0.76	0.902	0.808	0.067	8.244	36.89
C3	1.024	0.575	0.541	0.629	0.582	0.036	6.196	43.209
C4	0.819	0.372	0.42	0.495	0.429	0.051	11.811	47.619
C5	0.655	0.303	0.309	0.384	0.332	0.037	11.076	49.379
C6	0.419	0.212	0.219	0.263	0.231	0.023	9.728	44.832
control	0	0	0	0	0	average Δ'		
								42.108

SI Table 17: Measured concentrations at the beginning and at the end of the experiment in addition to the geometric mean.

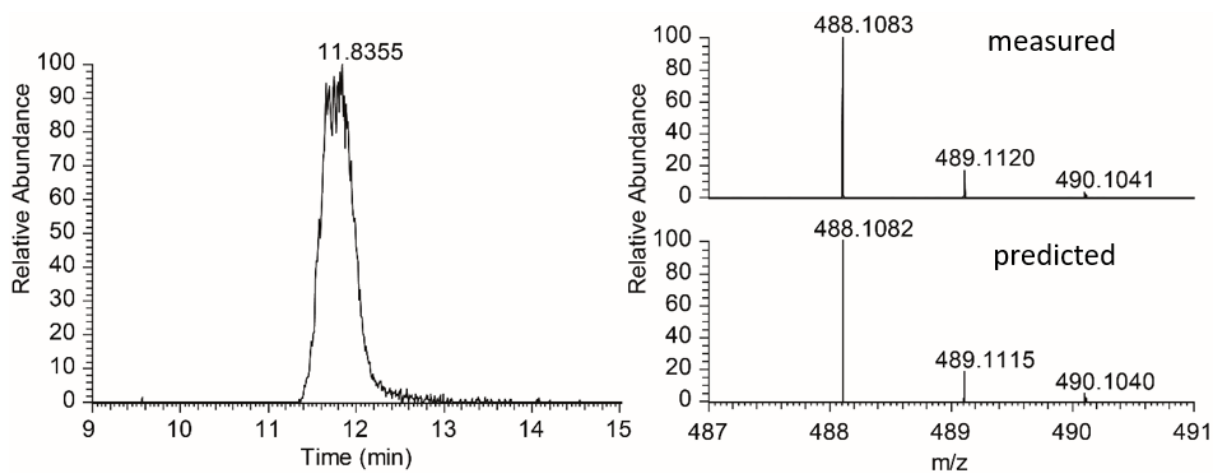
concentration	measured concentration [μg/ml]		
	C0h	C24h	geometric mean
C1	1.109	0.203	0.592
C2	0.808	0.046	0.375
C3	0.582	0.000	0.258
C4	0.429	0.000	0.195
C5	0.332	0.000	0.154
C6	0.231	0.000	0.110
control	0.000	0.000	0.000

SI Table 18: Mean of EC₅₀ and NtC values measured with the three fluorescent dyes Alamar Blue, 5-carboxyfluorescein diacetate acetoxy-methyl ester (CFDA-AM) and Neutral Red calculated based on nominal, measured and geometric mean of measured concentrations at the beginning and the end of the experiment (C_{0h} and C_{24h}).

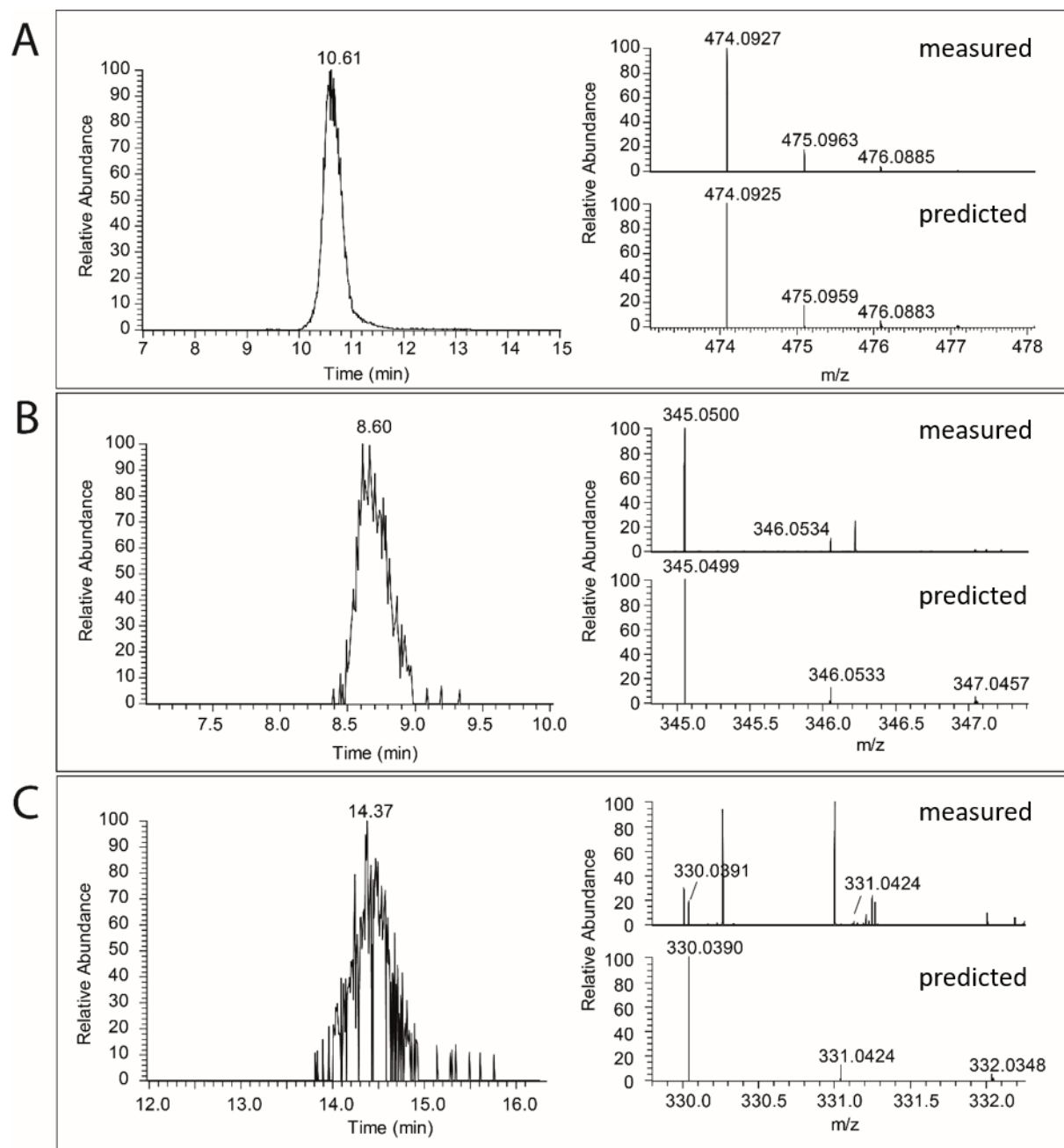
	nominal concentrations ng/ml	measured concentrations ng/ml	geometric mean (c0h and c24h) ng/ml
EC50	886	482	220
NtC	398	181	86



SI Figure 6: Dose-response curves representing cell viability measured with the use of three fluorescent dyes. A, B and C) Alamar Blue (metabolic activity), D, E and F) 5-carboxyfluorescein diacetate acetoxy-methyl ester (CFDA-AM, cell membrane integrity) and G, H and I) Neutral Red (lysosomal integrity) (Fischer et al. 2019; Tanneberger et al. 2013). Data is shown as % cell viability normalized to the CDNB-free solvent control as a function of log CDNB nominal concentration (A, D and G), log CDNB concentration measured in samples collected at the beginning of the experiments (B, E and H) and log CDNB geometric mean of concentrations measured in samples collected at the beginning (c_{0h}) and at the end of the experiments (c_{24h}) (C, F and I). The curve fit and the calculation of the non-toxic concentration (NtC) and the half-maximal effect concentration (EC_{50}) were performed with the use of an algorithm developed by Stadnicka-Michalak et al. (2018). The figure shows the fitted sigmoidal curve together with 95% confidence intervals and measured data where each dot represents one of three independent biological replicates. The NtC and EC_{50} values are indicated as a red and a blue cross, respectively. EC_{50_CI} represents the EC_{50} confidence interval. The EC_{50} values collected with the three fluorescent dyes did not differ significantly ($p > 0.01$, one-way ANOVA). The calculations based on the nominal concentrations yield an average EC_{50} of 886 ng/ml and an average NtC of 398 ng/ml. The calculations based on the measured concentrations yield an average EC_{50} of 482 ng/ml and an average NtC of 181 ng/ml. The calculations based on the geometric mean (c_{0h} and c_{24h}) yield an average EC_{50} of 220 ng/ml and an average NtC of 86 ng/ml.



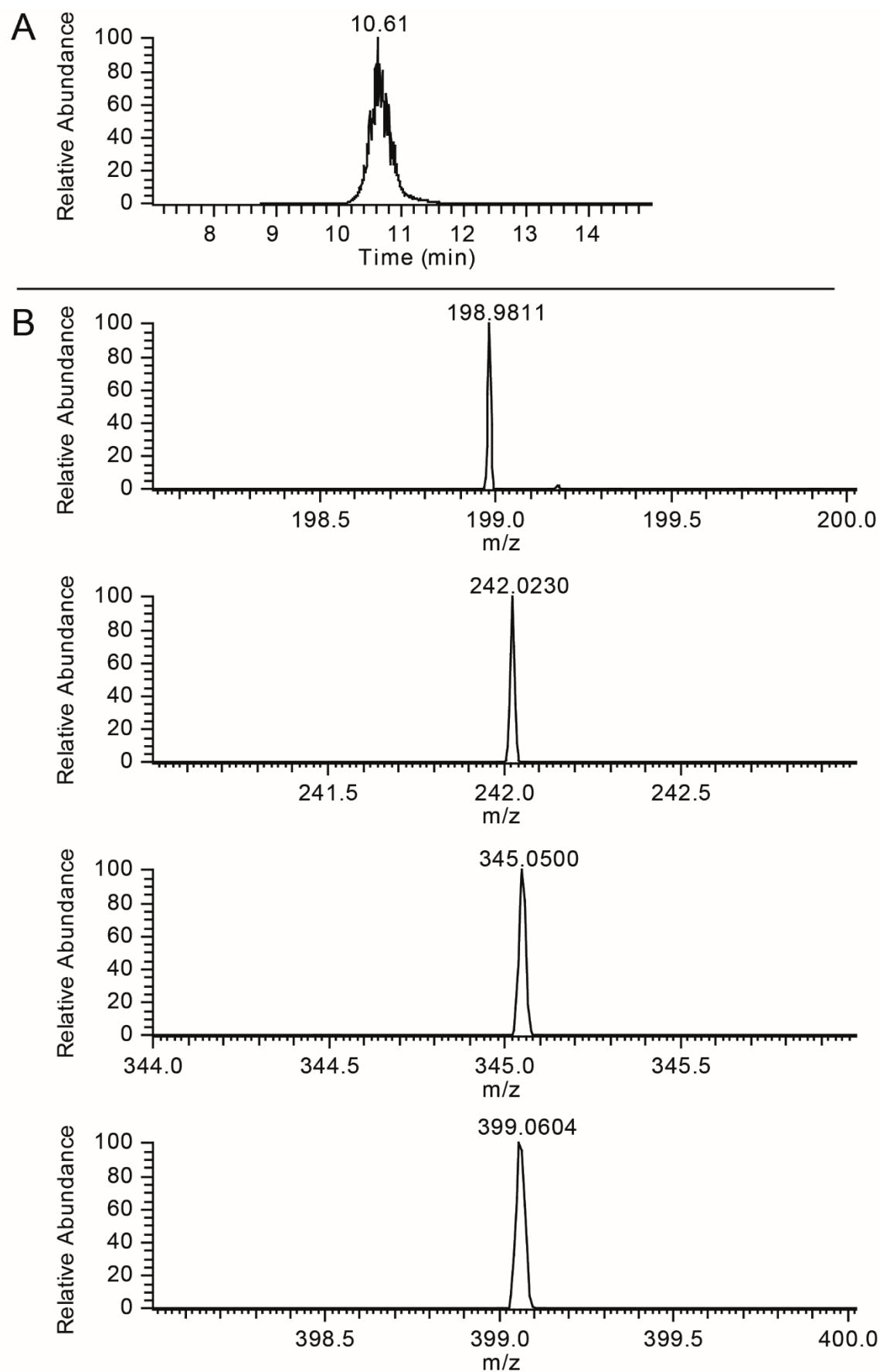
SI Figure 7: Chromatogram in full scan mode and mass spectra of 2,4-dinitrotoluene-S-glutathione (DNT-SG, internal standard). The measured isotope distribution is depicted on top of the predicted isotope distribution. m/z : mass-to-charge ratio.



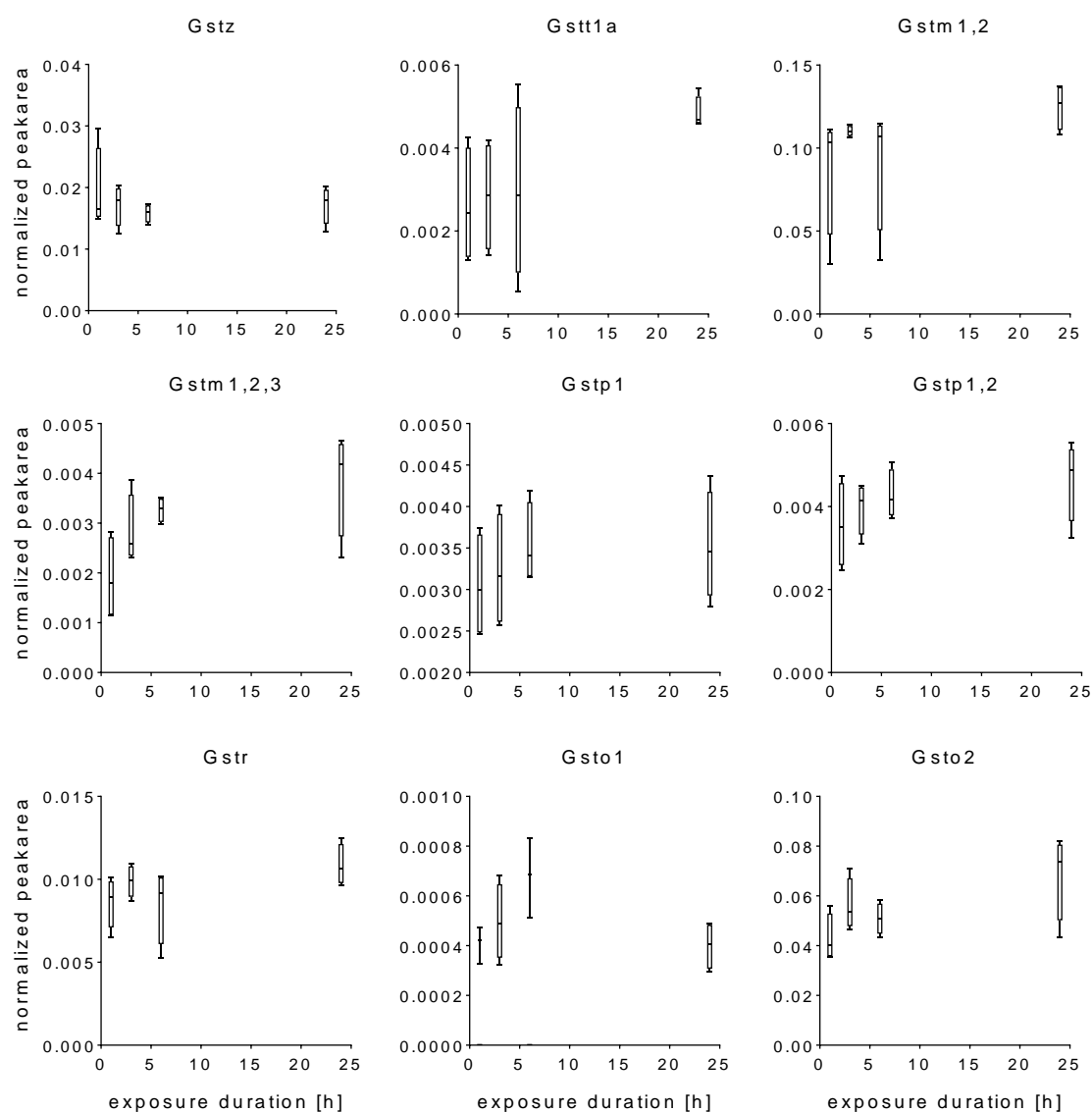
SI Figure 8: Chromatogram in full scan mode and mass spectra of A: 2,4-dinitrophenyl-S-glutathione (DNP-SG), B: 2,4-dinitrophenyl cysteinylglycine (DNP-CG) and C: 2,4-dinitrophenyl N-acetylcysteine (DNP-NAC). The measured isotope distribution is shown on top of the predicted isotope distribution. m/z : mass-to-charge ratio.

SI Table 19: Difference (ppm) between the measured and predicted isotopes of the protonated molecular ions of 2,4-dinitrotoluene-S-glutathione (DNT-SG, internal standard), 2,4-dinitrophenyl-S-glutathione (DNP-SG), 2,4-dinitrophenyl cysteinglycine (DNP-CG) and 2,4-dinitrophenyl N-acetylcysteine (DNP-NAC) in full scan (MS).

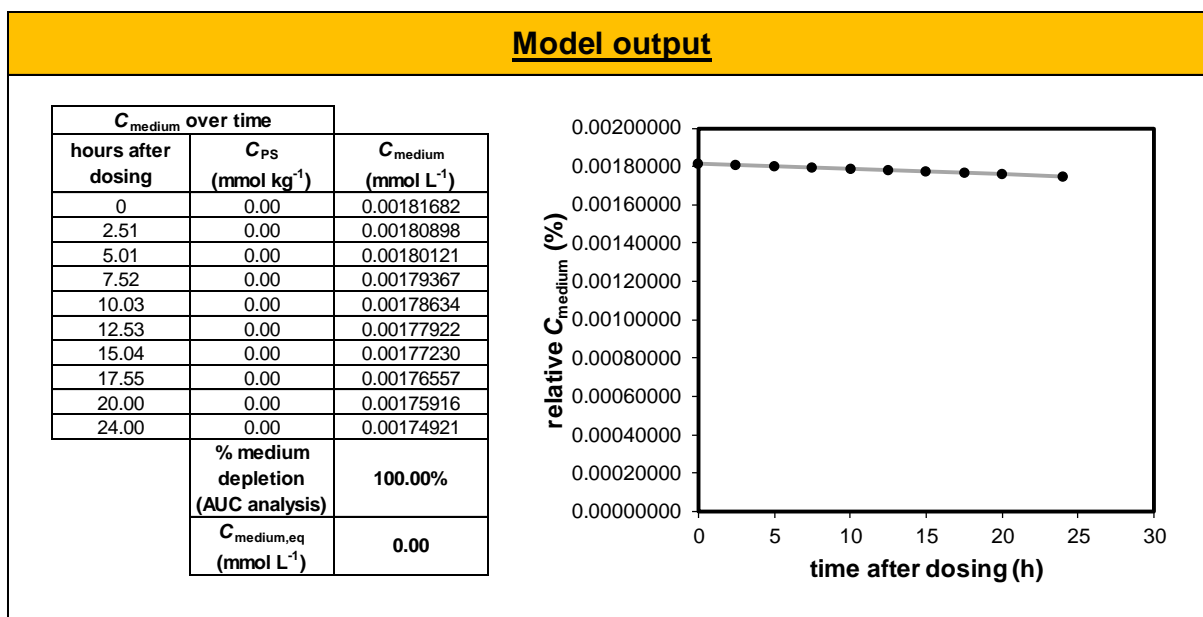
measured m/z	predicted m/z	difference ppm
DNT-SG		
488.1083	488.1082	0.20
489.1120	489.1115	1.02
490.1041	490.1040	0.20
DNP-SG		
474.0927	474.0925	0.42
475.0963	475.0959	0.84
476.0885	476.0883	0.42
DNP-CG		
345.0500	345.0499	0.29
346.0534	346.0533	0.29
DNP-NAC		
330.0391	330.0390	0.30
331.0424	331.0424	0.00



SI Figure 9: Reconstructed ion chromatogram of the $m/z=474.09$ (DNP-SG) precursor ion (A) and MS2 accurate mass spectra of the monoisotopic fragment ions (B). m/z : mass-to-charge ratio.



SI Figure 10: Expression of cytosolic GSTs within PAC2 cells cultured in L15 medium supplemented with 5% FBS for 1, 3, 6, and 24 h. The expression is shown as peak area normalized to the housekeeping proteins β -actin and 40S ribosomal protein S18. The values are shown as boxplots (minimum, first quartile, median, third quartile, and maximum) of 4 independent biological replicates. The normalized peak area of peptides belonging to the same enzyme (in case of proteotypic peptides) or several isoenzymes from the same class (in case of shared peptides) were cumulated. The number and characteristics of the cumulated peptides are summarized in Supplemental Information 2.



SI Figure 11: Kinetic model of the 1-chloro-2,4-dinitrobenzene (CDNB) concentration in T75 cell culture flasks filled with L15 medium supplemented with 5% FBS in a cell-free system. The concentration changes upon partitioning into plastic (Fischer et al. 2018).

Generation of DNP-CG through gas-phase reactions in the ESI source

In some sample chromatograms we observed a double peak at a retention time of 8.6 and 10.6 min with the mass $m/z=345.0500$. This mass corresponds to the 1-chloro-2,4-dinitrobenzene (CDNB) biotransformation product 2,4-dinitrophenyl cysteinglycine (DNP-CG). However, since the CDNB biotransformation product 2,4-dinitrophenyl-S-glutathione (DNP-SG) elutes at 10.6 min, with exactly the same retention time (RT) as the second peak, we conclude that the $m/z=345.0500$ signal detected at RT of 10.6 corresponds to a DNP-SG fragment produced in the ESI source through breaking of the peptide bond.

A similar formation of interfering fragment ions was observed in Chapter 4, however originating from the metabolites 2,4-dinitrophenyl cysteine (DNP-C) and 2,4-dinitrophenyl N-acetylcysteine (DNP-NAC).

SI Table 20: Analysis of biotransformation products in PAC2 cells during 1-chloro-2,4-dinitrobenzene (CDNB) exposure experiments.

2,4-dinitrotoluene-S-glutathione (DNT-SG); 2,4-dinitrophenyl-S-glutathione (DNP-SG); 2,4-dinitrophenyl N-acetylcysteine (DNP-NAC)
Zebrafish were exposed at 2 hpf (embryo) and 74 hpf (larva) for 2, 6, and 24 h. Control zebrafish (not exposed) were sampled at 26 and 98 hpf.

NF = not found

RT = retention time

S/N = signal-to-noise ratio

A	Sample	Sample name and identifiers
B	DNT-SG	Peak area of the standard DNT-SG
C	DNP-SG	Peak area of biotransformation products
D	Normalization	Data normalization to standard DNT-SG

Order of measurements		
Filename	Replicate	Time
191008_Sample_1	1	1h
191008_Sample_2	1	3h
191008_Sample_3	1	6h
191009_Sample_6	2	1h
191009_Sample_5	1	control
191009_Sample_4	1	24h
191009_Sample_17	4	3h
191009_Sample_11	3	1h
191009_Sample_9	2	24h
191009_Sample_20	4	control
191009_Sample_19	4	24h
191009_Sample_15	3	control
191009_Sample_10	2	control
191009_Sample_13	3	6h
191009_Sample_14	3	24h
191009_Sample_16	4	1h
191009_Sample_18	4	6h
191009_Sample_12	3	3h
191009_Sample_8	2	6h
191009_Sample_7	2	3h

A

Sample ID

Filename	Replicate	Time
191008_Sample_1	1*	1h
191008_Sample_2	1*	3h
191008_Sample_3	1*	6h
191009_Sample_4	1*	24h
191009_Sample_5	1*	control
191009_Sample_6	2	1h
191009_Sample_7	2	3h
191009_Sample_8	2	6h
191009_Sample_9	2	24h
191009_Sample_10	2	control
191009_Sample_11	3	1h
191009_Sample_12	3	3h
191009_Sample_13	3	6h
191009_Sample_14	3	24h
191009_Sample_15	3	control
191009_Sample_16	4	1h
191009_Sample_17	4	3h
191009_Sample_18	4	6h
191009_Sample_19	4	24h
191009_Sample_20	4	control

* due to technical difficulties during the measurements of the sample 1-3, as reflected in the DNT-SG standard, the replicate 1 was excluded from evaluation

B DNT-SG

Sample Name	Area (au)	Height (au)	RT (min)
191009_Sample_6	52512888.89	2928286.00	10.81
191009_Sample_7	5212751.72	397930.08	10.81
191009_Sample_8	2911663.71	253280.91	10.83
191009_Sample_9	NF	NF	NF
191009_Sample_10	NF	NF	NF
191009_Sample_11	98036001.09	5445058.50	10.75
191009_Sample_12	13870600.12	847379.19	10.70
191009_Sample_13	5796736.03	435455.13	10.82
191009_Sample_14	NF	NF	NF
191009_Sample_15	NF	NF	NF
191009_Sample_16	76084041.17	4544676.69	10.77
191009_Sample_17	4231686.01	337077.03	10.71
191009_Sample_18	2646688.36	220401.36	10.76
191009_Sample_19	NF	NF	NF
191009_Sample_20	NF	NF	NF

C DNP-SG

Sample Name	Area (au)	Height (au)	RT (min)
191009_Sample_6	1756878167.61	97586459.58	11.89
191009_Sample_7	1116426207.50	62691500.00	11.90
191009_Sample_8	1629386228.38	101308735.30	11.89
191009_Sample_9	1373839861.43	80243883.77	11.88
191009_Sample_10	1079096862.06	60244684.00	11.90
191009_Sample_11	1946083854.02	118570664.00	11.86
191009_Sample_12	1176570010.03	70053145.72	11.91
191009_Sample_13	1818708219.07	101418952.00	11.89
191009_Sample_14	1769824253.04	103852987.31	11.86
191009_Sample_15	1143772081.55	66545772.00	11.87
191009_Sample_16	1924355985.19	109072176.00	11.91
191009_Sample_17	908114698.70	52465408.00	11.90
191009_Sample_18	1536781313.60	93510712.00	11.90
191009_Sample_19	1305700730.00	74430157.95	11.84
191009_Sample_20	1027098082.33	57270422.23	11.89

D normalization

Filename	DNT-SG Area (au)	DNP-SG Area (au)	DNP-SG/DNT-SG Normalized
191009_Sample_6	1756878167.61	52512888.89	0.029889886
191009_Sample_7	1116426207.50	5212751.72	0.004669141
191009_Sample_8	1629386228.38	2911663.71	0.00178697
191009_Sample_9	1373839861.43	NF	0
191009_Sample_10	1079096862.06	NF	0
191009_Sample_11	1946083854.02	98036001.09	0.050376042
191009_Sample_12	1176570010.03	13870600.12	0.011789014
191009_Sample_13	1818708219.07	5796736.03	0.003187282
191009_Sample_14	1769824253.04	NF	0
191009_Sample_15	1143772081.55	NF	0
191009_Sample_16	1924355985.19	76084041.17	0.039537405
191009_Sample_17	908114698.70	4231686.01	0.004659859
191009_Sample_18	1536781313.60	2646688.36	0.001722228
191009_Sample_19	1305700730.00	NF	0
191009_Sample_20	1027098082.33	NF	0

SI Table 21: Analysis of biotransformation products in medium during 1-chloro-2,4-dinitrobenzene (CDNB) exposure experiments.

2,4-dinitrotoluene-S-glutathione (DNT-SG); 2,4-dinitrophenyl-S-glutathione (DNP-SG); 2,4-dinitrophenyl N-acetylcysteine (DNP-NAC)
 Zebrafish were exposed at 2 hpf (embryo) and 74 hpf (larva) for 2, 6, and 24 h. Control zebrafish (not exposed) were sampled at 26 and 98 hpf.

NF = not found

RT = retention time

S/N = signal-to-noise ratio

Content:

A	Sample	Sample name and identifiers
B	DNT-SG	Peak area of the standard DNT-SG
C	DNP-SG	Peak area of biotransformation products
D	DNP-CG	Peak area of biotransformation products
E	DNP-NAC	Peak area of biotransformation products
F	Normalization	Data normalization to standard DNT-SG

Measurement order		
Filename	Replicate	Timepoint
191011_Sample_Medium_13	3	6h
191011_Sample_Medium_10	2	control
191011_Sample_Medium_7	2	4h
191011_Sample_Medium_18	4	6h
191011_Sample_Medium_6	2	2h
191011_Sample_Medium_14	3	24h
191011_Sample_Medium_9	2	24h
191011_Sample_Medium_8	2	6h
191011_Sample_Medium_15	3	control
191011_Sample_Medium_17	4	4h
191011_Sample_Medium_20	4	control
191011_Sample_Medium_16	4	2h
191011_Sample_Medium_11	3	2h
191011_Sample_Medium_12	3	4h
191011_Sample_Medium_19	4	24h

B

Component Name

DNT-SG

Filename	Area	Height	RT	S/N
191011_Sample_Medium_6	483564894.49	28873834.89	11.81	INF
191011_Sample_Medium_7	472706358.74	25759446.00	11.75	INF
191011_Sample_Medium_8	633140379.78	33609352.00	11.76	INF
191011_Sample_Medium_9	580055975.60	30516298.00	11.77	INF
191011_Sample_Medium_10	480476830.52	27466688.00	11.75	INF
191011_Sample_Medium_11	981204.92	71352.23	11.81	INF
191011_Sample_Medium_12	72222392.81	3990004.96	11.79	641.90
191011_Sample_Medium_13	512923945.94	31725568.29	11.79	INF
191011_Sample_Medium_14	228926478.91	12038596.00	11.72	INF
191011_Sample_Medium_15	330525570.64	15561952.00	11.74	INF
191011_Sample_Medium_16	73264905.37	3030035.50	11.71	INF
191011_Sample_Medium_17	290324260.83	12652460.00	11.68	INF
191011_Sample_Medium_18	224025565.93	12471812.44	11.78	INF
191011_Sample_Medium_19	8281371.86	335695.16	11.84	INF
191011_Sample_Medium_20	106919645.10	4345512.50	11.70	INF

C

Component Name

DNP-SG

Filename	Area	Height	RT	S/N
191011_Sample_Medium_6	8284209117.47	406904640.00	10.64	466.36
191011_Sample_Medium_7	10533755566.02	505052288.00	10.59	419.01
191011_Sample_Medium_8	11978833953.82	517625408.00	10.61	347.47
191011_Sample_Medium_9	11579612066.61	491986944.00	10.61	325.21
191011_Sample_Medium_10	NF	NF	NF	NF
191011_Sample_Medium_11	1624438024.71	75475304.00	10.62	327.97
191011_Sample_Medium_12	1019416138.62	42997932.00	10.63	236.66
191011_Sample_Medium_13	9447164954.30	452778656.00	10.62	549.78
191011_Sample_Medium_14	4664081523.69	213448464.00	10.50	INF
191011_Sample_Medium_15	NF	NF	NF	NF
191011_Sample_Medium_16	1007892529.90	44676216.00	10.56	351.78
191011_Sample_Medium_17	5719325118.94	245176608.00	10.51	527.91
191011_Sample_Medium_18	5231984752.82	283003424.00	10.54	454.09
191011_Sample_Medium_19	135531869.15	5833443.00	10.54	457.47
191011_Sample_Medium_20	NF	NF	NF	NF

D

Component Name

DNT-CG

Filename	Area	Height	RT	S/N
191011_Sample_Medium_6	20383791.31	1997912.50	8.60	INF
191011_Sample_Medium_7	38732716.04	3313692.50	8.64	INF
191011_Sample_Medium_8	40485944.39	3658323.00	8.59	INF
191011_Sample_Medium_9	32943008.19	2771312.32	8.62	INF
191011_Sample_Medium_10	NF	NF	NF	NF
191011_Sample_Medium_11	19172259.21	1932702.63	8.63	INF
191011_Sample_Medium_12	28714047.15	2355632.50	8.65	1926.60
191011_Sample_Medium_13	37744570.62	3066930.75	8.58	434.73
191011_Sample_Medium_14	13290671.89	1877448.18	8.64	INF
191011_Sample_Medium_15	NF	NF	NF	NF
191011_Sample_Medium_16	5615162.60	1547491.38	8.70	INF
191011_Sample_Medium_17	16089197.12	1625135.79	8.63	INF
191011_Sample_Medium_18	9030931.21	2190717.28	8.66	INF
191011_Sample_Medium_19	2723236.04	323720.46	8.72	INF
191011_Sample_Medium_20	NF	NF	NF	NF

E

Component Name

DNT-NAC

Filename	Area	Height	RT	S/N
191011_Sample_Medium_6	NF	NF	NF	NF
191011_Sample_Medium_7	10594660.31	574917.75	14.48	INF
191011_Sample_Medium_8	12539423.09	709822.94	14.36	INF
191011_Sample_Medium_9	16832670.60	790777.56	14.45	INF
191011_Sample_Medium_10	NF	NF	NF	NF
191011_Sample_Medium_11	NF	NF	NF	NF
191011_Sample_Medium_12	NF	NF	NF	NF
191011_Sample_Medium_13	17652843.88	753302.94	14.38	INF
191011_Sample_Medium_14	NF	NF	NF	NF
191011_Sample_Medium_15	NF	NF	NF	NF
191011_Sample_Medium_16	NF	NF	NF	NF
191011_Sample_Medium_17	NF	NF	NF	NF
191011_Sample_Medium_18	NF	NF	NF	NF
191011_Sample_Medium_19	NF	NF	NF	NF
191011_Sample_Medium_20	NF	NF	NF	NF

F

Filename	DNT-SG	DNP-SG	DNP-CG	DNP-NAC	Normalization		
	Area	Area	Area	Area	DNP-SG	DNP-CG	DNP-NAC
191011_Sample_Medium_6	483564894.49	8284209117.47	20383791.31	NF	17.13153542	0.042153166	0
191011_Sample_Medium_7	472706358.74	10533755566.02	38732716.04	10594660.31	22.28393033	0.081938217	0.022412773
191011_Sample_Medium_8	633140379.78	11978833953.82	40485944.39	12539423.09	18.91971249	0.063944657	0.019805123
191011_Sample_Medium_9	580055975.60	11579612066.61	32943008.19	16832670.60	19.96292178	0.056792809	0.029019045
191011_Sample_Medium_10	480476830.52	NF	NF	NF	0	0	0
191011_Sample_Medium_11	981204.92	1624438024.71	19172259.21	NF	1655.554297	19.53950574	0
191011_Sample_Medium_12	72222392.81	1019416138.62	28714047.15	NF	14.11495935	0.397578175	0
191011_Sample_Medium_13	512923945.94	9447164954.30	37744570.62	17652843.88	18.4182568	0.073587071	0.034416104
191011_Sample_Medium_14	228926478.91	4664081523.69	13290671.89	NF	20.37370926	0.058056508	0
191011_Sample_Medium_15	330525570.64	NF	NF	NF	0	0	0
191011_Sample_Medium_16	73264905.37	1007892529.90	5615162.60	NF	13.75682566	0.076641914	0
191011_Sample_Medium_17	290324260.83	5719325118.94	16089197.12	NF	19.69978362	0.055418025	0
191011_Sample_Medium_18	224025565.93	5231984752.82	9030931.21	NF	23.35440927	0.040312056	0
191011_Sample_Medium_19	8281371.86	135531869.15	2723236.04	NF	16.36587167	0.328838759	0
191011_Sample_Medium_20	106919645.10	NF	NF	NF	0	0	0

SI Table 22: Cytosolic GST expression in PAC2 cells exposed to 1-chloro-2,4-dinitrobenzene (CDNB) non-toxic concentration (NtC).

Content:							
<p>Exposure Experiments Peak area of proteotypic peptides (PP) and shared peptides (SP)</p> <p>Peak area (normalized to internal standard GAPDH) of proteotypic peptides (PP) and shared peptides (SP) detected in PAC2 cells. Carbamidomethyl (C) cysteine is indicated as C, the position of the peptide in the protein (first and last amino acids) is indicated in square brackets.</p> <p>Zebrafish embryos were exposed at 2 hpf for 24 h.</p> <p>++ doubly charged</p> <p>+++ triply charged</p>							
peptide type	isoenzyme	peptide sequence and position within the protein	sample	Replicate			
				1	2	3	4
SP	Gstz1,2,3	DGGQQLTDQFK 618.7964++	Control 1h	0.00064947	0.000743048	0.000227112	0.001592473
			Control 3h	0.000950179	0.001087471	0.000811717	0.001038332
			Control 6h	0.000246135	0.001575719	0.001448269	0.001477475
			Control 24h	0.001039387	0.001396509	0.001000771	0.001245581
			Sample 1h	0.000987677	0.000861544	0.000938062	0.001514739
			Sample 3h	0.001101374	0.001450393	0.001523448	0.000982529
			Sample 6h	0.001122999	0.001201849	0.001717476	0.001785704
			Sample 24h	0.001162087	0.001459063	0.001701912	0.00044017
SP	Gstz1,2,3	LLPADPMQR 520.7815++	Control 1h	0.008731483	0.00785711	0.002262949	0.008854294
			Control 3h	0.006940108	0.007838006	0.010022485	0.009054611
			Control 6h	0.001596269	0.007539635	0.008182508	0.007475756
			Control 24h	0.007147532	0.010310773	0.009046534	0.009440691
			Sample 1h	0.008459565	0.010380243	0.008537738	0.009566558
			Sample 3h	0.007453141	0.010686993	0.01217399	0.010461682
			Sample 6h	0.007950759	0.01347644	0.009068957	0.008818157
			Sample 24h	0.007739865	0.012226815	0.008607277	0.010628441
SP	Gstz1,2,3	LNQTLVEIAFK 702.8903++	Control 1h	0.005573459	0.007480722	0.02706966	0.006651091
			Control 3h	0.004643403	0.008548338	0.009509833	0.008336335
			Control 6h	0.01210978	0.007483896	0.007653518	0.006515922
			Control 24h	0.004735689	0.008468692	0.00765159	0.007386454
			Sample 1h	0.006797613	0.008444639	0.008231369	0.00683231
			Sample 3h	0.00594056	0.010338264	0.006085585	0.006068341
			Sample 6h	0.005286811	0.009206989	0.007667891	0.007120393
			Sample 24h	0.004701488	0.011934434	0.007840166	0.006893711
PP	Gstta	AQVDFLSWQH TNIR 615.3077+++	Control 1h	0.000444467	0.000735532	0.000334493	0.000564117
			Control 3h	0.000599416	0.000604356	0.000511492	0.000884707
			Control 6h	0.000709583	0.000531941	0.000432448	0.000626852
			Control 24h	0.000628653	0.00066448	0.000677094	0.000472844
			Sample 1h	0.000615354	0.000659025	0.000627246	
			Sample 3h	0.000914629	0.000689265	0.000871938	
			Sample 6h	0.000677097	0.00094993	0.000651854	
			Sample 24h	0.000660677	0.000875139	0.000557704	
PP	Gstta	GVLPAVTGAPVP K 603.3663++	Control 1h	0.002124676		0.00033455	0.00369239
			Control 3h	0.003039902	0.000942703	0.002467133	
			Control 6h	0.003912583		0.001966315	0.00269775
			Control 24h	0.003832139	0.003212096	0.003127149	0.004196878
			Sample 1h	0.001820413		0.001356199	0.001652815
			Sample 3h	0.002220713		0.00170287	0.004879324
			Sample 6h	0.002095751	0.001862594	0.002448163	0.00262301

			Sample 24h	0.003543335	0.001914862	0.002832487	0.001937599
PP	Gstta	MDSALDLNMS LK 733.8469++	Control 1h	0.000703585	0.000842225	0.000639232	
			Control 3h	0.000545571	0.000464066	0.000738006	0.00052798
			Control 6h	0.000920566			
			Control 24h	0.000967842	0.000806385	0.000775599	
			Sample 1h	0.000796102	0.001135872	0.000867116	0.000957729
			Sample 3h	0.000674744		0.001719307	0.001027522
			Sample 6h	0.001100287	0.001713016		
			Sample 24h	0.000920375		0.000795404	
SP	Gstm1,2	CFLDHFESLEK 712.8294++	Control 1h	0.001988498	0.001307147	0.004665238	0.001498452
			Control 3h	0.003118377	0.002860644	0.003397997	0.001398065
			Control 6h	0.003245503	0.003253348	0.003763499	0.002077793
			Control 24h	0.003988223	0.004390999	0.003720085	0.002234074
			Sample 1h	0.002652252	0.002568427	0.002705434	0.001412603
			Sample 3h	0.002421421	0.003172889	0.003856894	0.00118535
			Sample 6h	0.004113446	0.001377499	0.002858114	0.001948552
			Sample 24h	0.004695713	0.003211979	0.004278353	0.00178218
SP	Gstm1,2	MFEPACLDLDFK 686.7992++	Control 1h	0.005102657	0.003638738	0.004265702	0.003497699
			Control 3h	0.009943851	0.004233252	0.004056221	0.004018988
			Control 6h	0.009691406	0.006117056	0.005534147	0.005217111
			Control 24h	0.010457303	0.008769643	0.007821753	0.003987181
			Sample 1h	0.005693702	0.003055149	0.004905029	0.002808989
			Sample 3h	0.006870673	0.003020251	0.001800729	0.002547087
			Sample 6h	0.007973908	0.002798958	0.005035127	0.002653114
			Sample 24h	0.011154413	0.004663267	0.008886396	0.003264174
SP	Gstm1,2	IVQSNAIMR 516.2870++	Control 1h	0.098217443	0.10632655	0.021069976	0.096517682
			Control 3h	0.093413457	0.102643944	0.103085913	0.108987801
			Control 6h	0.019646058	0.100945368	0.10542471	0.096812397
			Control 24h	0.093452066	0.121530823	0.125897512	0.113731958
			Sample 1h	0.090285398	0.104851887	0.103670761	0.097133666
			Sample 3h	0.091198936	0.11143095	0.098906778	0.093364902
			Sample 6h	0.089911133	0.124057181	0.107369639	0.096519105
			Sample 24h	0.09027189	0.123650044	0.116241455	0.119217068
SP	Gstm1,2,3	QFSDFLGDR 542.7565++	Control 1h	0.001261909	0.000864006		
			Control 3h	0.001844676	0.001100416	0.000741747	0.00089062
			Control 6h	0.001520205	0.00146125	0.001470878	0.001200036
			Control 24h	0.002331192	0.001825082	0.001767382	0.001164833
			Sample 1h	0.001111762	0.000649847	0.001336416	
			Sample 3h	0.001853178			
			Sample 6h	0.002000853	0.000560395	0.001021682	0.000560912
			Sample 24h	0.002655271	0.00120399	0.002024746	0.001024047
SP	Gstm1,2,3	VDILENQAMDFR 725.8534++	Control 1h	0.001142453	0.001960107	0.001189378	0.001148987
			Control 3h	0.002014474	0.001616012	0.001569667	0.001564747
			Control 6h	0.001991673	0.001977439	0.001695386	0.001775527
			Control 24h	0.002040918	0.002839049	0.002224149	0.001150068
			Sample 1h	0.001480918	0.001667502	0.001468217	0.001157461
			Sample 3h	0.001394598	0.001763439	0.001295612	0.001418454
			Sample 6h	0.001861172	0.001715354	0.001498617	0.00134891
			Sample 24h	0.002365478	0.00213839	0.002420507	0.00196689
PP	Gstp1	CFENVLAK 490.7471++	Control 1h	0.002552236	0.002460062	0.003741114	0.00342928
			Control 3h	0.002732235	0.002572221	0.004015911	0.003595132
			Control 6h	0.003154796	0.003171521	0.004192242	0.003641252
			Control 24h	0.003308686	0.003600663	0.004371572	0.002801154
			Sample 1h	0.002722745	0.002472674	0.004258461	0.002614986
			Sample 3h	0.003174374	0.002095994	0.002779788	0.002702059

			Sample 6h	0.003415729	0.001957794	0.004701997	0.002647022
			Sample 24h	0.003308352	0.003612889	0.004947099	0.003565247
SP	Gstp1,2	ALLECFNK 562.2762++	Control 1h	0.002963911	0.002462997	0.004740681	0.004040307
			Control 3h	0.003975641	0.003105853	0.004507883	0.004319074
			Control 6h	0.00434997	0.003720256	0.005078436	0.003990835
			Control 24h	0.005542714	0.004866887	0.004899	0.003239351
			Sample 1h	0.003644067	0.003037788	0.005339006	0.003594118
			Sample 3h	0.004167687	0.002237232	0.003742791	0.002869274
			Sample 6h	0.004343663	0.003518812	0.004076678	0.003933711
			Sample 24h	0.005129397	0.003669427	0.005953931	0.004660005
PP	Gstr	LMIALEEK 473.7675++	Control 1h	0.00449695	0.00327302		0.003161579
			Control 3h	0.004691044	0.003333659	0.003944345	0.003635633
			Control 6h		0.00315884	0.00392325	0.003698172
			Control 24h	0.004620499	0.004318362	0.005455224	0.003723527
			Sample 1h	0.003445304	0.002721322	0.003658467	0.003136454
			Sample 3h	0.004607832	0.002561011	0.002565044	0.002737378
			Sample 6h	0.004467679	0.002977331	0.004384311	0.003198077
			Sample 24h	0.005192576	0.004225886	0.005148639	0.003719841
PP	Gstr	LIPDNPAE- MALVYQR 865.4507++	Control 1h	0.002260457	0.002215428	0.00363721	0.001907891
			Control 3h	0.002068656	0.002042912	0.00238081	0.002562763
			Control 6h	0.002733878	0.001955785	0.002301845	0.00183088
			Control 24h	0.001915136	0.002648634	0.002612094	0.002079433
			Sample 1h	0.001807009	0.002391548	0.002374257	0.002168133
			Sample 3h	0.002070199	0.00283142	0.003230359	0.002049703
			Sample 6h	0.002356918	0.002694288	0.002571175	0.001938361
			Sample 24h	0.002120382	0.002852709	0.002814872	0.002411564
		LIPDNPAE- MALVYQR 577.3029+++	Control 1h	0.001242014	0.001323929	0.002378044	0.001536707
			Control 3h	0.000926015	0.001172469	0.000935755	0.001702536
			Control 6h	0.002026836	0.001103134	0.001157607	0.001316544
			Control 24h	0.000604055	0.001099775	0.000995092	0.001318099
			Sample 1h	0.000904494	0.0013122	0.001220384	0.00124463
			Sample 3h	0.001018224	0.00194584	0.001620736	0.001311903
			Sample 6h	0.000900002	0.001848963	0.001002073	0.001484233
			Sample 24h	0.000896191	0.00175713	0.001200043	0.002320542
PP	Gstr	MFETENLQKQ 634.3030++	Control 1h	0.002145852	0.002280861	0.000516007	0.002209381
			Control 3h	0.002582217	0.002167364	0.002383446	0.003056131
			Control 6h	0.000532533	0.002285049	0.002817001	0.003024801
			Control 24h	0.002492233	0.00298406	0.003432974	0.003083207
			Sample 1h	0.002258986	0.001689081	0.00225459	0.002709517
			Sample 3h	0.0027008	0.002003684	0.001870538	0.003447866
			Sample 6h	0.002452098	0.00234167	0.002582314	0.003035106
			Sample 24h	0.002527546	0.003440997	0.003321652	0.002476268
PP	Gsto1	MLLELFSSK 490.7779++	Control 1h	0.000422375	0.000475212	0.000326778	
			Control 3h	0.000683861	0.000538072	0.000436364	0.000322987
			Control 6h		0.000831433	0.000512969	0.000686434
			Control 24h	0.000489323	0.000346226	0.000467185	0.0002944
			Sample 1h	0.00040227	0.000384977	0.00053814	
			Sample 3h	0.000451756	0.000412283		0.00055735
			Sample 6h	0.000459052		0.000415684	0.000793991
			Sample 24h	0.000403952	0.00034682	0.000431985	0.000704313
PP	Gsto2	LLPSDPFER 537.2849++	Control 1h	0.055550043	0.042431284	0.034033917	0.03600828
			Control 3h	0.070100807	0.045558523	0.05432599	0.051118415
			Control 6h	0.042649955	0.051611718	0.056966051	0.047834262

			Control 24h	0.075578555	0.070231892	0.080505282	0.042231105
			Sample 1h	0.049894877	0.035615146	0.059234433	0.028198365
			Sample 3h	0.061552655	0.03395348	0.033311233	0.032338995
			Sample 6h	0.071682259	0.036137305	0.060819492	0.034172613
			Sample 24h	0.081719168	0.053534571	0.083417833	0.041028462
PP	Gsto2	ECSAPGPVPNG QIR 741.3619++	Control 1h	0.00053358	0.001010539	0.001345981	0.000821706
			Control 3h	0.000922373	0.001021045	0.001024855	0.000591316
			Control 6h	0.000858753	0.001024678	0.001366549	0.000897777
			Control 24h	0.00057604	0.000975951	0.001614185	0.000947729
			Sample 1h	0.000884463	0.001242572	0.001319614	0.000825731
			Sample 3h	0.000799637	0.001032685	0.001210385	0.001135978
			Sample 6h	0.000601489		0.001484821	0.00045635
			Sample 24h	0.000925529	0.001127139	0.002049624	0.00083717

SI Table 23: Analysis of CDNB in medium during the exposure experiments.

T0 0 h exposure
T1 1 h exposure
T2 3 h exposure
T3 6 h exposure
T4 24 h exposure

EXP_Cell : Exposure cell: medium from flasks containing cells

EXP_Chem: Exposure chem: medium from flasks not containing cells

	mz 171	mz 183	mz 200	mz201	mz 232	
Filename	Area	Area	Area	Area	Area	SUM
191017_EXP_Cell_Blank_1	NF	NF	NF	NF	NF	0.00
191017_EXP_Cell_Blank_2	NF	NF	NF	NF	NF	0.00
191017_EXP_Cell_Blank_3	NF	NF	NF	NF	NF	0.00
191017_EXP_Cell_Blank_4	NF	NF	NF	NF	NF	0.00
191017_EXP_Cell_Blank_5	NF	NF	NF	NF	NF	0.00
191017_EXP_Cell_Blank_6	NF	NF	NF	NF	NF	0.00
191017_EXP_Cell_C_R1	NF	NF	NF	NF	NF	0.00
191017_EXP_Cell_C_R2	NF	NF	NF	NF	NF	0.00
191017_EXP_Cell_C_R3	NF	NF	NF	NF	NF	0.00
191017_EXP_Cell_C_R4	NF	NF	NF	NF	NF	0.00
191017_EXP_Cell_T0_R1	6528646.76	873091146.93	11497345.24	5840830.07	7654397.47	904612366.46
191017_EXP_Cell_T0_R2	10992379.23	1242644876.45	16604223.21	8648105.79	11746877.15	1290636461.84
191017_EXP_Cell_T0_R3	9064866.99	1107270748.91	15185253.76	8388830.97	10553570.80	1150463271.44
191017_EXP_Cell_T0_R4	7648346.05	1155849098.68	13704851.93	7109996.53	8897747.30	1193210040.49
191017_EXP_Cell_T1_R1	252188.23	54120538.05	470483.25	86805.53	320704.82	55250719.89
191017_EXP_Cell_T1_R2	1136436.44	158452993.39	1995821.42	843238.94	1360105.35	163788595.55
191017_EXP_Cell_T1_R3	844042.78	119448103.16	1420132.25	597233.36	929610.28	123239121.83
191017_EXP_Cell_T1_R4	322884.07	75559917.82	764311.72	154879.26	389896.04	77191888.91
191017_EXP_Cell_T2_R1	141226.98	915640.78	NF	NF	NF	1056867.76
191017_EXP_Cell_T2_R2	177101.19	1778475.94	NF	NF	NF	1955577.12
191017_EXP_Cell_T2_R3	192609.64	6899608.02	NF	NF	NF	7092217.66
191017_EXP_Cell_T2_R4	138665.57	1131715.79	NF	NF	NF	1270381.35
191017_EXP_Cell_T3_R1	147190.06	NF	NF	NF	NF	147190.06
191017_EXP_Cell_T3_R2	129841.99	2823832.02	NF	NF	NF	2953674.01
191017_EXP_Cell_T3_R3	142748.79	NF	NF	NF	NF	142748.79
191017_EXP_Cell_T3_R4	89529.41	NF	NF	NF	NF	89529.41
191017_EXP_Cell_T4_R1	NF	NF	NF	NF	NF	0.00
191017_EXP_Cell_T4_R2	NF	NF	NF	NF	NF	0.00

191017_EXP_Cell_T4_R3	NF	NF	NF	NF	NF	0.00
191017_EXP_Cell_T4_R4	NF	NF	NF	NF	NF	0.00
191017_EXP_Chem_Blank_1	NF	NF	NF	NF	NF	0.00
191017_EXP_Chem_Blank_2	NF	NF	NF	NF	NF	0.00
191017_EXP_Chem_Blank_3	NF	NF	NF	NF	NF	0.00
191017_EXP_Chem_Blank_4	NF	172388.30	NF	NF	NF	172388.30
191017_EXP_Chem_T1_R1	9982766.64	1224996797.91	19558372.81	8296925.22	11901892.69	1274736755.27
191017_EXP_Chem_T1_R2	7457921.57	870321598.55	13188290.60	6177323.91	8101762.53	905246897.16
191017_EXP_Chem_T1_R3	43346561.08	1925661946.78	24040929.58	46428379.22	15436901.75	2054914718.41
191017_EXP_Chem_T2_R1	6865960.20	915403205.96	12532496.41	5785699.55	8381209.74	948968571.86
191017_EXP_Chem_T2_R2	5315494.78	673053048.80	9292518.28	4733647.43	5906024.23	698300733.51
191017_EXP_Chem_T2_R3	6121129.66	828138397.54	10601893.75	4978383.42	7114798.23	856954602.60
191017_EXP_Chem_T3_R1	5350807.22	689027638.80	9549076.04	4254641.77	6090472.50	714272636.32
191017_EXP_Chem_T3_R2	3326778.14	429071239.34	5553334.99	2865606.91	3572468.65	444389428.03
191017_EXP_Chem_T3_R3	4282276.20	553776281.23	7634718.14	3228249.06	5138074.00	574059598.62
191017_EXP_Chem_T4_R1	793924.98	117830778.70	1257567.48	578412.60	766988.36	121227672.13
191017_EXP_Chem_T4_R2	NF	24656594.00	NF	NF	NF	24656594.00
191017_EXP_Chem_T4_R3	96595.42	34230575.38	160309.38	NF	76793.46	34564273.64

Measured concentration [µg/ml]					
	1	2	3	4	
Cell Control	0	0	0	0	
Exposure cell t0	0.242241	0.322073	0.293084	0.301924	
Exposure cell t1	0.066587	0.089033	0.080647	0.071125	
Exposure cell t2	0.055379	0.055565	0.056628	0.055424	
Exposure cell t3	0.055191	0.055772	0.05519	0.055179	
Exposure cell t4	0	0	0	0	
Exposure chem t1	0	0.318785	0.242372	0.48013	
Exposure chem t2	0	0.251414	0.199574	0.232385	
Exposure chem t3	0	0.202877	0.147063	0.17388	
Exposure chem t4	0	0.080231	0.06026	0.062309	

Acknowledgements

Many people made my stay at Eawag an unforgettable journey of professional and personal growth. With this letter, I would like to gratefully thank my supervisors, colleagues, friends and family who supported and motivated me throughout my doctoral studies.

Foremost, I would like to express my sincere gratitude to my thesis supervisors Kristin Schirmer, Marc J-F Suter and Ksenia J Groh for giving me the opportunity to design my own project and providing guidance and support throughout this research. I wish to thank Kristin for her valuable feedback throughout my thesis, her support with manuscript writing and for keeping me on the right track throughout the project. Special thanks go to Marc for teaching me everything I know about mass spectrometry, fruitful discussions and for always having an open door to listen, not only to scientific, but also to all kinds of problems. I would like to thank Ksenia: за поддержку моего проекта своим огромным знаниям о биологических системах, ее интересные идеи и мотивацию.

I would like to gratefully thank my PhD jury committee members, Urs von Gunten, Sandrine Gerber, Shana Sturla and Paola Picotti for dedicating their time and energy to reading my thesis and attending my defence. Thank you for the nice atmosphere during my defense, a fruitful discussion and valuable feedback.



I wish to express my deepest gratitude to René Schönenberger, who supported me with my laboratory work and mass spectrometric analysis. Without René's humor and marvelous help the laboratory work would have been more difficult, stressful and, above all, boring. His all-around capabilities and helpful attitude are in every sense inspiring.

Furthermore, I would like to thank my colleagues at the department of environmental toxicology (Utox) for supporting me in the laboratory (Melanie, Sebastian, Hannah and all members of the Fish Group), and my colleagues at the department of environmental

chemistry (Uchem) for their support with mass spectrometry (Jonas, Bernadette, Philipp, Martin).

A big thank you goes out to my colleagues and friends at Utox and Uchem (especially the Spring/Summer/Autumn/Winter-fun group, the pět ručníků and Ash) for all the fun and creative coffee breaks, social events and leisure activities. The ability of those departments to create an excellent work environment for employees makes them truly special.

I am very grateful to be a part of the feminno program, and I would like to thank Ute Budliger and my fellow members of the program for their encouragement and for broadening my horizon in so many ways.

At last, but not least, I would like to thank my family and friends for their love, encouragement and unconditional support during the hard times and their warm and cheerful nature during the good times. I feel really lucky to have you in life. Огромное спасибо! Danke! Thank you!

Thank you



Curriculum Vitae – Alena Tierbach



Contact

Address: Roswiesenstrasse 133,
8051 Zuerich, Switzerland

E-mail: alena.tierbach@eawag.ch
Phone: +41 58 765 5802
Mobile: +49 774 970 490

Date & place of birth: 08.11.1987,
Uljanowsk, Russia

Academic Societys

Society of Environmental Toxicology
and Chemistry (SETAC)

Swiss Group for Mass Spectrometry
(SGMS)

Swiss Chemical Society
(SCS)

Volunteer Experience

Nov. '11 - May. '12

Voluntary social work with the
organisation Cultural Canvas
Thailand, Chiang Mai, Thailand.
Planning and support of projects
focused on art therapy and education

Languages

German ☐

Russian ☐

English ☐

Spanish ☐

ALENA TIERBACH

Education and work experience

Jan. '16 - Mar. '20

PhD Student, École Polytechnique Fédérale de
Lausanne (EPFL), and Department of Environmental
Toxicology, Eawag, Duebendorf, Switzerland

PhD thesis: Role of glutathione S-transferases and
the mercapturic acid pathway in the biotransformation
potential of two zebrafish (*Danio rerio*) test systems:
early life stages and PAC2 cells

Oct. '14 - Dez. '15

Research Assistant, Department of Environmental
Toxicology, Eawag, Duebendorf, Switzerland
Research topic: targeted proteomics in zebrafish

Oct. '12 - Sep. '14

Master of Science in Environmental Toxicology,
University of Duisburg-Essen, Essen, Germany.

Master thesis: Mechanistic and systematic
understanding of the toxicity of manufactured
nanomaterials in the alga *Chlamydomonas reinhardtii*
(performed at Eawag, Duebendorf, Switzerland)

Nov. '13 - Feb. '14

Research Internship, Eawag, Duebendorf,
Switzerland

Oct. '08 - Sep. '11

Bachelor of Science in Biology Rheinische
Friedrich-Wilhelms-University, Bonn, Germany.

Bachelor thesis: Membrane protein interactions
between different *Arabidopsis thaliana* MRS2-type
magnesium transporters using mbSUS in
Saccharomyces cerevisiae.

Awards and scholarships

Jun. '17

DAS Young Analytical Scientist Travel Award

Oct. '16

SGMS Annual meeting, best poster presentation

Aug. '16

SGMS - Student Travel Award

Sep. '16

SETAC GLB annual meeting 2016
best platform presentation

Sep. '15

Young Scientist Award SETAC GLB
best master thesis

Jun. '15

ZWU Young Scientist Award
(Zentrum fuer Wasser- und Umweltforschung)

Mar. '13 - Oct. '14

German Academic Scholarship Foundation



ALENA TIERBACH

Conference organisation

Student assistant at the SETAC GLB 20th annual meeting, Sep. '15, Zuerich, Switzerland.

Student assistant at the SETAC Europe 24th Annual Meeting, May. '14, Basel, Switzerland.

Member of the organizing committee and student assistant at the SETAC GLB 18th annual meeting, Sep. '13, Essen, Germany

Student assistant

Apr '11 - Sep '11

Student assistant in the research group of Molecular Evolution, University of Bonn, Germany
Protein-protein interaction studies of magnesium transport proteins in *Arabidopsis thaliana*

Sep '10 - Jan '11

Student assistant in the research group of Gravitation Biology, University of Bonn, Germany
Gravity-sensing and gravity-oriented tip-growth in Characean rhizoid

Career Development

2019
feminno

Interests



art



aerial silk



yoga

Teaching experience

Jun. '17/'18/'19 Guest lecturer and teaching assistant, Practical Course in Molecular Ecotoxicology (M.Sc.), Eawag, Switzerland (1x 1h lecture, assist in practical work and exercises)

Jun. '14/'15/'16 Teaching assistant, Practical Course in Molecular Ecotoxicology (M.Sc.), Eawag, Switzerland (assist in practical work and exercises)

Summer '11 Teaching assistant, Practical Course in Plant Physiology and Molecular Genetics of Plants (B.Sc.), University of Bonn, Germany (assist in practical work and exercises)

Courses

Safety Pharmacology - Swiss Society of Toxicology (SST)

Cellular Toxicology - Swiss Society of Toxicology (SST)

Xenobiotic Metabolism and Toxicokinetics - Swiss Society of Toxicology (SST)

DIA/SWATH Course (Mass spectrometry) ETHZ

12th Mass Spectrometry School in Biotechnology and Medicine (MSBM)

Alternatives to Animal Testing in Aquatic Toxicology (PEAK Eawag-course)

LTK Module 20E - Introductory Course in Laboratory Animal Science: "Non rodent" species

Research Ethics (ETHZ)

Design of Experiments - EPFL

ALENA TIERBACH

Publications

- 2020 Expression of cytosolic glutathione S-transferases and performance of the mercapturic acid pathway in the zebrafish embryo cell line, PAC2; Tierbach, A; Groh, KJ; Schoenenberger, R; Schirmer, K; Suter MJ-F; *in preparation*
- Biotransformation capacity of zebrafish (*Danio rerio*) early life stages: Functionality of the mercapturic acid pathway; Tierbach, A; Groh, KJ; Schoenenberger, R; Schirmer, K; Suter MJ-F; *under review in Toxicological Sciences*
- LC-APCI(-)-MS determination of 1-chloro-2,4-dinitrobenzene, a model substrate for glutathione S-transferases; Tierbach, A; Groh, KJ; Schoenenberger, R; Schirmer, K; Suter MJ-F; Journal of the American Society for Mass Spectrometry, 2020, doi: 10.1021/jasms.9b00116.
- 2019 „Umwelttoxikologie“. Toxikologie; Schirmer, K; Schug, H; Tierbach, A; Eds. Marquardt, H; Schäfer, SG; Barth, H; Wissenschaftliche Verlagsgesellschaft, 2019, 1151-1158.
- 2018 Glutathione S-transferase protein expression in different life stages of zebrafish (*Danio rerio*), Tierbach, A; Groh, KJ; Schoenenberger, R; Schirmer, K; Suter MJ-F; Toxicological Sciences. 2018. *Editor's Highlights*
- 2013 Membrane protein interactions between different *Arabidopsis thaliana* MRS2-type magnesium transporters are highly permissive; Schmitz, J; Tierbach, A; Lenz, H; Meschenmoser, K; Knoop, V. Biochimica et Biophysica Acta (BBA)-Biomembranes. 2013, 1828 (9), 2032-2040.

Talks

- 2018 Detoxification capacity of zebrafish (*Danio rerio*) early life stages: Characterization of the glutathione conjugation pathway by targeted proteomics and metabolite analysis; A Tierbach, KJ Groh, R Schoenenberger, K Schirmer, MJ-F Suter; SETAC Europe, 25.-30. May 2019, Helsinki, FIN
- Glutathione S-transferase protein expression in different life stages of the vertebrate model zebrafish (*Danio rerio*); A Tierbach, KJ Groh, K Schirmer, MJ-F Suter; CHanalysis, 12./13. April 2018, Beatenberg, CH
- 2017 Glutathione S-transferase protein expression in different life stages of the vertebrate model zebrafish (*Danio rerio*); A Tierbach, KJ Groh, K Schirmer, MJ-F Suter; SGMS, 25.-27. October 2017, Beatenberg, CH
- 2016 Glutathion S-Transferasen in unterschiedlichen Entwicklungsstadien des Zebrafischblings – der erste Einblick in Proteinanalysen von Phase II Enzymen; A Tierbach, KJ Groh, K Schirmer, MJ-F Suter; SETAC GLB 5.-8. September 2016, Tübingen, D
- 2015 Interactions of silver nanomaterials with *Chlamydomonas reinhardtii*; A Tierbach, S Pillai, MJ-F Suter, K Schirmer; SETAC GLB, September 7.-10. 2015, Zurich, CH
- Case Study: Effects of NP on molecular endpoints in algae; Tierbach, A; Peak-Course V40/15, Ecotoxicological Effects of Synthetic Nanoparticles, 2015, Duebendorf, CH

ALENA TIERBACH

Poster

- 2019** Mercapturic acid pathway is complete and functional in early stages of zebrafish (*Danio rerio*) development; Tierbach, A; Groh, KJ; Schoenenberger, R; Schirmer, K; Suter MJ-F; CHanalysis, April 11/12. 2019, Beatenberg, CH
- 2018** Zebrafish (*Danio rerio*) early life stages biotransform the reference compound 2,4-dinitrochlorobenzene via glutathione-conjugation; Tierbach, A; Groh, KJ; Schoenenberger, R; Schirmer, K; Suter MJ-F; Fish and amphibian embryos as alternative models in toxicology and teratology, November 29/30. 2018 Aulnay-sous-Bois/Paris, F
- Biotransformation of the reference compound 2,4-dinitrochlorobenzene in zebrafish (*Danio rerio*) early life stages; Tierbach, A; Groh, KJ; Schoenenberger, R; Schirmer, K; Suter MJ-F; SGMS, October 25/26. 2018, Beatenberg, CH
- In vivo* GSH conjugation of the reference substrate CDNB in zebrafish early life stages; Tierbach, A; Groh, KJ; Schoenenberger, R; Schirmer, K; Suter MJ-F; 12th Mass Spectrometry School in Biotechnology and Medicine, July 8-14. 2018, Dubrovnik, HR
- 2017** Expression of Glutathione S-Transferases in different life stages of zebrafish - a targeted proteomics approach; Tierbach, A; Groh, KJ; Schoenenberger, R; Schirmer, K; Suter MJ-F; Proteomics Forum, April 2-5. 2017, Potsdam, D
- 2016** Members of GST family are differently expressed in early life stages of zebrafish; Tierbach, A; Groh, KJ; Schoenenberger, R; Schirmer, K; Suter MJ-F; SGMS, October 27/28. 2016, Beatenberg, CH
- Can we use targeted proteomics to explore dynamics in glutathione S-transferase expression in zebrafish embryos? Tierbach, A; Groh, KJ; Schoenenberger, R; Schirmer, K; Suter MJ-F; SCS Fall Meeting, September 15. 2016, Zürich, CH
- Expression of glutathione S-transferases in the developing zebrafish embryo - a targeted proteomic approach; Tierbach, A; Groh, KJ; Schoenenberger, R; Schirmer, K; Suter MJ-F; IMSC2016, August 20-26. 2016, Toronto, CA
- 2015** Glutathione S-transferase: the first step towards mapping of biotransformation enzymes in zebrafish embryos; Tierbach, A; Groh, KJ; Schoenenberger, R; Schirmer, K; Suter MJ-F; SGMS, October 26/27. 2015 Beatenberg, CH
- Expression of phase II biotransformation enzymes at early life stages of zebrafish (*Danio rerio*); Tierbach, A; Groh, KJ; Schoenenberger, R; Schirmer, K; Suter MJ-F; SETAC GLB, September 7-10. 2015, Zurich, CH
- The biotransformation potential of zebrafish embryos; Tierbach, A; Groh, KJ; Schoenenberger, R; Schirmer, K; Suter MJ-F; SETAC Europe 25th Annual Meeting, May 3-7. 2015, Barcelona, ES
- The role of free metal ions in the interaction of zinc oxide and silver nanoparticles with *Chlamydomonas reinhardtii*; A Tierbach, S Pillai, MJ-F Suter, K Schirmer; SETAC Europe 25th Annual Meeting, May 3-7. 2015, Barcelona, ES
- The biotransformation potential of zebrafish embryos; Tierbach, A; Groh, KJ; Schoenenberger, R; Schirmer, K; Suter MJ-F; 8th Swiss Zebrafish meeting, April 10. 2015 Fribourg, CH